VALIDITY OF DOSE DISTRIBUTION OF ELECTRON BEAM THERAPY OF ADAC PINNACLE ^{3} TREATMENT PLANNING SYSTEM VERSION 7.6C

SAENGDUEAN SONGSRI

A THESIS SUBMITTED IN PARTIAL FULFILLMENT
OF THE REQUIREMENTS FOR
THE DEGREE OF MASTER OF SCIENCE
(MEDICAL PHYSICS)
FACULTY OF GRADUATE STUDIES
MAHIDOL UNIVERSITY
2008

Thesis

Entitled

VALIDITY OF DOSE DISTRIBUTION OF ELECTRON BEAM THERAPY OF ADAC PINNACLE ^{3} TREATMENT PLANNING SYSTEM VERSION 7.6C

……
Miss. Saengduean Songsri
Candidate

……
Dr. Puangpen Tangboonduangjit,
Ph.D. (Medical Radiation Physics)
Major-Advisor

……..
Asst.Prof. Chirapha Tannanonta,
M.Sc. (Medical Physics)
Co-Advisor

…….
Asst. Prof. Auemphorn Mutchimwong,
Ph.D
Acting Dean
Faculty of Graduate Studies

……..
Assoc. Prof. Vipa Boonkitticharoen,
Ph.D. (Radiation Biology)
Chair
Master of Science Programme
In Medical Physics
Faculty of Medicine
Ramathibodi Hospital

Thesis

Entitled

VALIDITY OF DOSE DISTRIBUTION OF ELECTRON BEAM THERAPY OF ADAC PINNACLE ^{3} TREATMENT PLANNING SYSTEM VERSION 7.6C

was submitted to the Faculty of Graduate Studies, Mahidol University

For the degree of Master of Science (Medical Physics)

on

23 May, 2008

……..
Miss.Saengduean Songsri
Candidate

……...
Assoc.Prof.Sivalee Suriyapee
M.Eng (Nuclear Technology)
Chair

……
Dr. Puangpen Tangboonduangjit,
Ph.D. (Medical Radiation Physics)
Member

…….
Asst.Prof. Chirapha Tannanonta
M.Sc. (Medical Physics)
Member

……..
Asst. Prof. Auemphorn Mutchimwong,
Ph.D
Acting Dean
Faculty of Graduate Studies
Mahidol University

……
Professor Rajata Rajatanavin,
M.D., F.A.C.E.
Dean
Faculty of Medicine
Ramathibodi Hospital,
Mahidol University

ACKNOWLEDGEMENT

I would like to express my gratitude to all those who gave me the possibility to complete this thesis. I want to thank the Deviation of Radiation Oncology, Department of Radiology, Faculty of Medicine, Ramathibodi Hospital for giving me permission to commence this thesis in the first instance, to do the necessary research work and to use the materials in this experiments.

I am deeply indebted to my major advisor, Dr. Puangpen Tangboonduangjit for her guidance, supervision and encouragement helped me in all the time of research and writing of this thesis. I am equally grateful to my co-advisor, Asst. Prof. Chirapha Tannanonta for her kind suggestion, constructive comments in the experiment.

I wish to thank Assoc.Prof.Sivalee Suriyapee who was to chair and external examiner of the thesis defense for her kindness in examining the research and providing suggestions for improvement.

I would like to thank Assoc. Prof. Dr. Vipa Boonkitticharoen, program Director of Medical physics for her advice and comments in the research proposal.

My heartfelt thanks to my friends in the school of Medical Physics for their help and encouragement thought the entire course of study. Especially I am obliged to Ms.Patchareeporn Dejsupa for helping me in doings all thought the experiment.

I am grateful to all teachers, lecturers and staffs in the Medical Physics School of Faculty of Medicine, Ramathibodi Hospital for their kind support and teaching me in the Medical Physics Program.

Finally, I am grateful to my family for their valuable encouragement, entirely care and understanding during the entire course of study.

Saengduean Songsri

VALIDITY OF DOSE DISTRIBUTION OF ELECTRON BEAM THERAPY OF ADAC PINNACLE ^{3} TREATMENT PLANNING SYSTEM VERSION 7.6C

SAENGDUEAN SONGSRI 4836290 RAMP/M

M.Sc. (MEDICAL PHYSICS)

THESIS ADVISORS: PUANGPEN TANGBOONDUANGJIT, Ph.D. (MEDICAL RADIATION PHYSICS), CHIRAPHA TANNANONTA, M.Sc. (MEDICAL PHYSICS)

ABSTRACT

The purpose of this study is to investigate the accuracy of the dose computation of the implemented electron beam dose calculation algorithm in Pinnacle^{3} treatment planning system version 7.6C (Philips radiation Oncology System, Milpitas, CA). The investigation includes comparisons of measured relative dose distribution with calculated dose distributions and also comparisons of measured and calculated relative output factor. The testing process consisted of five experiments which were designed to represent typical clinical applications for electron beam therapy. The experiments consisted of standard fields, shaped fields, extended SSDs, oblique fields and internal heterogeneities (air and bone) and were most often irradiated with 6, 9 and 12 MeV electrons from the Varian Clinac 2100C linear accelerator. The accuracy of relative doses in standard fields with perpendicular incidences at standard and extended SSD, shaped fields and internal heterogeneities conditions was reasonably in agreement with the results. However, for the inhomogeneity test, the deviation between measurements and calculations at the interface area of an air cavity was up to 7%. The dose calculation in the interface area of a bone cavity was closer to the measurement than that in the border area of an air cavity and was within criteria of acceptability (<7%). The agreement between calculations and measurements in the SSD correction factor was smaller than 2%. For shaped fields and oblique beam incidence condition, the deviations of the output factor were smaller than 5%. This study indicates that the Pinnacle TPS is appropriated for electron dose calculations in the clinical radiation therapy. However, the physicist and clinician should be aware of the limitations of the dose calculation at the interface area of the internal heterogeneities.

KEY WORDS: VALIDITY OF DOSE DISTRIBUTION / ELECTRON BEAM / PENCIL BEAM / TREATMENT PLANNING

164 pp.

การตรวจสอบความถูกต้องในการคำนวณปริมาณรังสีอิเลกตรอนของเครื่องวางแผนการรักษา ADAC Pinnacle^3 เวอร์ชั่น 7.6C
(VALIDITY OF DOSE DISTRIBUTION OF ELECTRON BEAM THERAPY OF ADAC PINNACLE^3 TREATMENT PLANNING SYSTEM VERSION 7.6C)

แสงเดือน ทรงศรี 4836290 RAMP/M

วท.ม. (ฟิสิกส์การแพทย์)

คณะกรรมการควบคุมวิทยานิพนธ์ : พวงเพ็ญ ตั้งบุญดวงจิตร, Ph.D. (MEDICAL RADIATION PHYSICS), จีระภา ตันนานนท์, M.Sc. (MEDICAL PHYSICS)

บทคัดย่อ

งานวิจัยนี้มีวัตถุประสงค์เพื่อตรวจสอบความถูกต้องในการคำนวณปริมาณรังสีอิเลกตรอนของเครื่องวางแผนการรักษา ADAC Pinnacle^3 เวอร์ชั่น 7.6C (Philips radiation Oncology System, Milpitas, CA). ซึ่งได้ทำการเปรียบเทียบทั้ง Relative dose distribution และ relative output factor ระหว่างการวัดและการคำนวณของเครื่องวางแผนการรักษา โดยแบ่งการทดลองออกเป็น 5 การทดลอง และในแต่ละการทดลองได้จำลองจากเทคนิคที่แพทย์ใช้ในการรักษาให้กับผู้ป่วยจริง ซึ่งได้แก่ standard fields, shaped fields, extended SSDs, oblique fields และ internal heterogeneities (โพรงอากาศและโพรงกระดูก) และฉายด้วยอิเลกตรอนพลังงาน 6,9 และ 12 เมกะอิเลกตรอนโวลต์ โดยลำรังสีอิเลกตรอนผลิตจากเครื่องเร่งอนุภาค Varian Clinac 2100C ซึ่งจากการเปรียบเทียบ Percent Depth Dose (PDD) และ Beam profiles ระหว่างการวัดและการคำนวณของเครื่องวางแผนการรักษาในแต่ละการทดลองของ standard fields, shaped fields, extended SSDs และ internal heterogeneities พบว่าโดยส่วนใหญ่มีความแตกต่างอยู่ในเกณฑ์มาตรฐานที่กำหนดโดย Van dyk และคณะ ในการทดลองของ internal heterogeneities พบว่าที่บริเวณขอบของโพรงอากาศมีความแตกต่างระหว่างการวัดและการคำนวณมากกว่า 7% ส่วนที่บริเวณขอบของโพรงกระดูกมีความแตกต่างอยู่ภายในเกณฑ์มาตรฐานที่กำหนด สำหรับการเปรียบเทียบค่า Relative output factor พบว่าในการทดลอง extended SSDs มีความแตกต่างน้อยกว่า 2% ส่วนการทดลองของ shaped fields และ oblique fields มีความแตกต่างน้อยกว่า 5% กล่าวโดยสรุปได้ว่าเครื่องวางแผนการรักษา ADAC Pinnacle^3 เวอร์ชั่น 7.6C สามารถนำมาใช้ในการวางแผนการรักษาให้กับผู้ป่วยได้ แต่อย่างไรก็ตามแพทย์และนักฟิสิกส์ต้องระวังข้อจำกัดของการคำนวณปริมาณรังสีในบริเวณขอบของ inhomogeneity ด้วย
164 หน้า

CONTENTS

LIST OF TABLES

LIST OF TABLES (Continued)

LIST OF TABLES (Continued)

LIST OF TABLES (Continued)

LIST OF TABLES (Continued)

LIST OF TABLES (Continued)

LIST OF TABLES (Continued)

LIST OF TABLES (Continued)

LIST OF TABLES (Continued)

LIST OF FIGURES

LIST OF FIGURES (Continued)

LIST OF FIGURES (Continued)

LIST OF FIGURES (Continued)

LIST OF FIGURES (Continued)

LIST OF FIGURES (Continued)

LIST OF FIGURES (Continued)

LIST OF FIGURES (Continued)

LIST OF FIGURES (Continued)

LIST OF FIGURES (Continued)

LIST OF FIGURES (Continued)

LIST OF FIGURES (Continued)

LIST OF FIGURES (Continued)

LIST OF ABBREVIATIONS

Abbreviation	Term
2D	Two Dimensional
3D	Three Dimensional
A	Ampere
AAPM	American Association of Physicist in Medicine
AgBr	Silver Bromide
BEV	Beam's eye view
BP	Beam profile
°C	Degree Celsius
cGy	Centigray
cm	centimeter
cm^2	Square centimeter
cm^3	Cubic centimeter
^{60}Co	Cobalt-60
CT	Computed Tomography
D	Dose
Dcalc	Calculation dose
Dmeas	Measured dose
Dmeas,cax	Measured dose at central beam axis
Dmax	Dose at the maximum depth
$D_{W,Q}$	Absorbed dose to water
d_{max}	Depth of maximum dose
$d_{90\%}$	Depth of 90% dose or ionization
$d_{50\%}$	Depth of 50% dose or ionization
ECWG	Electron Collaborative Working Group
$E_{p,0}$	Most proable energy at phantom surface
Eq.	Equation
FMCS	Water Scatter Correction Factor

LIST OF ABBREVIATIONS (Continued)

Abbreviation	Term
g/cm	Gram per centimeter
g/cm^3	Gram per cubic centimeter
Gy	Gray
Gy/min	Gray per minute
Gy.min	Gray minute
IAEA	International Atomic Energy Agency
k_{elec}	Electrometer correction factor
k_{pol}	Correction factor for the polarity effect
k_s	Recombination correction factor
k_{TP}	Temperature and pressure correction factor
$k_{Q,Q0}$	The correction factor for the effects of the difference between the reference beam quality and the actual user quality
kVp	Kilovolt (peak)
LAN	Lacal Area Network
mm	Millimeter
mm^2	Square millimeter
mm^3	Cubic millimeter
M	Electrometer reading
MCS	Multiple Coulomb Scatter
MCU	Main Control Unit
MeV	Megaelectron Volt
MU	Monitor Unit
nrc	Non-reference condition
$N_{D,W}$	Absorb dose to water calibration factor
OF	Relative Output Factor
P	Air Pressure
P_0	Reference air pressure

LIST OF ABBREVIATIONS (Continued)

Abbreviation	Term
PDD	Percentage Depth Dose
Q	Beam quality
Q_0	Reference beam quality
rc	Reference condition
R	Roentgen
R_{50}	Depth of 50% dose or ionization
R/min	Roengent per minute
Rp	Practical range
Rp+ 2cm	Two centimeter beyond the practical range
RFA	Radiation Field Analyzer
RTP	Radiotherapy Treatment Planning
RW_{50}	Radiological width
SSD	Source to Surface Distance
Sw,air	Ratio of average stopping power for water to air
Sv	Sivert
T, T_0	Temperature of the chamber cavity air during measurement (T_0 is the reference temperature)
TLD	Thermoluminescence dosimeter
TPS	Treatment Planning System
TRS	Technical Report Series
V	Polarizing or collecting of ionization chamber
z_{ref}	Reference depth
µm	Micrometer
$\sigma_{\theta x}$	Angular scattering in air

CHAPTER I
INTRODUCTION

Electron beams are often used to deliver uniform dose to superficial target volumes while sparing normal tissues at depth with a characteristically sharp rapid fall-off in dose beyond the tumor[1, 2]. Typical electron energies can range from 6 to 20 MeV[3]. Its selection in clinical use is usually based on depth of the most distal disease, as the depth dose of an electron beam is a strong function of its incident energy. However, the dose characteristics can change depending on irregular surfaces and blocked fields, as well as heterogeneities encountered inside a patient's body due to scattering[4]. As a result, clinical decisions are frequently made based on isodose treatment plans generated by radiotherapy treatment planning (RTP) systems. Three dimensional (3D) RTP systems now provide the necessary tools to better support such decision-making process through enhanced visualization of patient anatomy, target volumes, beam arrangements, treatment aids, as well as dose distributions. Consequently, it is very important for the users of any 3D RTP system to have a clear understanding of the limitations of the implemented electron dose calculation algorithm. This paper was made for an investigation of the accuracy of the dose computation in three dimensions of the implemented electron beam dose calculating algorithm in Pinnacle^3 treatment planning system version 7.6C (Philips Radiation Oncology System, Milpitas, CA). The electron dose calculation uses the Hogstrom pencil beam algorithm [5, 6].

The investigation includes comparisons of measured relative dose distribution with calculated dose distributions and also comparisons of measured and calculated relative output factor. The relative measurements were mainly presented as dose profiles and depth dose curves. All experiments in this work are based on the International Atomic Energy Agency: Technical reports series no.430[7]. The testing process consisted of five experiments, which were designed to represent typical clinical applications for electron beam therapy. The experiments consists of standard

fields, shaped fields, extended SSDs, oblique fields and internal heterogeneities and irradiated with 6, 9 and 12 MeV electron beam energies. Criteria for clinical acceptability are defined by Van Dyk *et al*. [8].

Effects of tissue heterogeneities[9]

The distribution of dose in tissue irradiated with electron beams can be significantly distorted by the presence of tissue heterogeneities such as bone, lung and air cavities. Electron beams are absorbed more rapidly by denser media and are absorbed less rapidly by less dense media. The deposition of dose is related to the collision stopping power, which varies with the electron density (electron per gram) of the medium. However, the scattering of electrons also is affected by the medium, and under some circumstances, the dose distributions may be altered in complex ways.

In the case of broad inhomogeneities, the effects on the dose distribution may be more easily measured, Figure 1.1 is a graph of percent depth dose measured in water, as well as in phantom composed of a layer of water above a layer of cork representing lung. The increased penetration of the electron beam through the lung materials is clearly demonstrated. A small reduction in dose on the proximal side of the cork boundary is seen, resulting from reduced backscattering of electrons into the water. This small perturbation due to backscattering is generally neglected when manual heterogeneity corrections are performed, but the increased penetration through low-density material must be determined.

Small inhomogeneities present a more complex problem because scattering of electrons within thin heterogeneity becomes quite important. Figure 1.2 indicates schematically the scattering of electrons at edges formed between high-and low-density media. As expected, absorption of electrons within the high-density heterogeneity causes a reduction in dose directly behind the heterogeneity. In addition, the increased scattering to electrons laterally from the heterogeneity causes an increase in dose beyond the edges of the heterogeneity. Conversely, the transmission of an electron beam through a low-density heterogeneity causes an increase in dose directly behind the heterogeneity but a reduction in dose laterally to the edges of the heterogeneity. This reduction is due to a lack of scattering of electron into these regions. The presence of these hot and cold spots have important implications when

small heterogeneities such as ribs and air cavities exist, or when high atomic number shielding materials are placed on or near the patients surface.

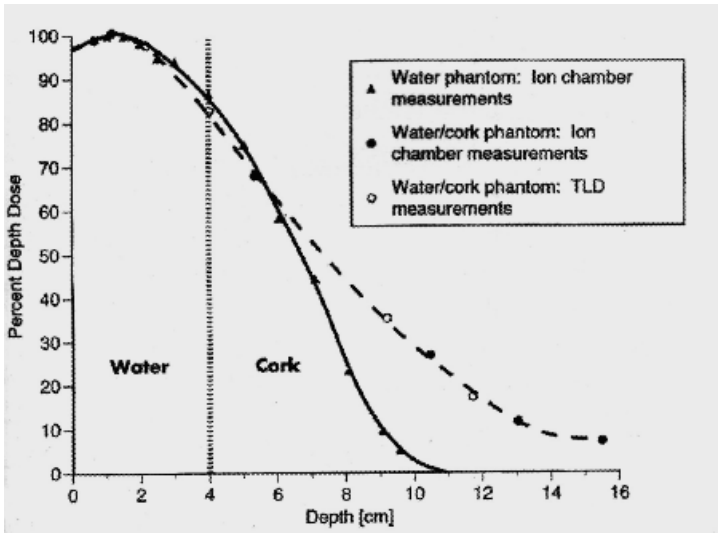

Figure 1.1 Electron beam depth dose curves measured in water and in a combination of water and cork

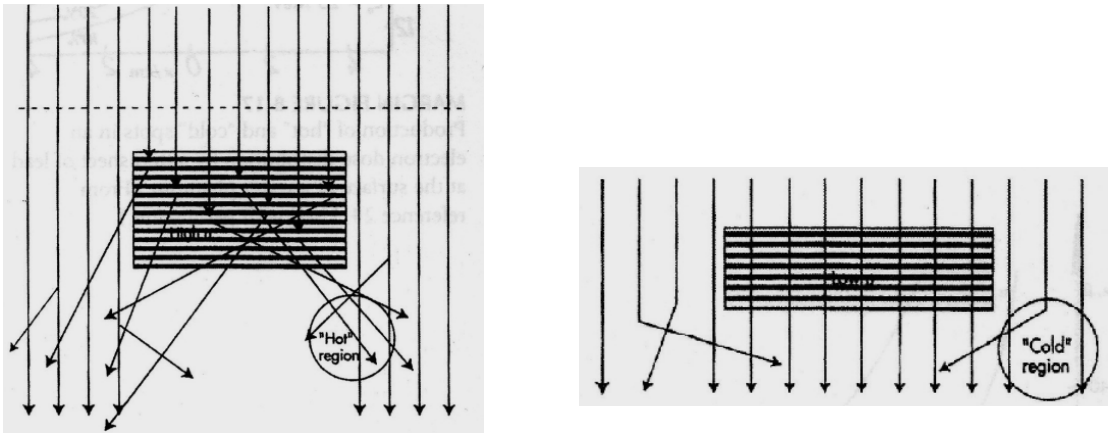

A B

Figure 1.2 A: Electron encountering a high-density heterogeneity are scattered at a steeper angle than electrons passing through the adjacent unit-density medium, and high dose regions are produced. B: Conversely, electrons encountering a low-density heterogeneity are scattered less, resulting in low-dose regions.

Electron dose algorithm in Pinnacle TPS

The electron dose calculation uses the Hogstrom pencil-beam algorithm (Hogstrom, 1981, 1984 and 1987). The algorithm uses a combination of measured data and model parameters that characterize the electron beam physics [5, 6]. The Hogstrom approximates the spatial distribution of pencil beams with radially symmetric Gaussian function[10]. The electron field is divided into a set of square pencil beams uniformly distributed. Each pencil beam can have its own intensity and lateral scatter spread, which are depth and energy dependent. Dose to any point of interest in the broad electron beam would then be the sum of dose contributions, over the beam cross section, from each of pencil beams. The dose contribution from each pencil beam is calculated as if the medium under the central ray of a pencil beam is infinite in their lateral. The advantage of this type of calculation is that it allows each pencil beam to be individually manipulated to make the calculation more sensitive to changes in patient anatomy in all three dimensions[3].

Measured data required as input, for each energy and cone size, are percent depth dose (%DD) in water at normal distances, cross-axis beam profile in water at depths of (1/2)R_{90}, R_{90}, R_{70}, R_{50} and Rp + 2 cm at normal distances and output factors at normal distances and extended distances. The electron model parameters required by the algorithm are the most probable incident electron energy at the phantom surface ($E_{p,0}$) , the angular scattering of electrons in air ($\sigma_{\theta x}$), the virtual source to the surface distance, photon contamination measurements depth, the setup source to surface distance (SSD), drift distance (the distance from the downstream edge of the beam-defining collimator to the surface of the phantom), the Off-Axis Ratio (OAR) and Water Scatter Correction Factor (FMCS) as shown in figure 1.3. The latter two parameters can be adjusted to fit the computed data with measured data[5, 6]. The FMCS corrects for the angular scattering of electrons in the computation medium relative to air. For each CT scanner, the user enters a table that correlates CT number to electron densities. To construct such a table, a phantom with known materials is scanned with the same kVp that is used for treatment planning. CT numbers for each material are obtained from the transferred images according to a procedure described in the Pinnacle users' manual[19].

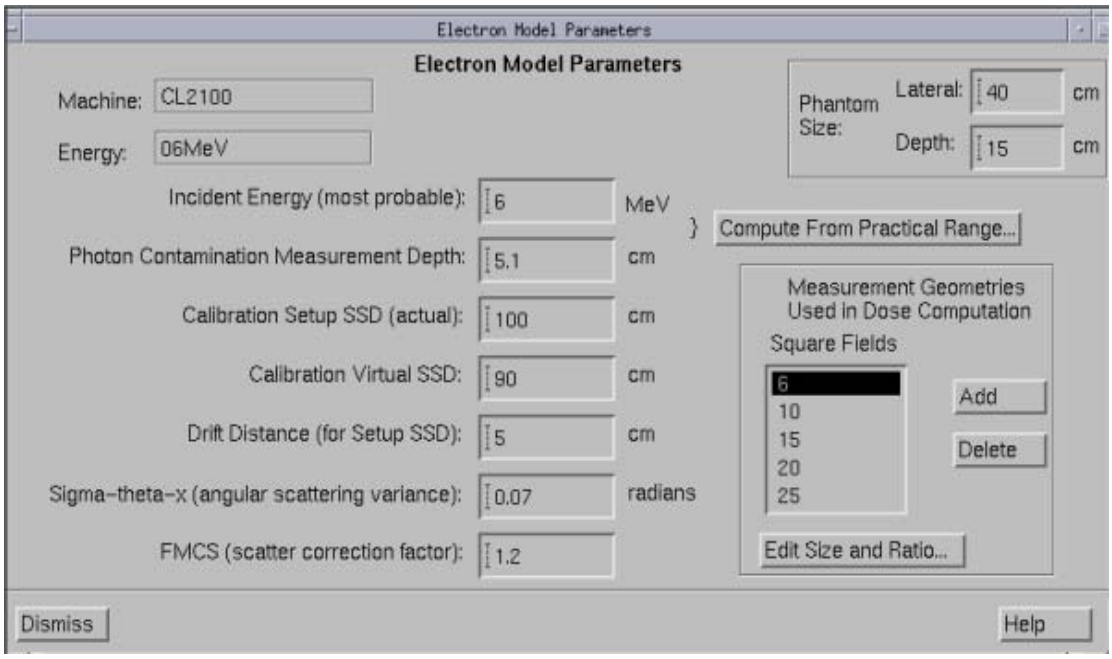

Figure 1.3 The electron model parameter screen shot

Methods for dosimetric comparison and verification

Dose calculation verification tests are compared between calculated and measured dose distributions. The standard method of comparison for 2D dose distributions consists of overlaying hard copy plots of measured and calculated dose in the form of cross-beam profiles, depth dose, or isodose distributions. For quantitative comparisons of entire 3D dose distributions, more sophisticated techniques are also needed to perform the analysis. [11].

Deviations between results of calculations and measurements can be expressed as a percentage of the locally measured dose according to:

$$\delta = 100\% \times \frac{(D\text{calc} - D\text{meas})}{D\text{meas}} \qquad (1)$$

Venselaar *et al.* [12] have defined a set of criteria of acceptability for dose calculations based on different tolerances for δ based on the knowledge that dose calculation algorithms provide better accuracy in some regions than in others. The difference between calculated and measured dose values is compared as a percentage of the dose measured locally. Normalization to this local dose D is preferred instead of to the dose at d_{max} (D_{max}).

The criteria of acceptability of dose calculations to be applied in such a comparison are related to uncertainties which are inevitably presented in dose measurements and to errors which follow from (expected) inadequacies of the dose calculation model or its implementation in the TPS. Different tolerances for δ are proposed for different regions in the beam which can be distinguished, analogous to the paper of Van Dyk *et al.* [8]and the report of AAPM Task Group 53[11]:as

- δ_1: for data point on the central beam axis beyond the depth of $d_{max:}$ the high dose and small dose gradient region.
- δ_2: for data point in the build up region, in the penumbra, and in region close to interfaces of inhomogeneities: the high dose and large dose gradient regions. This criterion can be applied in the region between the phantom surface and the depth of 90% isodose surfaces, as well as in the penumbra region. As an alternative, it is often proposed to use the shift of isodose line expressed in mm. A large dose gradient is generally defined as being larger than 3% per mm.
- δ_3: for data points beyond d_{max}, within the beam but outside the central beam axis: again this region is a high dose and small dose gradient region.
- δ_4: for data points off geometrical beam edges and below shielding blocks, generally beyond d_{max}: the region is a low dose and small dose gradient region, for instance below 7% of the central ray normalization dose.

The last criterion, δ_4, is applied in low dose regions where the dose calculations are inherently less accurate. It is therefore sometimes not useful to relate deviations between calculations and measurements in such cases to the value of the locally measured dose. An alternative is to replace expression (2) in those cases by:

$$\delta = 100\% \times \frac{(D\text{calc} - D\text{meas})}{D\text{meas,cax}} \qquad (2)$$

in which the deviation for point outside the beam is related to the dose measured at a point at the same depth as the point under the consideration, but now on the central beam axis (*D*meas,cax). The same approach can be applied for points where the dose is very low, such as below shielding blocks. Then, the deviation might be related to the dose measured at a point at the same depth on the central axis of the

open beam. It is recommended to include both values of the criterion δ_4 from equation (1) and (2) in such an evaluation.

Two other quantities are sometimes proposed which can be useful in comparing results of isodose calculations and profiles, especially for the reproduction of the basic beam data by the treatment planning system.

- RW_{50}: the radiological width, defined as the width of a profile measured at half its height compared to the value at the beam axis.
- $\delta_{50\text{-}90}$: the distance between the 50% and the 90% point (relative to the maximum of the profile) in the penumbra, which is sometimes called 'beam fringe'.

The region of validity of the above mentioned criteria are shown in the graphical examples of the depth-does curves and beam profiles of Fig 1.4.

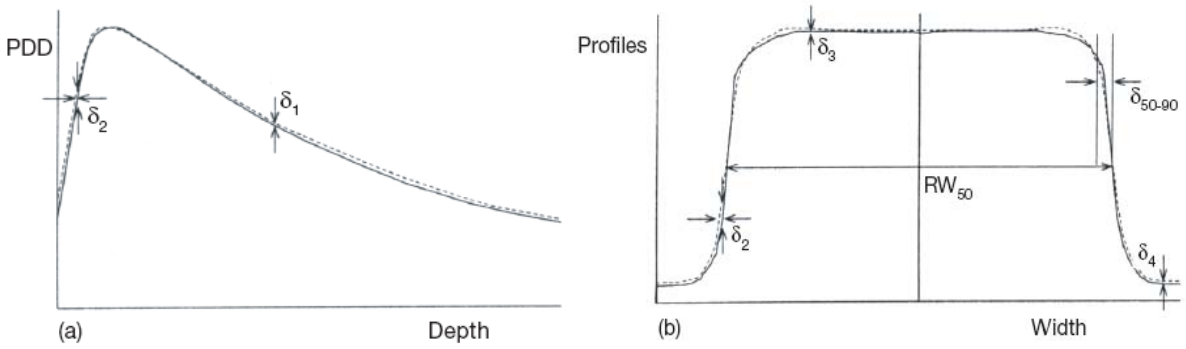

Fig 1.4 Regions of validity of the criteria δ_1-δ_4, radiological width RW_{50}, and beam fringe$\delta_{50\text{-}90}$ to compare calculated and measured depth-dose (PDD) curves (a) and beam profiles (b).

Criteria for acceptability of dose calculations

The tolerance considerations are the differences between measurements and calculations. These differences are dependent on the location within the beam and on the patient geometry.

Recommended values for the tolerances δ1 - δ4 are summarized in Table 1.1, subdivided according to increasing complexity of the test configurations. The different levels of complexity of geometry are:

1. Homogeneous, simple geometry. For calculation of dose values in homogeneous phantom for fields without special accessories and without asymmetric collimator setting, the tolerances of the descriptor A can be applied. These test situations include variation of SSD, rectangular field sizes, oblique incidence.
2. Complex geometry. For dose calculations for complex case, larger tolerances are allowed. Theses situations include beam with wedges, inhomogeneitis, shields, irregular fields, missing tissue and asymmetric collimator settings.

Table 1.1 Criteria of acceptability for electron beam dose calculation. [8]

Descriptor	δs	Criterion
A. Homogeneous calculation (no shields)		
1.Central ray data (except in build up region)	δ_1	2%
2.High dose region – low dose gradient	δ_3	4%
3.Large dose gradient(> 30% / cm)	δ_2 , $\delta_{50\text{-}90}$	4 mm
4.Small dose gradients in low dose region (i.e.< 7% of normalization dose)	δ_4	4%
B. Inhomogeneity corrections		
1. Central ray (slab geometry, in regions of electron equilibrium)	δ_1	5%
C. Composition uncertainty,anthromorphic phantom		
Contour correction,		
Inhomogeneities,		
Shields		
Irregular fields		
Off axis		
1. High dose region – low dose gradient	δ_3	7%
2. Large dose gradient(> 30% / cm)	δ_2 , $\delta_{50\text{-}90}$	5 mm
3. Small dose gradients in low dose region (i.e.< 7% of central ray dose)	δ_4	5%

Electron calculation verification experiments [7]

International atomic energy agency: Technical Reports Series no.430 (IAEA. TRS no.430) proposed a grade series of checks of various types of electron beam dose calculation, which should be used as guidance for the creation of individualized sets of checks to be used in any particular institution. Table 1.2 contains a summary of the experiments that might be required for verification and clinical testing of an electron beam dose calculation algorithm. The amount and sophistication of testing required for the verification of a calculation algorithm depends directly on the number of different capabilities of the TPS system that will be used clinically in the user' s institution. This table consists of a series of tests that describes increasing levels of complexity for each case (field shaping, set-up, etc.); these will be requiring additional checks.

Table 1.2 Electron beam planning techniques requiring verification checks

Level of complexity		Test	Test for each beam
Field shaping	Square and rectangular fields	Electron test 1	Yes
	Shaped apertures	Electron test 2	Yes
	Shielding and skin collimator	Electron test 3	Low energy only
Set-up	SSD dependence	Electron test 4	Yes
Bolus	Slab bolus	Electron test 5	One energy
	Shaped bolus	Electron test 6	Low and high energy
Patient shape	Oblique incidence	Electron test 7	Low and high energy
	Complex surface shapes	Electron test 8	Yes
Inhomogeneities	Bulk	Electron test 9	Yes
	CT based	Electron test 10	Yes
Arcs	Arcs	Electron test 11	Yes

Absorb dose calculation [13]

The charged reading from parallel plate ionization chamber at the depth of maximum in the water phantom, the absorbed dose to water at the reference depth (z_{ref}) in water, in an electron beam of quality Q and in the absence of the chamber, which can be calculated by using IAEA protocol from Technical Reports Series No.398 [8], is using by

$$D_{W,Q} = M_Q N_{D,W,Qo} k_{Q,Qo} \quad (3)$$

where M_Q is the reading of the dosimeter corrected for the influence quantities temperature and pressure, polarity effect, ion recombination and electrometer calibration by

$$M_Q = M \cdot k_{TP} \cdot k_{pol} \cdot k_s \cdot k_{elec} \quad (4)$$

where M is electrometer reading, k_{TP} is the factor to correct the effect of non reference temperature and pressure.

$$k_{TP} = \frac{(273.2 + T)}{(273.2 + T_0)} \frac{P_0}{P} \quad (5)$$

where P and T are the cavity air pressure (mmPb) and temperature (°C) at the time of measurements, P_0 and T_0 are the reference values (generally 1013 mmPb and 20°C) . k_{pol} is the correction factor for polarity effect.

$$k_{pol} = \frac{|M_+| + |M_-|}{2M} \quad (6)$$

where M_+ and M_- are the electrometer readings obtained at the positive and negative polarity, respectively. M is the electrometer reading recommended by the detector manual. k_s is the recombination correction factor which derived using the two voltages method. This method assumes a linear dependence of 1/M on 1/V and uses the measured values of the collected charges M_1 and M_2 at the polarizing voltages V_1 and V_2, respectively, measured with the same irradiation condition. V_1 is the normal operating voltage and V_2 a lower voltage; the ratio V_1/V_2 should ideally be equal to or larger than 3. The recombination correction factor k_s at the normal operating V_1 is obtained from

$$k_s = a_0 + a_1(M_1/M_2) + a_2 (M_1/M_2)^2 \quad (7)$$

where a_i is the constant. k_{elec} is the electrometer calibration factor. If the ionization and the electrometer are calibrated together, a value for k_{elec} is unity. When the ionization

chamber and the electrometer are calibrated separately, the calibration factor for each is given by the calibration laboratory.

N_{D,W,Q_o} is the calibration factor in terms of absorbed dose to water for the dosimeter at the reference quality Q_0 and k_{Q,Q_o} is a chamber specific factor which corrects for differences between the reference beam quality Q_0 and the actual beam quality Q. When the reference quality Q_0 is ^{60}Co, the factor k_{Q,Q_o} is denoted by k_Q. Calculated values for k_Q are given in table 18 of TRS 398. It is a function of beam quality R_{50} and a number of chamber types; values for non-tabulated qualities may be obtained by interpolation.

For a chamber calibrated at a series of electron beam qualities, the data from the calibration laboratory will ideally be presented as a single calibration factor N_{D,W,Q_o} determined in a reference electron beam of quality Q_0 and one or more measured factors k_{Q,Q_o} corresponding to the other calibration qualities Q.

However, if the calibration data are in the form of a set of calibration factors $N_{D,W,Q}$, then one of the calibration qualities should be chosen as the reference calibration quality Q_0. The corresponding calibration factor is denoted N_{D,W,Q_o} and the remaining calibration factors $N_{D,W,Q}$ are expressed as a series of factor k_{Q,Q_o} using the relation

$$k_{Q,Q_o} = \frac{N_{D,W,Q}}{N_{D,W,Q_o}} \qquad (8)$$

If the quality of the user beam Q does not match any of the calibration qualities, the values for k_{Q,Q_o} to be used in Eq.(3) can be obtained by interpolation.

Relative output factor (OF) [13]

For a given electron beam, output factor should be measured at z_{max} for the non-reference field sizes and SSDs used for the treatment of patients. Output factor may be determined as the absorbed dose at z_{max} for a given set of non-reference conditions relative to the absorbed dose at z_{ref} (z_{max}) under the appropriate reference conditions (FS. 10×10 cm^2, SSD 100 cm) that given by Eq.(9).

$$OF = \frac{M_Q^{nrc}(z_{max}) \cdot S^{nrc}_{w,air}}{M_Q^{rc}(z_{max}) \cdot S^{rc}_{w,air}} \qquad (9)$$

where M_Q is the dosimeter reading corrected for the influence qualities temperature and pressure, polarity effect, ion recombination and electrometer calibration, as shown in Eq.(4). $S_{w,air}$ is the stopping power ratio of water to air at the point of measurement, the values of $S_{w,air}$ are shown in table 20 of TRS 398 as a function of beam quality (R_{50}) and relative depth in water (z/R_{50}).

For detectors such as diodes, diamonds, etc., the output factor will be adequately approximated by the detector reading under the non-reference conditions relative to that under reference conditions. If an ionization chamber is used, the measured ratio of corrected ionization currents or charges should be corrected for the variation in $S_{w,air}$ with depth.

Film dosimetry

Film dosimetry has been used extensively as a convenient and rapid means of measuring dose distribution of therapeutic electron beams. Film is especially important for the dosimetry of scanning electron beams where automated dosimetry system using diode or ion chambers cannot be easily employed. Film also has the property of high spatial resolution and can provide a permanent record of dose distributions. [4, 14]

The film response is nonlinear with dose, therefore the data were converted to absorbed dose by the use of the optical density versus dose curve (sensitometric curve). For the linear portion can be used in relative dose measurement.

A commonly employed film in Radiotherapy department is the Kodak X-Omat V film, which has a dose range of about 0-100 cGy [15]. The x-ray film emulsion consists of microscopic grains of silver bromide (AgBr) dispersed in a gelatin layer on either one side or both sides of a supporting film. The AgBr content of the emulsion is typically 30%-40% by weight and the emulsion layer is 10-25 μm thick with a physical density of 2 g/cm. The measured density of the supporting film-emulsion layer combination is 1.39 g/cm^3 with a thickness of 0.2 mm [16].

CHAPTER II
OBJECTIVES

The main objectives:

To verify the accuracy of the dose computation for electron beam in the ADAC Pinnacle^3 radiotherapy treatment planning system version 7.6C. The electron dose calculation uses the Hogstrom pencil beam algorithm.

The sub-objectives:

1. To investigate the limitation of dose computation for electron beam in the ADAC Pinnacle^3 radiotherapy treatment planning system version 7.6C.
2. To be used as a guideline for evaluating the accuracy of other radiotherapy treatment planning system.
3. To be used as a guideline for evaluating the accuracy of other algorithms.

CHAPTER III
LITERATURE REVIEWS

The clinical radiation therapy process is complex and involves multiple steps. The process begins with patients' diagnosis and disease staging and culminating in the treatment of a specified target volume with predetermined radiation energies and beam parameters[7]. The accuracy of each step in a process has a direct impact on treatment outcome. One component of this process is computerized treatment planning dose calculations. Uncertainties or errors in this part of the therapy process could result in reduced cure or even serious complications.

Prior to their clinical implementation, it is important to carry out an evaluation of the accuracy of pencil-beam calculations in situations likely to be encountered clinically.

Anna Samuelsson et al. [17] investigated the accuracy of the recently implemented three-dimensional electron beam dose calculating algorithm in CADPLAN version 2.62 manufactured by Varian Dosetek. The algorithm used a generalized Gaussian pencil beam model and the dose distributions are calculated as the sum of three weighted Gaussians. To use the calculating program in an optimum way, one needs to know the dose calculation accuracy of the algorithm as well as its limitations. This investigation includes comparisons of measured relative dose distributions with calculated dose distributions and also comparisons of measured and calculated monitor units. The geometries tested were quadratic fields, irregularly shaped fields, oblique fields, irregularly shaped phantom surfaces and internal heterogeneities and were most often irradiated with 8 and 20 MeV electrons. The results indicate that the algorithm is well suited for clinical three-dimensional dose planning. Some deviations occurred but they were most often the limits of international criteria of acceptability.

Abel Cheng et al. [3] studied a three-dimensional electron beam dose calculation algorithm implemented on a commercial radiotherapy treatment planning

system. The calculation is based on the M.D. Anderson Hospital (M.D.A.H.) pencil beam model which uses the Fermi-Eyges theory of thick target multiple Coulomb scattering. To establish the calculation algorithm's accuracy as well as its limitations, it was systematically and extensively tested and evaluated against a set of benchmark measurements. The algorithm's ability to accurately simulate commonly used clinical setup geometries, including standard or extended SSDs, blocked fields, irregular surfaces, and heterogeneities, is demonstrated. Various levels of dose and spatial tolerances were used to validate the calculation quantitatively. Based on the ECWG data set, 77%, 90%, 96% and 98% of the calculated dose points agree with those of the measurements to within 2% or 2 mm, 3% or 3 mm, 4% or 4 mm, and 5% or 5 mm, respectively. The dose calculation algorithm is capable of modeling open fields at standard and extended SSDs, block fields, sloping or irregular surfaces, and high-or low-density heterogeneities. Disagreement between calculation and measurements, in most cases, are quite predictable and are associated with inherent algorithmic assumptions.

G.X. Ding et al. [18] evaluated a commercial three dimensional (3D) electron beam treatment planning system (CADPLAN version 2.7.9) using both experimentally measured and Monte Carlo calculated dose distributions to compare with those predicted by CADPLAN calculations. Tests were carried out at various field sizes and electron beam energies from 6 to 20 MeV. For a homogeneous water phantom the agreement between measured and CADPLAN calculated dose distributions is very good except at the phantom surface (< 4 mm) where CADPLAN significantly underestimates the doses. CADPLAN is able to predict hot and cold spots cause by a simple 3D inhomogeneity but unable to predict dose distributions for a more complex geometry where CADPLAN underestimates dose changes caused by inhomogeneity. For open electron cones, values of CADPLAN monitor unit calculations can be adjusted to match the measured values. The electron cut-out factors calculated by CADPLAN agree with measured values within 1%-2% in most cases except for very small electron cut-outs, such as 3×3 cm^2, where over 5% differences have been observed.

Renate Muller-Runkel and Sang-Hyun Cho [19] studied the results from beta testing of a commercially available three-dimensional electron pencil beam algorithm in CMS FOCUS. Straight on beams were evaluated at normal and extended distances, and obliquely incident beams at angle up to 40°. Shaped electron fields with small circular cutouts, and narrow elongated, centered and off centered, rectangular field shapes were investigated. Slab inhomogeneities were studied for lung and bone equivalent material, and isodose distributions for small inhomogeneities of these materials were compared with film and TLD measurements. All tests reported were performed with electrons of 6, 12 and 20 MeV from a Cl-1800 accelerator. The FOCUS 3D pencil beam algorithm is capable of representing open and moderately shaped fields for perpendicular beam incidence at normal and extended distances. It also accounts reasonably well for the change in beam penetration caused by wide inhomogeneities. Small circular cutouts use with medium and high energies require additional input data for small “cones” in order to achieve better accuracy. Similarly, accuracy for narrow elongated fields can be improved by defining psuedocones for commonly used rectangular field shapes. When a treatment plan calls for oblique beam incidence (important for chest wall irradiation), the clinician should be aware of the limitations the algorithm. Buildup dose or dose falloff inside small inhomogeneities like bone or air cavities may need verification by measurement for the individual case. With these caveats, general acceptance criteria for clinical electron beams, as formulated by Van Dyk et al., are well met by the FOCUS 3D electron pencil beam algorithm.

CHAPTER IV
MATERIALS AND METHODS

4.1 Materials

The materials used for the dose measurements consist of Varian Clinac 2100C linear accelerator, RFA-300 scanning system, Kodak X-OMAT V film, Vidar 12 plus scanner, Image J software, plane-parallel ionization chamber (Roos 34001), PTW UNIDOS electrometer , CIRS pelvis phantom, Philips CT simulation and Wellhofer 1D water phantom. For the dose calculation, the ADAC Pinnacle^3 treatment planning system version 7.6C of Radiotherapy and Oncology Division at Ramathibodi Hospital was used.

4.1.1 Linear accelerator

Varian Clinac 2100C linear accelerator was used for all tests as shown in figure 4.1. This accelerator was manufactured by Varian Oncology system, Palto Alto, U.S.A. It can generate electron beam with energies of normally 6, 9, 12, 16 and 20 MeV. In this investigation, the nominal energies 6, 9 and 12 MeV were used. The accelerator has a double scattering foils system to create broad uniform beam of electrons and employs cones to limit the therapeutic beam to five different square field sizes from 6×6 to 25×25 cm^2. For this study, five standard cone sizes of 4×4, 6×6, 10×10, 15×15 and 20×20 cm^2 were used. Each cone can accommodate custom-shaped inserts that are fabricated from a low melting point alloy (Lipowitz's metal, MPC-96), with cadmium free (52% bismuth, 30% lead, and 18% tin).

Figure 4.1 The Varian Clinac 21000C linear accelerator with an electron cone installed at Ramathibodi Hospital.

4.1.2 RFA-300 scanning system

Most of the relative measurements were performed with a diode in a water phantom. A p-type silicon diode detector in a RFA-300 radiation field analyzer from Scanditronix was used (see figure 4.2). It is high precision water phantom system and consists of a main control unit (MCU), a field and reference semiconductor detectors and a 3-D servo with a water phantom. The field detector allows fields measurements with spatial resolution due to the small size of the active semiconductor chip. The chip can be positioned near the phantom surface since it is very close (0.5 mm) to the front of the field detector. The active area of the detector is 2.5×2.5 mm^2.

The water phantom is fitted with a precision servo mechanism for full three-dimensional detector positioning. It also allows positioning of the field detector to measure both vertical and horizontal beams with scanning volume $495 \times 495 \times 495$ mm^3.

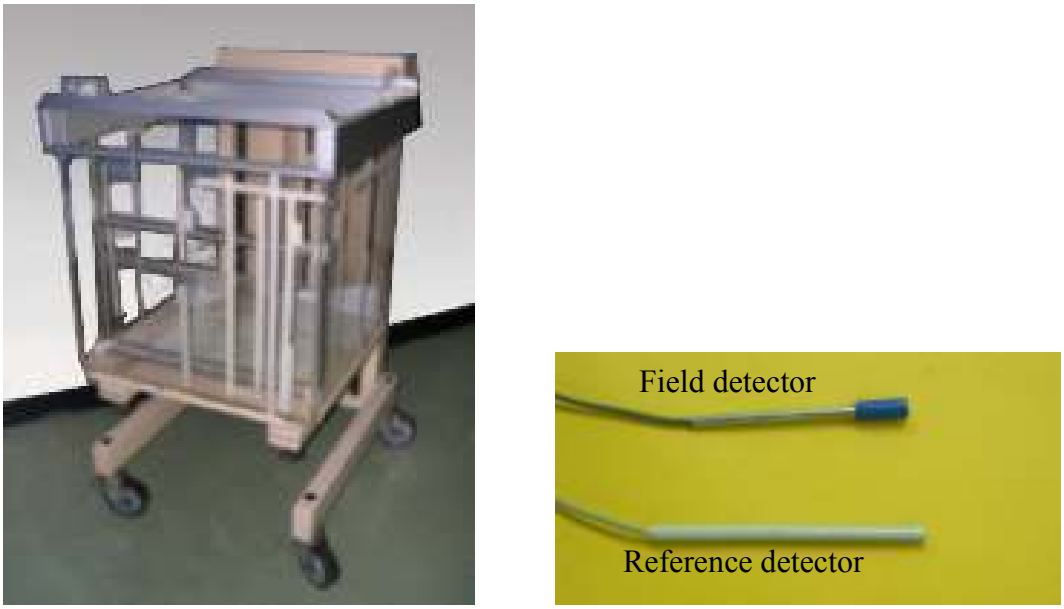

(a) (b)

Figure 4.2 The Scanditronix RFA-300 Radiation Field Analyzer: (a) 3D water phantom and (b) reference and field detectors.

4.1.3 Kodak X-Omat V film

X-Omat V film was used for the relative measurement made in BEV planes (see figure 4.3). It is a relatively low speed film designed for verifying the orientation and for approximating patient dosage in radiation therapy procedures. It features the ready-pack which eliminates the need for loading cardboard cassette.

Figure 4.3 The Kodak X-Omat V film

4.1.4 Film digitizer and Image J program software

Figure 4.5 show the Vidar film digitizer (VXR-12 plus, Vidar System Corporation, Herndon, VA, USA). Its 12 bit gray scale (496 shades of gray scale) imaging system can capture in any medical films including those with optical densities ranging from 0 to 3. Image J is a public domain image processing program which is used for processing and analyzing images (see figure 4.4). It is a public domain Java image processing program. It runs, either as an online applet or as a downloadable application, on any computer with a Java 1.1 or later virtual machine. It can display, edit, analyze, process, save and print 8-bit, 16-bit and 32-bit images in TIFF, GIF, JPEG, BMP, DICOM, FITS or "raw" formats. The Image J websites (http:// rsb.info.nih.gov/ij/) has instructions for use of the program and links to useful resources.

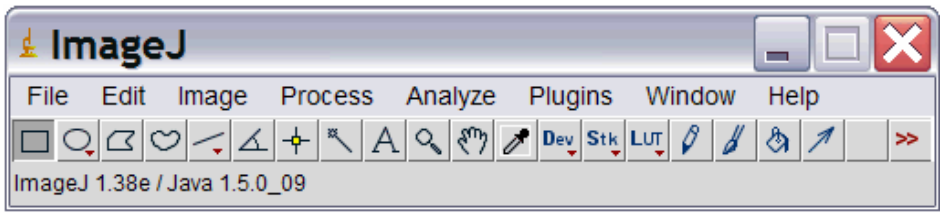

Figure 4.4 The Image J program software screen shot

Figure 4.5 The VXR – 12 plus film digitizer

4.1.5 Plane-parallel ionization chamber (Roos 34001)

The Roos ionization chamber type 34001 is a parallel plate chamber for use with therapy dosimeters for the measurement of electron radiation as shown in Fig 4.6. It can be implemented for the measurement of dose or dose rate using the measuring quantity the absorbed energy to water in a solid or water phantom in radiation therapy. It has a wide guard ring for eliminating field perturbations at low electron energies and in the build-up region of photon radiation. The energy dependence of the chamber is only given by the stopping power correction in a range of 2 MeV to 50 MeV. The direction of radiation is perpendicular to the entrance window. The chamber has sensitive volume of 0.35 cm^3 and the window thickness is 1 mm. The reference point of chamber is situated on the inner side of the entrance window, i.e. 1 mm behind the entrance plane. The chamber is waterproof for use in a water phantom.

Figure 4.6 The Roos chamber type 34001

4.1.6 PTW UNIDOS electrometer

The PTW UNIDOS is a high performance secondary standard and reference class dosimeter/ electrometer for universal use as shown in Fig 4.7. UNIDOS displays the measured values of dose and dose rate in Gy, Sv, R, Gy/min, Sv/h, R/min or Gy.m. The electrical values of charge and current are displayed in C and A. Polarization voltage and polarity adjustable from 0 V to ±400 V in 50 V increments.

Figure 4.7 The PTW UNIDOS electrometer

4.1.7 CIRS IMRT phantom pelvic 3-D Model 74-034

Figure 4.8 shows the CIRS Model 74-034 IMRT Pelvic phantom[21] . It is designed to address the complex issues surrounding commissioning and comparison of treatment planning systems and verification of individual patient plans and delivery. The CIRS 74-034 Phantom properly represents human pelvic anatomy in shape, proportion and structures as well as density. This enables thorough analysis of both the imaging and dosimetry system. The phantom is 20 × 30 cm in elliptical shape, approximates the size of and average patient, and has a tissue equivalent, three dimensional skeletons. Tissue equivalent interchangeable rod inserts for ionization chambers allow for point dose measurements in multiple planes in the phantom and film calibration. The phantom also supports film dosimetry with not only standard radiographic films but also Gafchromic® media. Optional inserts are available to support a variety of other detectors including TLD's, MOSFET and diodes. The Model 74-034 includes four different electron density reference plugs which can be interchanged in five separate locations within the phantom. The surface of the phantom is etched with groove to ensure proper orientation of the CT slices and accurate film to plan registration.

Figure 4.8 The CIRS Model 74-034 IMRT Pelvic Phantom

4.1.8 Wellhofer 1D water phantom (WP-manual water phantom)

Figure 4.9 shows one dimensional, stand-alone water phantom for absolute dose measurements according to TG-51 (lead filter option needed) and IAEA TRS-398 dosimetry protocols. The measurement depth can be manually adjusted with 0.1 mm steps and read out on the incremental encoder with integrated display.

Figure 4.9 Wellhofer 1D Water phantoms

4.1.9 Barometer and thermometer

Barometer and thermometer used to measure air pressure and water temperature while collecting measured data are shown in Fig 4.10. The pressure and temperature are essential for the correction factor ($k_{t,p}$) for relative output factor measurements.

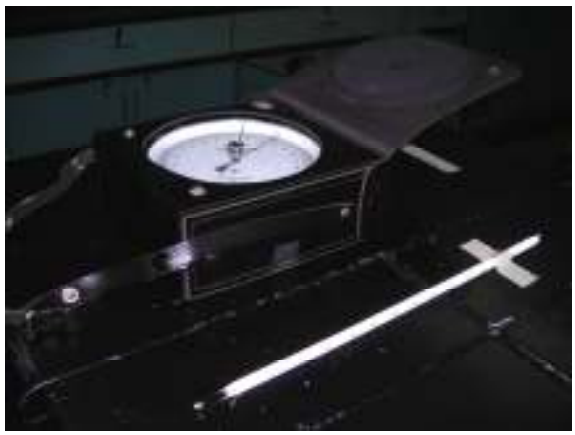

Figure 4.10 Barometer and thermometer

4.1.10 CT simulation

Figure 4.11 shows a Phillips CT machine; model Mx IDT 8000 with 16 slices. It was used as a patient imaging device with corresponding to tissue density. The quality of the images depends on the level and energy of x-rays delivered to the tissue. The CT imaging displays both high density tissue, such as bone, and low density such as lung and soft tissue. The image data can be transferred to the Pinnacle planning system by DICOM 3. A set of Gammex moveable lasers with three positions, one on the roof and two on the opposite walls for patient positioning and isocenter defining is available in the CT room.

Figure 4.11 The Phillips CT machine; model Mx IDT 8000 with 16 slices

4.1.11 ADAC Pinnacle treatment planning system

The Pinnacle^3 Radiotherapy Treatment Planning (RTP) system version 7.6 C (ADAC Laboratories, Milpitas, CA) was used for all dose computation (see figure 4.12). The electron dose calculation is done by using the Hogstrom pencil beam algorithm. This algorithm uses a combination of measured data and model parameters that characterize the electron beam physics. The Pinnacle^3 3DRTP system consists of a server, one work station and a physician review console. These are run by the Solaris 8 operating system on a UNIX work station and are networked together over the Local Area Network (LAN) for image acquisition. The CT image data then can be transferred from the CT workstation into the treatment planning. Tissue densities can be derived from CT numbers for pixel by pixel heterogeneities corrections.

Figure 4.12 Computerized treatment planning system: ADAC Pinnacle Radiation Therapy planning System version 7.6 C of Ramathibodi Hospital

4.2 Methods

The procedures were divided into three majors parts; measurement, calculation and comparison. The electron test consists of square fields, shaped fields, extended SSDs, oblique beam incidence and internal heterogeneities and irradiated with 6, 9 and 12 MeV electrons. The investigation includes comparisons of measured relative dose distribution with calculated dose distribution and also comparisons of measured and calculated relative output factor. The relative measurements were mainly presented as dose profiles and depth dose curves. All measured data used for the relative measurements were obtained in two ways: (1) diode detector in a water phantom or (2) X-Omat V film in the CIRS phantom. In order to check the accuracy of the monitor unit calculation, measurements were performed with a plane-parallel ionization chamber (Roos 34001) that placed in the 1D water phantom. Table 4.1 summarizes the experiments included in this work.

Table 4.1 Summary of the experiments included in this work

Tests		Phantom	Applicator cone (cm^2)	Insert / block (cm^2)	SSD (cm)	Detector	Measurement
1.	Square fields	water	4 × 4	-	100	RFA - 300	PDD / BP
			6 × 6				
			10 × 10				
			15 × 15				
			20 × 20				
2.	Shaped fields	water	10 × 10	∅ 5.2 cm	100	RFA – 300 / Roos chamber	PDD / BP / Output factor
				8.7×6.8			
				9.5×4.2			
			15 × 15	6.7×13.7			
				4.7×14.6			
3.	SSD dependence	water	4 × 4	-	105/110	RFA - 300	PDD / BP
			10 × 10				
			20 × 20				
			10 × 10		105/110	Roos chamber	Output factor
4.	Oblique beam incidence	water / G25°	15 × 15	-	105	RFA - 300	Output factor
5.	Small inhomogeneities	CIRS phantom	10 × 10	-	100	X O-mat V film	BP

4.2.1 Measurements of relative dose distribution and relative output factor

Test 1: Square fields

The purpose of the first experiment of any radiation dose calculation algorithm is its ability to predict (or at least reproduce) the measured dose distribution in a water phantom at the standard treatment distance[20] as shown in figure 4.13(a). The relative measurements were performed in a water phantom using p-type silicon diode detectors in conjunction with a Scanditronix RFA 300 scanning system. The beam was scanned along a major coordinate axis through the beam center, with the central axis of the field diode detector perpendicular to the beam. For percent depth

dose (PDD), scans started from beyond the practical range and proceeded, with small step 1 mm and large step 2 mm, went up to the water surface. Beam profiles were scanned at the depth of d_{max}, $d_{90\%}$, $d_{50\%}$, R_p with small step 1 mm and large step 2 mm and R_{p+2cm} with small step 0.1 mm and large step 0.5 mm for applicator cone raging from 4 × 4 cm^2 to 20 × 20 cm^2 and all energies. All beam profile measurement values were normalized to the d_{max} for each field size and depth.

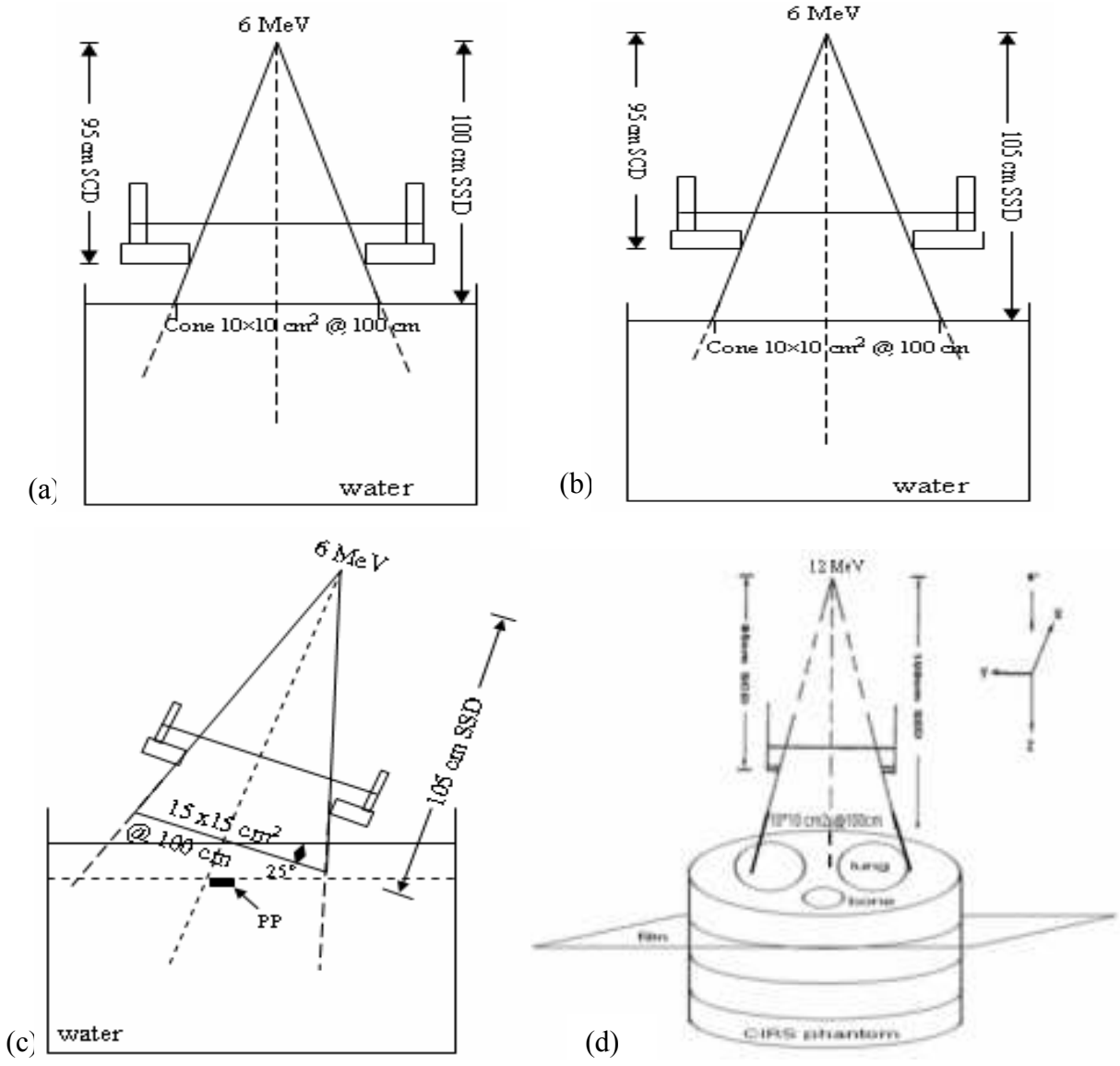

Fig 4.13 Schematic of irradiation geometry of water phantom (a) square fields at standard SSD (100 cm), (b) extended SSD 105 cm, (c) 25° oblique incidence for cone 15 × 15 cm^2 at the central-axis SSD of 105 cm of a 6 MeV beam into a water phantom and (d) internal heterogeneities tests.

Test 2: Shaped fields

The purpose of this experiment is to test the Pinnacle TPS prediction in the forward shift of maximum dose buildup and diminished beam penetration when substantial area of the open field is blocked. We studied the circular cutout with diameter 5.2 cm and rectangular cutouts of 8.7 × 6.8, 9.5 × 4.2, 4.7 × 14.6 and 6.7 × 13.7 cm^2 that are centered in the cone. The relative measurements were performed in a water phantom with a Scanditronix RFA 300 scanning system. Beam profiles were scanned at the maximum depth of electron energies 6, 9 and 12 MeV for each cutout combination. All beam profile measurement values were normalized to the d_{max} for each field size and depth

For relative output factor, measurements were performed with a plane-parallel ionization chamber (Roos 34001). The chamber was placed in the water phantom at the reference depth and perpendicular to central axis of beam. The measurements were related to a situation with field size 10 × 10 cm^2 and standard treatment distance (100 cm). Relative output factor were calculated according to the recommendation of TRS-398 as shown in Equation 9 (see Chapter I).

Test 3: Extended SSDs

One characteristic of the algorithm is its ability to predict dose distributions at extended treatment distances. The relative measurements were performed in a water phantom with a Scanditronix RFA 300 scanning system. Measurements were made in water phantom at 105 and 110 cm source to surface distance with applicator cone 4 × 4, 10 × 10 and 20 × 20 cm^2 as shown in figure 4.13(b). Beam profiles were scanned at the maximum depth of electron energies 6, 9 and 12 MeV with SSD and applicator cone combination. All beam profile measurement values were normalized to the d_{max} for each field size, SSD and depth.

For relative output factor, measurements were performed with a plane-parallel ionization chamber (Roos 34001). The chamber was placed in the water phantom at the reference depth of electron energies 6, 9 and 12 MeV, for field size 10 × 10 cm^2 at extended SSD 105 and 110 cm, respectively. The measurements were related to a situation with field size 10 × 10 cm^2 and standard treatment distance (100 cm).

Relative output factor was calculated according to the recommendation of TRS-398 as shown in Equation 9 (see Chapter I).

Test 4: Oblique incidence

This technique is often inevitable in electron treatments of the head and neck cancer. The experiment examined a 25° beam incidence on a plane phantom. A SSD of 105 cm, rather than the standard treatment SSD of 100 cm, was required to prevent the treatment applicator colliding with the phantom as shown in figure 4.13(c). In this experiment; we studied the accuracy of the Monitor Units calculation, measurements were performed with a plane-parallel ionization chamber (Roos 34001). The chamber was placed in the water phantom at the reference depth of electron energies 6, 9 and 12 MeV, for field size 15 × 15 cm^2. The measurements were related to a situation with perpendicular incidence, field size 10 × 10 cm^2 and standard treatment distance (100 cm). Relative output factor was calculated according to the recommendation of TRS-398 as shown in Equation 9 (see Chapter I).

Test 5: Computed Tomography based Inhomogeneity correction (small inhomogeneities)

The experiment was performed by using the XV film with the following steps:

A. Film calibration

Film calibration defines the relation between the net optical density and absorbed dose. The calibration curve is called sensitometric curve. The sensitometric curves of Kodak X-Omat V films were determined by irradiating known dose of electron beams in the perpendicular direction with the film. Each film was cut into six equal sections. This process was done in the dark room and each packet was sealed with black masking tapes to protect film from the light. The air bubbles were removed by using pinprick of the film at the corner then the air can be squeezed out. The film was placed in the CIRS phantom at the specified depth and perpendicular to the central axis of the beam and the known absorbed dose at each electron energy was given to each film. The radiation output was calibrated to be 1 cGy/MU for field size 10 × 10

cm^2 at d_{max} and SSD 100 cm. The dose given on the film was ranged from 10-60 cGy. Table 4.2 shows the MU setting for the exposing films in the experiments. The films were processed by an automatic film processor. The background (base plus fog) is the measurement of optical density of processed film, which has not been exposed to radiation. The background density has to be determined for every film batch. After the development of the film in an automatic process, the film was scanned with Vidar 12 plus scanner. The film scanner was operated with a pixel resolution of 0.42 mm or 60 DPI (dot per inch) and a depth of 8 bits. The Image J software was used to read the optical density to the pixel value. Then the sensitometric curves of 6, 9 and 12 MeV electron beams were constructed by the variation of the dose with the pixel values at each energy. After calibration, the film will be read in the term of the dose.

Table 4.2 The MU setting for exposing the films in calibration curve measurement for field size of 10 × 10 cm^2 at depth 2 cm for 6 MeV electron beams and depth 3 cm for 9 and 12 MeV electron beams.

Dose (cGy)	MU setting		
	d = 2 cm	d = 3 cm	
	6 MeV	9 MeV	12 MeV
10	12	12	10
20	23	23	20
30	35	34	30
40	46	45	40
50	58	57	50
60	69	68	60

B. Film measurement

For test geometries with heterogeneities inside the phantom, the measurements were performed in a CIRS pelvis phantom with a graphic film (Kodak X-Omat V film). The heterogeneity tests were performed with air cavity and hard bone substitute cavity. The phantom is a 20 cm × 30 cm in elliptical shape and 1 cm thick solid water slab with the cavity inside. The cavity has a diameter of 2.5 cm and 1 cm thick. The top of the cavity is recessed from the phantom surface by 1 cm as shown in

fig 4.14. The hard bone disk was inserted into the cavity. The electron density relative to water was 1.506 for the hard bone substitute[21]. The film was placed perpendicular to the beam between two plates at the specified depth (see table 4.3). Figure 4.13 (d) shows the schematic geometry for the internal inhomogeneity. Measurements were made at 100 cm SSD with field size 10 × 10 cm^2. For 6 MeV electrons beam, the measurement was performed only with air cavity. The film was irradiated to approximately 35 cGy. After the development of the film in an automatic process, the film was scanned by using Vidar - 12 plus scanner. The Image J software was used to read the optical density to the pixel value. The pixel values were converted to dose by using calibration curve.

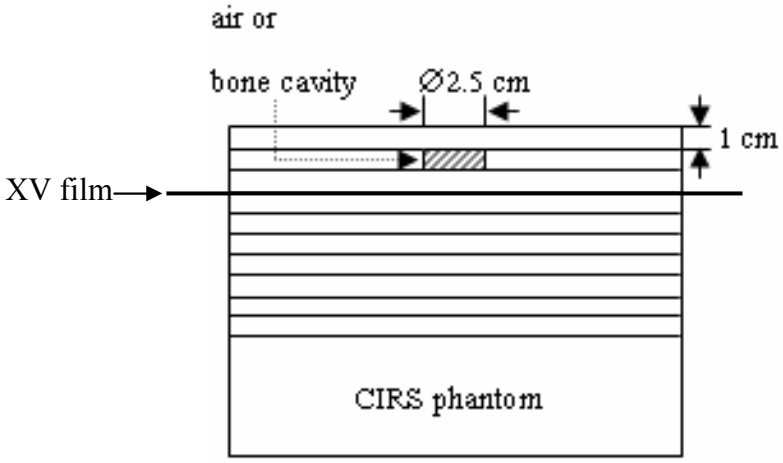

Fig 4.14 Schematic of geometry of an air and hard bone substitute cavity (1 cm thick by 2.5 cm diameter) within a CIRS pelvis phantom.

Table 4.3 The specified depths and MU setting of dose 35 cGy for beam profile measurement by using X-Omat V film in CIRS phantom.

Energy (MeV)	Depth (cm)	MU setting
6	2	41
9	3	40
12	3	35

4.2.2 Pinnacle TPS Calculations

A large water phantom was created in Pinnacle TPS and the dose distribution for different fields was computed. Dose calculations were performed on a 3D beam grid, or calculation grid. The pencil beam calculation grid is 0.2 cm for all experiments. The dose profiles were extracted from planar dose distribution with a 0.1 or 0.2 cm step between points regardless of the grid size of calculation, using the planar dose computation utility.

4.2.3 Comparisons

The measured data were evaluated by comparing to the calculated dose of the Pinnacle TPS. The difference between them was presented as the distance in cm between the curves if the dose gradient was larger than 30% per cm otherwise the difference was presented in percent of the normalization dose.

For the depth dose curves, the measured data were compared with the calculated dose of the TPS on a point by point and the average difference was used to compare with the criteria of acceptability. In the buildup region (from surface to depth of maximum dose), the difference was presented in percent relative dose while the dose value between 20% and 80% of the normalization dose was presented as the difference of the distance in mm[17].

The dose profile curves were normalized to 1 in the center of the field at each depth and were compared for different regions in the beam. Different tolerances for δ are proposed in this study, which can be defined as:

δ_1: the dose difference at central beam axis

δ_2: the distance difference between the 80% and the 20% dose

δ_3: the dose difference at the outside central beam axis and that point is about 2/3 of half of field size from the central beam axis

δ_4: the dose difference for data point off geometrical beam edges and that point has the dose below 7% of central ray normalization dose

$\delta_{50\text{-}90}$: the distance difference between the 90% and the 50% dose

RW_{50}: field width at the 50% dose

The results from the relative output factor were presented in percent difference. Van Dyk *et al.* provided guidelines for the evaluation of treatment planning system. The cited percentages are defined relative to the central ray normalization dose. They have presented a detailed description of the limits of acceptance for electron beam dose calculations as shown in Table 1.1.

Table 1.1 Criteria of acceptability for electron beam dose calculation (from Chapter I)

Descriptor	δs	Criterion
A. Homogeneous calculation (no shields)		
1.Central ray data (except in build up region)	δ_1	2%
2.High dose region – low dose gradient	δ_3	4%
3.Large dose gradient(> 30% / cm)	δ_2 , $\delta_{50\text{-}90}$	4 mm
4.Small dose gradients in low dose region (i.e.< 7% of normalization dose)	δ_4	4%
B. Inhomogeneity corrections		
1. Central ray (slab geometry, in regions of electron equilibrium)	δ_1	5%
C. Composition uncertainty,anthromorphic phantom		
Contour correction,		
Inhomogeneities,		
Shields		
Irregular fields		
Off axis		
1. High dose region – low dose gradient	δ_3	7%
2. Large dose gradient(> 30% / cm)	δ_2 , $\delta_{50\text{-}90}$	5 mm
3. Small dose gradients in low dose region (i.e.< 7% of central ray dose)	δ_4	5%

Note: Percentages are quoted as a % of the central ray normalization dose

CHAPTER V
RESULTS AND DISCUSSIONS

5.1 Relative dose distributions

Some results have been selected for graphical representation in this work. All dose profiles and depth dose curves were presented in diagrams. When analyzing the results, the deviations in the diagrams were measured and compared with the criteria of the acceptability recommended by Van dyk *et al*[8].

A. Square fields

The most fundamental test of any radiation dose calculation algorithm is its ability to predict the measured dose distribution in a water phantom at the standard treatment distance (100 cm SSD) with no additional cerrobend insert or blocking. The comparisons of diode-measured and Pinnacle-calculated central axis percent depth dose are shown in figures 5.1 to 5.3 (a-e) for 6, 9, 12 MeV with 4 × 4, 6 × 6, 10 × 10, 15 × 15, and 20 × 20 cm^2 standard cone sizes. The overall agreement was within 4% or 0.4 cm, except the buildup region of electron energy 6 MeV. The deviations were found in standard cone 6 × 6 cm^2 and 15 × 15 cm^2 and were about 4.2% and 5.59%, respectively. At the rapid dose fall-off region, the Pinnacle TPS had the reduction of dose faster than the measurement for all applicator cones and energies. The maximum shift toward the surface of the Pinnacle TPS calculation is about 0.325 cm for 9 MeV electron beam with 4 × 4 cm^2 applicator size as shown in Table 5.1. Table 5.1 shows the average of % dose difference and distance difference at buildup region and fall-off region between diode measurements and Pinnacle calculations of Percent Depth Dose (PDD) for standard cone 4 × 4, 6 × 6, 10 × 10, 15 × 15 and 20 × 20 cm^2 at standard SSD 100 cm.

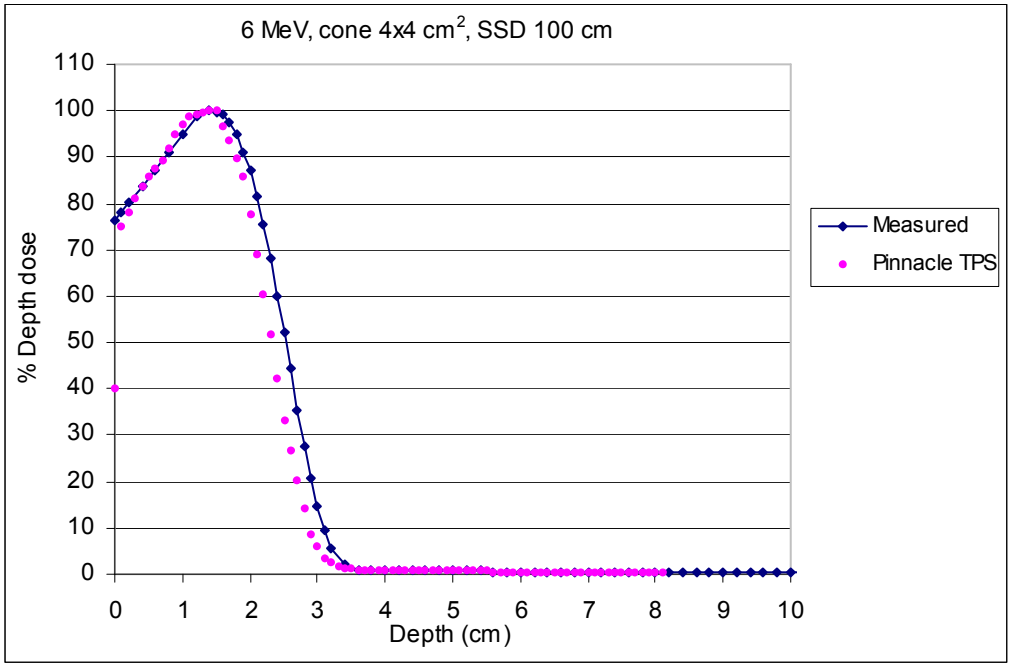
6 MeV, cone 4x4 cm2, SSD 100 cm
% Depth dose
Depth (cm)
Measured
Pinnacle TPS

(a)

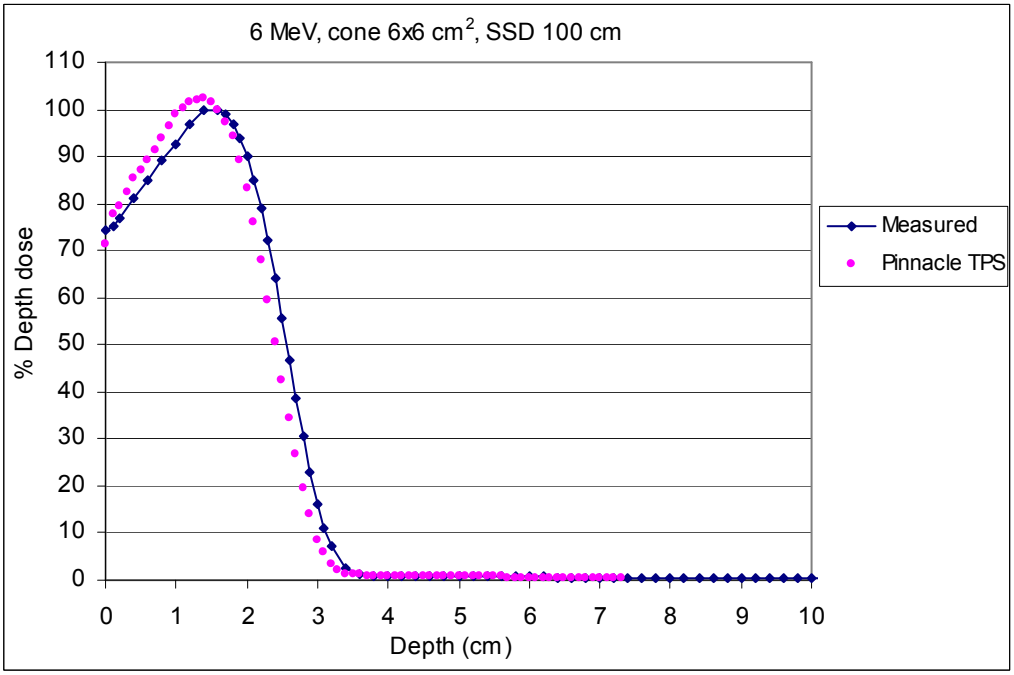
6 MeV, cone 6x6 cm2, SSD 100 cm
% Depth dose
Depth (cm)
Measured
Pinnacle TPS

(b)

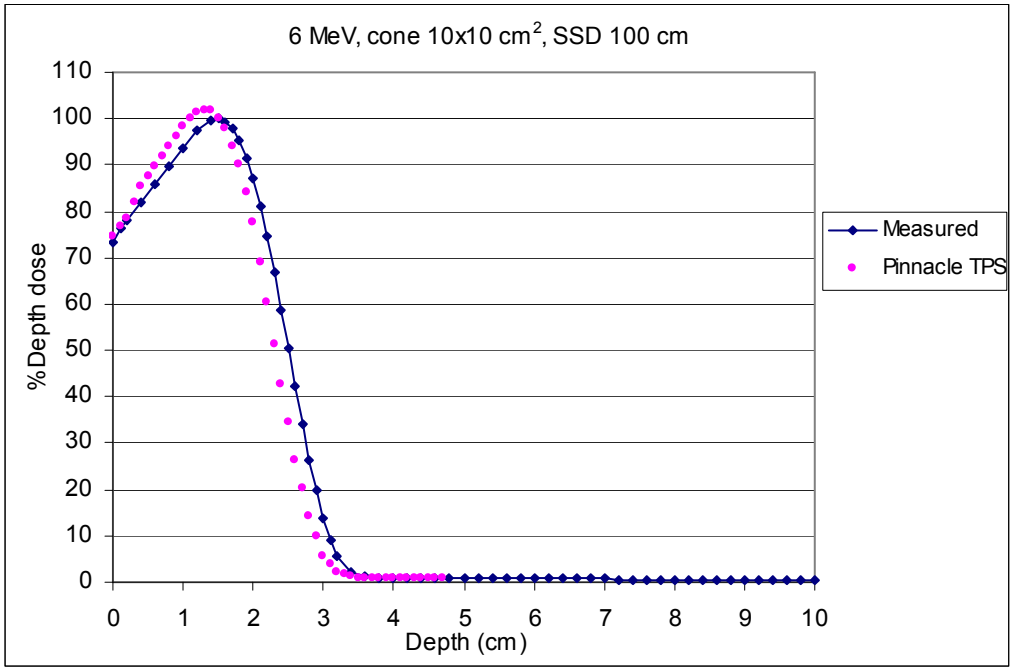
6 MeV, cone 10x10 cm2, SSD 100 cm
%Depth dose
Depth (cm)
Measured
Pinnacle TPS

(c)

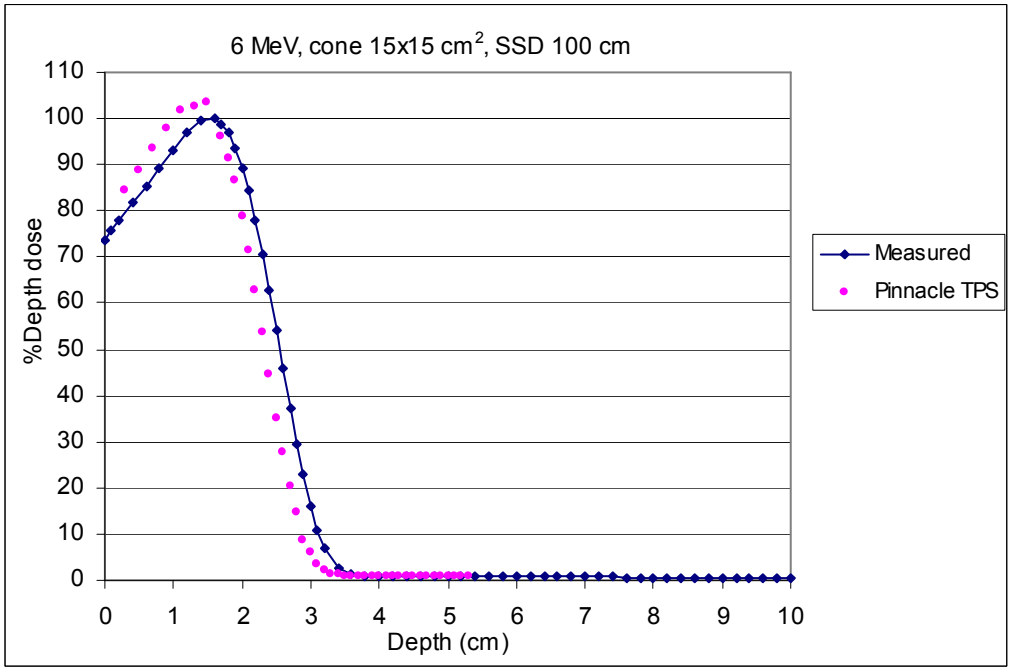
6 MeV, cone 15x15 cm2, SSD 100 cm
%Depth dose
Depth (cm)
Measured
Pinnacle TPS

(d)

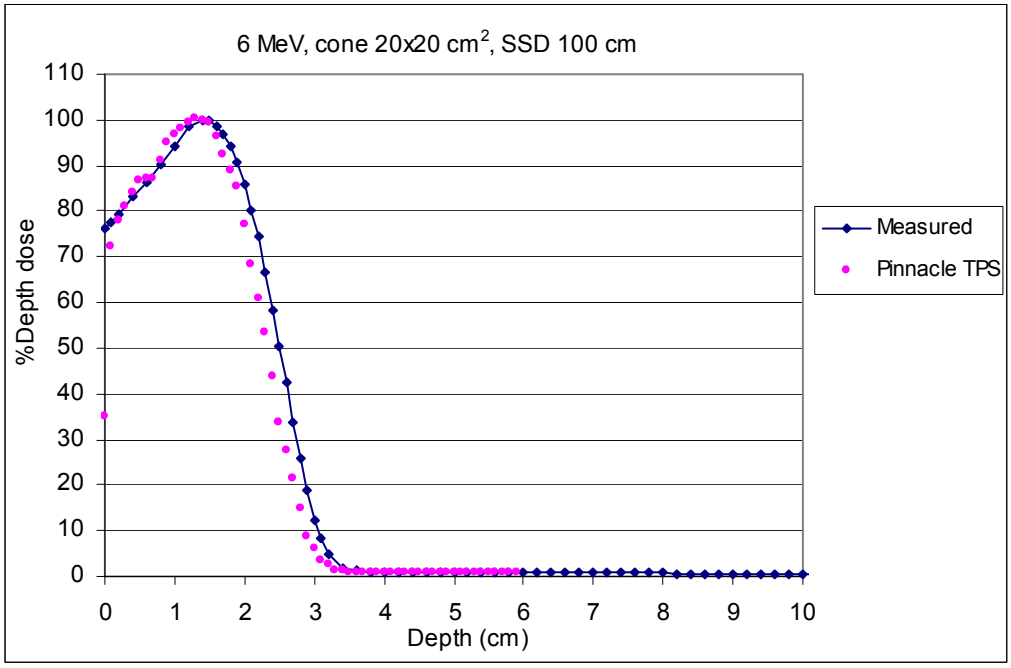

(e)

Figures 5.1 The comparison of percent depth dose for 6 MeV electron beams of Pinnacle calculation and diode measurement for standard cone (a) 4 × 4, (b) 6 × 6, (c) 10 × 10, (d) 15 × 15 and (e) 20 × 20 cm^2.

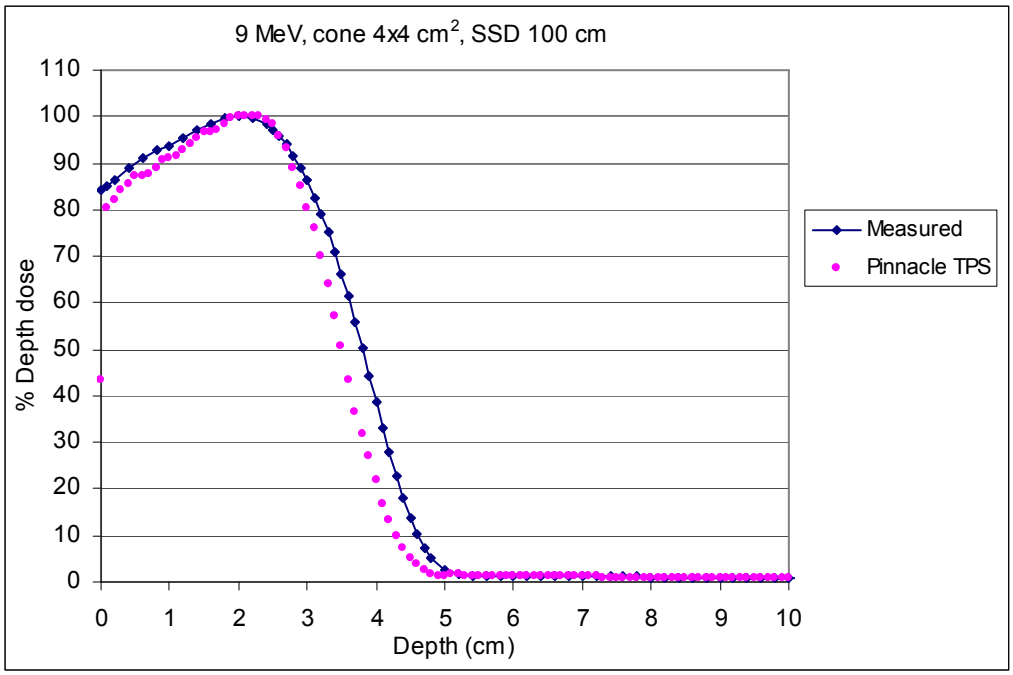
9 MeV, cone 4x4 cm2, SSD 100 cm
% Depth dose
Depth (cm)
Measured
Pinnacle TPS

(a)

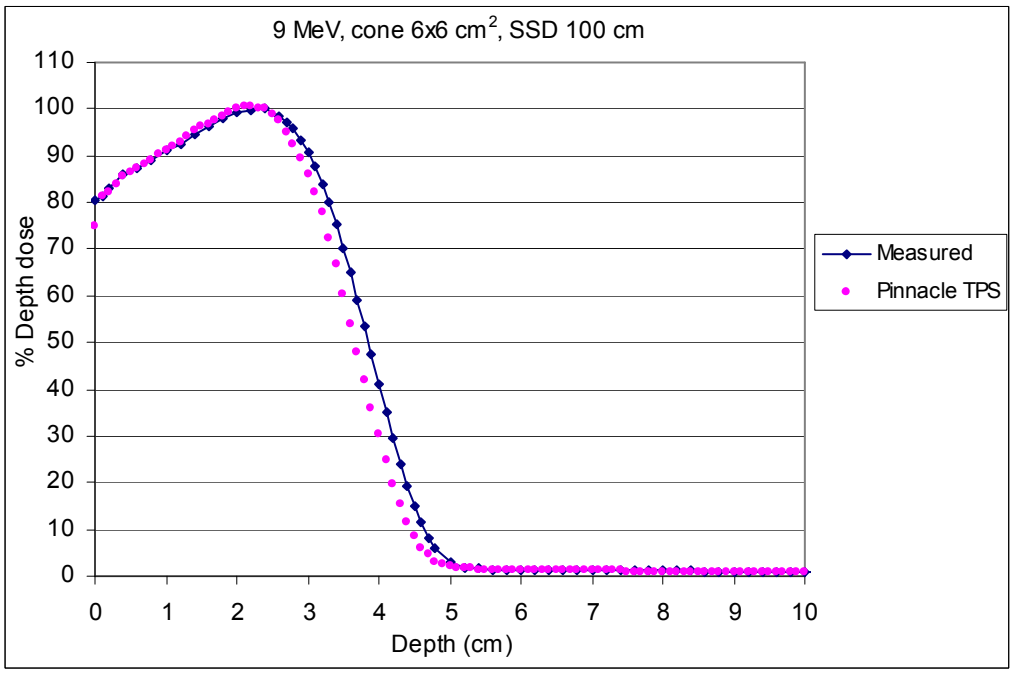
9 MeV, cone 6x6 cm2, SSD 100 cm
% Depth dose
Depth (cm)
Measured
Pinnacle TPS

(b)

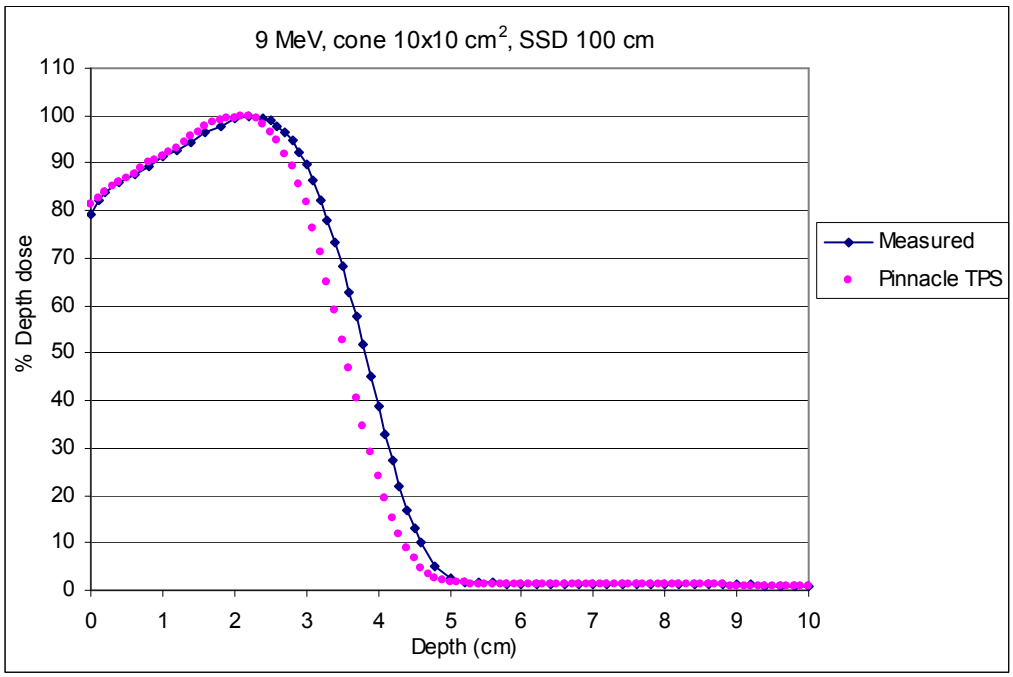
9 MeV, cone 10x10 cm2, SSD 100 cm
% Depth dose
Depth (cm)
Measured
Pinnacle TPS

(c)

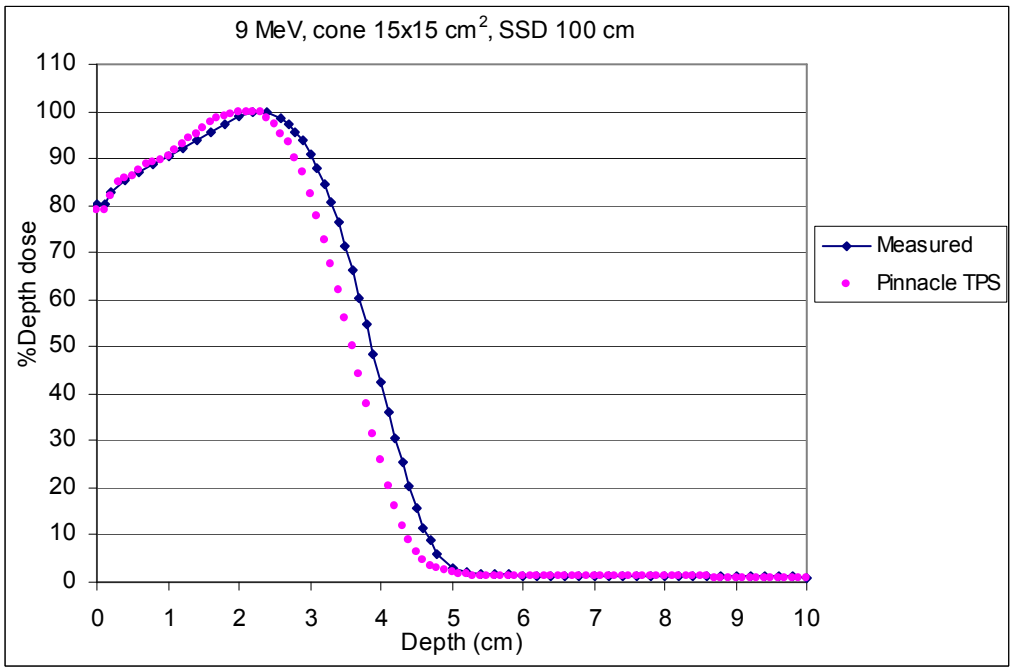
9 MeV, cone 15x15 cm2, SSD 100 cm
%Depth dose
Depth (cm)
Measured
Pinnacle TPS

(d)

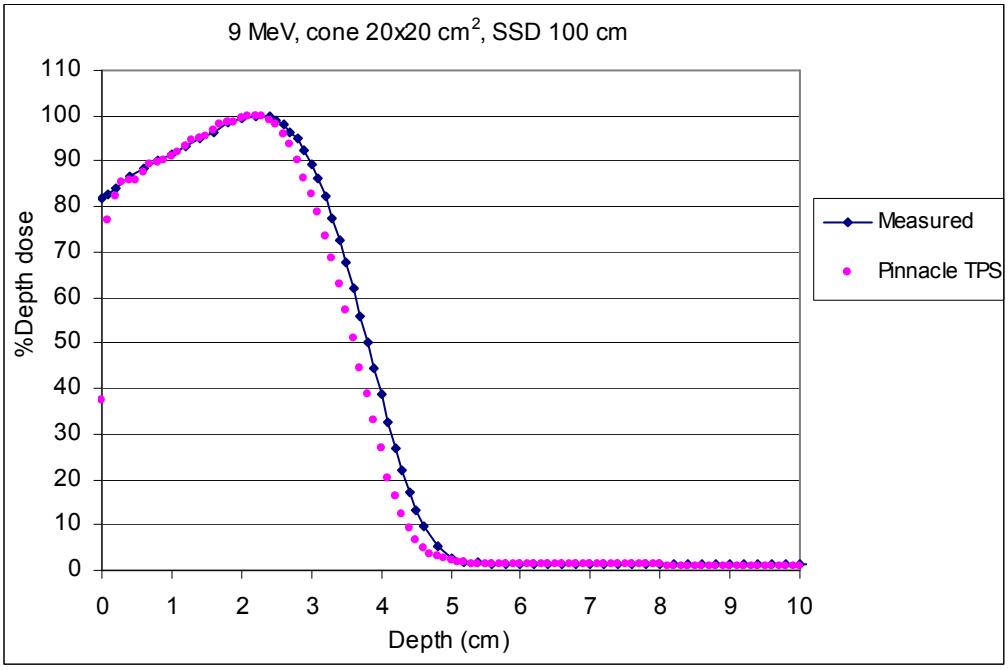

(e)

Figures 5.2 The comparison of percent depth dose for 9 MeV electron beams of Pinnacle calculation and diode measurement for standard cone (a) 4 × 4, (b) 6 × 6, (c) 10 × 10, (d) 15 × 15 and (e) 20 × 20 cm^2.

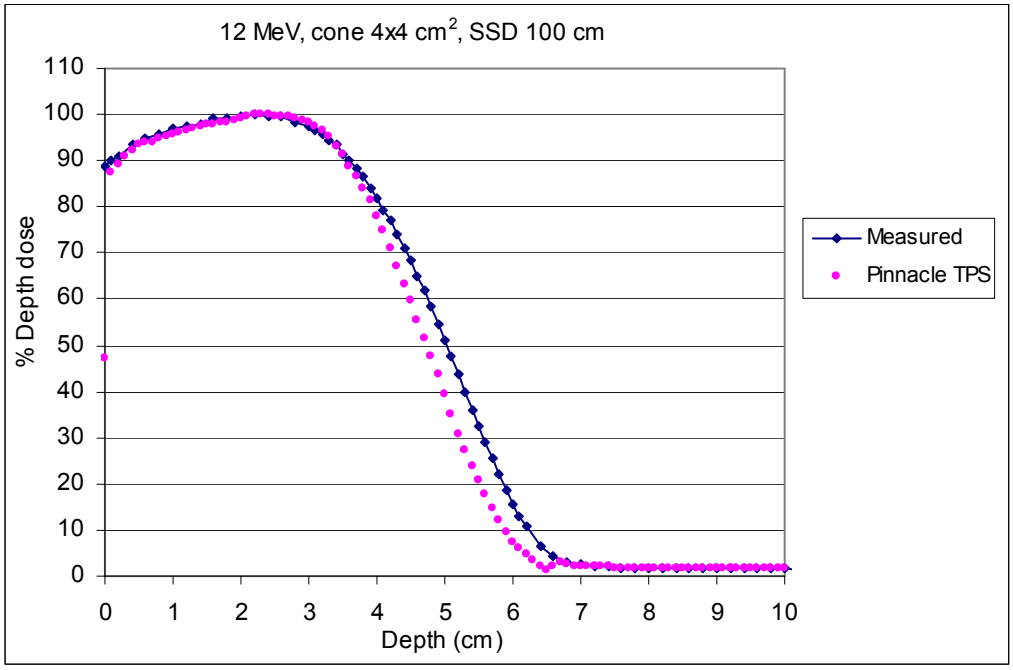
12 MeV, cone 4x4 cm2, SSD 100 cm
% Depth dose
Depth (cm)
Measured
Pinnacle TPS

(a)

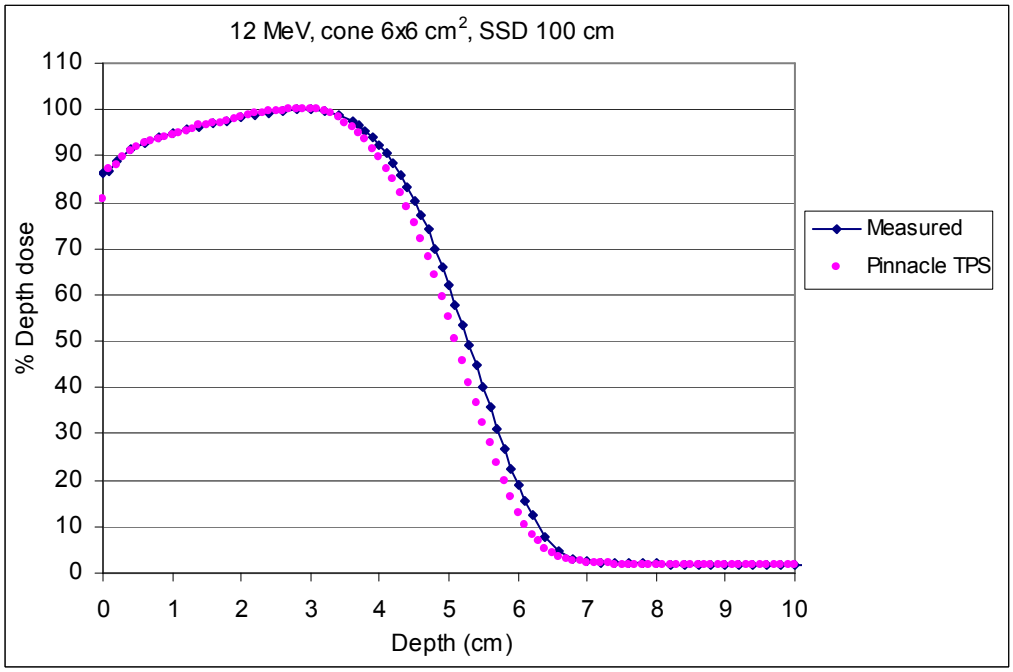
12 MeV, cone 6x6 cm2, SSD 100 cm
% Depth dose
Depth (cm)
Measured
Pinnacle TPS

(b)

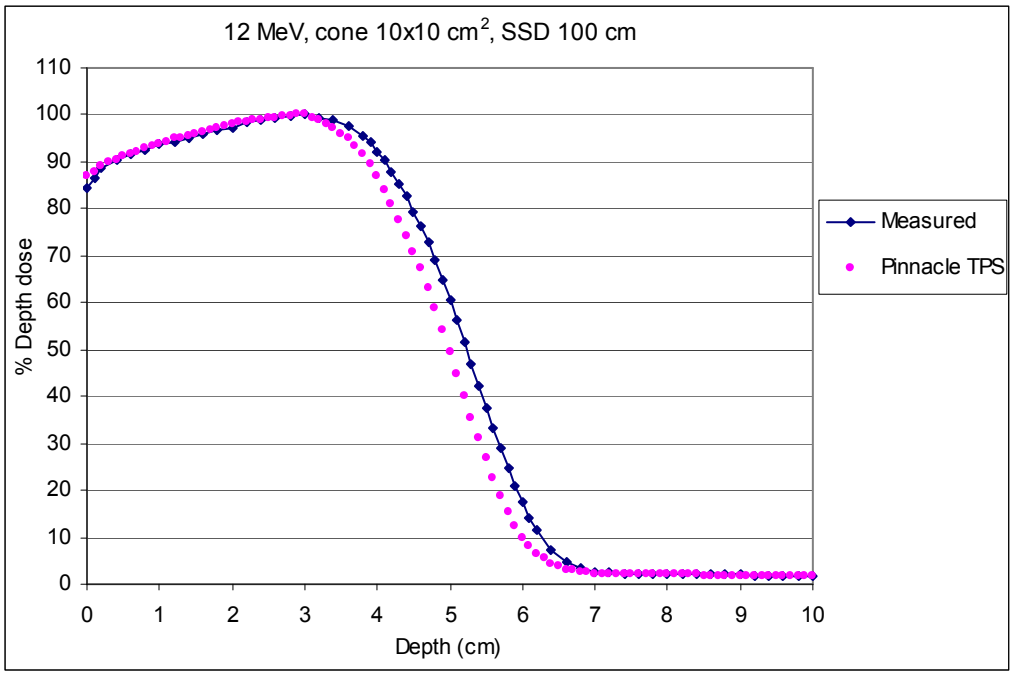
12 MeV, cone 10x10 cm2, SSD 100 cm
% Depth dose
Depth (cm)
Measured
Pinnacle TPS

(c)

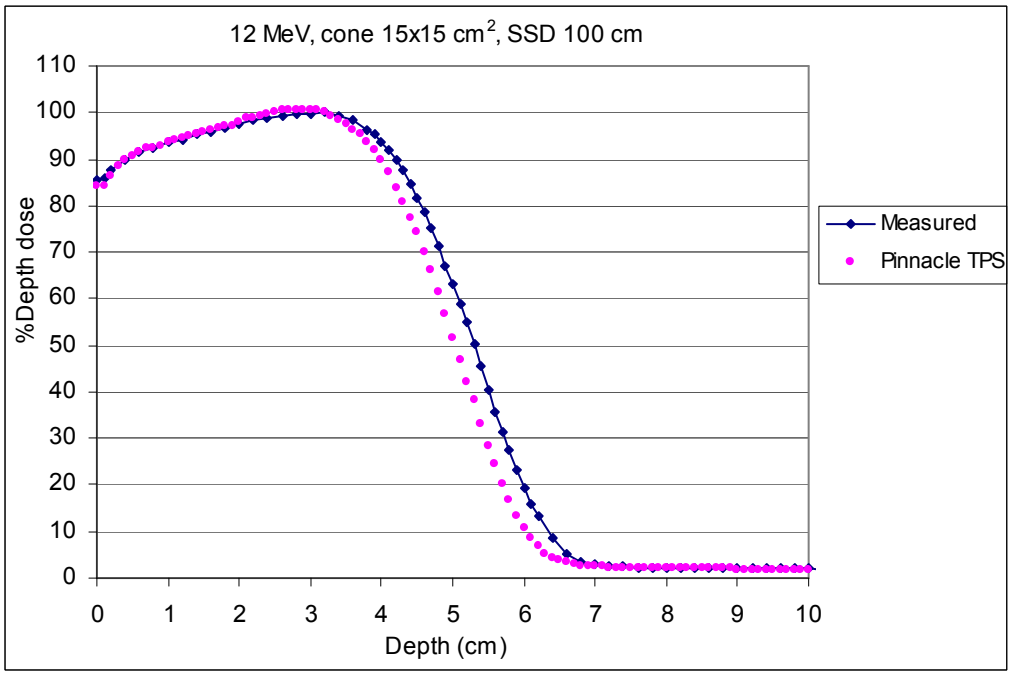
12 MeV, cone 15x15 cm2, SSD 100 cm
%Depth dose
Depth (cm)
Measured
Pinnacle TPS

(d)

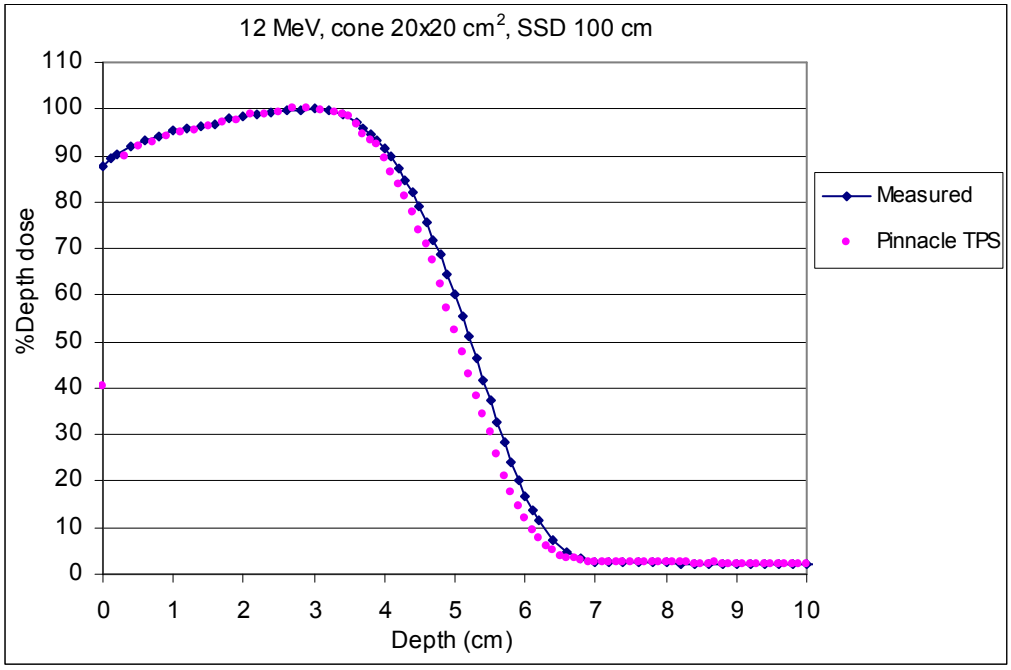

(e)

Figures 5.3 The comparison of percent depth dose for 12 MeV electron beams of Pinnacle calculation and diode measurement for standard cone (a) 4 × 4, (b) 6 × 6, (c) 10 × 10, (d) 15 × 15 and (e) 20 × 20 cm^2.

Table 5.1 Average % dose difference and distance difference of buildup region and fall-off region between diode-measurements and Pinnacle calculations of Percent Depth Dose (PDD) for standard cone 4 × 4, 6 × 6, 10 × 10, 15 × 15 and 20 × 20 cm^2 at standard SSD treatment.

Region	Cone (cm^2)	**% dose difference**		
		6 MeV	**9 MeV**	**12 MeV**
Buildup region	4 × 4	0.145 %	-2.868%	-0.9295%
	6 × 6	4. 2%	0.241%	-0.165%
	10 × 10	3.14%	-0.486%	0.296%
	15 × 15	5. 59%	0.76%	0.072%
	20 × 20	-0.308%	-0.977%	-0.895%
Region	Cone (cm^2)	**Distance to agreement (cm)**		
		6 MeV	**9 MeV**	**12 MeV**
Fall-off region	4 × 4	- 0.230	-0.325	-0.274
	6 × 6	-0.150	-0.178	-0.164
	10 × 10	-0.184	-0.260	-0.252
	15 × 15	-0.209	-0.275	-0.253
	20 × 20	-0.170	-0.194	-0.156

Figures 5.4 to 5.12 show the comparison between dose profiles calculated with Pinnacle TPS and diode-measured at depth of d_{max}, $d_{90\%}$, $d_{50\%}$, Rp and Rp+2 cm for standard cone 6 × 6, 10 × 10 and 15 × 15 cm^2 of 6, 9 and 12 MeV electron beams. The difference of dose profiles at d_{max} and $d_{90\%}$ shows good agreement. For the dose profiles at $d_{50\%}$ and Rp, the deviation was found near the field edges and penumbra width because the modeling of dose profiles were compromised between the depths of 90%, 70%, 50% and the shallow depth was paid more attention than the deeper depth. Table 5.2-5.4 show the difference between Pinnacle calculation and diode-measurement for standard cone 6 × 6, 10 × 10 and 15 × 15 cm^2 at the depths of d_{max}, $d_{90\%}$ $d_{50\%}$, Rp and Rp + 2 cm and irradiated with electron energy 6, 9 and 12 MeV electron beams. The penumbra width of Pinnacle calculation was overestimated than the diode measurement because in the Pinnacle implementation of the algorithm,

Water Scatter Correction Factor (FMCS) is selected for each energy with ignoring depth and cone size. As a result, it increases electron scatter at shallow depth, such as $d_{90\%,}$ which improves upstream penumbra agreement but it overestimates the scatter at the deeper depth [3]. For the outside beam region of dose profiles at R_{p+2cm}, the measured dose is higher than the calculation due to the higher response of the diode detector to low energy of electron beams.

The deviation at the outside beam edges (< 7% of norm. dose) of electron energy 9 MeV was larger than 4%, except the dose profiles at $d_{90\%}$ (see figures 5.5 (a-e)). Disagreements between calculations and measurements are associated with inherent algorithmic modeling. This error could be seen through most of the geometry in the test.

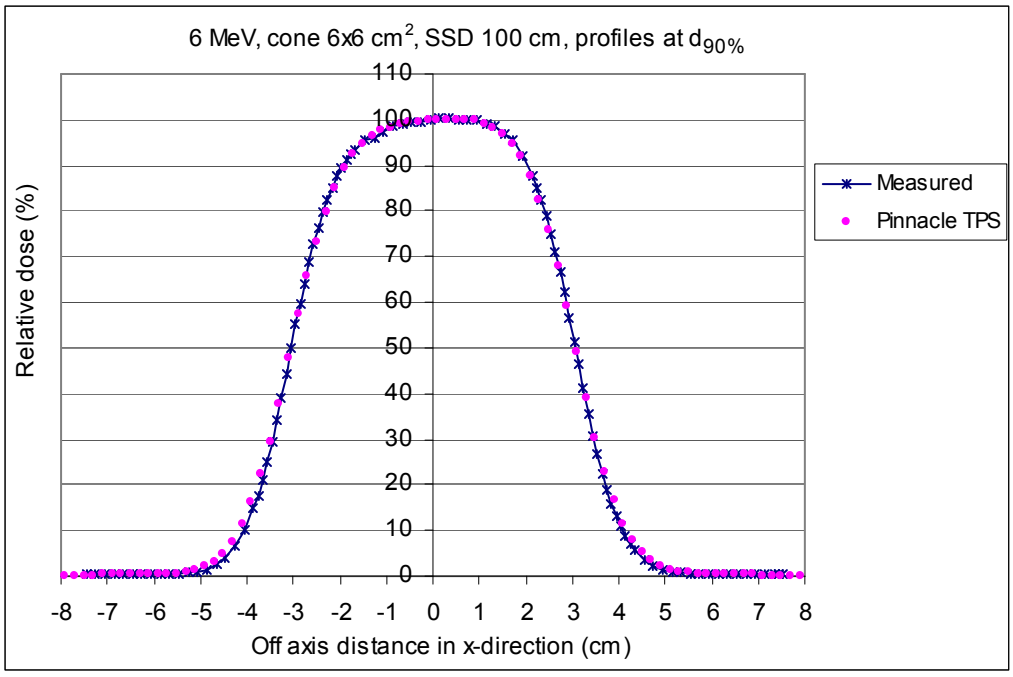

(a)

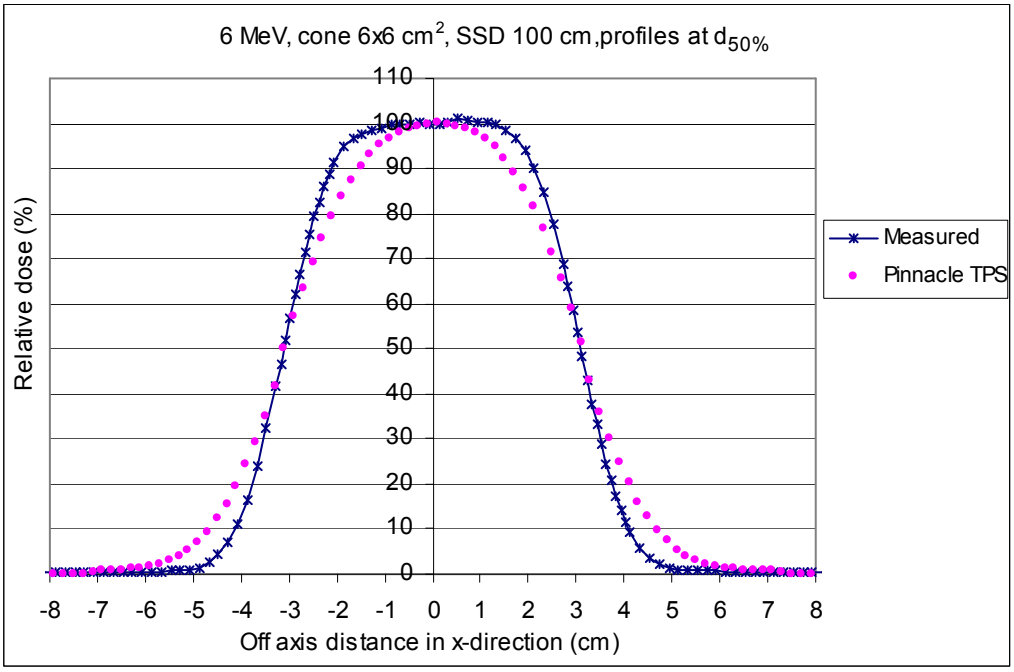

(b)

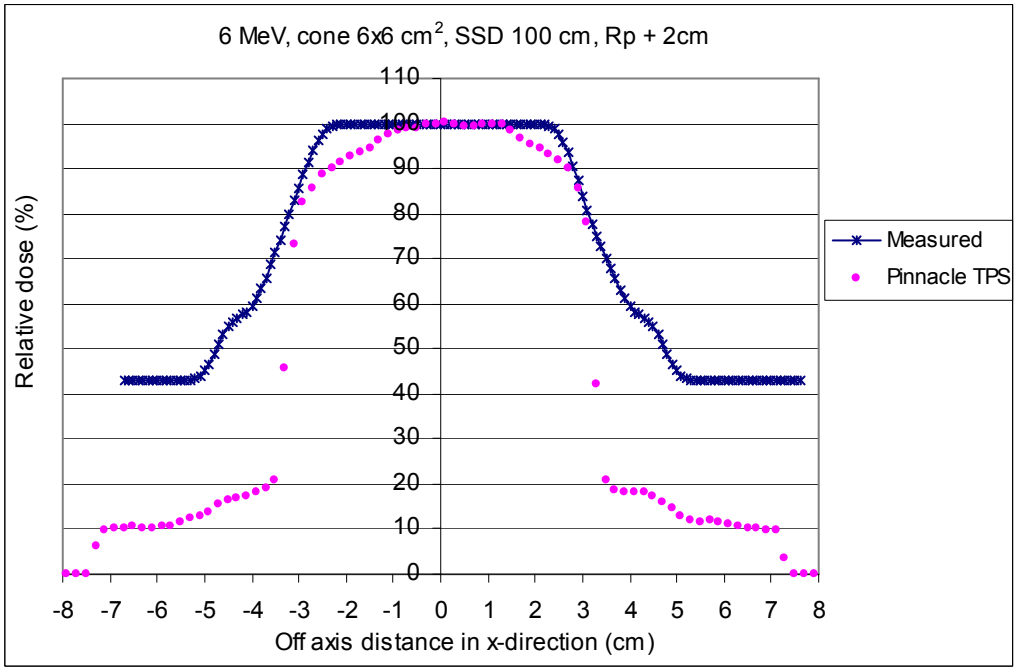

(c)

Figure 5.4 The comparison of relative dose profiles between Pinnacle TPS and diode measurement is shown for electron energy 6 MeV, SSD 100 cm and field size 6 × 6 cm^2 at (a) depth of dose 90%, (b) depth of dose 50%, and (c) depth R_P + 2 cm.

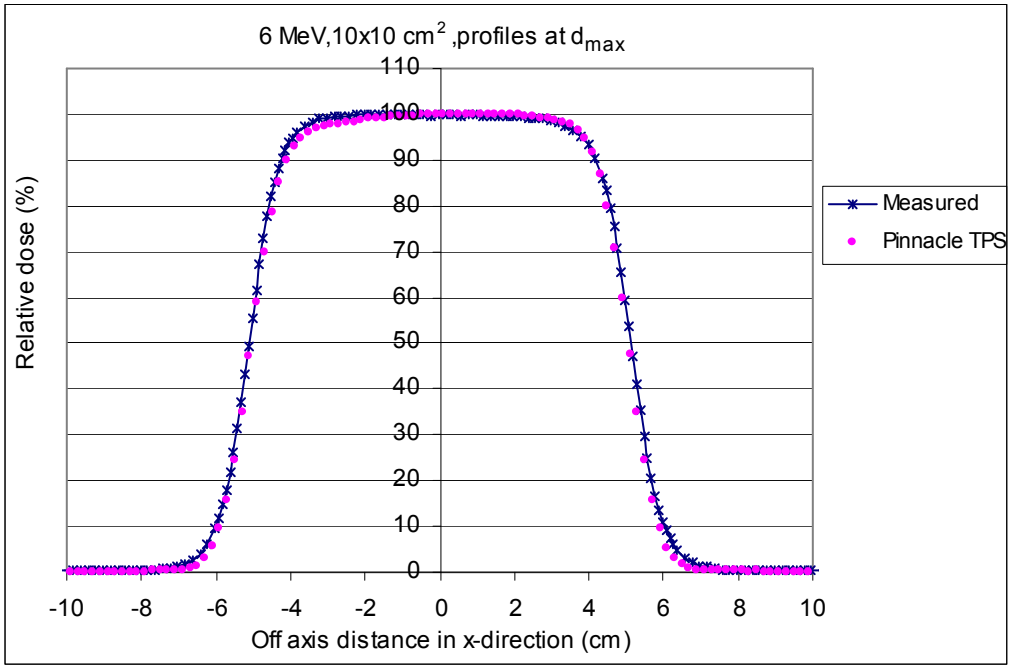
6 MeV,10x10 cm2 ,profiles at dmax
Relative dose (%)
110
100
90
80
70
60
50
40
30
20
10
0
-10 -8 -6 -4 -2 0 2 4 6 8 10
Off axis distance in x-direction (cm)
Measured
Pinnacle TPS

(a)

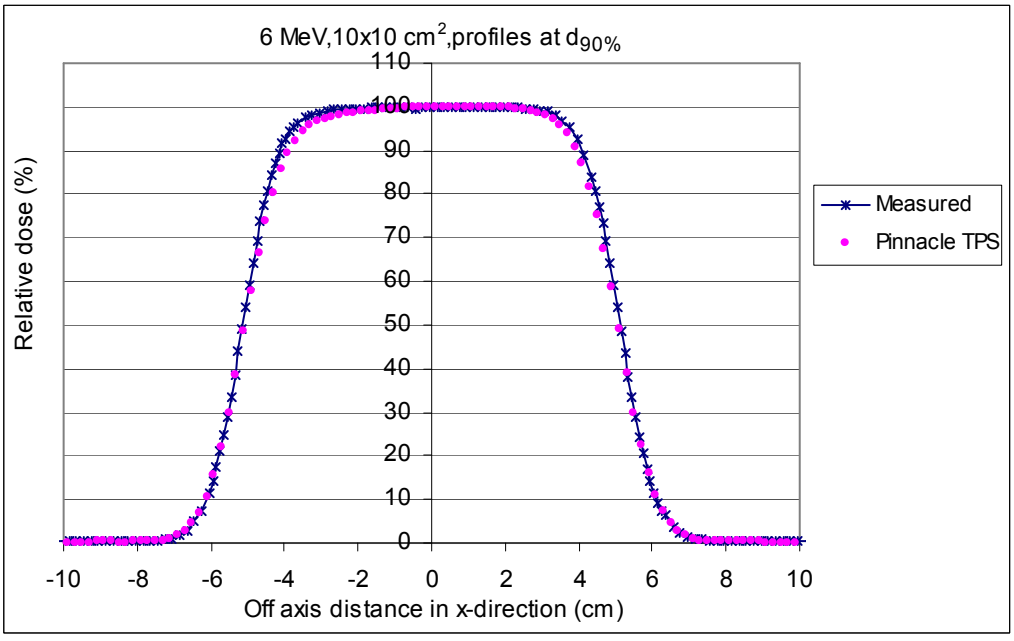
6 MeV,10x10 cm2,profiles at d90%
Relative dose (%)
110
100
90
80
70
60
50
40
30
20
10
0
-10 -8 -6 -4 -2 0 2 4 6 8 10
Off axis distance in x-direction (cm)
Measured
Pinnacle TPS

(b)

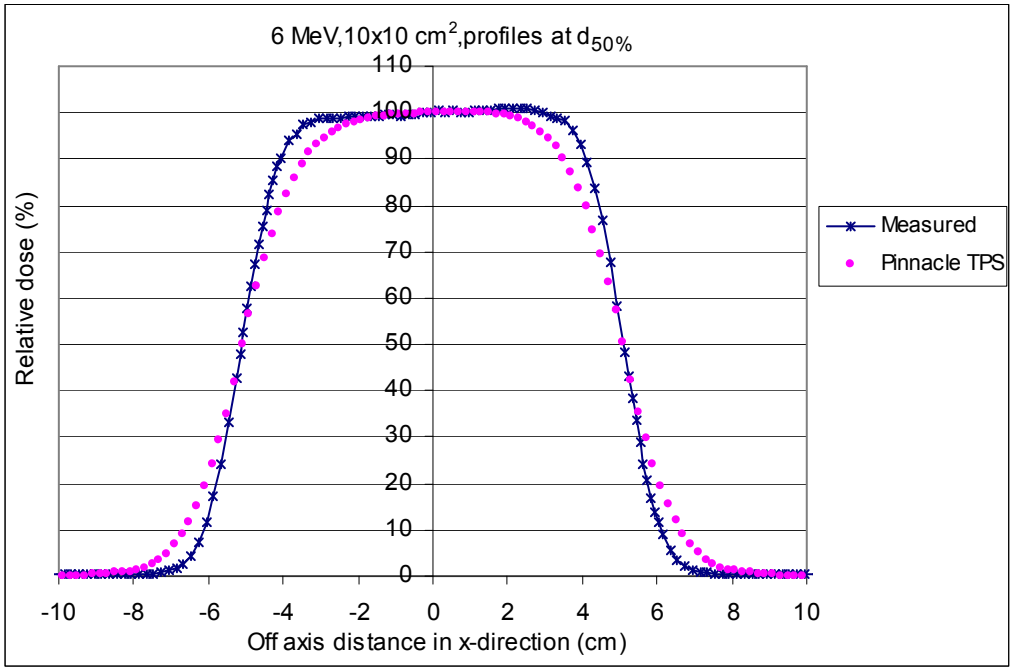
6 MeV,10x10 cm2,profiles at d50%
Relative dose (%)
110
100
90
80
70
60
50
40
30
20
10
0
-10
-8
-6
-4
-2
0
2
4
6
8
10
Off axis distance in x-direction (cm)
Measured
Pinnacle TPS

(c)

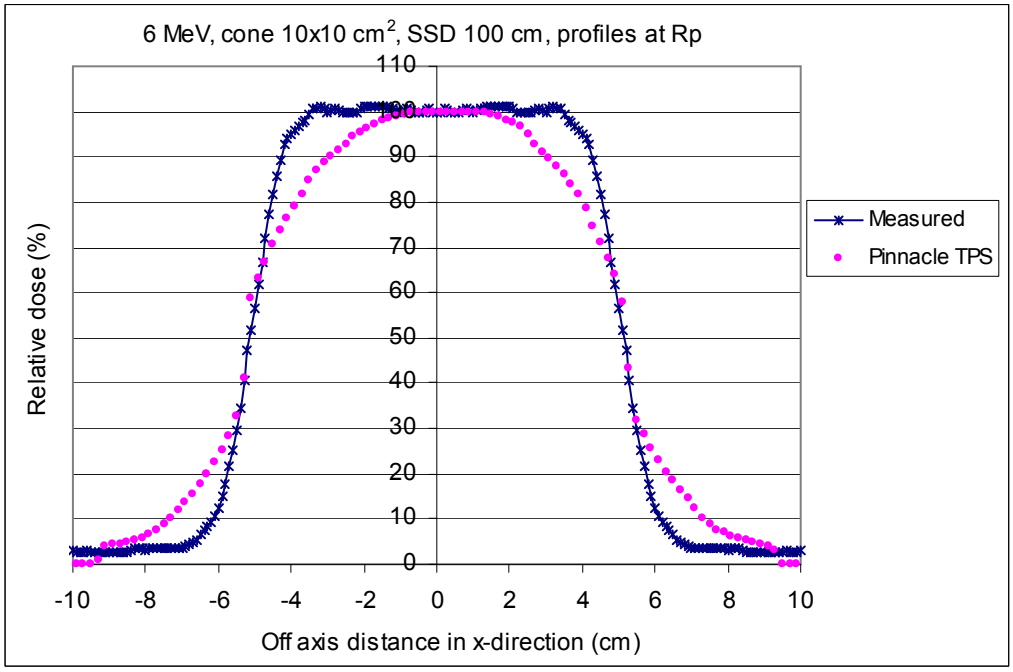
6 MeV, cone 10x10 cm2, SSD 100 cm, profiles at Rp
Relative dose (%)
110
100
90
80
70
60
50
40
30
20
10
0
-10
-8
-6
-4
-2
0
2
4
6
8
10
Off axis distance in x-direction (cm)
Measured
Pinnacle TPS

(d)

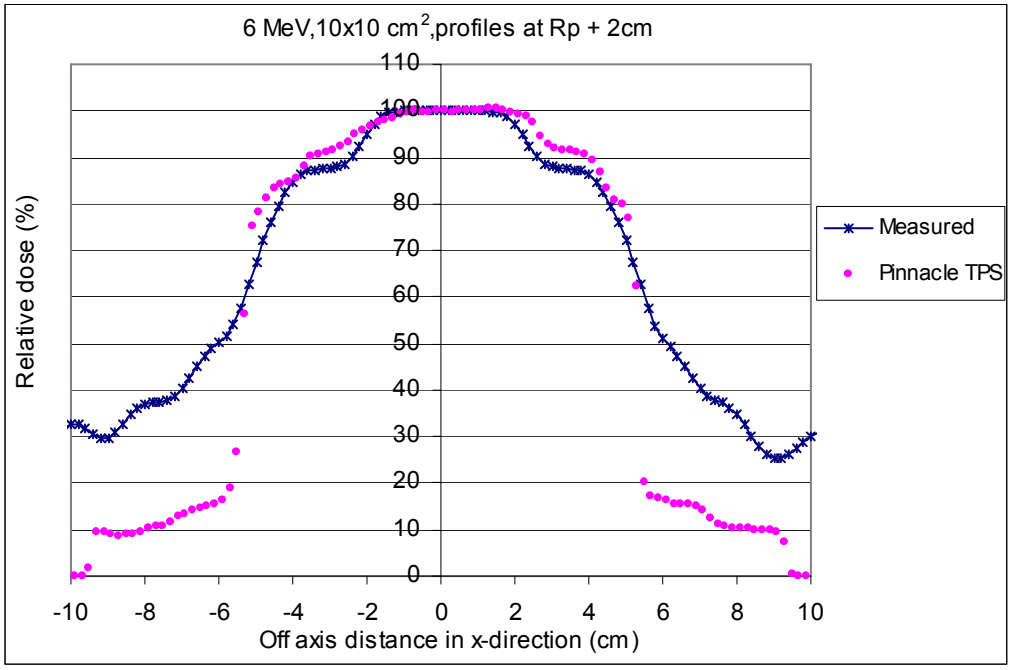

(e)

Figure 5.5 The comparison of relative dose profiles between Pinnacle TPS and diode measurement is shown for electron energy 6 MeV, SSD 100 cm and field size 10 × 10 cm^2 at (a) depth of dose maximum, (b) depth of dose 90%, (c) depth of dose 50%, (d) depth R_P, and (e) depth R_P + 2 cm.

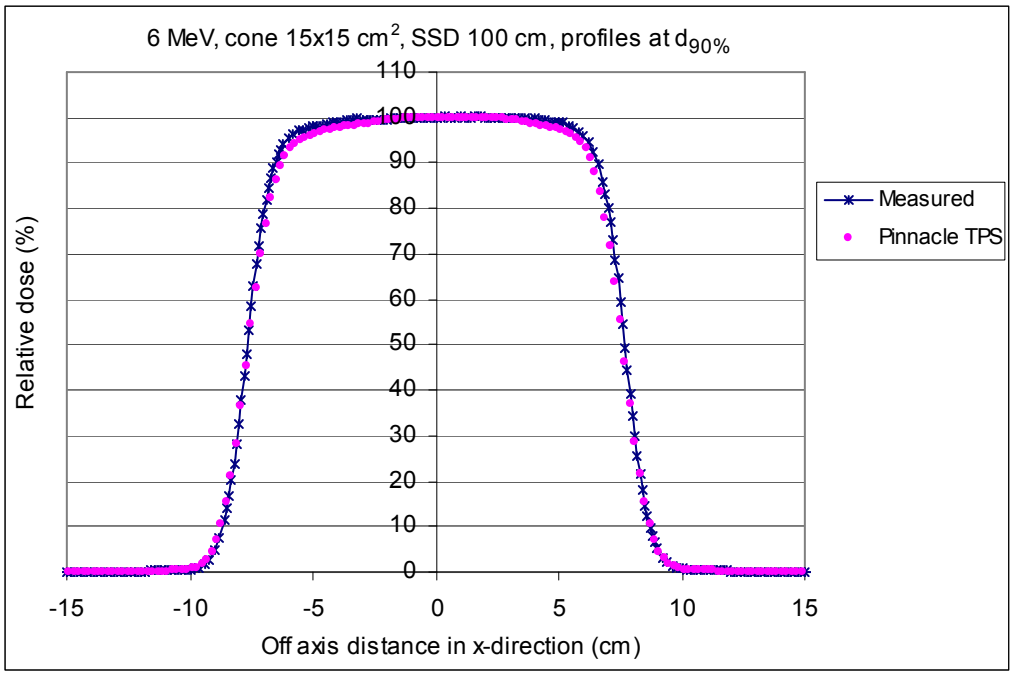
6 MeV, cone 15x15 cm2, SSD 100 cm, profiles at d90%
Relative dose (%)
110
100
90
80
70
60
50
40
30
20
10
0
-15
-10
-5
0
5
10
15
Off axis distance in x-direction (cm)
Measured
Pinnacle TPS

(a)

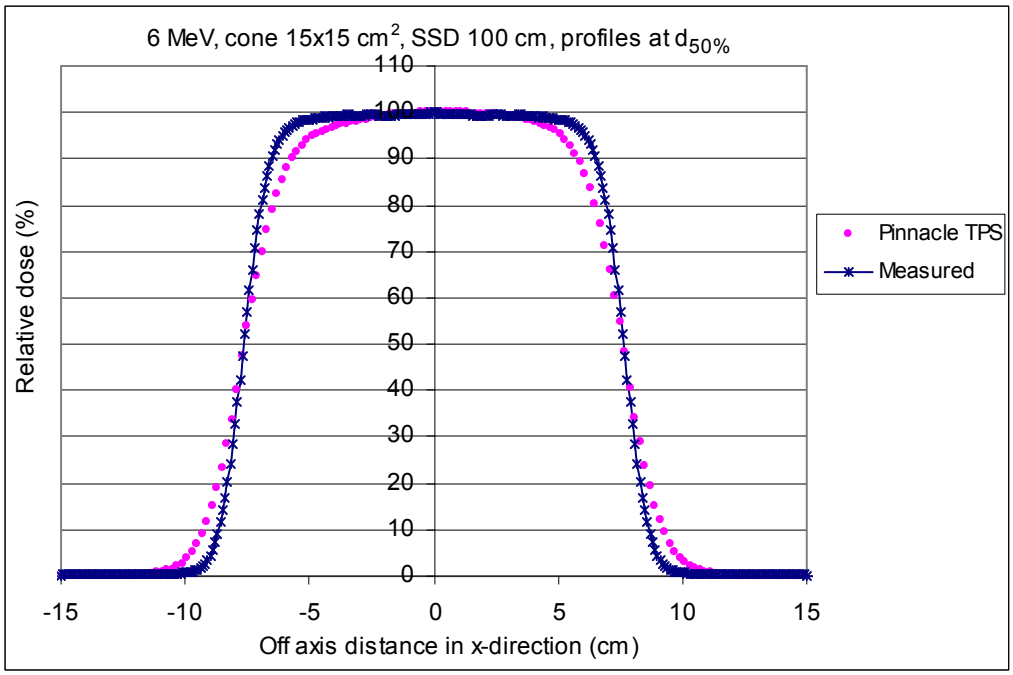
6 MeV, cone 15x15 cm2, SSD 100 cm, profiles at d50%
Relative dose (%)
110
100
90
80
70
60
50
40
30
20
10
0
-15
-10
-5
0
5
10
15
Off axis distance in x-direction (cm)
Pinnacle TPS
Measured

(b)

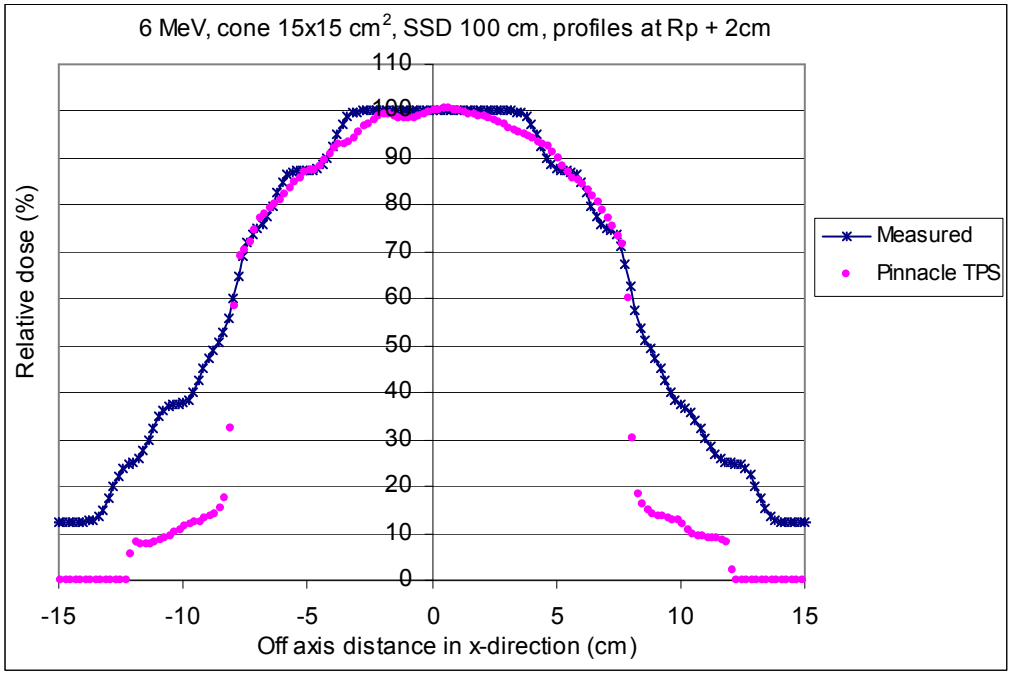

(c)

Figure 5.6 The comparison of relative dose profiles between Pinnacle TPS and diode measurement is shown for electron energy 6 MeV, SSD 100 cm and field size 15 × 15 cm^2 at (a) depth of dose 90%, (b) depth of dose 50%, and (c) depth R_P + 2 cm.

Table 5.2 The difference of beam fringe ($\delta_{50\text{-}90}$), radiological width (RW_{50}), penumbra width (δ_2), outside central beam axis region (δ_3) and outside beam edges (δ_4) between Pinnacle calculation and diode measurement for standard cone 6 × 6, 10 × 10 and 15 × 15 cm^2 at the depths of d_{max}, $d_{90\%}$ $d_{50\%}$, Rp and Rp + 2 cm and irradiated with electron energy 6 MeV electron beams of 100 cm SSD.

	Depth	**Distance to agreement (cm)**		
		6 × 6 cm^2	**10 × 10 cm^2**	**15 × 15 cm^2**
$\delta_{50\text{-}90}$	Dmax	-	0.072	-
	d90%	0.246	0.195	0.042
	d50%	0.57	0.6	0.68
	Rp	-	1.68	-
	Rp+2cm	1.4	2	1.2
RW_{50}	Dmax	-	0.13	-
	d90%	0.05	0.2	0.1
	d50%	0.05	0.04	0.016
	Rp	-	0.04	-
	Rp+2cm	2.95	1.4	1.4
δ_2 (80-20%)	Dmax	-	0.034	-
	d90%	0.206	0.165	0.068
	d50%	0.82	0.66	0.76
	Rp	-	1.43	-
	Rp+2cm	-	0.72	0.51
	Depth	**% dose difference**		
		6 × 6 cm^2	**10 × 10 cm^2**	**15 × 15 cm^2**
δ_3	Dmax	-	1.965%	-
	d90%	1.165%	2.62%	1.84%
	d50%	11.85%	6.99%	4.54%
	Rp	-	14.34%	-
	Rp+2cm	-	5%	3.115%
δ_4	Dmax	-	1.83%	-
	d90%	1.35%	0.94%	0.66%
	d50%	5.57%	5.45%	5.75%
	Rp	-	3.64%	-
	Rp+2cm	-	-	-

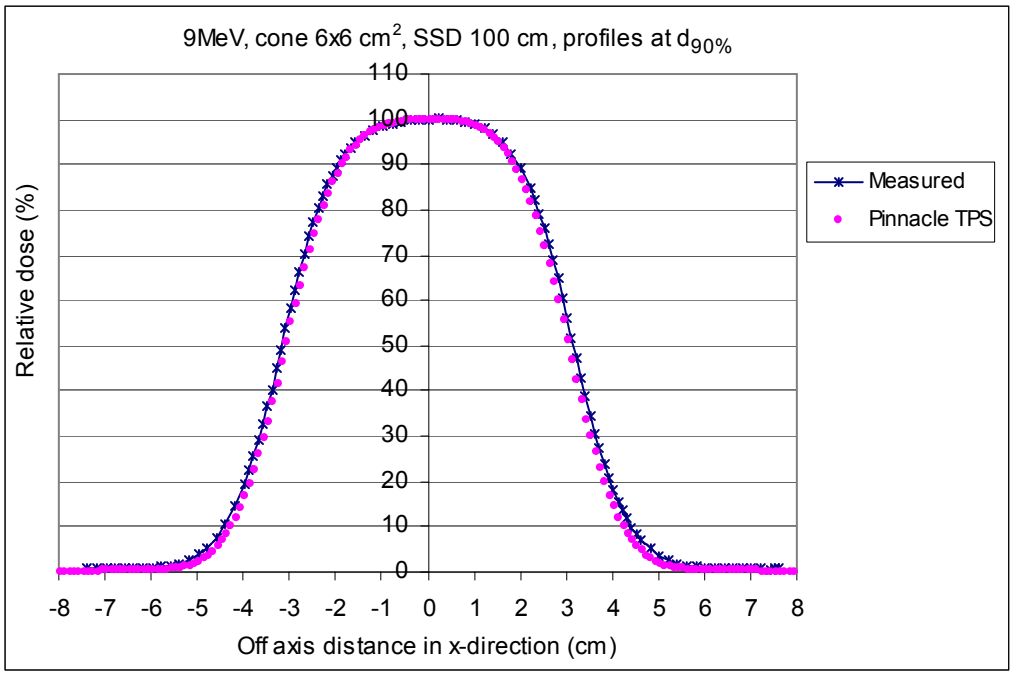
9MeV, cone 6x6 cm2, SSD 100 cm, profiles at d90%
Relative dose (%)
110
100
90
80
70
60
50
40
30
20
10
0
-8 -7 -6 -5 -4 -3 -2 -1 0 1 2 3 4 5 6 7 8
Off axis distance in x-direction (cm)
Measured
Pinnacle TPS

(a)

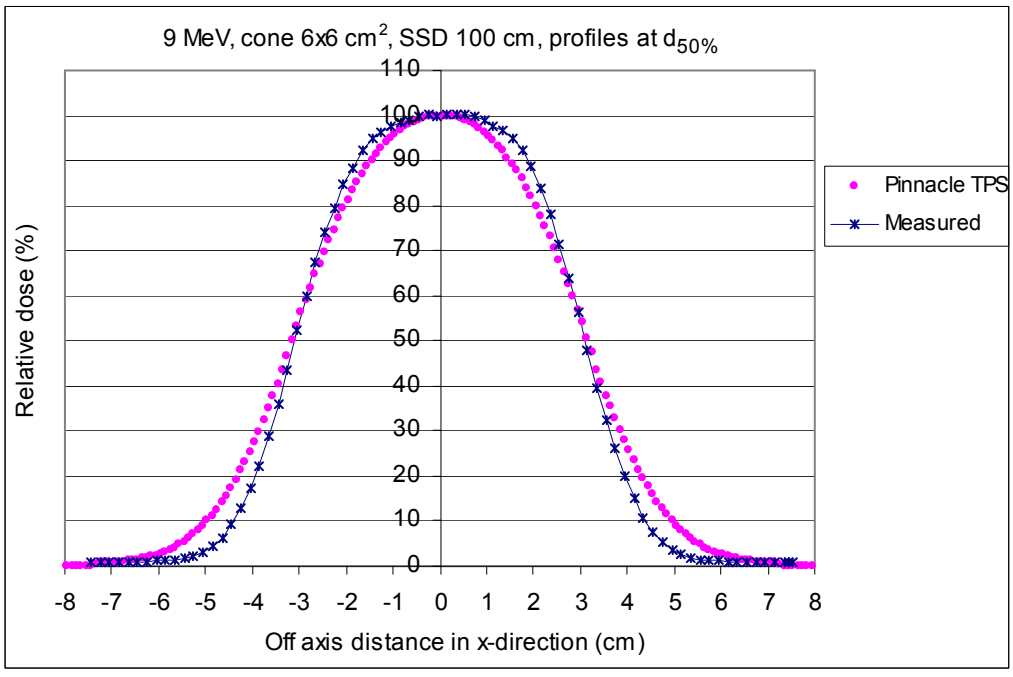
9 MeV, cone 6x6 cm2, SSD 100 cm, profiles at d50%
Relative dose (%)
110
100
90
80
70
60
50
40
30
20
10
0
-8 -7 -6 -5 -4 -3 -2 -1 0 1 2 3 4 5 6 7 8
Off axis distance in x-direction (cm)
Pinnacle TPS
Measured

(b)

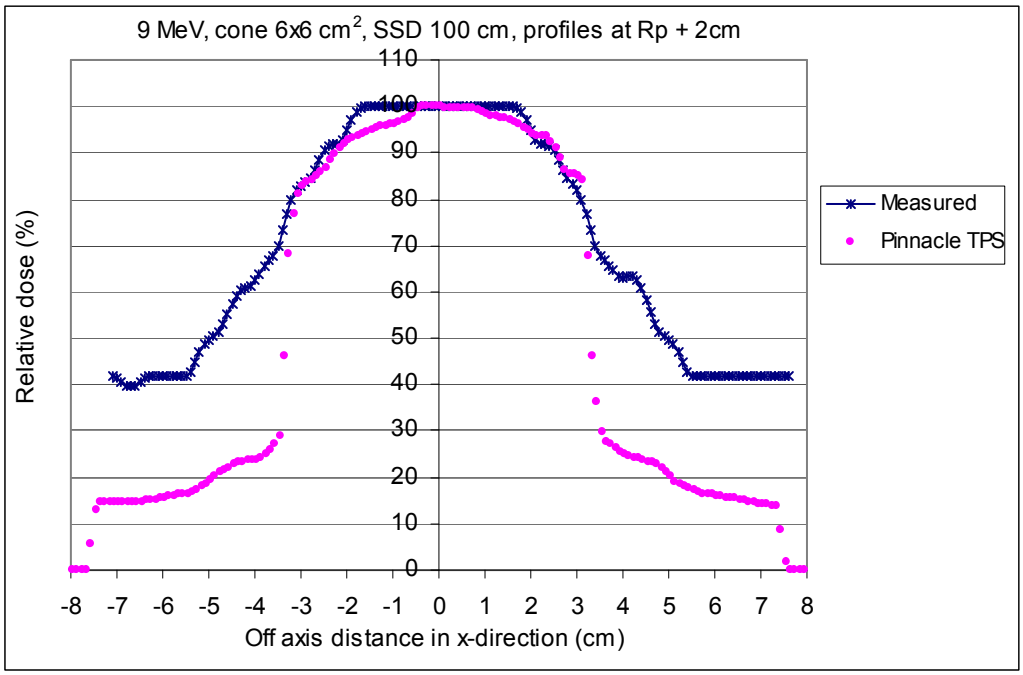

(c)

Figure 5.7 The comparison of relative dose profiles between Pinnacle TPS and diode measurement is shown for electron energy 9 MeV, SSD 100 cm and field size 6 × 6 cm^2 at (a) depth of dose 90%, (b) depth of dose 50%, and (c) depth R_P + 2 cm .

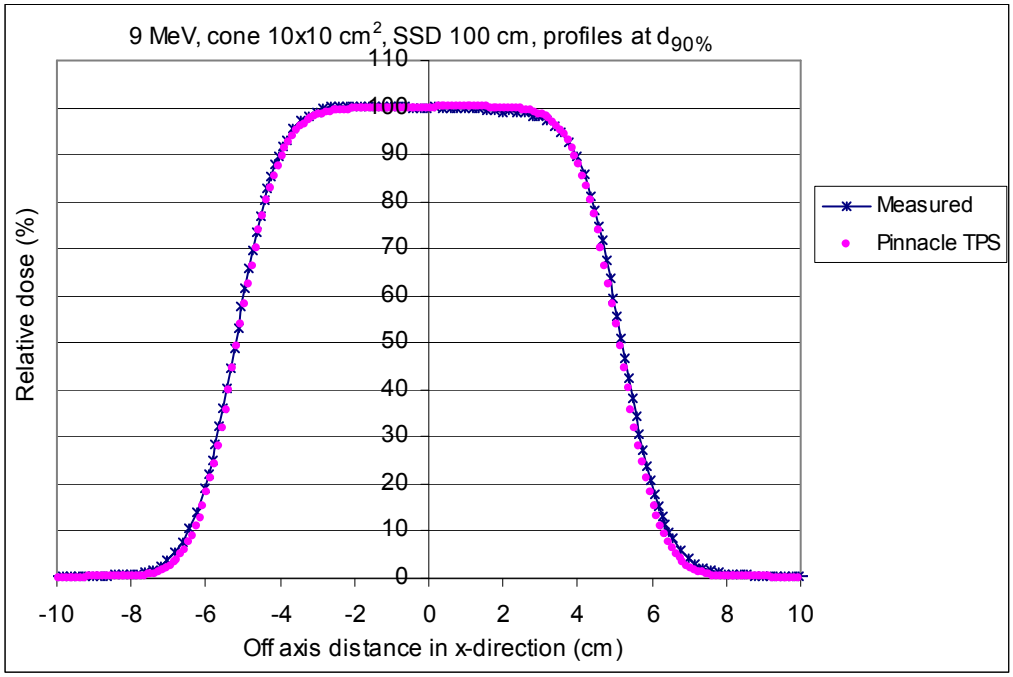
9 MeV, cone 10x10 cm2, SSD 100 cm, profiles at d90%
Relative dose (%)
110
100
90
80
70
60
50
40
30
20
10
0
-10
-8
-6
-4
-2
0
2
4
6
8
10
Off axis distance in x-direction (cm)
Measured
Pinnacle TPS

(a)

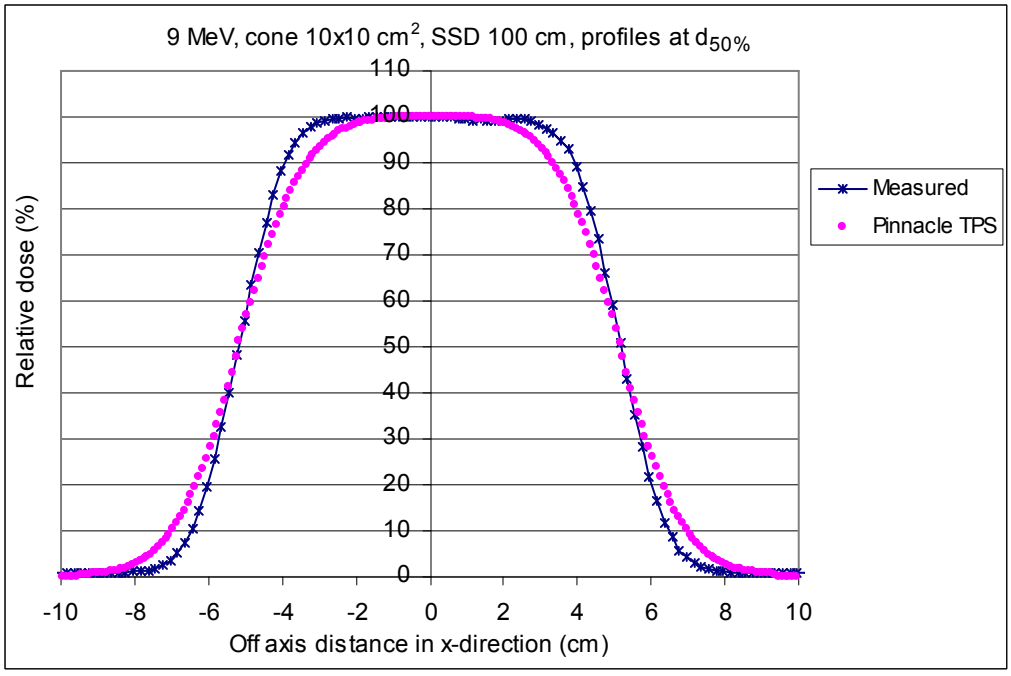
9 MeV, cone 10x10 cm2, SSD 100 cm, profiles at d50%
Relative dose (%)
110
100
90
80
70
60
50
40
30
20
10
0
-10
-8
-6
-4
-2
0
2
4
6
8
10
Off axis distance in x-direction (cm)
Measured
Pinnacle TPS

(b)

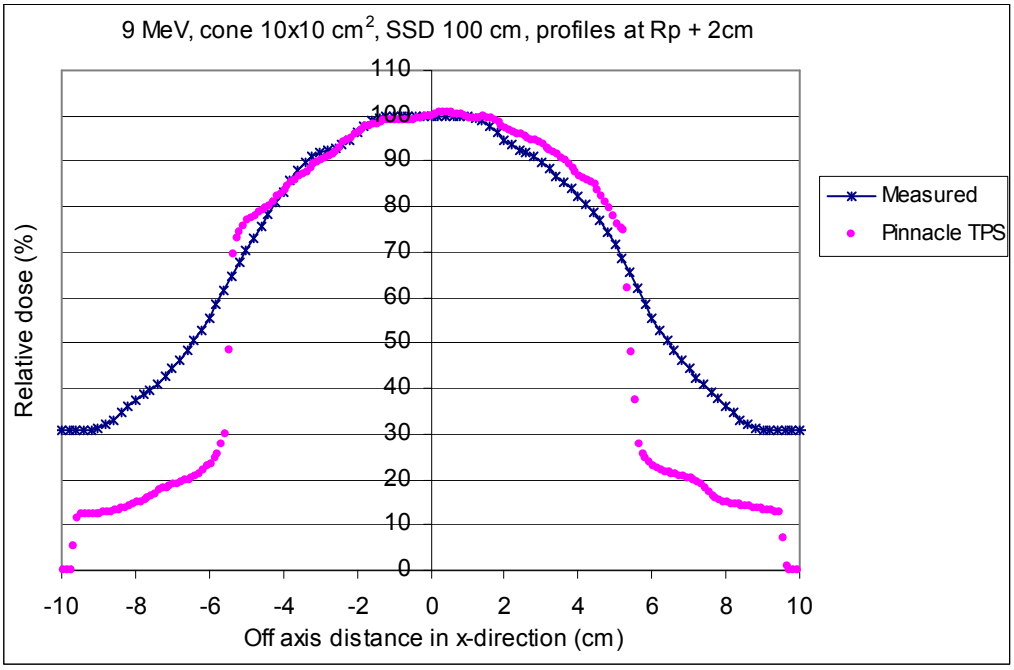

(c)

Figure 5.8 The comparison of relative dose profiles between Pinnacle TPS and diode measurement is shown for electron energy 9 MeV, SSD 100 cm and field size 10 × 10 cm^2 at (a) depth of dose 90%, (b) depth of dose 50%, and (c) depth R_P + 2 cm.

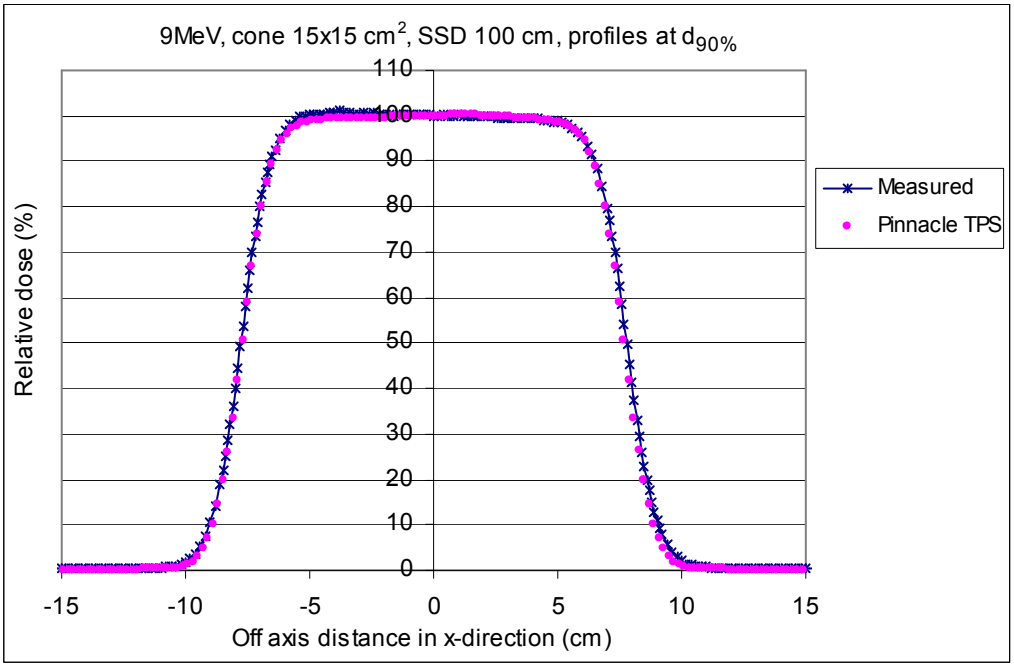
9MeV, cone 15x15 cm2, SSD 100 cm, profiles at d90%
Relative dose (%)
110
100
90
80
70
60
50
40
30
20
10
0
-15
-10
-5
0
5
10
15
Off axis distance in x-direction (cm)
Measured
Pinnacle TPS

(a)

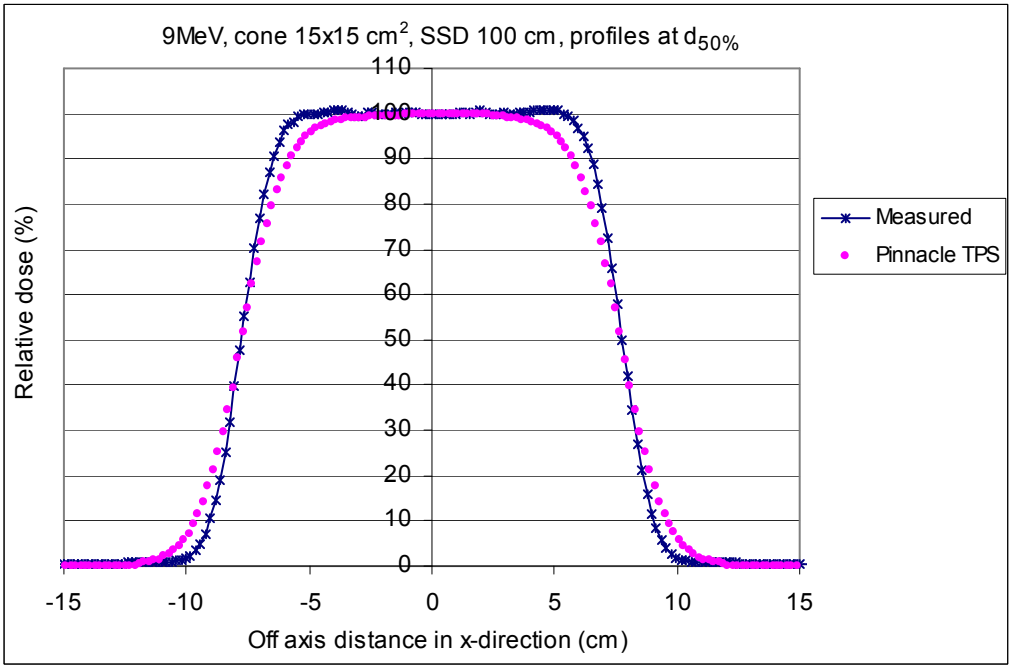
9MeV, cone 15x15 cm2, SSD 100 cm, profiles at d50%
Relative dose (%)
110
100
90
80
70
60
50
40
30
20
10
0
-15
-10
-5
0
5
10
15
Off axis distance in x-direction (cm)
Measured
Pinnacle TPS

(b)

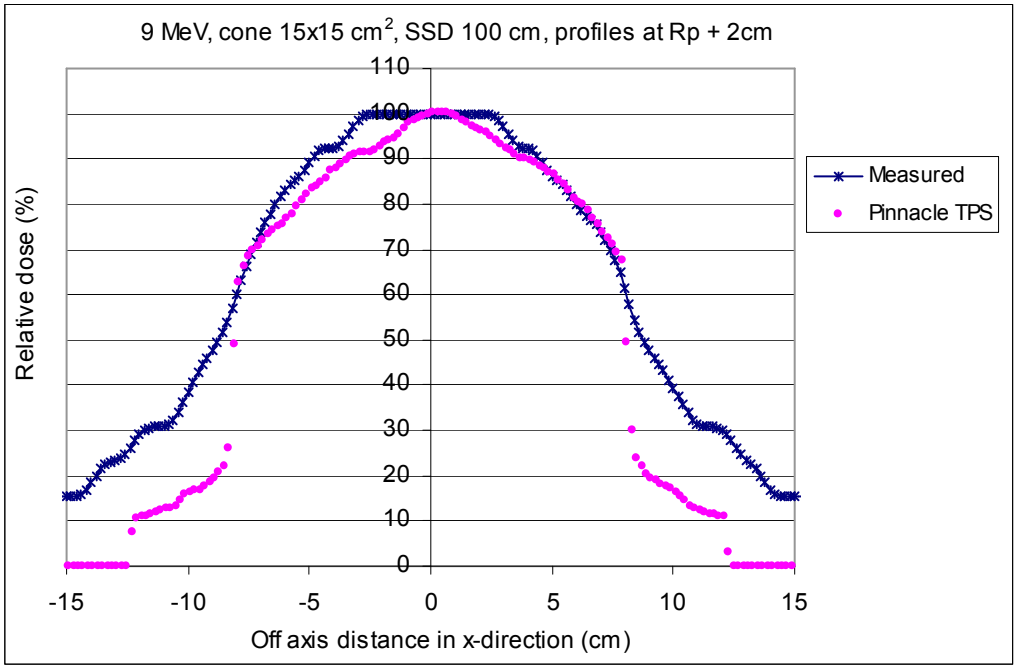

(c)

Figure 5.9 The comparison of relative dose profiles between Pinnacle TPS and diode measurement is shown for electron energy 9 MeV, SSD 100 cm and field size 15 × 15 cm^2 at (a) depth of dose 90%, (b) depth of dose 50%, and (c) depth R_P + 2 cm.

Table 5.3 The difference of beam fringe ($\delta_{50\text{-}90}$), radiological width (RW_{50}), penumbra width (δ_2), outside central beam axis region (δ_3) and outside beam edges (δ_4) between Pinnacle calculation and diode measurement for standard cone 6 × 6, 10 × 10 and 15 × 15 cm^2 at the depths of $d_{90\%}$ $d_{50\%}$, and Rp + 2 cm and irradiated with electron energy 9 MeV electron beams of 100 cm SSD.

	Depth	**Distance to agreement (cm)**		
		6 × 6 cm^2	**10 × 10 cm^2**	**15 × 15 cm^2**
$\delta_{50\text{-}90}$	d90%	0.028	0.067	0.013
	d50%	0.46	0.65	0.87
	Rp+2cm	1.75	1.6	0.7
RW_{50}	d90%	0.26	0.1	0.2
	d50%	0.11 c	0	0
	Rp+2cm	3.3	2.1	1.6
δ_2 (80-20%)	d90%	0.024	0.065	0.02
	d50%	0.63	0.72	0.9
	Rp+2cm	-	6.8	4.8
	Depth	**% dose difference**		
		6 × 6 cm^2	**10 × 10 cm^2**	**15 × 15 cm^2**
δ_3	d90%	1.67%	0.593%	1.42%
	d50%	7.31%	7.48%	4.98%
	Rp+2cm	0.85%	5%	7%
δ_4	d90%	2.34%	2.034%	2.30%
	d50%	4.69%	5%	5.19%
	Rp+2cm	-	-	-

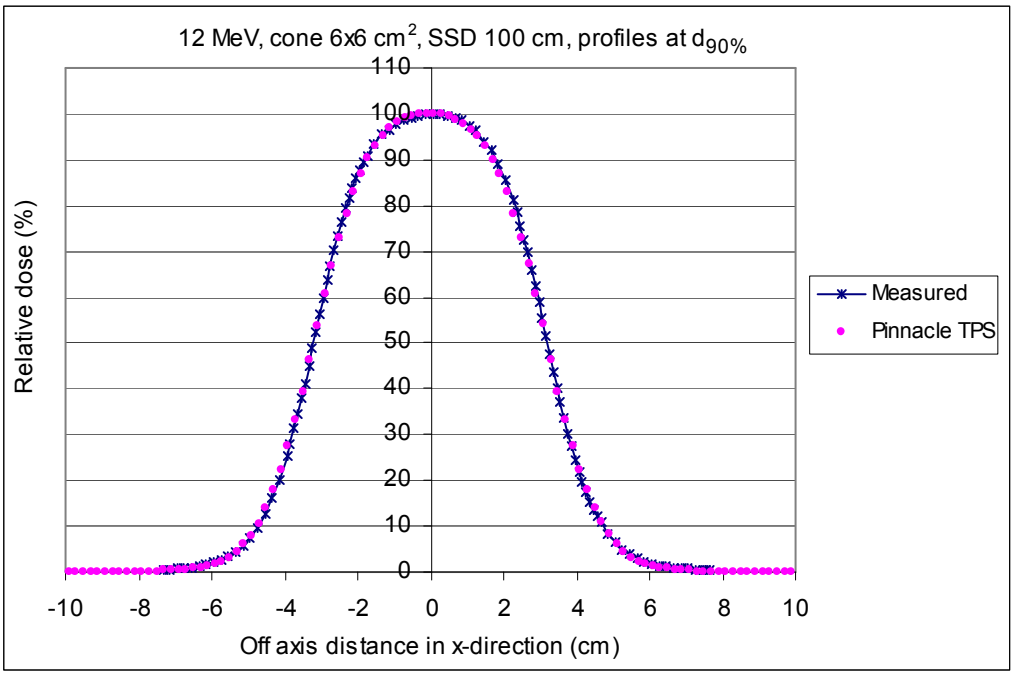
12 MeV, cone 6x6 cm2, SSD 100 cm, profiles at d90%
Relative dose (%)
110
100
90
80
70
60
50
40
30
20
10
0
-10
-8
-6
-4
-2
0
2
4
6
8
10
Off axis distance in x-direction (cm)
Measured
Pinnacle TPS

(a)

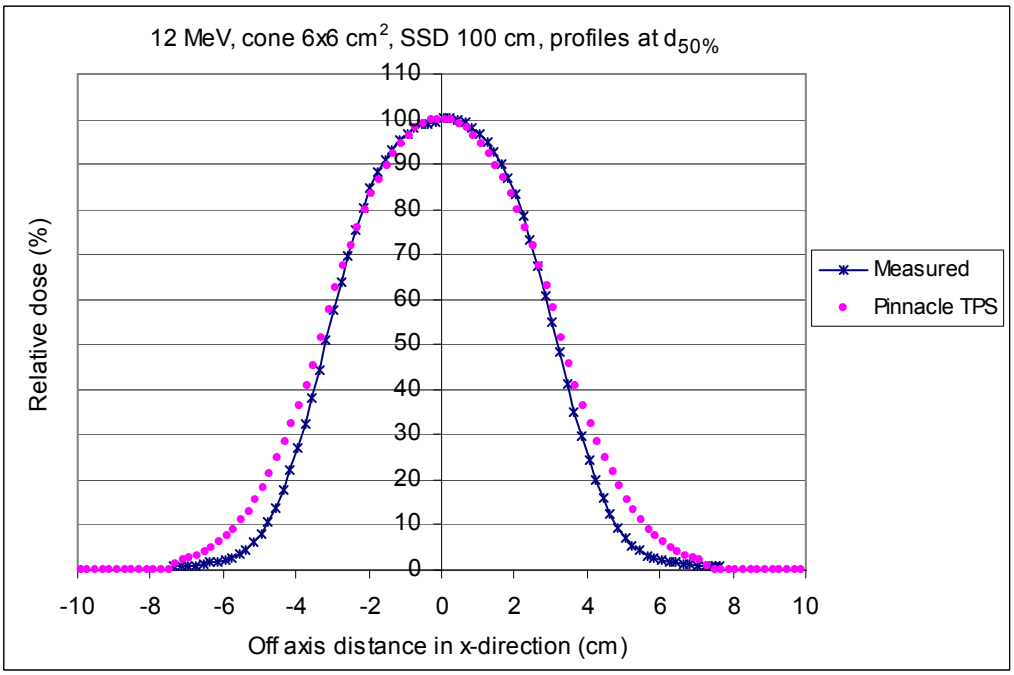
12 MeV, cone 6x6 cm2, SSD 100 cm, profiles at d50%
Relative dose (%)
110
100
90
80
70
60
50
40
30
20
10
0
-10
-8
-6
-4
-2
0
2
4
6
8
10
Off axis distance in x-direction (cm)
Measured
Pinnacle TPS

(b)

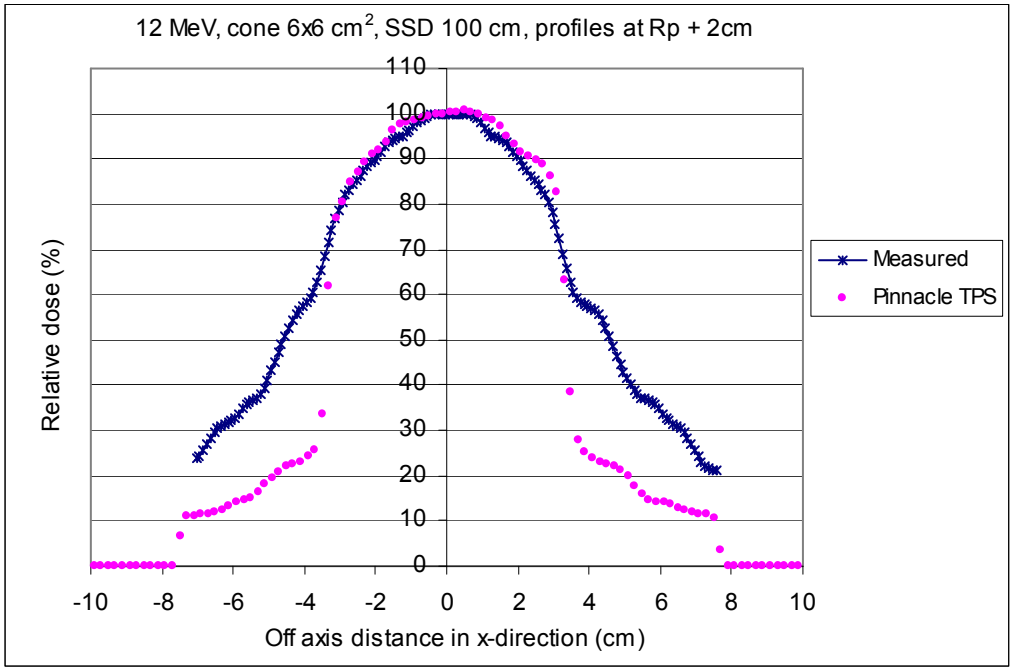

(c)

Figure 5.10 The comparison of relative dose profiles between Pinnacle TPS and diode measurement is shown for electron energy 12 MeV, SSD 100 cm and field size 6×6 cm^2 at (a) depth of dose 90%, (b) depth of dose 50% and (c) depth $R_P + 2$ cm.

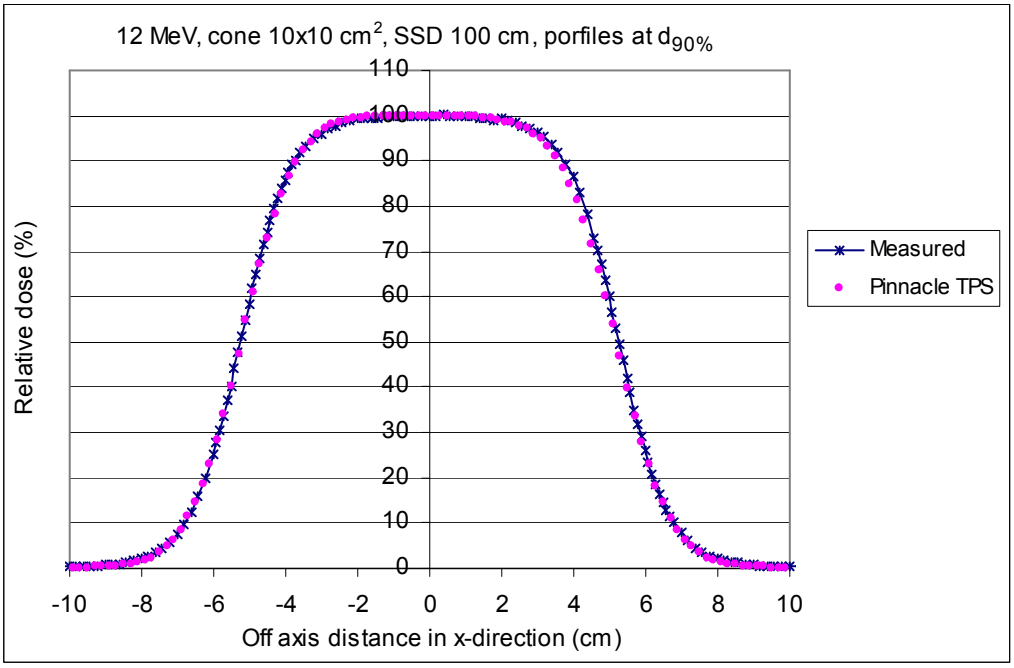
12 MeV, cone 10x10 cm2, SSD 100 cm, porfiles at d90%
Relative dose (%)
110
100
90
80
70
60
50
40
30
20
10
0
-10 -8 -6 -4 -2 0 2 4 6 8 10
Off axis distance in x-direction (cm)
Measured
Pinnacle TPS

(a)

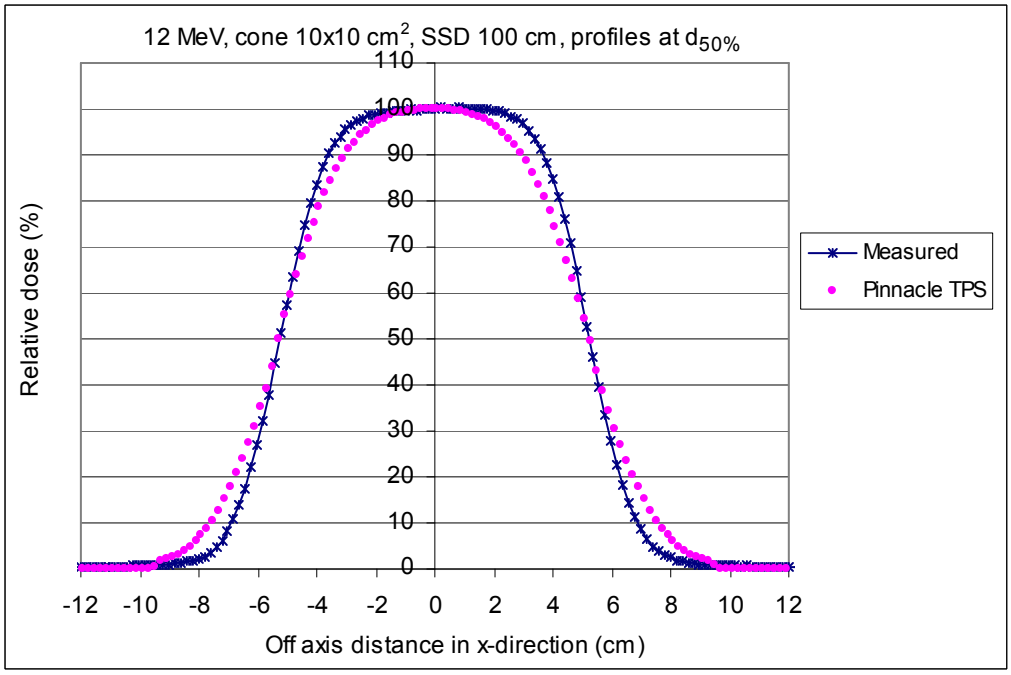
12 MeV, cone 10x10 cm2, SSD 100 cm, profiles at d50%
Relative dose (%)
110
100
90
80
70
60
50
40
30
20
10
0
-12 -10 -8 -6 -4 -2 0 2 4 6 8 10 12
Off axis distance in x-direction (cm)
Measured
Pinnacle TPS

(b)

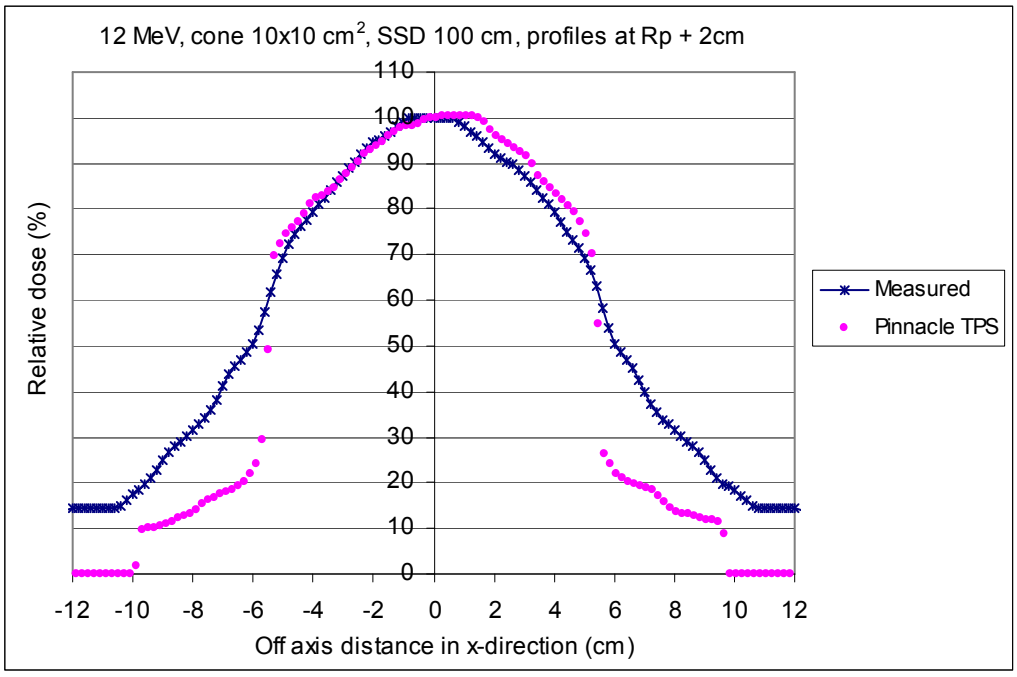

(c)

Figure 5.11 The comparison of relative dose profiles between Pinnacle TPS and diode measurement is shown for electron energy 12 MeV, SSD 100 cm and field size 10×10 cm^2 at (a) depth of dose 90%, (b) depth of dose 50% and (c) depth $R_P + 2$ cm.

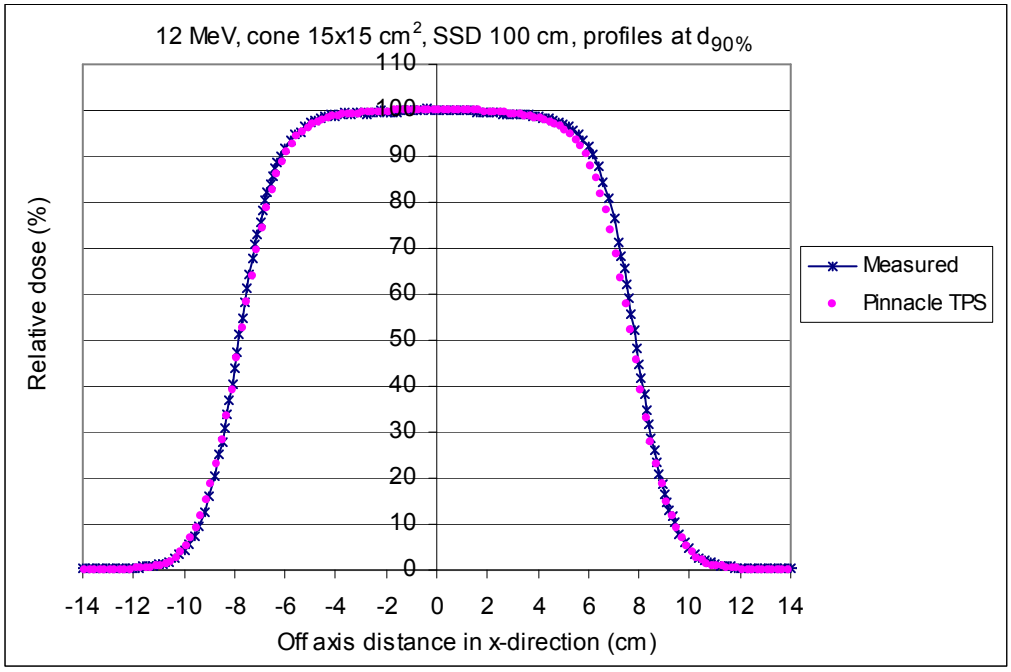
12 MeV, cone 15x15 cm2, SSD 100 cm, profiles at d90%
Relative dose (%)
110
100
90
80
70
60
50
40
30
20
10
0
-14 -12 -10 -8 -6 -4 -2 0 2 4 6 8 10 12 14
Off axis distance in x-direction (cm)
Measured
Pinnacle TPS

(a)

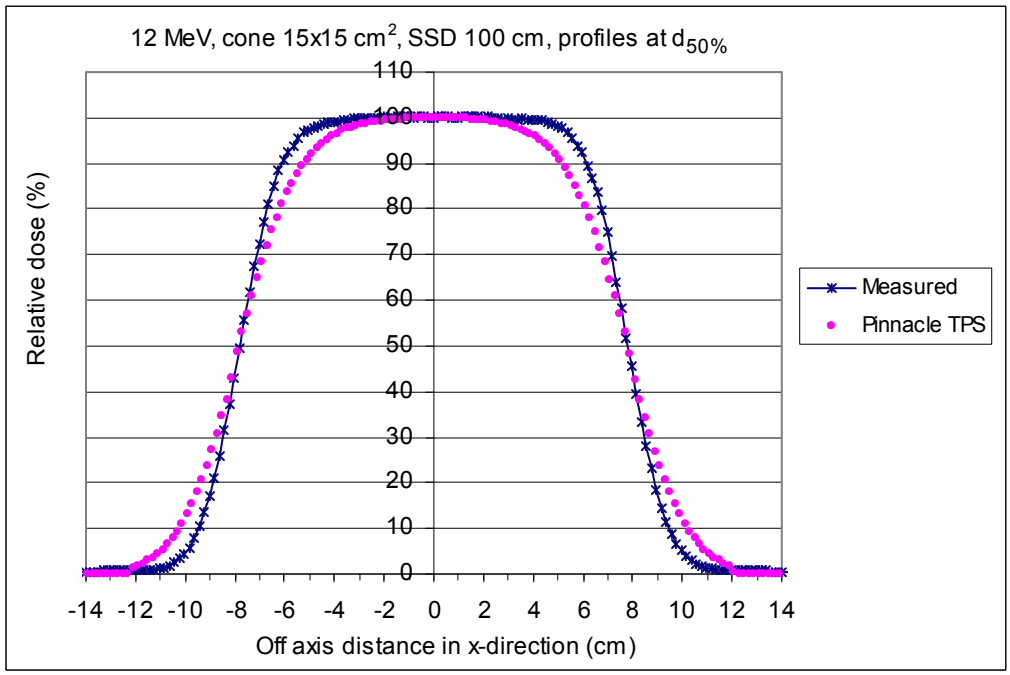
12 MeV, cone 15x15 cm2, SSD 100 cm, profiles at d50%
Relative dose (%)
110
100
90
80
70
60
50
40
30
20
10
0
-14 -12 -10 -8 -6 -4 -2 0 2 4 6 8 10 12 14
Off axis distance in x-direction (cm)
Measured
Pinnacle TPS

(b)

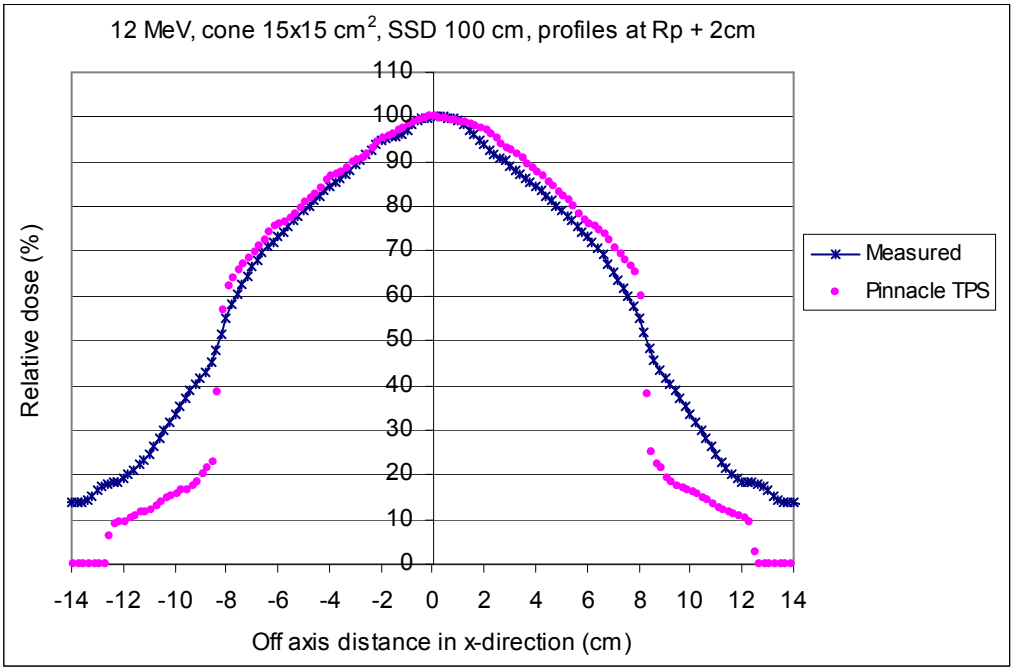

(c)

Figure 5.12 The comparison of relative dose profiles between Pinnacle TPS and diode measurement is shown for electron energy 12 MeV, SSD 100 cm and field size 15 × 15 cm^2 at (a) depth of dose 90%, (b) depth of dose 50% and (c) depth R_P + 2 cm.

Table 5.4 The difference of beam fringe (δ_{50-90}), radiological width (RW_{50}), penumbra width (δ_2), outside central beam axis region (δ_3) and outside beam edges (δ_4) between Pinnacle calculation and diode measurement for standard cone 6 × 6, 10 × 10 and 15 × 15 cm^2 at the depths of $d_{90\%}$ $d_{50\%}$ and Rp + 2 cm and irradiated with electron energy 12 MeV electron beams of 100 cm SSD.

	Depth	**Distance to agreement (cm)**		
		6 × 6 cm^2	**10 × 10 cm^2**	**15 × 15 cm^2**
δ_{50-90}	d90%	0.097	0.093	0.204
	d50%	0.33	0.72	0.96
	Rp+2cm	1.7	1.2	0.9
RW_{50}	d90%	0	0.08	0.1
	d50%	0.3	0	0.04
	Rp+2cm	2.4	0.1	0.2
δ_2 (80-20%)	d90%	0.136	0.143	0.255
	d50%	0.623	0.9	1.06
	Rp+2cm	-	-	0.33
	Depth	**% dose difference**		
		6 × 6 cm^2	**10 × 10 cm^2**	**15 × 15 cm^2**
δ_3	d90%	2.10%	1.49%	0.96%
	d50%	2.64%	8.53%	7%
	Rp+2cm	2.46%	6%	5%
δ_4	d90%	0.6%	0.62%	0.829%
	d50%	4.98%	4.78%	5%
	Rp+2cm	-	-	-

B. Shaped fields

The majority of clinical electron fields are custom shapes using Cerrobend cutouts to encompass target volumes and minimize the amount of normal tissue in the field. The comparisons of diode-measured and Pinnacle-calculated central axis percent depth dose are shown in figures 5.13 to 5.15 (a-e). The agreement was within 5% or 0.5 cm. At the rapid dose fall-off region, the Pinnacle TPS had the drop of dose faster than the measurement for all insert cutouts and energies. Table 5.5 shows the average of %dose difference and distance difference at buildup region and fall-off region between diode measurements and Pinnacle calculations of Percent Depth Dose (PDD) for insert circular cutout diameter 5.2 cm and rectangular cutout of 8.7 × 6.8, 9.5 × 4.2, 6.7 × 13.7 and 4.7 × 14.6 cm^2 at standard 100 cm SSD .

Figure 5.16 to 5.24 (a-b) show the comparison of dose profiles at the maximum depth between Pinnacle calculations and diode measurements for insert circular cutout diameter 5.2 cm and rectangular cutout of 8.7 × 6.8 and 9.5 × 4.2 cm^2 of 6, 9 and 12 MeV electron beams. The accuracy of the calculation for relative dose profiles at the maximum depth in circular and rectangular shaped fields showed overall good agreement within 5% or 0.5 cm as illustrated in Table 5.6-5.8.

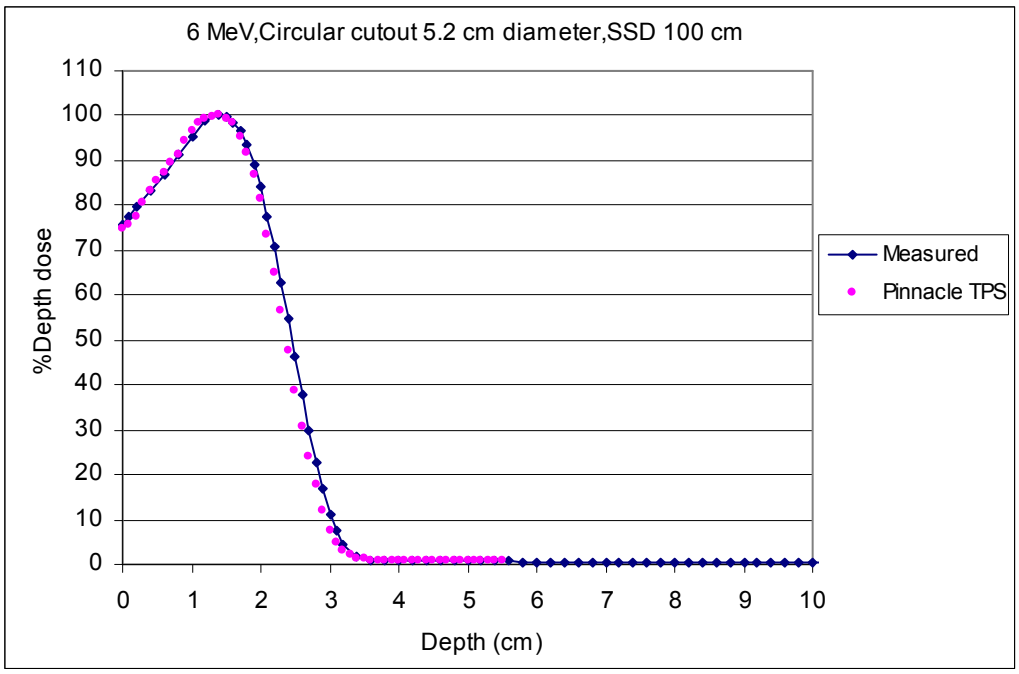

(a)

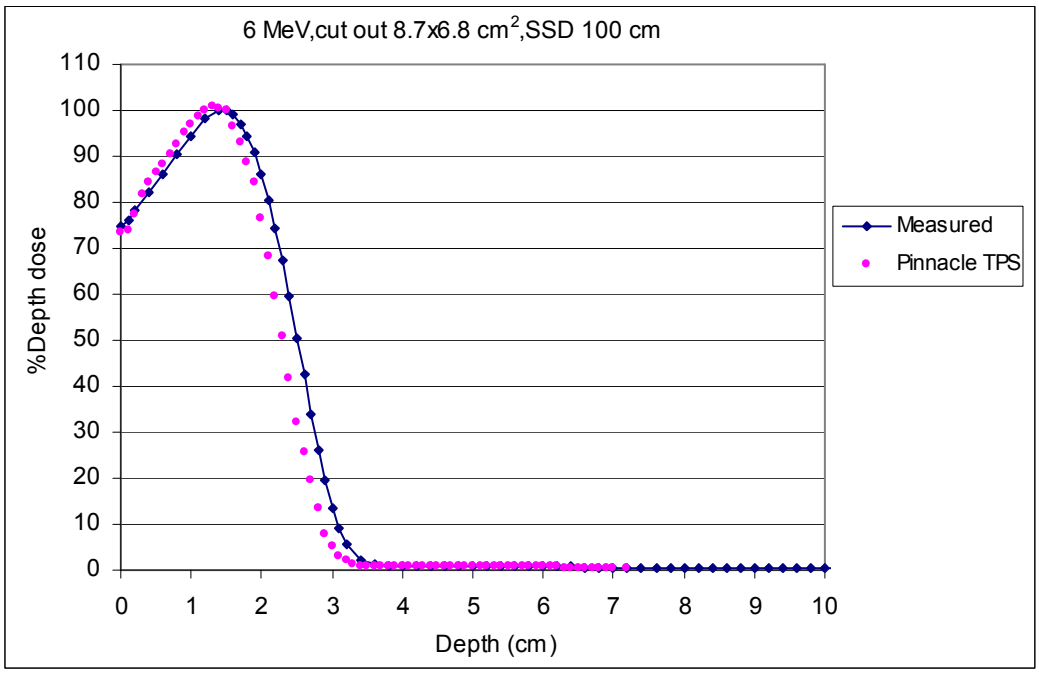
6 MeV,cut out 8.7x6.8 cm2,SSD 100 cm
%Depth dose
Depth (cm)
Measured
Pinnacle TPS

(b)

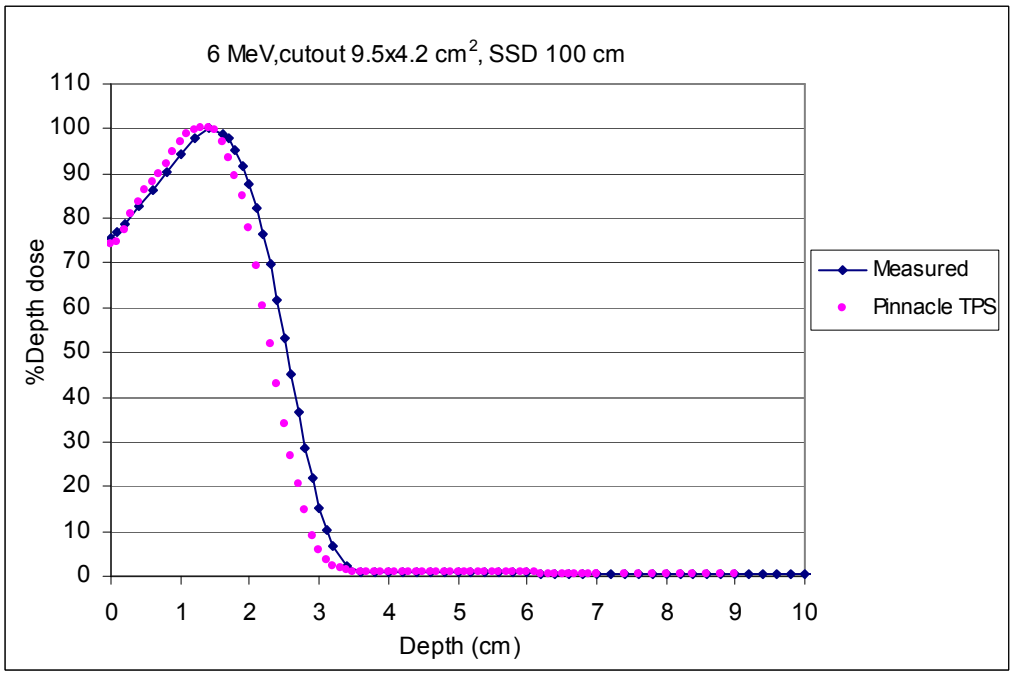
6 MeV,cutout 9.5x4.2 cm2, SSD 100 cm
%Depth dose
Depth (cm)
Measured
Pinnacle TPS

(c)

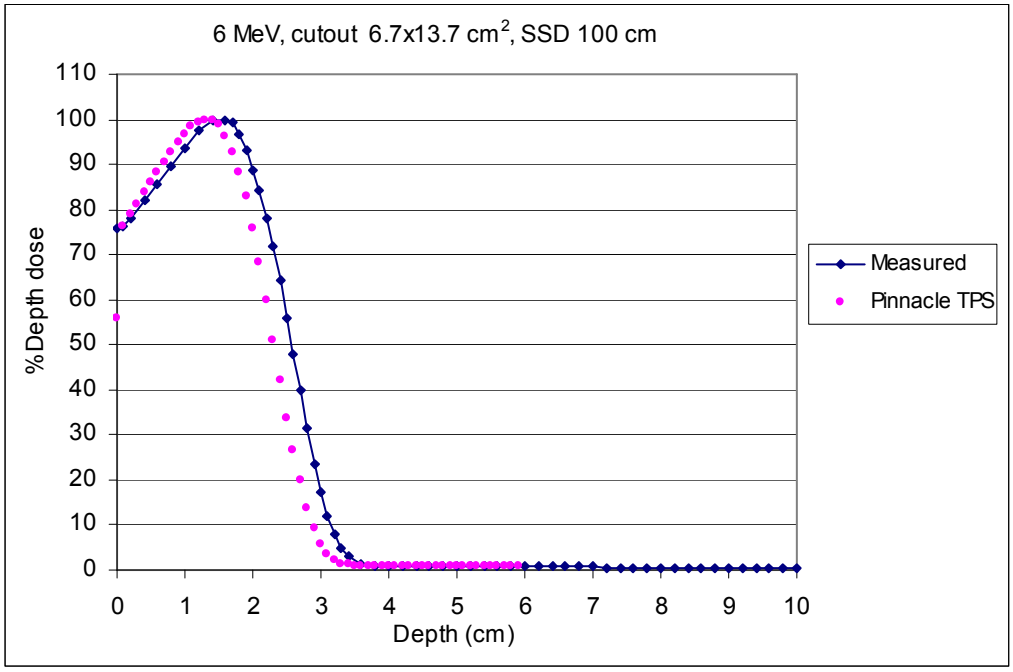

(d)

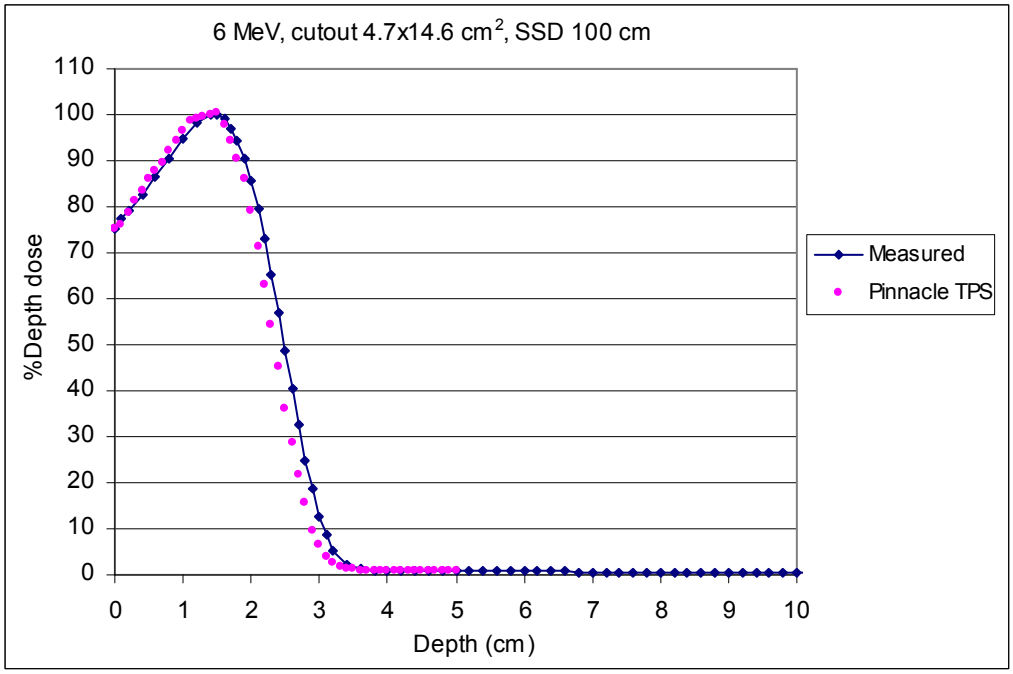

(e)

Figure 5.13 The comparison of percent depth dose for 6 MeV electron beams between Pinnacle calculation and diode measurement for insert (a) circular cutout diameter 5.2 cm and rectangular cutout of (b) 8.7 × 6.8, (c) 9.5 × 4.2, (d) 6.7 × 13.7 and (e) 4.7 × 14.6 cm^2.

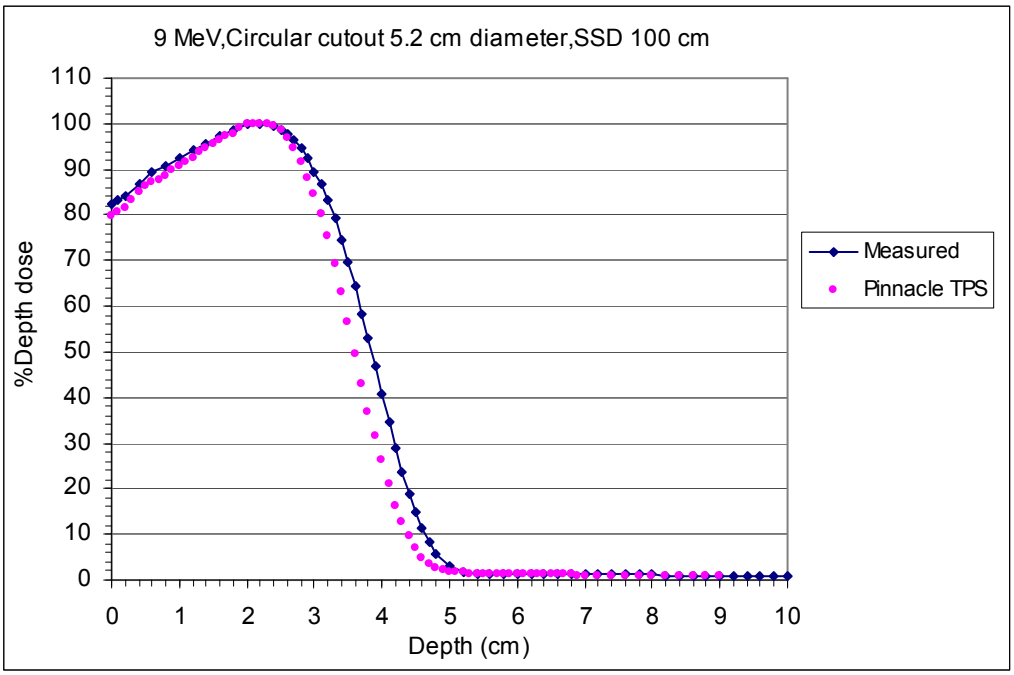
9 MeV,Circular cutout 5.2 cm diameter,SSD 100 cm
%Depth dose
Depth (cm)
Measured
Pinnacle TPS

(a)

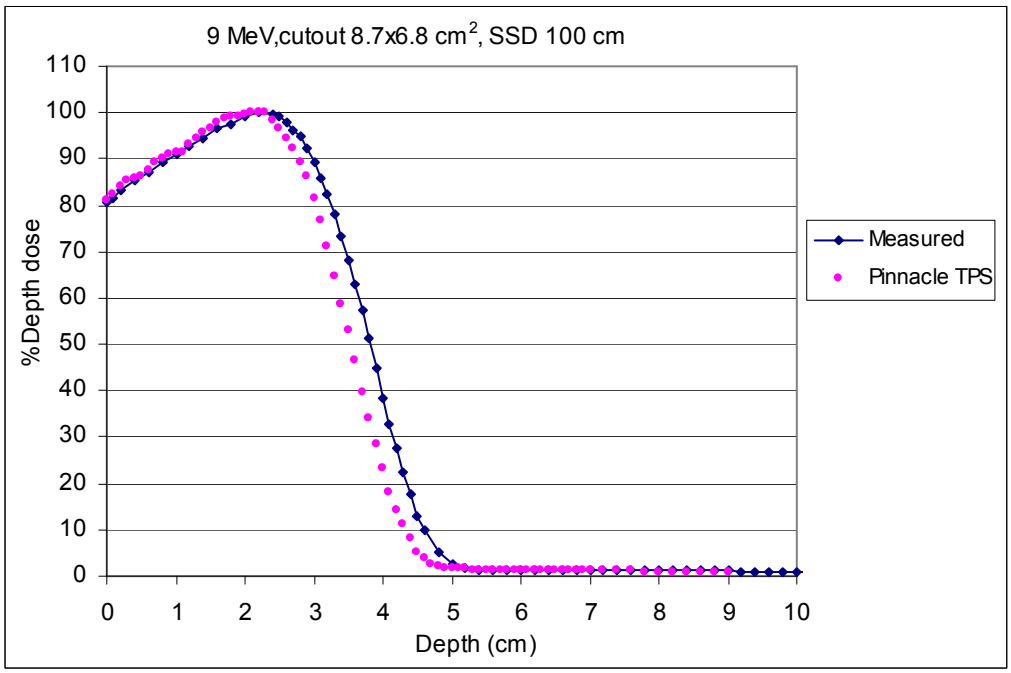
9 MeV,cutout 8.7x6.8 cm2, SSD 100 cm
%Depth dose
Depth (cm)
Measured
Pinnacle TPS

(b)

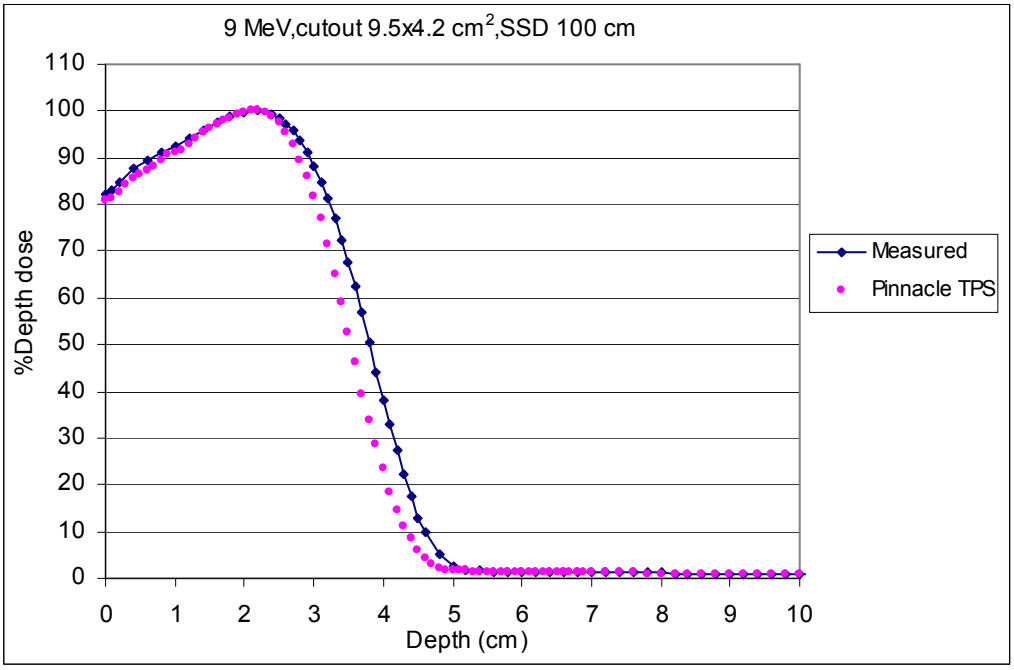
9 MeV,cutout 9.5x4.2 cm2,SSD 100 cm
%Depth dose
Depth (cm)
Measured
Pinnacle TPS

(c)

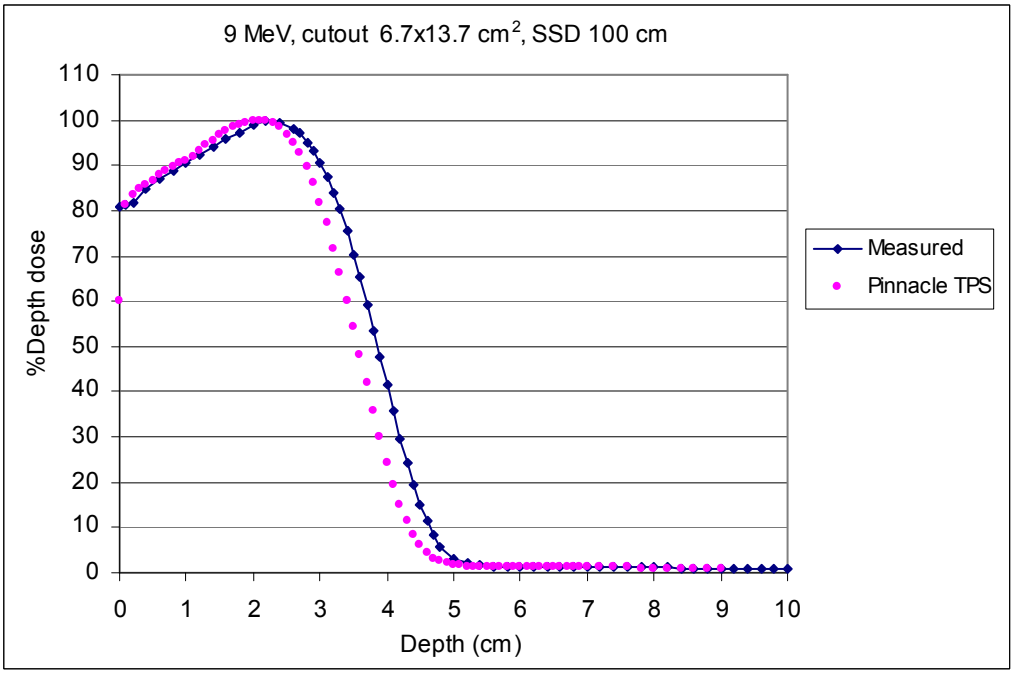
9 MeV, cutout 6.7x13.7 cm2, SSD 100 cm
%Depth dose
Depth (cm)
Measured
Pinnacle TPS

(d)

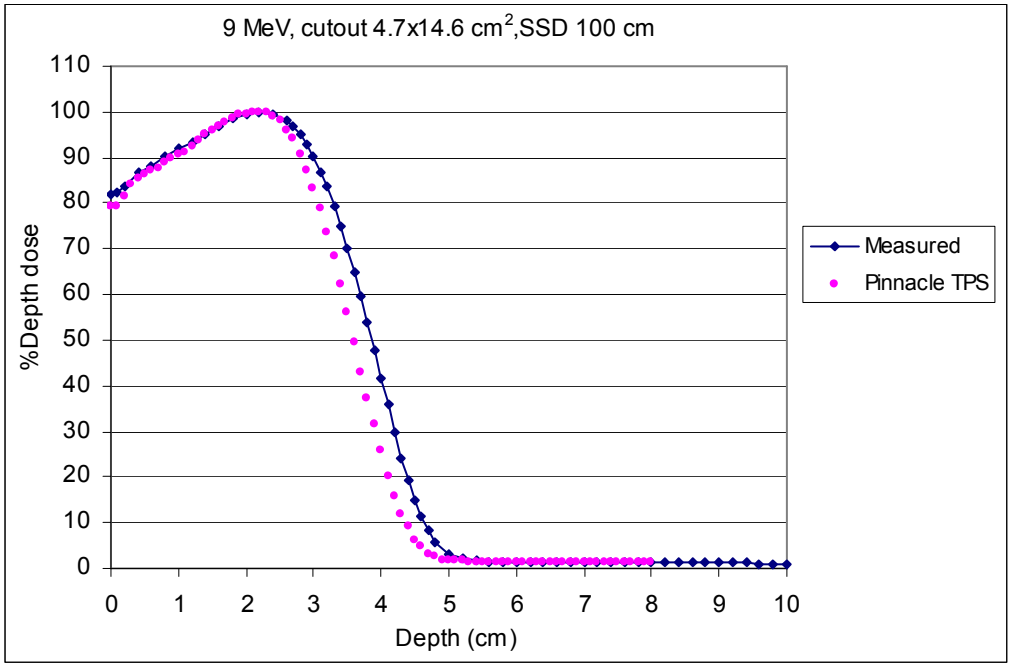

(e)

Figure 5.14 The comparison of percent depth dose for 9 MeV electron beams between Pinnacle calculation and diode measurement for insert (a) circular cutout diameter 5.2 cm and rectangular cutout of (b) 8.7 × 6.8, (c) 9.5 × 4.2, (d) 6.7 × 13.7 and (e) 4.7 × 14.6 cm^2.

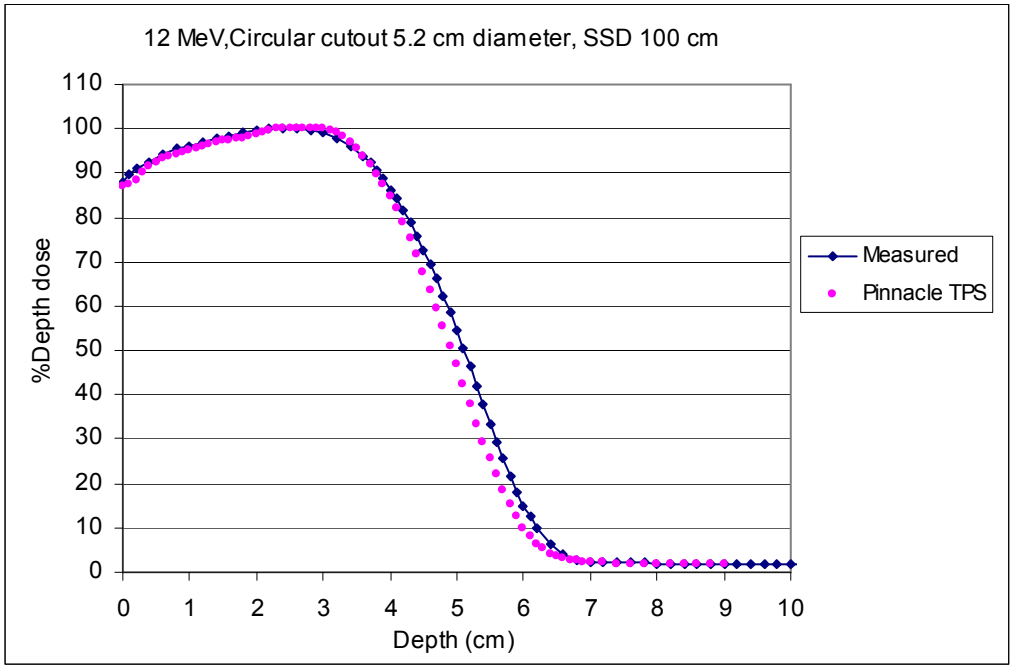
12 MeV,Circular cutout 5.2 cm diameter, SSD 100 cm
%Depth dose
Depth (cm)
Measured
Pinnacle TPS

(a)

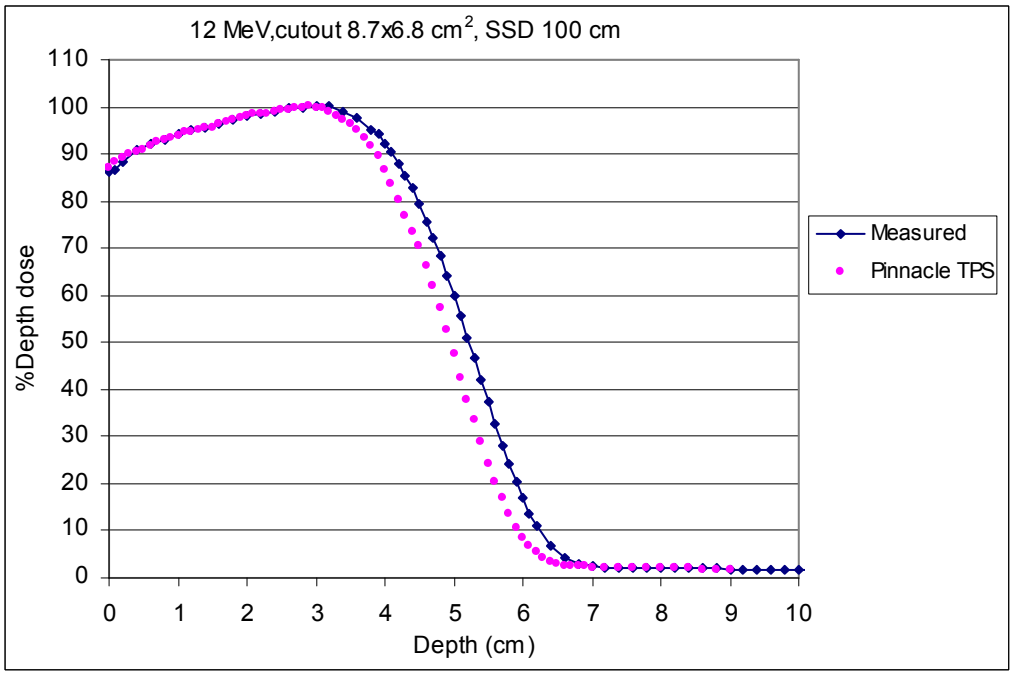
12 MeV,cutout 8.7x6.8 cm2, SSD 100 cm
%Depth dose
Depth (cm)
Measured
Pinnacle TPS

(b)

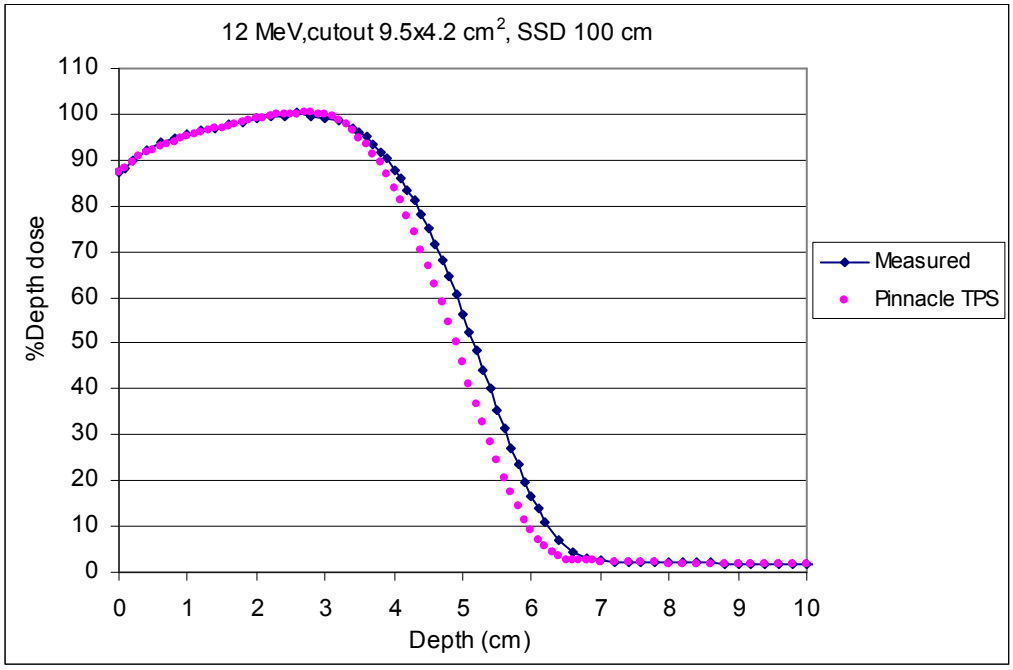
12 MeV,cutout 9.5x4.2 cm2, SSD 100 cm
%Depth dose
Depth (cm)
Measured
Pinnacle TPS

(c)

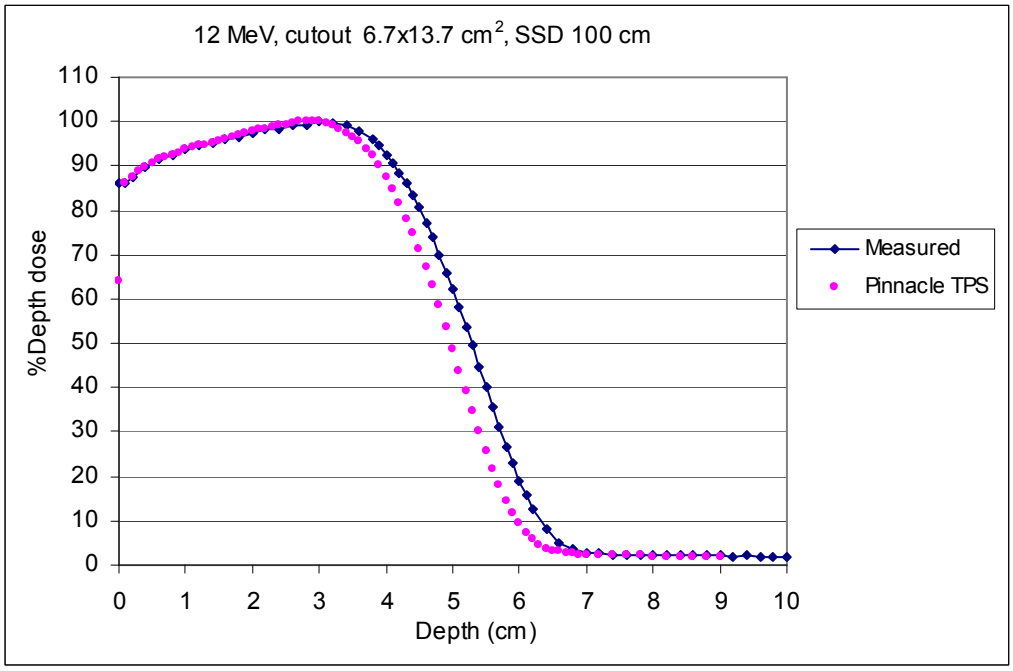
12 MeV, cutout 6.7x13.7 cm2, SSD 100 cm
%Depth dose
Depth (cm)
Measured
Pinnacle TPS

(d)

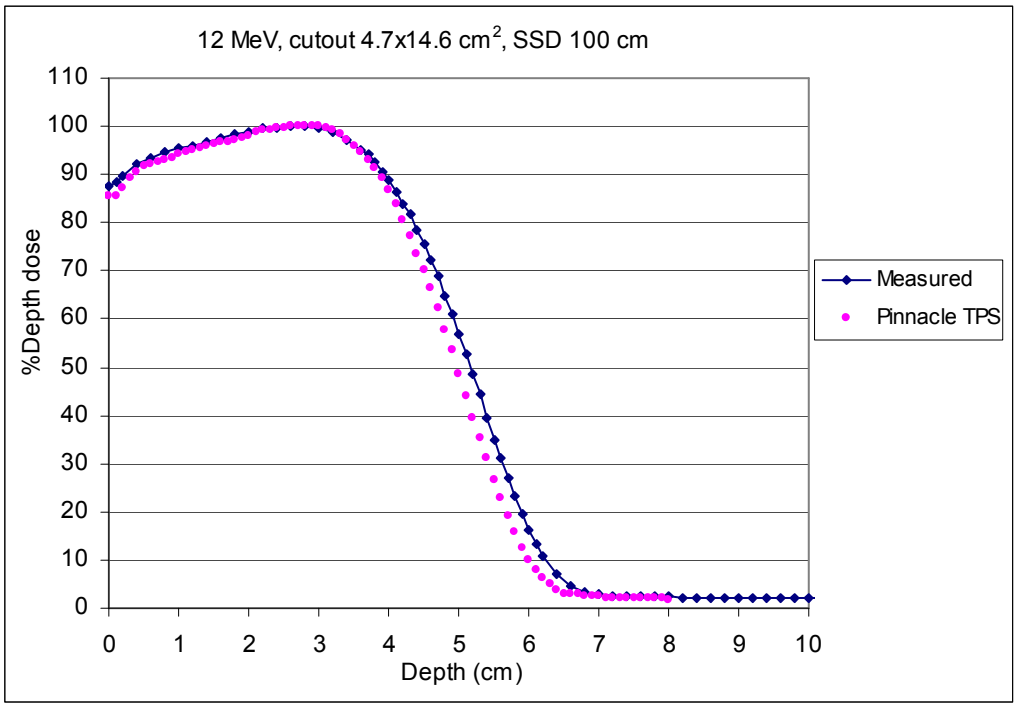

(e)

Figure 5.15 The comparison of percent depth dose for 12 MeV electron beams between Pinnacle calculation and diode measurement for insert (a) circular cutout diameter 5.2 cm and rectangular cutout of (b) 8.7 × 6.8, (c) 9.5 × 4.2, (d) 6.7 × 13.7 and (e) 4.7 × 14.6 cm^2.

Table 5.5 Average %dose difference and distance difference of buildup region and fall-off region between diode measurement and Pinnacle calculation for Percent Depth Dose (PDD) with insert circular cutout ∅5.2 cm and rectangular cutout of 8.7 × 6.8, 9.5 × 4.2, 6.7 × 13.7 and 4.7 × 14.6 cm^2.

Region	Cone (cm^2)	**% dose difference**		
		6 MeV	**9 MeV**	**12 MeV**
Buildup region	∅5.2cm	-0.114%	-1.626%	-1.253%
	8.7 × 6.8	1.355%	0.82%	0.053%
	9.5 × 4.2	0.986%	-1.26%	-0.352%
	6.7 × 13.7	2.2%	1.12%	0.162%
	4.7 × 14.6	0.813%	-0.931%	-1.242%
Region	Cone (cm^2)	**Distance to agreement (cm)**		
		6 MeV	**9 MeV**	**12 MeV**
Fall-off region	∅5.2cm	-0.077	-0.233	-0.17
	8.7 × 6.8	-0.194	-0.265	-0.274
	9.5 × 4.2	-0.212	-0.253	-0.25
	6.7 × 13.7	-0.256	-0.286	-0.299
	4.7 × 14.6	-0.135	-0.259	-0.183

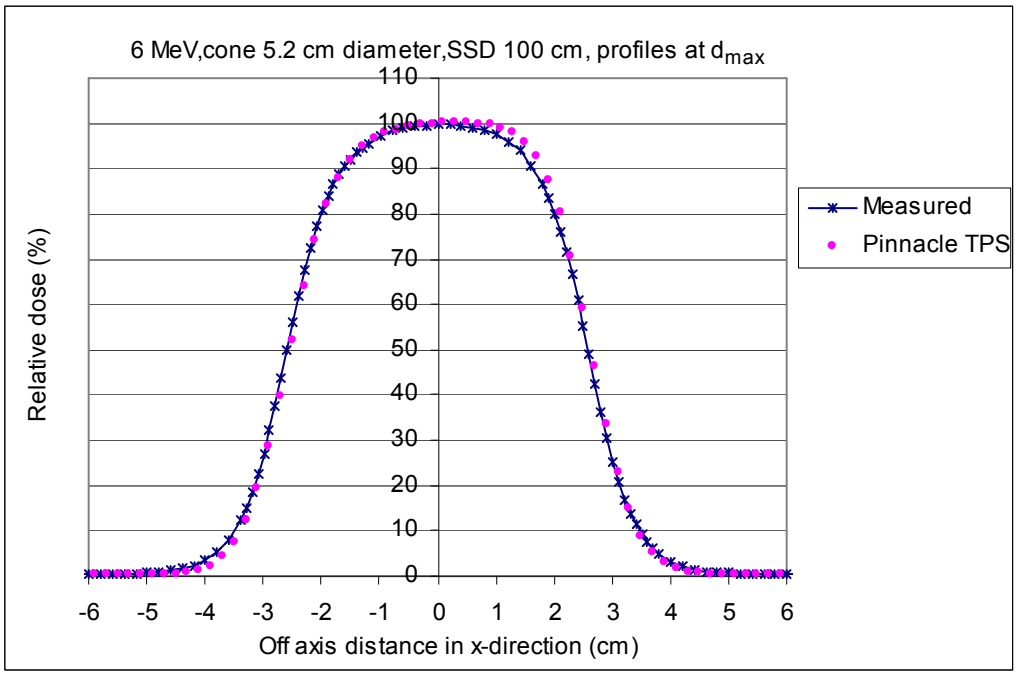

(a)

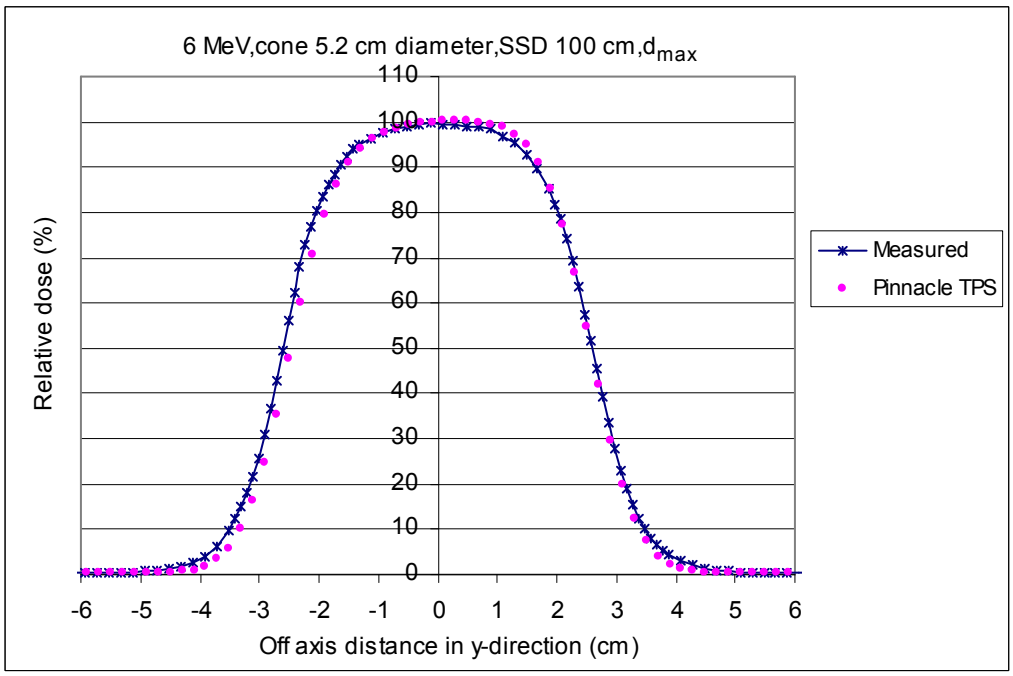

(b)

Figure 5.16 The comparison of relative dose profiles at the depth of maximum dose between Pinnacle TPS and diode measurement is shown for circular cutout diameter 5.2 cm, SSD 100 cm with electron energy 6 MeV both in x-direction (a) and y-direction (b).

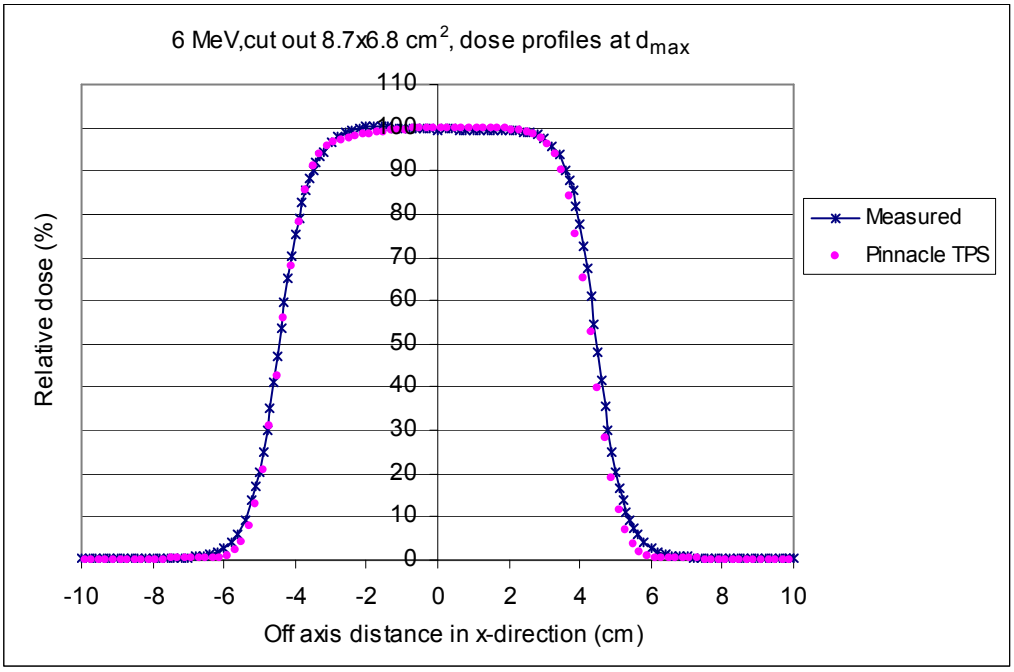

(a)

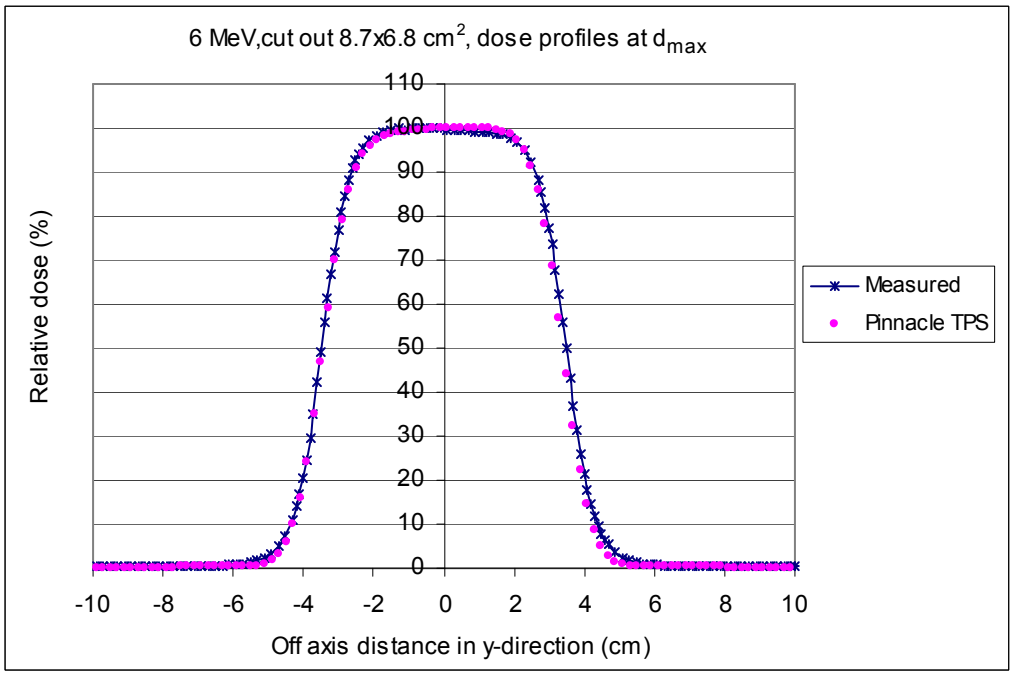

(b)

Figure 5.17 The comparison of relative dose profiles at the depth of maximum dose between Pinnacle TPS and diode measurement is shown for insert cutout 8.7 × 6.8 cm^2, SSD 100 cm with electron energy 6 MeV both in x-direction (a) and y-direction (b).

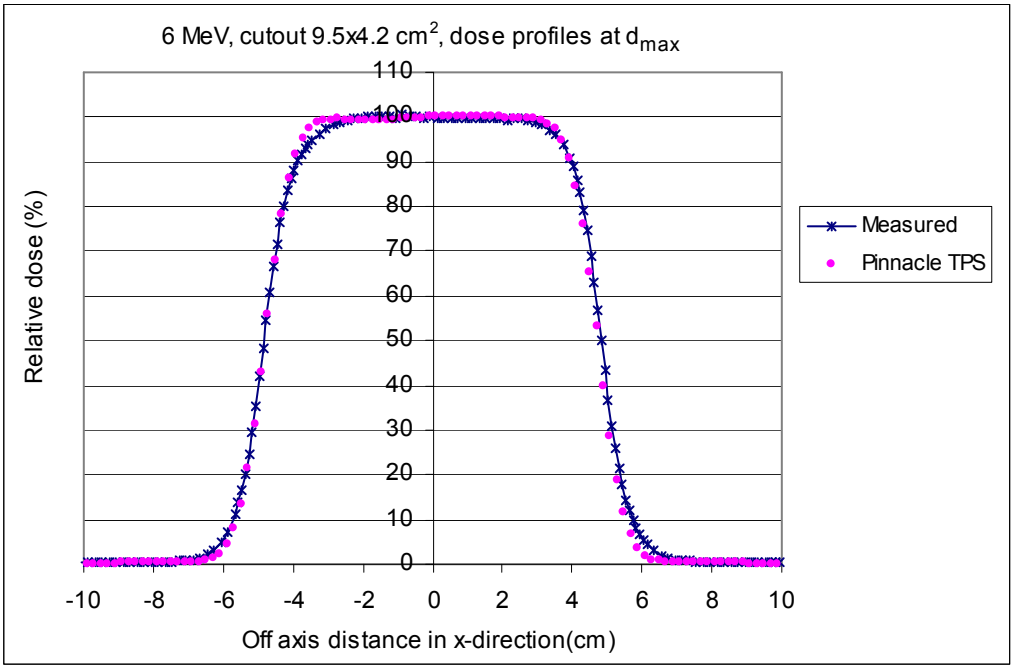

(a)

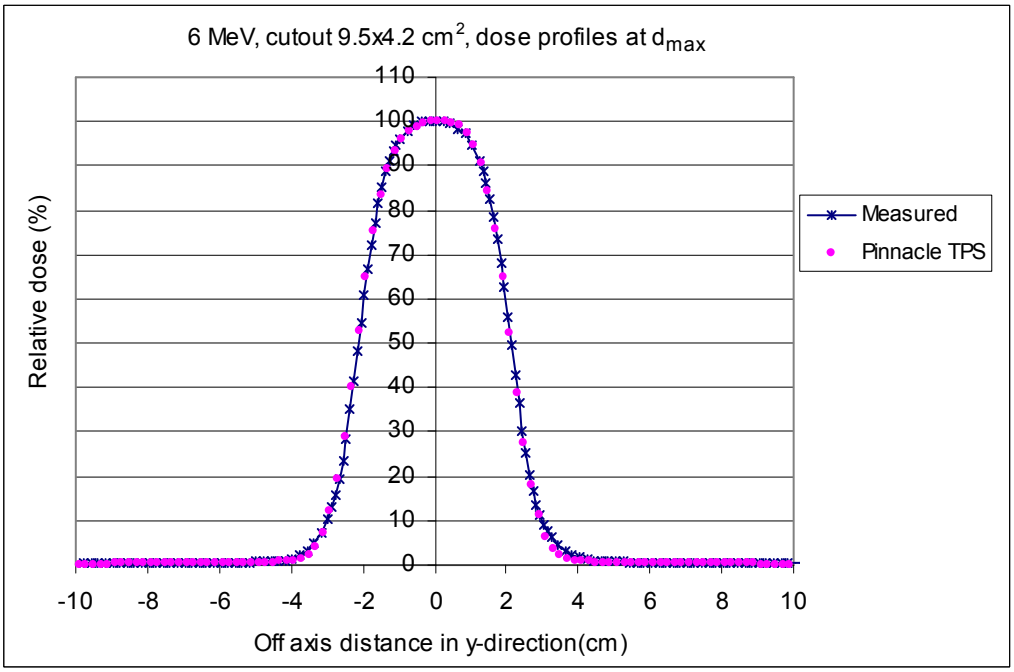

(b)

Figure 5.18 The comparison of relative dose profiles at the depth of maximum dose between Pinnacle TPS and diode measurement is shown for insert cutout 9.5 × 4.2 cm^2, SSD 100 cm with electron energy 6 MeV both in x-direction (a) and y-direction (b).

.

Table 5.6 The difference of beam fringe ($\delta_{50\text{-}90}$), radiological width (RW_{50}), penumbra width (δ_2), outside central beam axis region (δ_3) and outside beam edges (δ_4) between Pinnacle calculation and diode measurement for circular cutout diameter 5.2 cm and rectangular cutout of 8.7 × 6.8 and 9.5 × 4.2 cm^2 at the maximum depth that insert to standard cone 10 × 10 cm^2 and irradiated with electron energy 6 MeV electron beams.

	Direction	**Distance to agreement (cm)**		
		∅ 5.2 cm	**8.7 × 6.8 cm^2**	**9.5 × 4.2 cm^2**
$\delta_{50\text{-}90}$	X	0.096	0.017	0.033
	Y	0.038	0.167	0.018
RW_{50}	X	0.1	0.3	0.16
	Y	0.17	0.15	0
δ_2 (80-20%)	X	0.09	0.002	0.028
	Y	0.011	0.053	0.01
	Depth	**% dose difference**		
		∅ 5.2 cm	**8.7 × 6.8 cm^2**	**9.5 × 4.2 cm^2**
δ_3	X	-	0.596%	2.2%
	Y	-	1.47%	-
δ_4	X	0.95%	2.52%	2.83%
	Y	2.88%	2.67%	2.56%

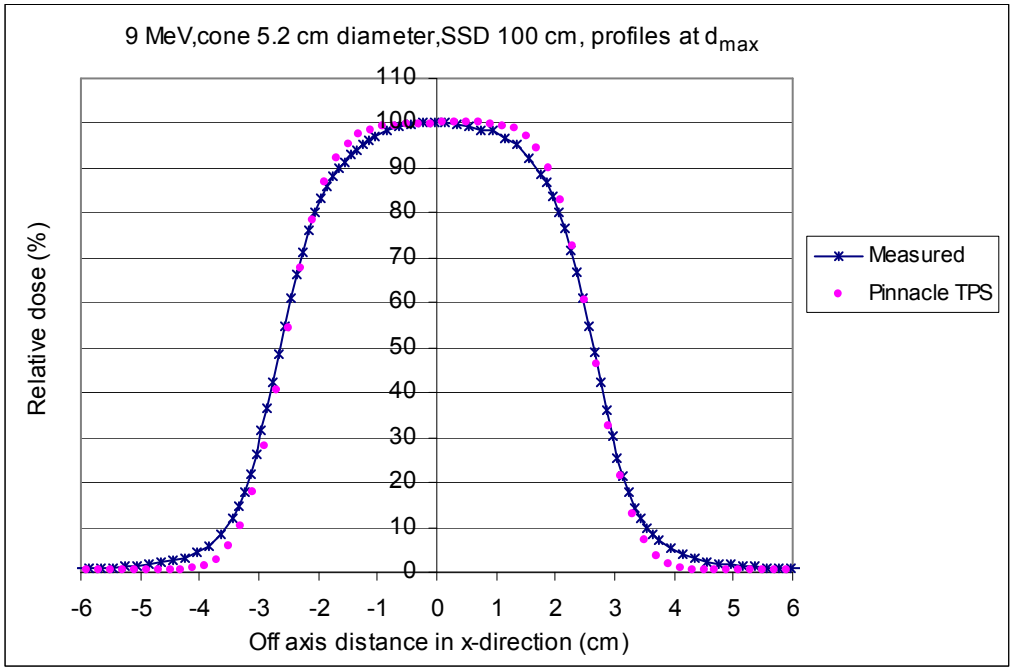

(a)

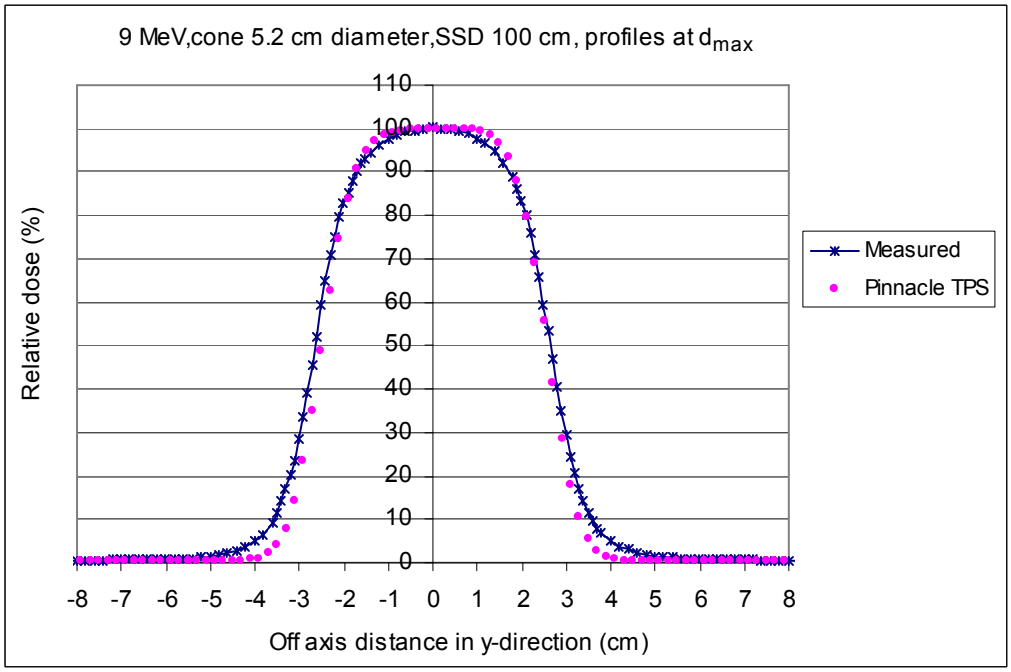

(b)

Figure 5.19 The comparison of relative dose profiles at the depth of maximum dose between Pinnacle TPS and diode measurement is shown for circular cutout diameter 5.2 cm, SSD 100 cm with electron energy 9 MeV both in x-direction (a) and y-direction (b).

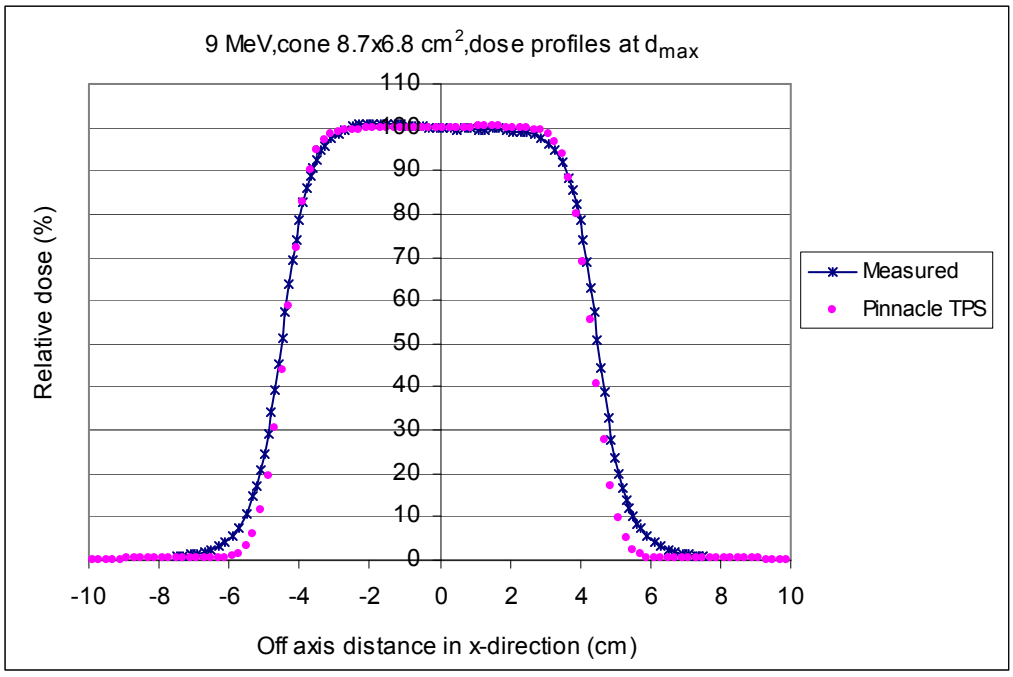

(a)

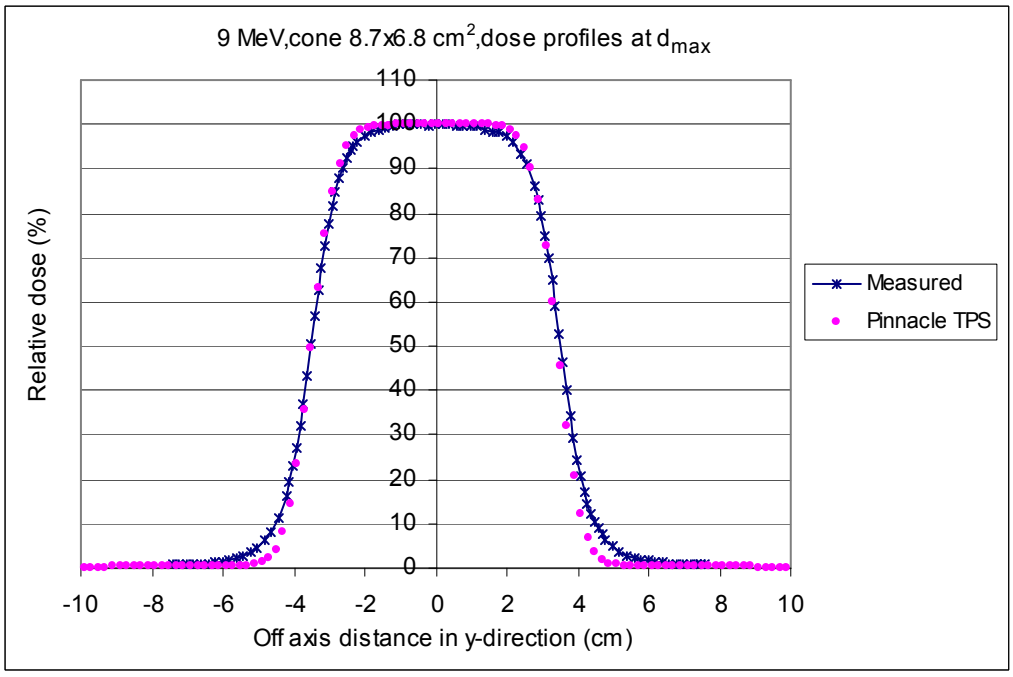

(b)

Figure 5.20 The comparison of relative dose profiles at the depth of maximum dose between Pinnacle TPS and diode measurement is shown for insert cutout 8.7 × 6.8 cm^2, SSD 100 cm with electron energy 9 MeV both in x-direction (a) and y-direction (b).

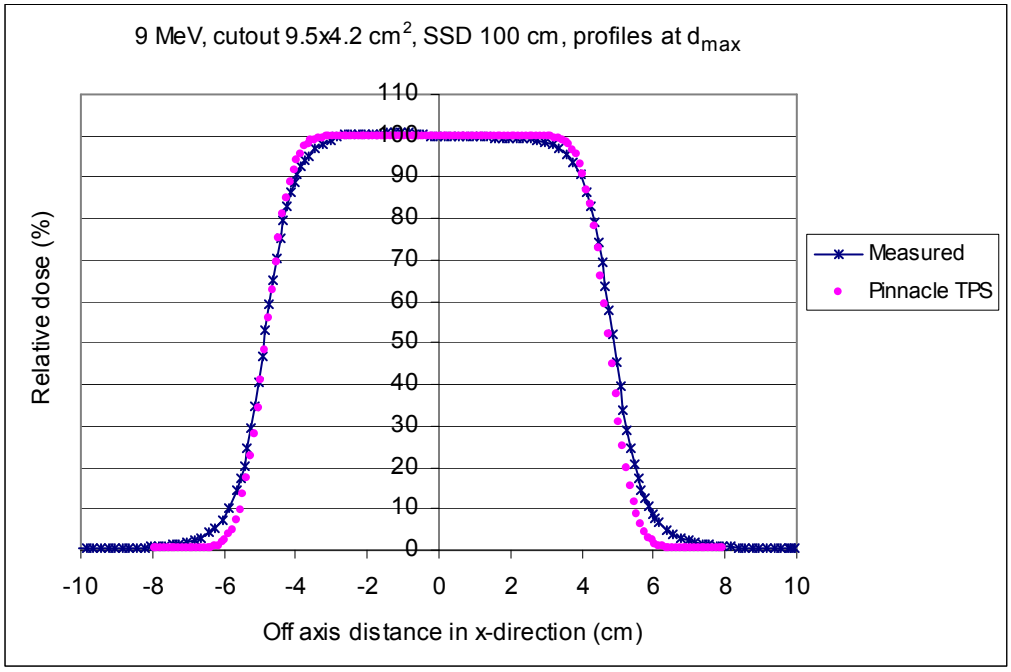

(a)

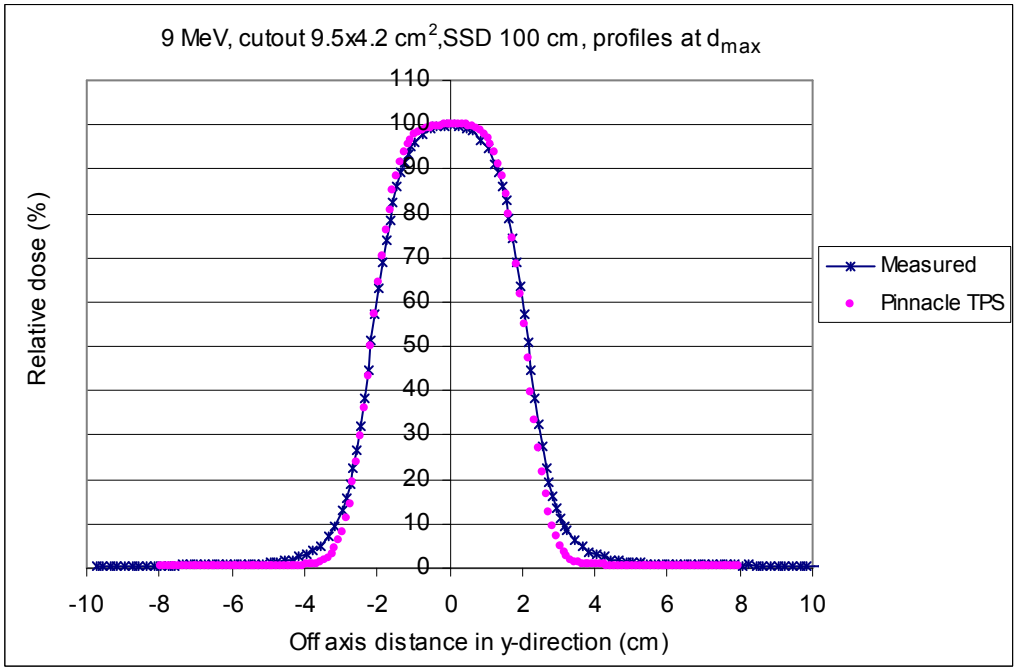

(b)

Figure 5.21 The comparison of relative dose profiles at the depth of maximum dose between Pinnacle TPS and diode measurement is shown for insert cutout 9.5 × 4.2 cm^2, SSD 100 cm with electron energy 9 MeV both in x-direction (a) and y-direction (b).

Table 5.7 The difference of beam fringe ($\delta_{50\text{-}90}$), radiological width (RW_{50}), penumbra width (δ_2), outside central beam axis region (δ_3) and outside beam edges (δ_4) between Pinnacle calculation and diode measurement for circular cutout diameter 5.2 cm and rectangular cutout of 8.7 × 6.8 and 9.5 × 4.2 cm^2 at the maximum depth that insert to standard cone 10 × 10 cm^2 and irradiated with electron energy 9 MeV electron beams.

	Direction	**Distance to agreement (cm)**		
		∅ 5.2 cm	**8.7 × 6.8 cm^2**	**9.5 × 4.2 cm^2**
$\delta_{50\text{-}90}$	X	0.16	0.17	0.17
	Y	0.01	0.38	0.13
RW_{50}	X	0.1	0.2	0.15
	Y	0.21	0.02	0.02
δ_2 (80-20%)	X	0.18	0.23	0.20
	Y	0.04	0.33	0.17
	Depth	**%dose difference**		
		∅ 5.2 cm	**8.7 × 6.8 cm^2**	**9.5 × 4.2 cm^2**
δ_3	X	-	0.54%	1.84%
	Y	-	2.77%	-
δ_4	X	4.25%	4.8%	5.48%
	Y	5.1%	5.2%	5.04%

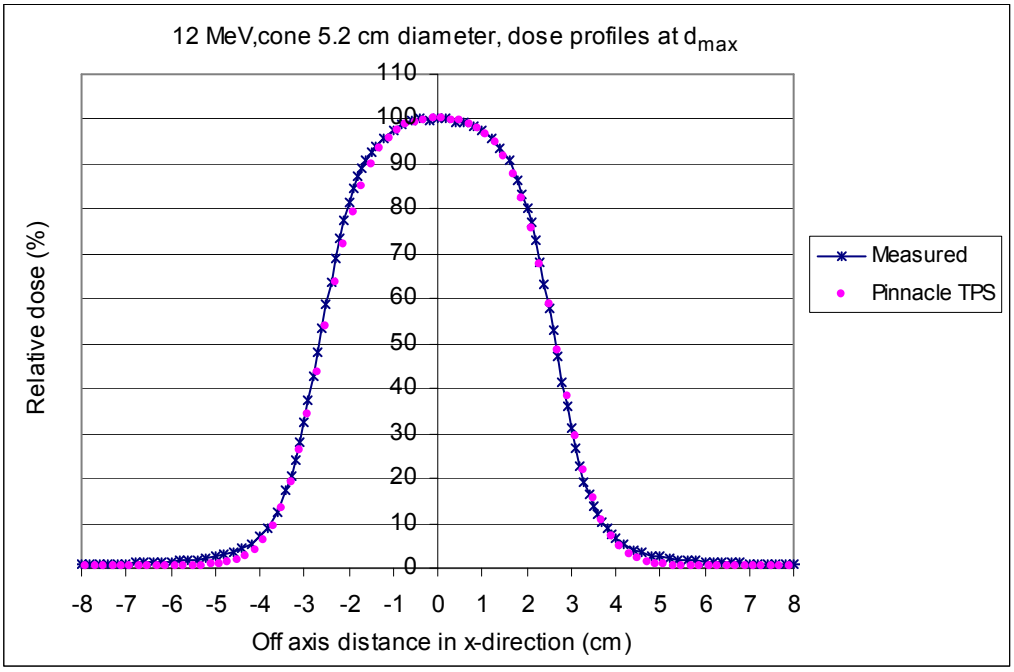

(a)

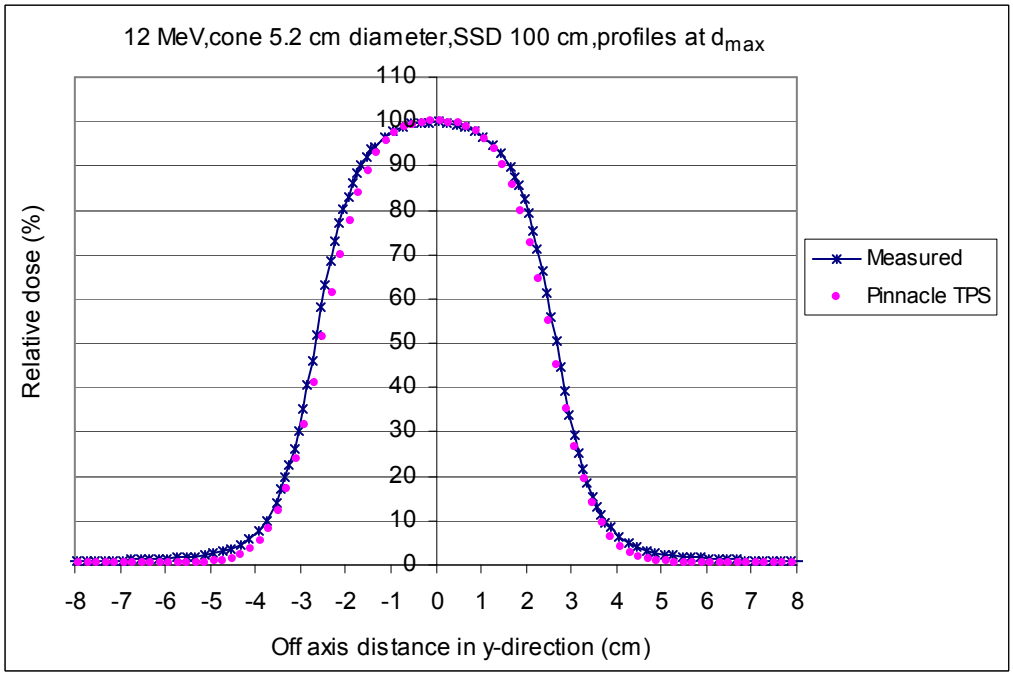

(b)

Figure 5.22 The comparison of relative dose profiles at the depth of maximum dose between Pinnacle TPS and diode measurement is shown for circular cutout diameter 5.2 cm, SSD 100 cm with electron energy 12 MeV both in x-direction (a) and y-direction (b).

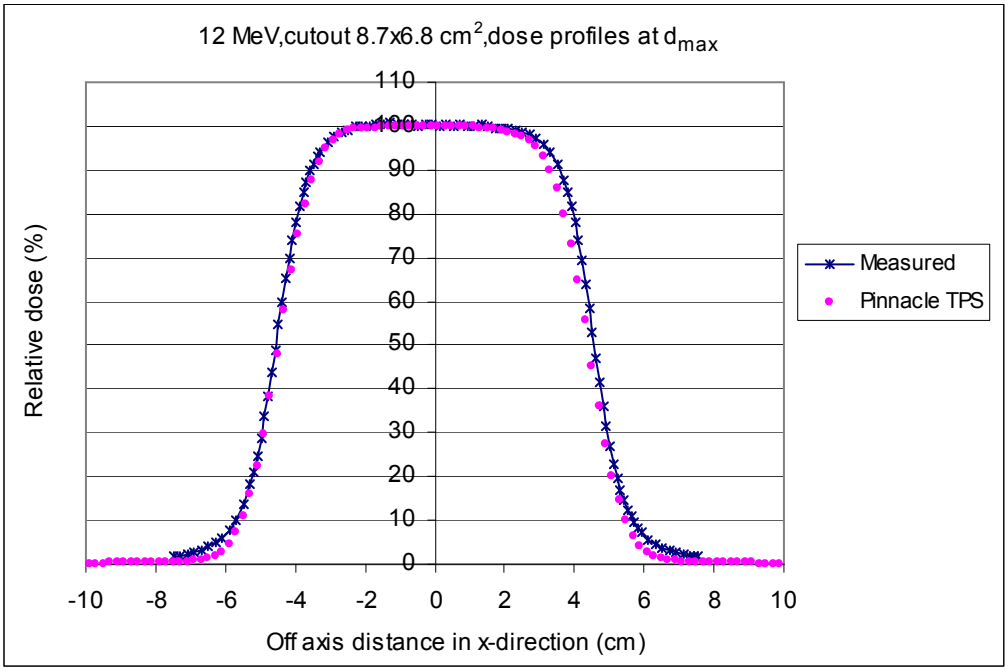

(a)

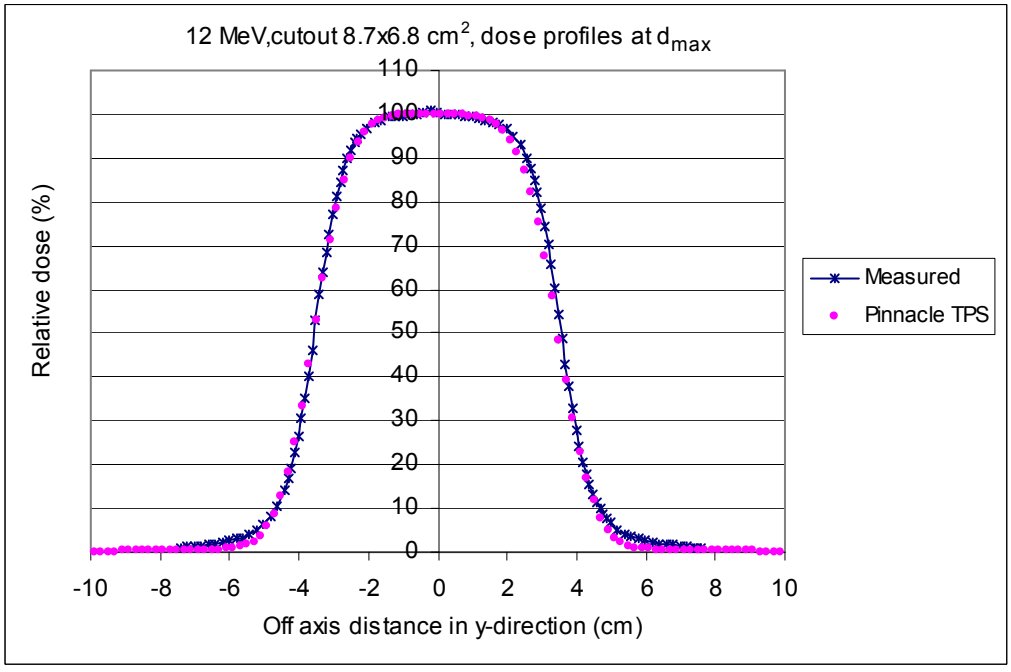

(b)

Figure 5.23 The comparison of relative dose profiles at the depth of maximum dose between Pinnacle TPS and diode measurement is shown for insert cutout 8.7 × 6.8 cm^2, SSD 100 cm with electron energy 12 MeV both in x-direction (a) and y-direction (b).

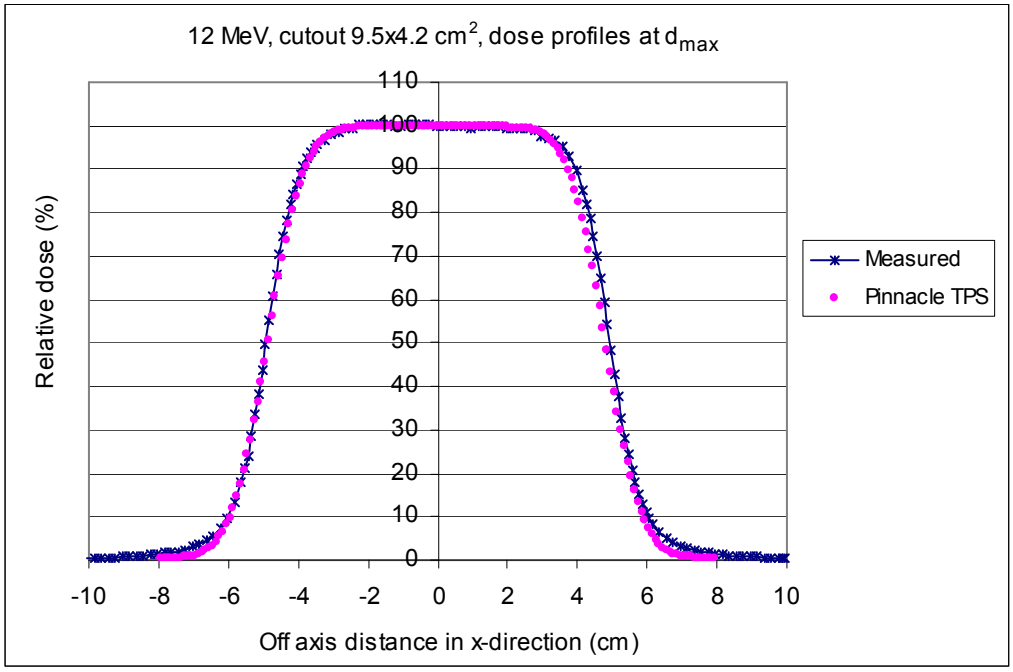

(a)

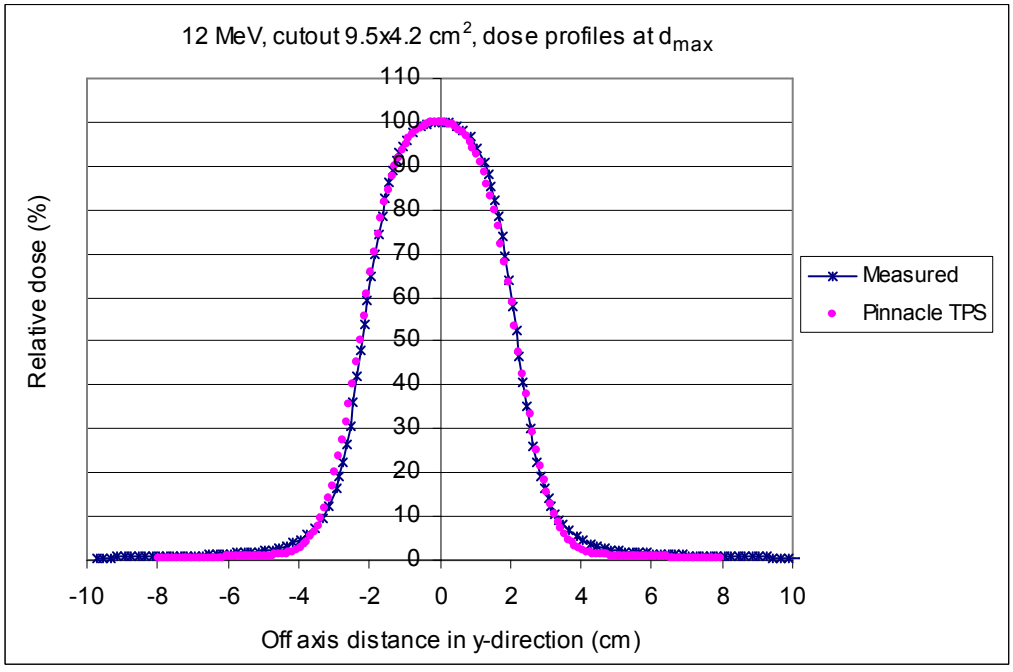

(b)

Figure 5.24 The comparison of relative dose profiles at the depth of maximum dose between Pinnacle TPS and diode measurement is shown for insert cutout 9.5 × 4.2 cm^2, SSD 100 cm with electron energy 12 MeV both in x-direction (a) and y-direction (b).

Table 5.8 The difference of beam fringe ($\delta_{50\text{-}90}$), radiological width (RW_{50}), penumbra width (δ_2), outside central beam axis region (δ_3) and outside beam edges (δ_4) between Pinnacle calculation and diode measurement for circular cutout diameter 5.2 cm and rectangular cutout of 8.7 × 6.8 and 9.5 × 4.2 cm^2 at the maximum depth that insert to standard cone 10×10 cm^2 and irradiated with electron energy 12 MeV electron beams.

	Direction	**Distance to agreement (cm)**		
		∅ 5.2 cm	**8.7 × 6.8 cm^2**	**9.5 × 4.2 cm^2**
$\delta_{50\text{-}90}$	X	0.082	0.124	0.085
	Y	0.135	0.327	0.118
RW_{50}	X	0.1	0.3	0.2
	Y	0.2	0.13	0.02
δ_2 (80-20%)	X	0.028	0.163	0.123
	Y	0.116	0.31	0.14
	Depth	**% dose difference**		
		∅ 5.2 cm	**8.7 × 6.8 cm^2**	**9.5 × 4.2 cm^2**
δ_3	X	-	1.75%	0.283%
	Y	-	2.62%	-
δ_4	X	0.824%	2.87%	2.63%
	Y	2.27%	2.50%	1.87%

C. Extended SSD

In this experiment, the influence of SSD variation on TPS dose calculations was investigated. The comparisons between diode-measured and Pinnacle-calculated central axis percent depth dose are shown in figures 5.25 to 5.33 (a-b). The agreement was within 4% or 0.4 cm, except the buildup region of electron energy 6 MeV. The deviation was found in standard cone 4 × 4 cm^2 at extended SSD 110 cm and was about 5%. At the rapid dose fall-off region, the Pinnacle TPS had the diminished dose faster than the measurement for all applicator cones, SSDs and energies. Table 5.9 shows the average of % dose difference and distance difference at buildup region and fall-off region between diode measurements and Pinnacle calculations of Percent Depth Dose (PDD) for standard cone 4 × 4, 10 × 10 and 20 × 20 cm^2 at extended SSD 105 and 110 cm.

Figure 5.34 to 5.42 (a-b) show the comparison of relative dose profiles at the maximum depth between Pinnacle calculations and diode measurements for standard cone 4 × 4, 10 × 10 and 20 × 20 cm^2 with a 105 cm and 110 cm SSD. The agreement of dose profiles was reasonable. Table 5.10-5.12 show the difference between Pinnacle calculation and diode measurement for standard cone 4 × 4, 10 × 10 and 20 × 20 cm^2 at the maximum depths with a 105 cm and 110 cm SSD and irradiated with electron energy 6, 9 and 12 MeV electron beams. Table 5.10 shows that the maximum differences are within 4%/0.4 cm for both SSDs with 6 MeV electron beam. However 9 MeV electron beam which shown in Table 5.11, gives the maximum difference at 110 cm SSD and applicator size 20 × 20 cm^2 which is 6.43% for the δ_4 (the point off geometrical beam edges) and 0.54 cm for the δ_2 (penumbra width: distance between the 20%-80% point dose). For the 12 MeV, Table 5.12 shows that the maximum difference appears at 110 cm SSD and applicator size 10 × 10 cm^2 which is about 5% for the δ_3 (point outside the central beam axis) and 0.9 cm for the δ_2 (penumbra width: distance between the 20%-80% point dose). Better models are produced for lower energies (6 and 9 MeV) than medium energy (12 MeV). The most noticeable differences were found near the field edges and penumbra width because the dose profile was modeled at standard treatment distance (100 cm) but not the extended SSD.

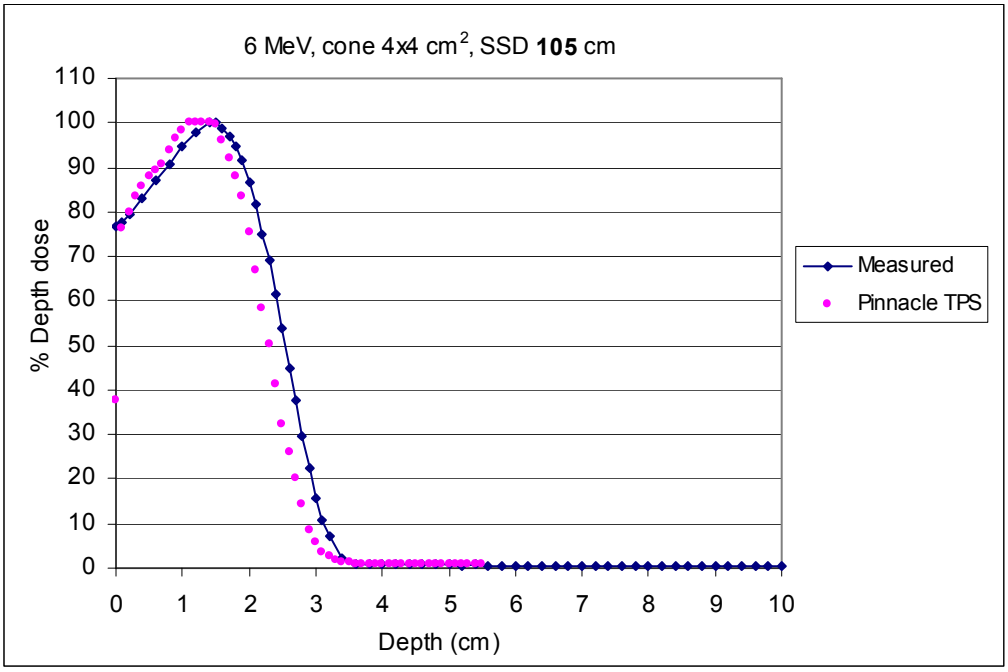

(a)

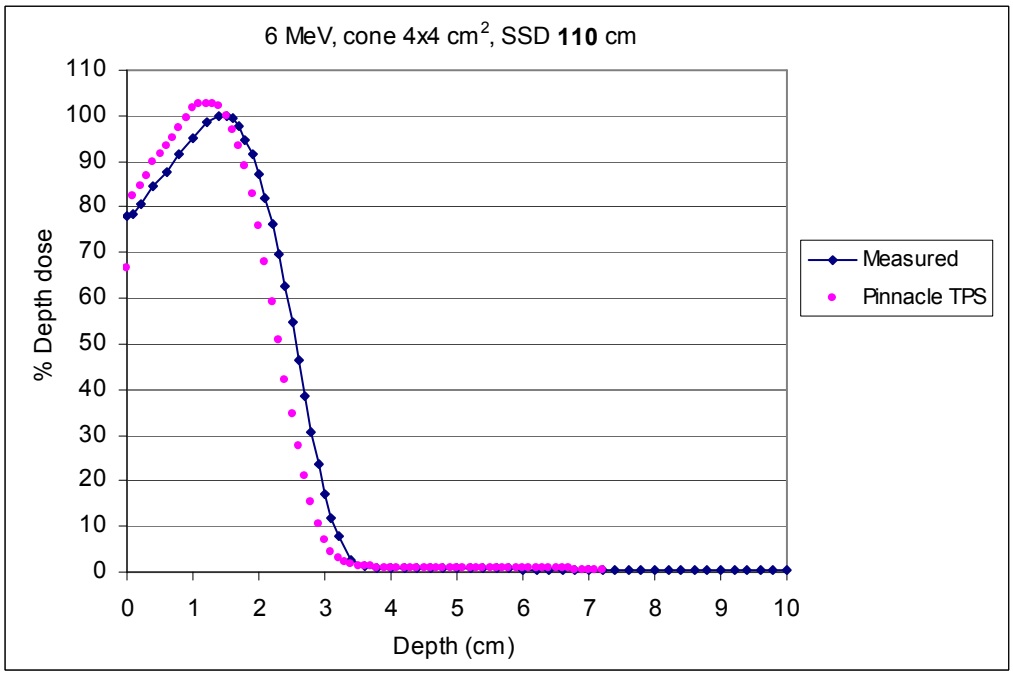

(b)

Figure 5.25 The comparison of percent depth dose for 6 MeV electron beams of Pinnacle calculation and diode measurement for standard cone 4 × 4 cm^2 at extended SSD (a) 105 cm and (b) 110 cm.

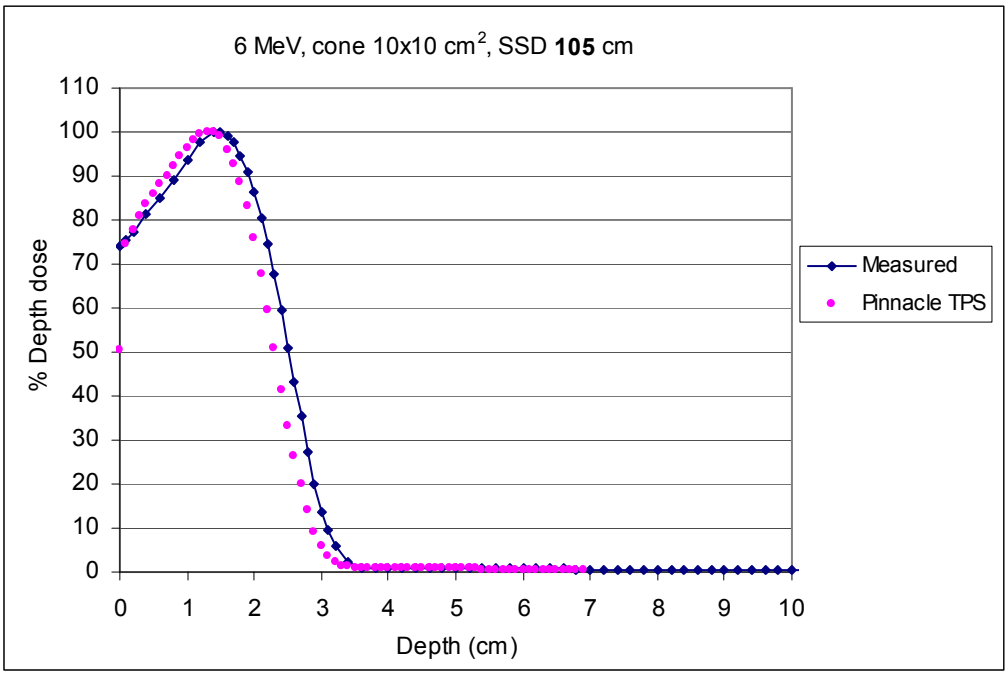

(a)

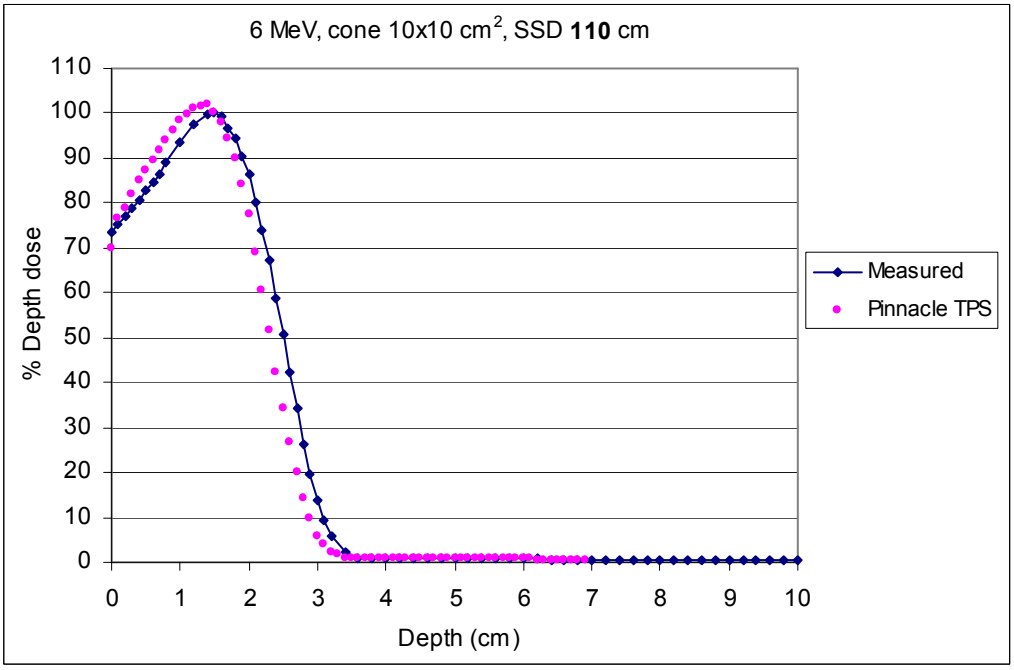

(b)

Figure 5.26 The comparison of percent depth dose for 6 MeV electron beams of Pinnacle calculation and diode measurement for standard cone 10 × 10 cm^2 at extended SSD (a) 105 cm and (b) 110 cm.

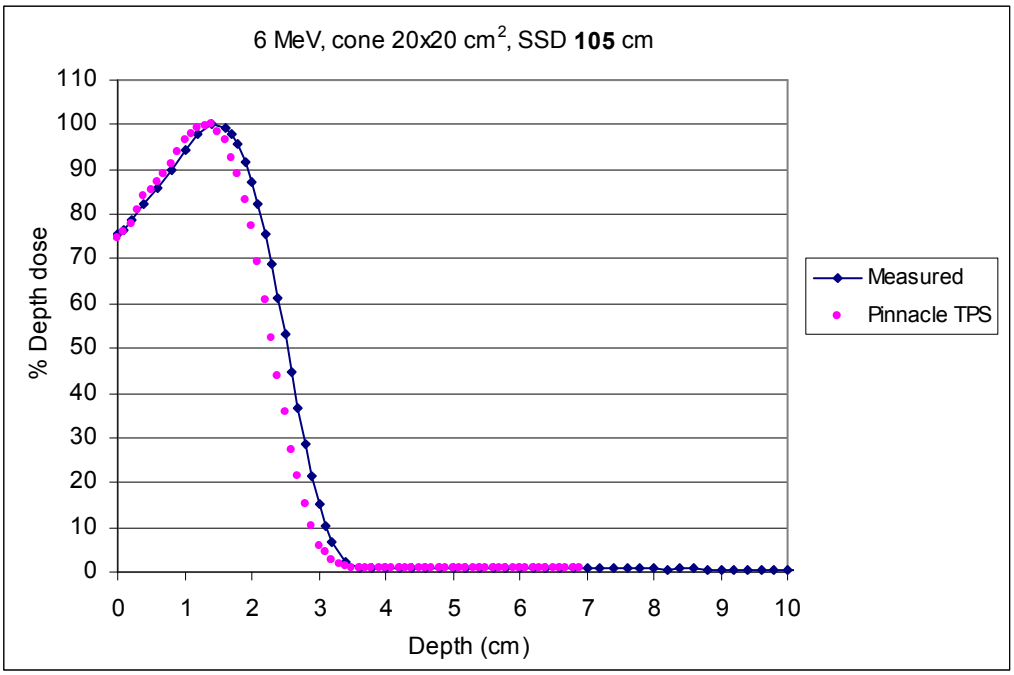

(a)

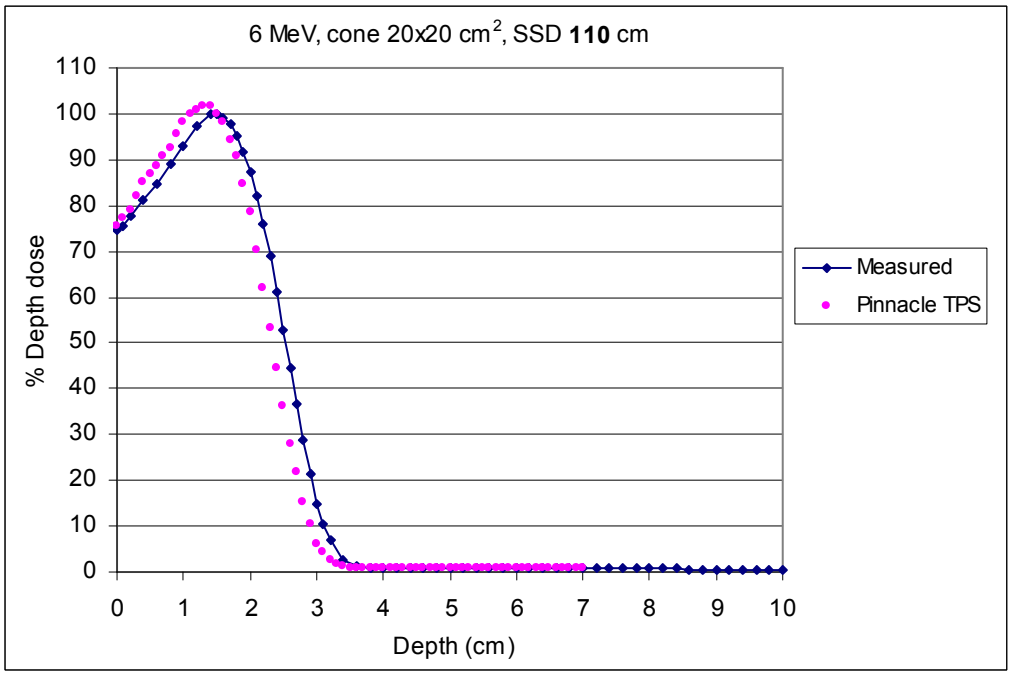

(b)

Figure 5.27 The comparison of percent depth dose for 6 MeV electron beams of Pinnacle calculation and diode measurement for standard cone 20 × 20 cm^2 at extended SSD (a) 105 cm and (b) 110 cm.

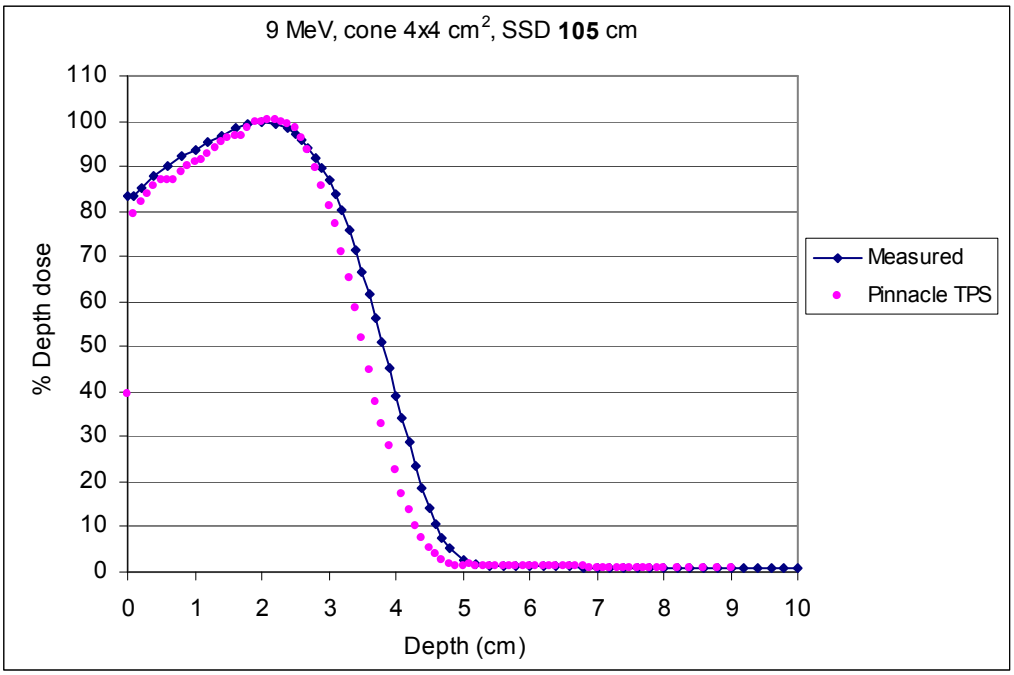

(a)

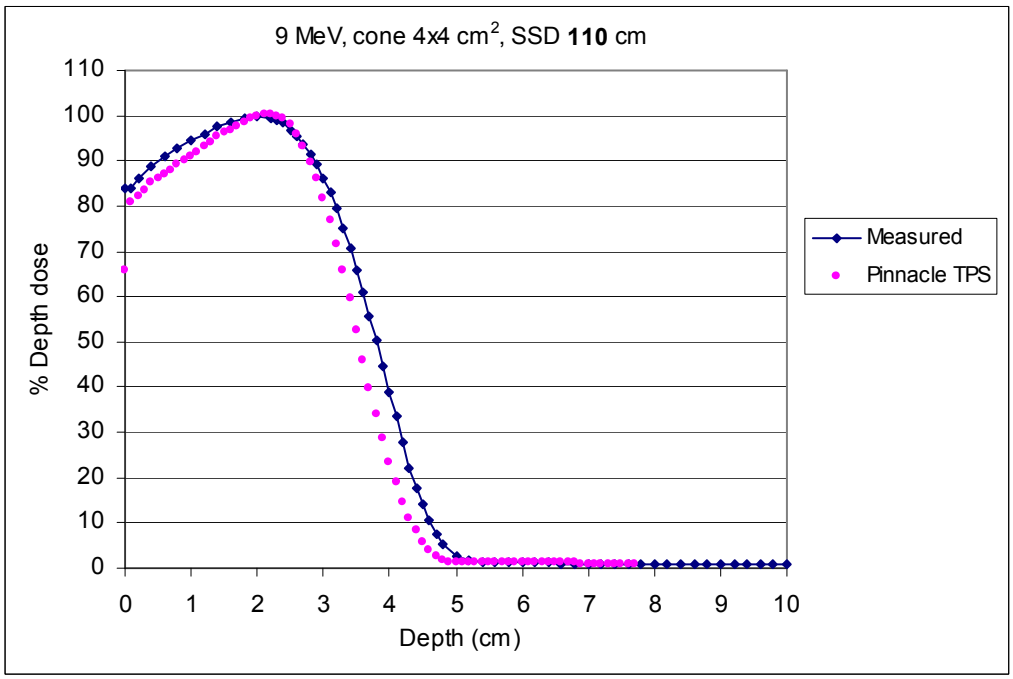

(b)

Figure 5.28 The comparison of percent depth dose for 9 MeV electron beams of Pinnacle calculation and diode measurement for standard cone 4 × 4 cm^2 at extended SSD (a) 105 cm and (b) 110 cm.

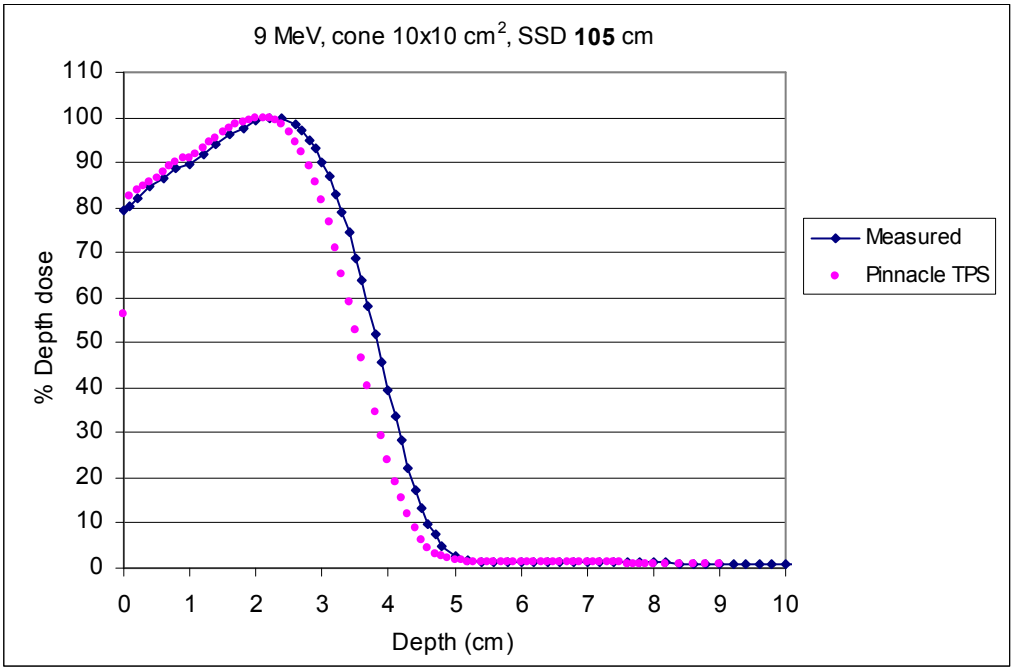

(a)

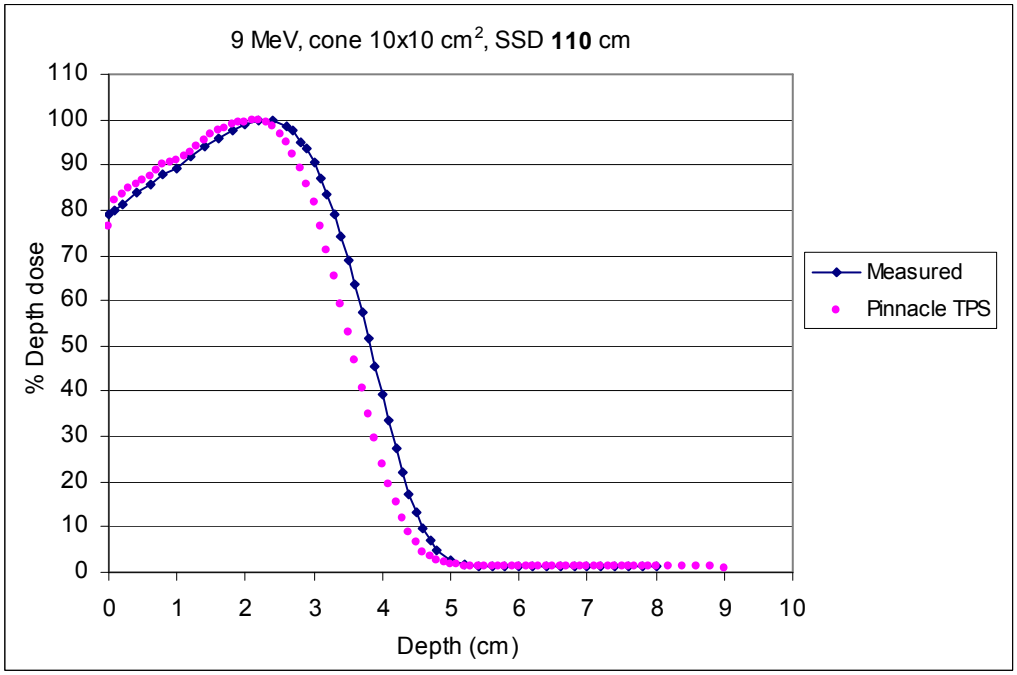

(b)

Figure 5.29 The comparison of percent depth dose for 9 MeV electron beams of Pinnacle calculation and diode measurement for standard cone 10 × 10 cm^2 at extended SSD (a) 105 cm and (b) 110 cm.

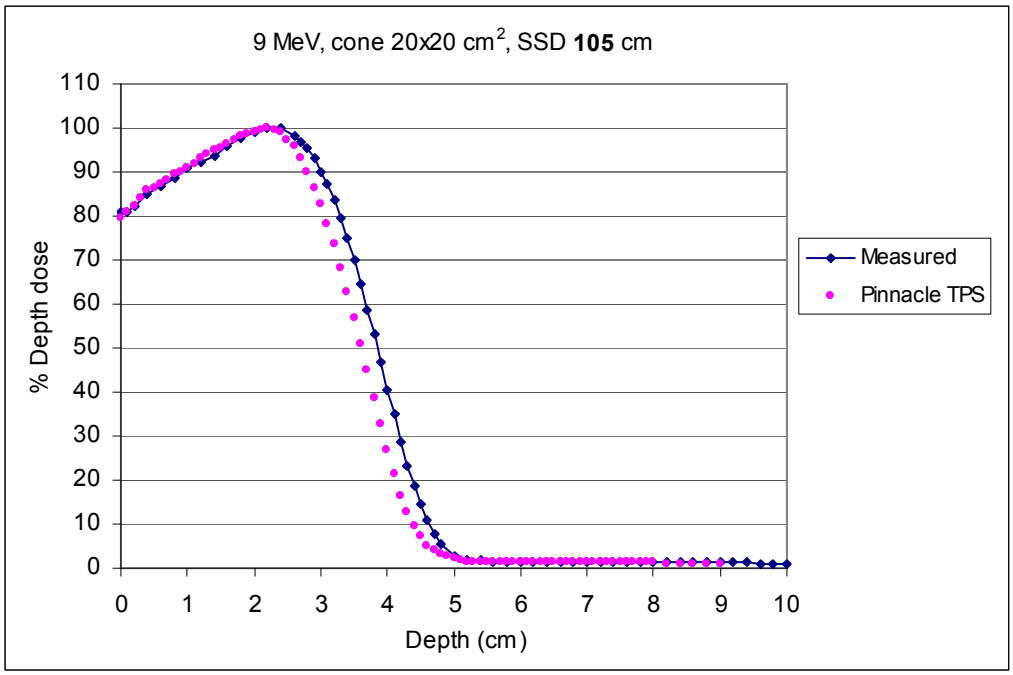

(a)

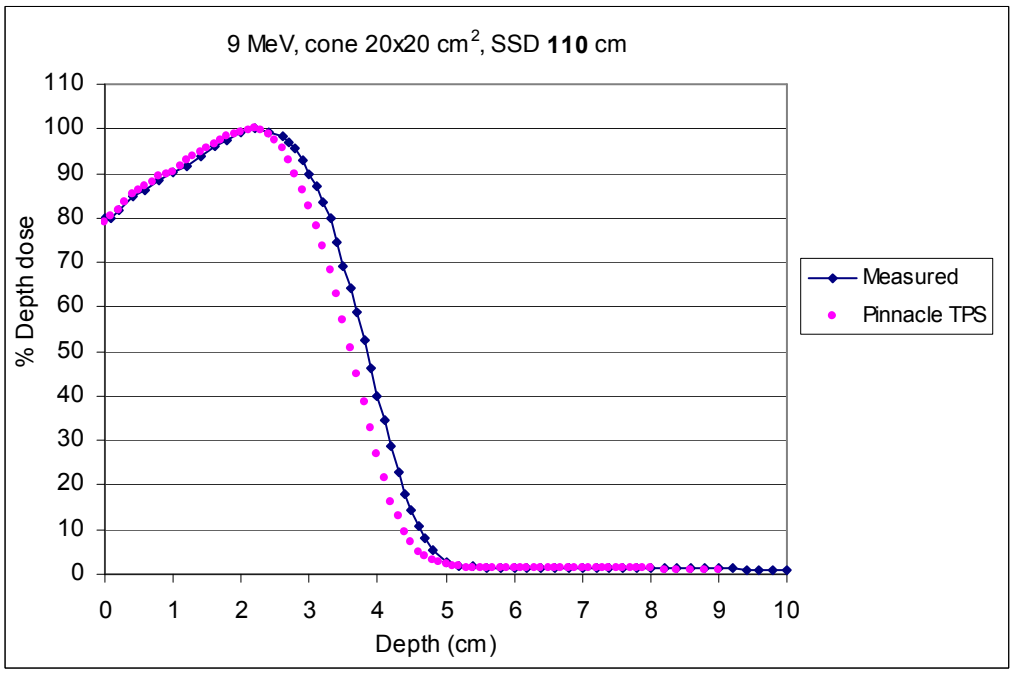

(b)

Figure 5.30 The comparison of percent depth dose for 9 MeV electron beams of Pinnacle calculation and diode measurement for standard cone 20 × 20 cm^2 at extended SSD (a) 105 cm and (b) 110 cm.

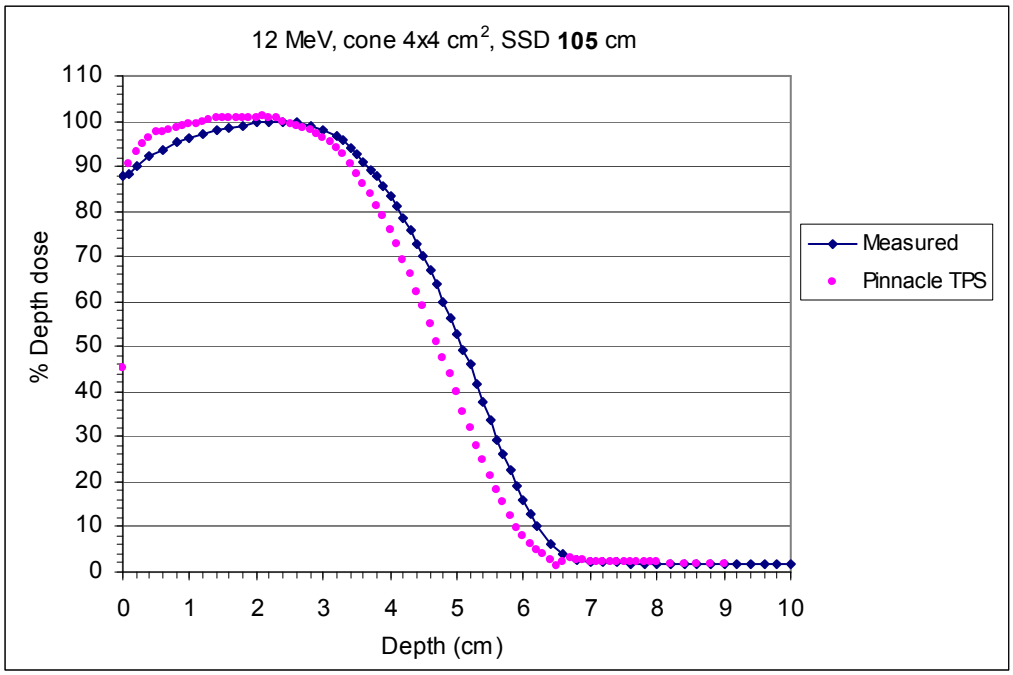

(a)

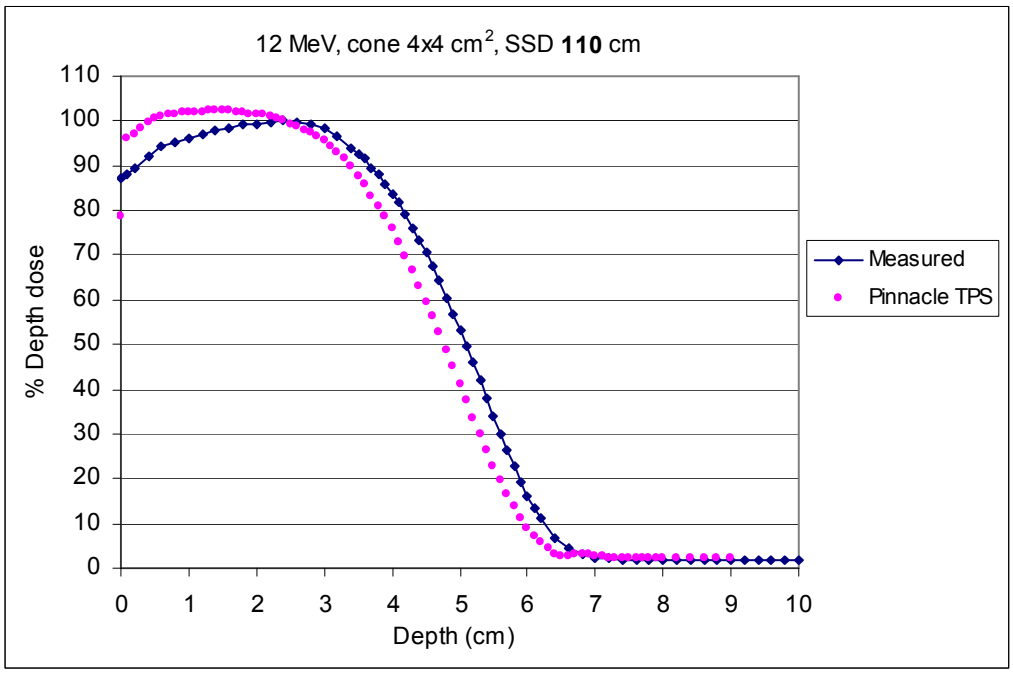

(b)

Figure 5.31 The comparison of percent depth dose for 12 MeV electron beams of Pinnacle calculation and diode measurement for standard cone 4 × 4 cm^2 at extended SSD (a) 105 cm and (b) 110 cm.

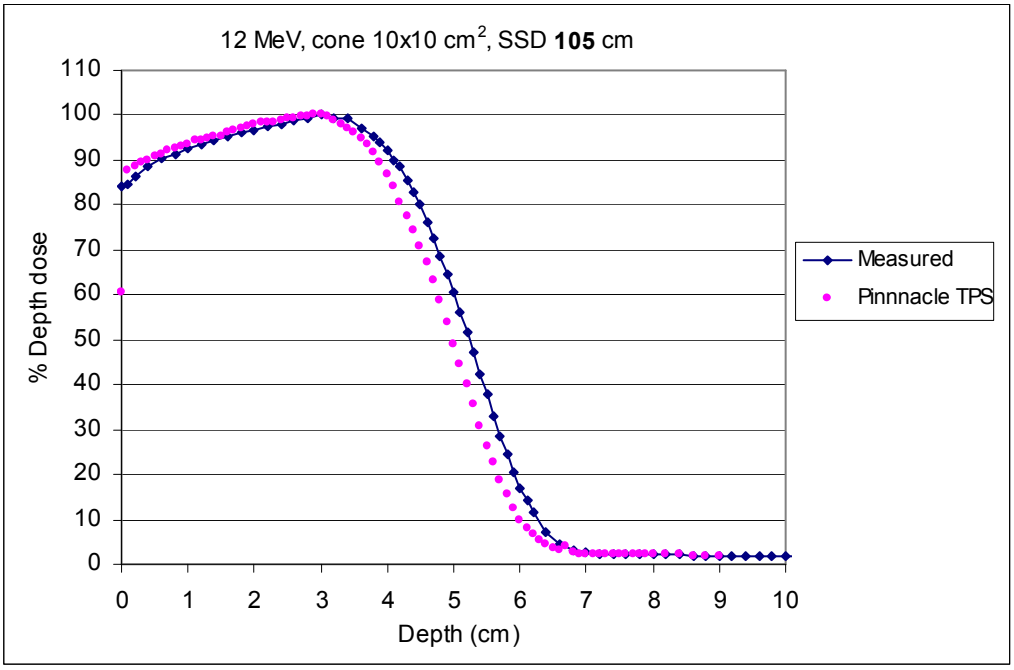

(a)

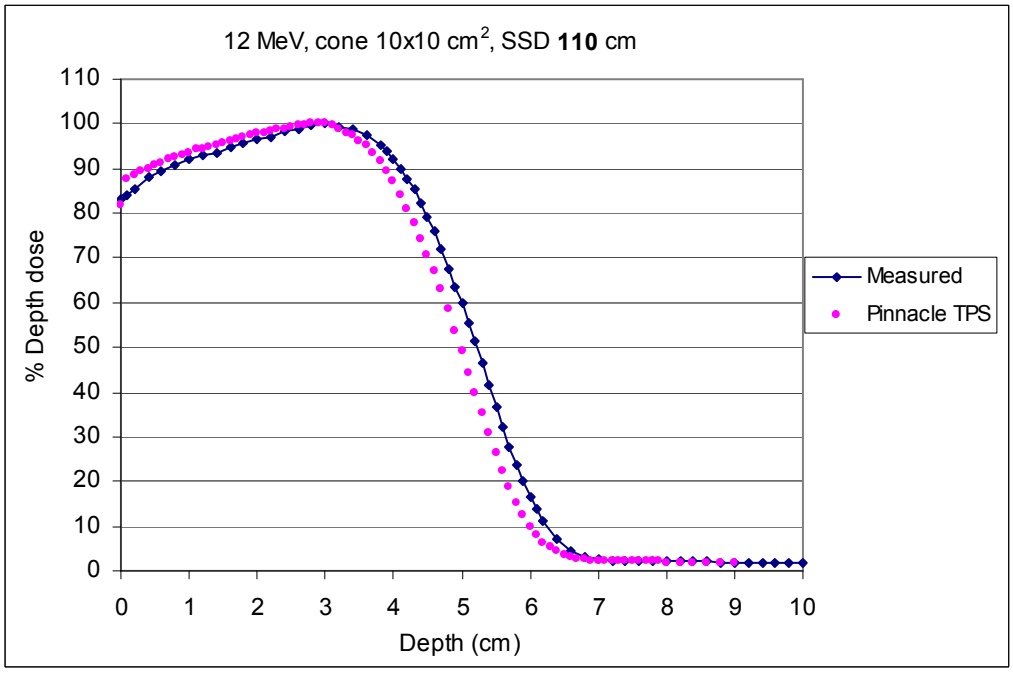

(b)

Figure 5.32 The comparison of percent depth dose for 12 MeV electron beams of Pinnacle calculation and diode measurement for standard cone 10 × 10 cm^2 at extended SSD (a) 105 cm and (b) 110 cm.

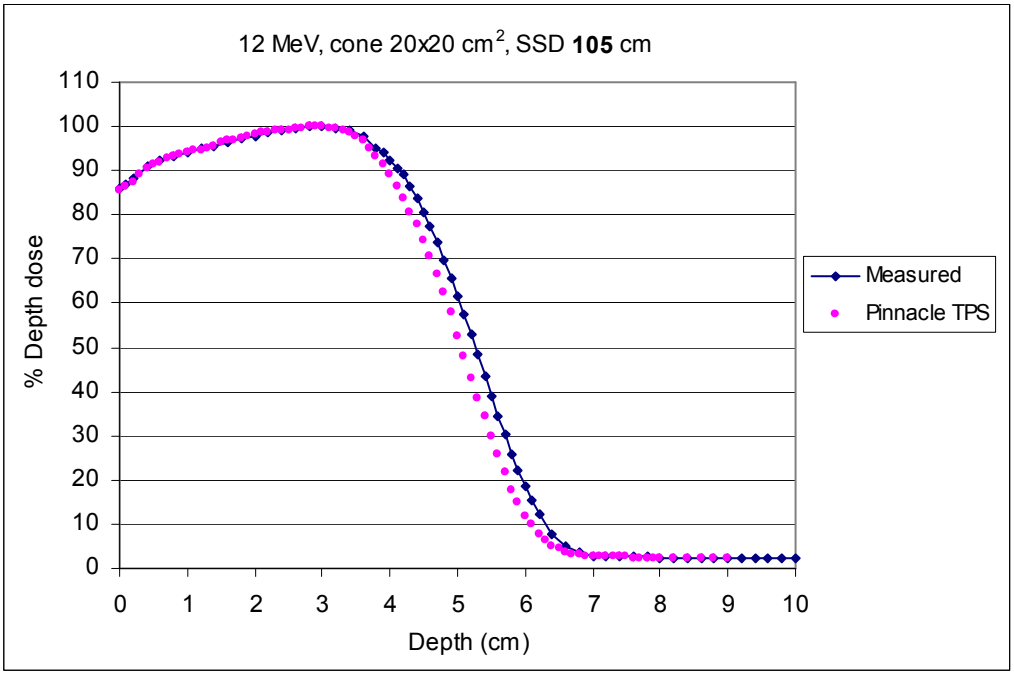

(a)

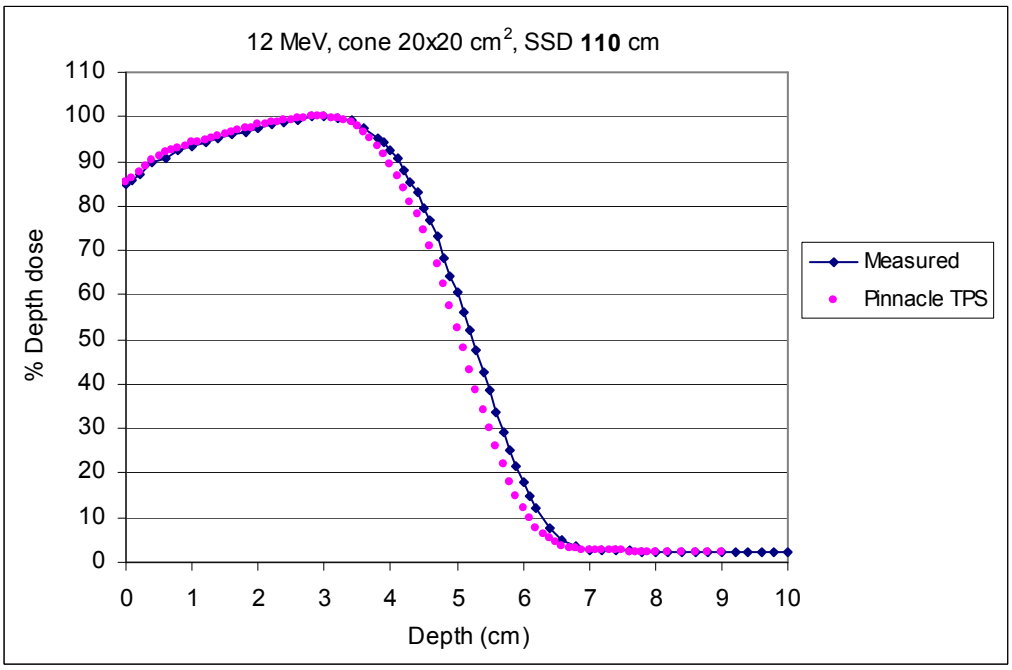

(b)

Figure 5.33 The comparison of percent depth dose for 12 MeV electron beams of Pinnacle calculation and diode measurement for standard cone 20 × 20 cm^2 at extended SSD (a) 105 cm and (b) 110 cm.

Table 5.9 Average of % dose difference and distance difference at buildup region and fall-off region between diode measurements and Pinnacle calculations of Percent Depth Dose (PDD) for standard cone 4 × 4, 10 × 10 and 20 × 20 cm^2 at extended SSD 105 and 110 cm of electron energy 6, 9 and 12 MeV.

SSD 105 cm				
Region	Cone (cm^2)	**% dose difference**		
		6 MeV	**9 MeV**	**12 MeV**
Buildup region	4 × 4	2.300%	-2.420%	2.596%
	10 × 10	2.218%	1.404%	1.060%
	20 × 20	0.978%	0.324%	-0.059%
Region	Cone (cm^2)	**Distance to agreement (cm)**		
		6 MeV	**9 MeV**	**12 MeV**
Fall-off region	4 × 4	-0.232	-0.268	-0.331
	10 × 10	-0.202	-0.272	-0.251
	20 × 20	-0.20	-0.234	-0.20
SSD 110 cm				
Region	Cone (cm^2)	**% dose difference**		
		6 MeV	**9 MeV**	**12 MeV**
Buildup region	4 × 4	5%	-2.95%	3.82%
	10 × 10	3.98%	1.64%	1.56%
	20 × 20	3.66%	0.49%	0.57%
Region	Cone (cm^2)	**Distance to agreement (cm)**		
		6 MeV	**9 MeV**	**12 MeV**
Fall-off region	4 × 4	-0.234	-0.239	-0.314
	10 × 10	-0.182	-0.265	-0.235
	20 × 20	-0.191	-0.228	-0.174

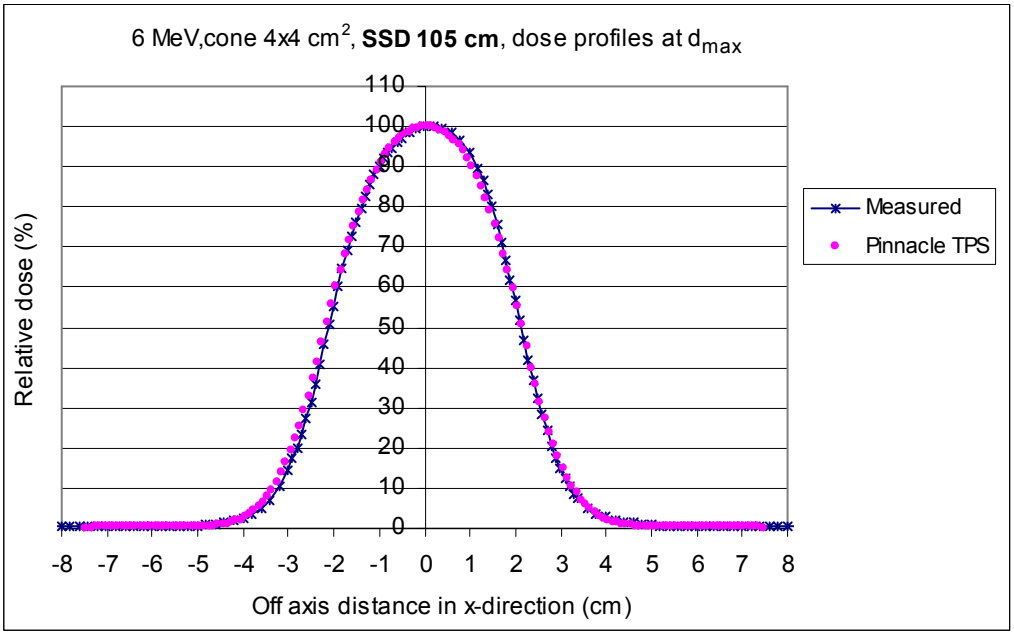

(a)

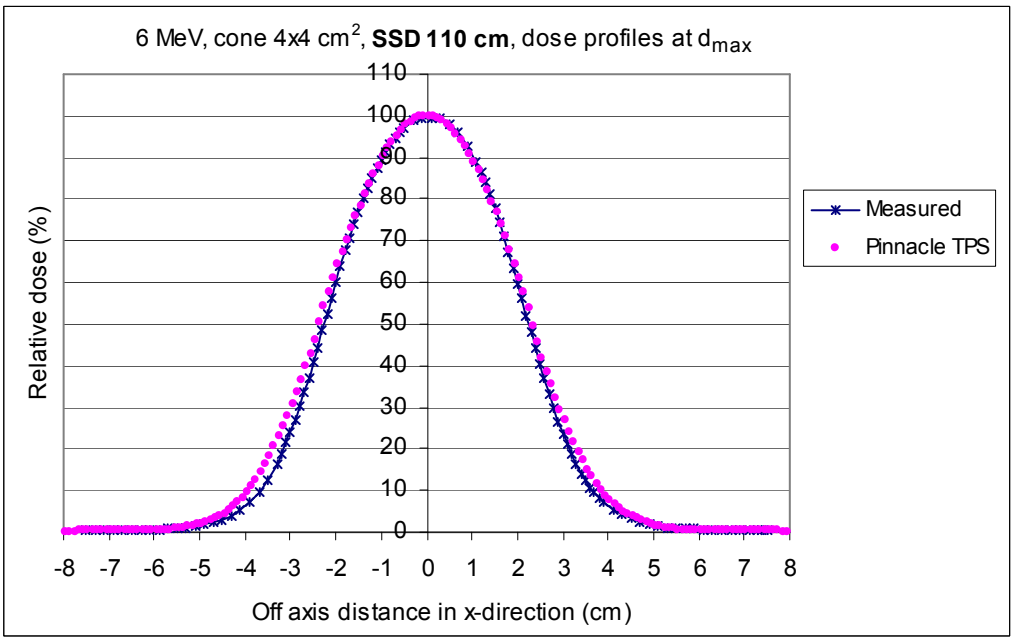

(b)

Figure 5.34 The comparison of relative dose profiles at the depth of maximum dose between Pinnacle TPS and diode measurement is shown for electron energy 6 MeV and field size 4×4 cm^2 at SSD (a) 105 cm and (b) 110 cm.

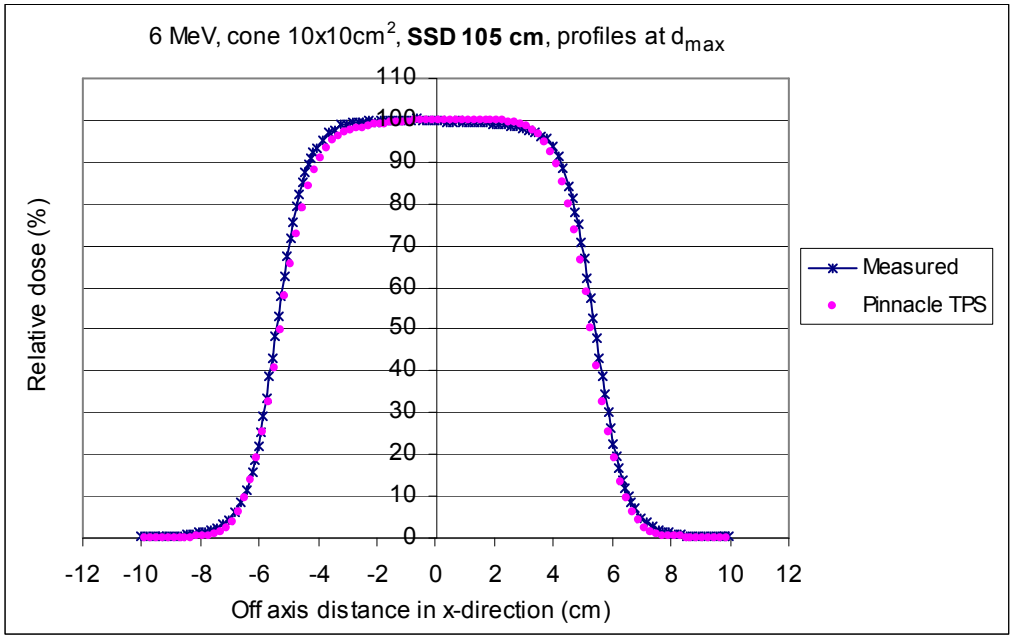

(a)

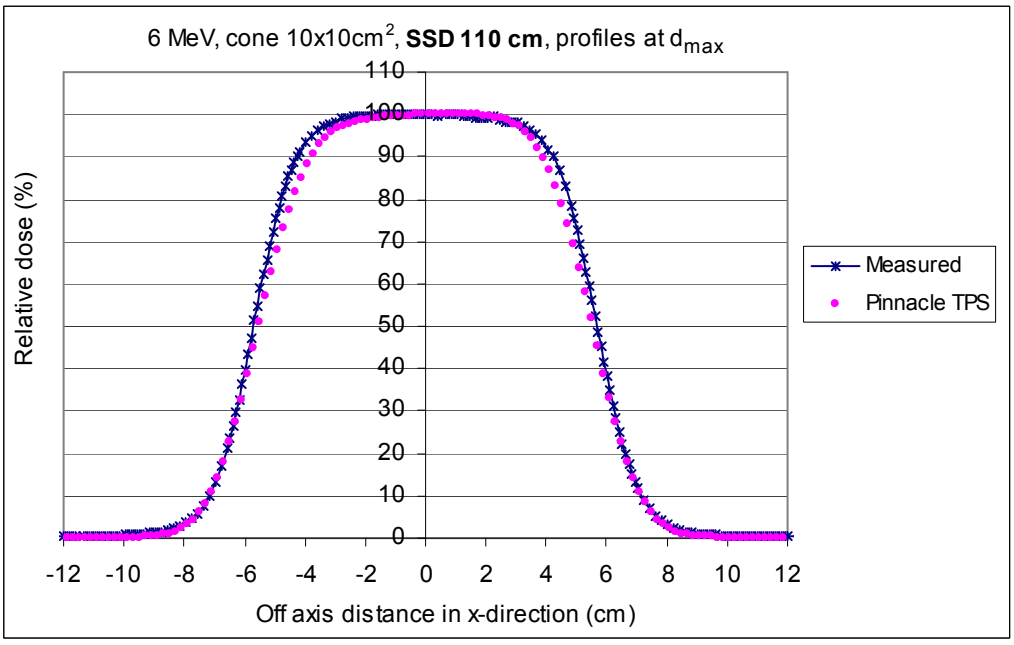

(b)

Figure 5.35 The comparison of relative dose profiles at the depth of maximum dose between Pinnacle TPS and diode measurement is shown for electron energy 6 MeV and field size $10 \times 10 cm^2$ at SSD (a) 105 cm and (b) 110 cm.

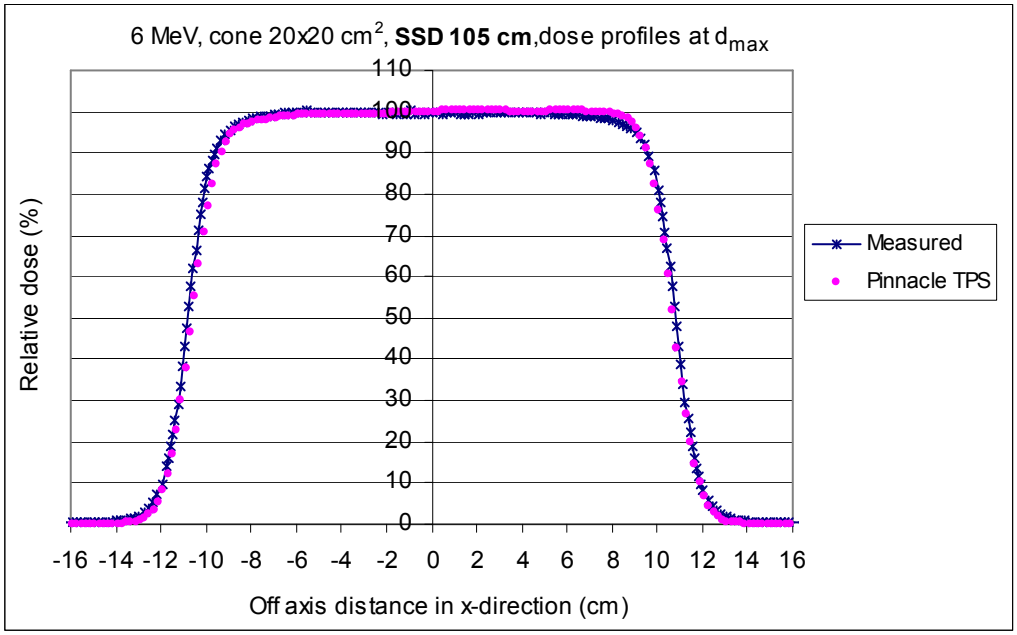

(a)

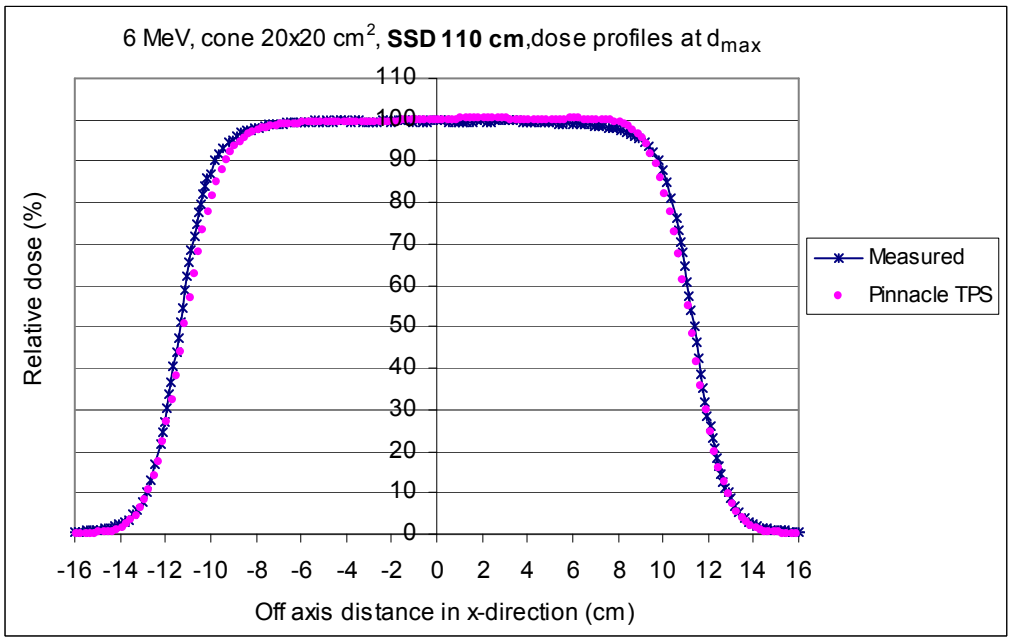

(b)

Figure 5.36 The comparison of relative dose profiles at the depth of maximum dose between Pinnacle TPS and diode measurement is shown for electron energy 6 MeV and field size 20 × 20 cm^2 at SSD (a) 105 cm and (b) 110 cm.

Table 5.10 The difference of beam fringe ($\delta_{50\text{-}90}$), radiological width (RW_{50}), penumbra width (δ_2), outside central beam axis region (δ_3) and outside beam edges (δ_4) between Pinnacle calculation and diode measurement for standard cone 4 × 4, 10 × 10 and 20 × 20 cm^2 at the maximum depths with extended SSD 105 and 110 cm, respectively and irradiated with electron energy 6 MeV electron beams.

SSD 105 cm			
	Distance to agreement (cm)		
	4 × 4 cm^2	**10 × 10 cm^2**	**20 × 20 cm^2**
$\delta_{50\text{-}90}$	0.016	0.27	0.08
RW_{50}	0.04	0.2	0.35
δ_2 (80-20%)	0.002	0.20	0.062
	% dose difference		
	4 × 4 cm^2	**10 × 10 cm^2**	**20 × 20 cm^2**
δ_3	-	2.50%	1.34%
δ_4	0.87%	1.79%	1.75%
SSD 110 cm			
	Distance to agreement (cm)		
	4 × 4 cm^2	**10 × 10 cm^2**	**20 × 20 cm^2**
$\delta_{50\text{-}90}$	0.103	0.352	0.001
RW_{50}	0.15	0.24	0.3
δ_2 (80-20%)	0.211	0.387	0.263
	% dose difference		
	4 × 4 cm^2	**10 × 10 cm^2**	**20 × 20 cm^2**
δ_3	-	3.27%	1.202%
δ_4	2.15%	0.087%	0.36%

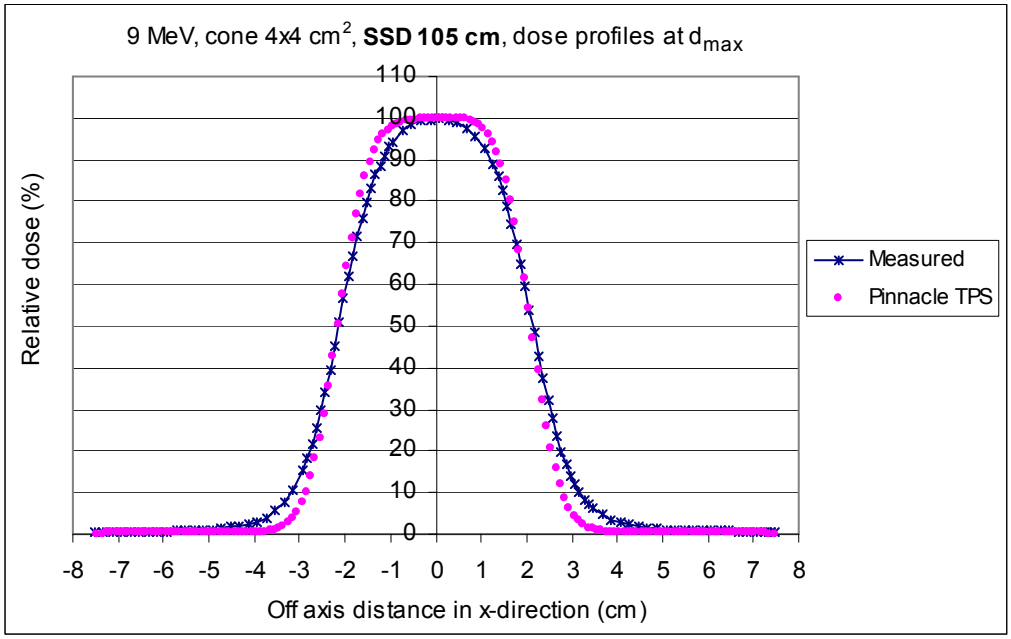

(a)

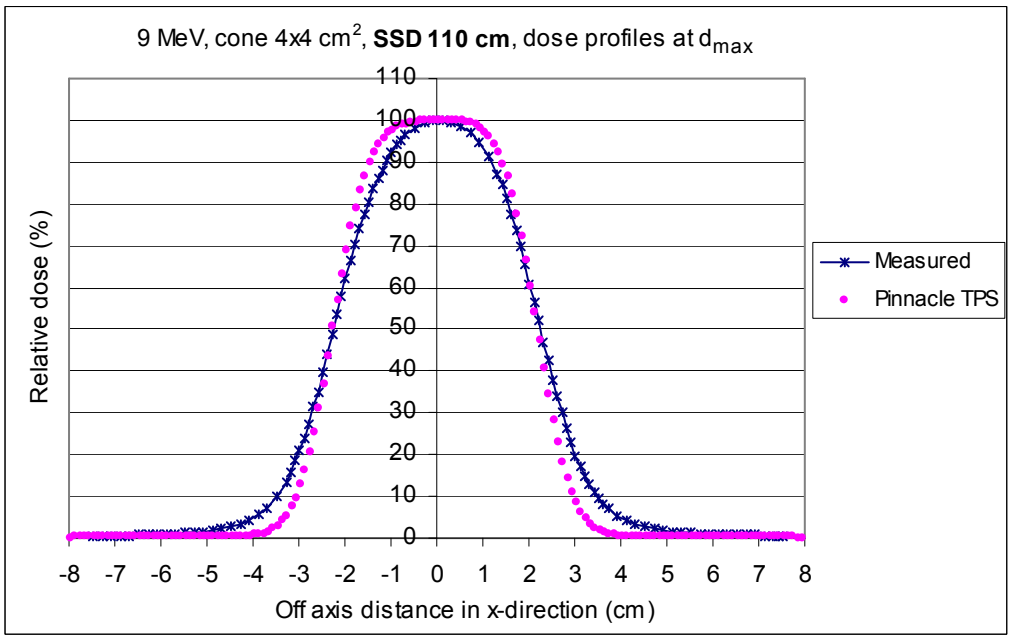

(b)

Figure 5.37 The comparison of relative dose profiles at the depth of maximum dose between Pinnacle TPS and diode measurement is shown for electron energy 9 MeV and field size 4×4 cm^2 at SSD (a) 105 cm and (b) 110 cm .

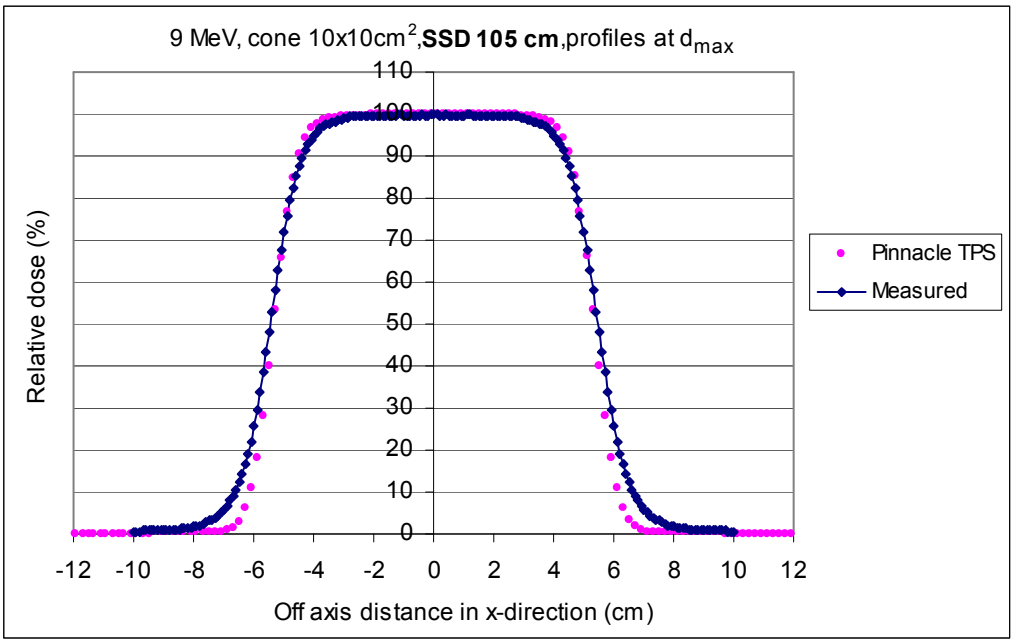

(a)

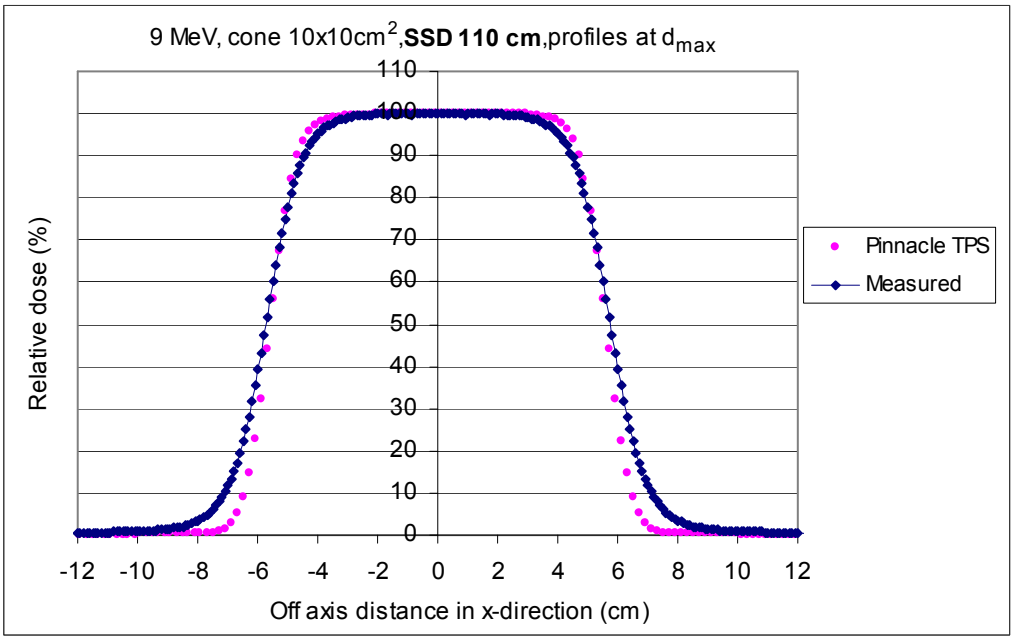

(b)

Figure 5.38 The comparison of relative dose profiles at the depth of maximum dose between Pinnacle TPS and diode measurement is shown for electron energy 9 MeV and field size 10 × 10 cm^2 at SSD (a) 105 cm and (b) 110 cm .

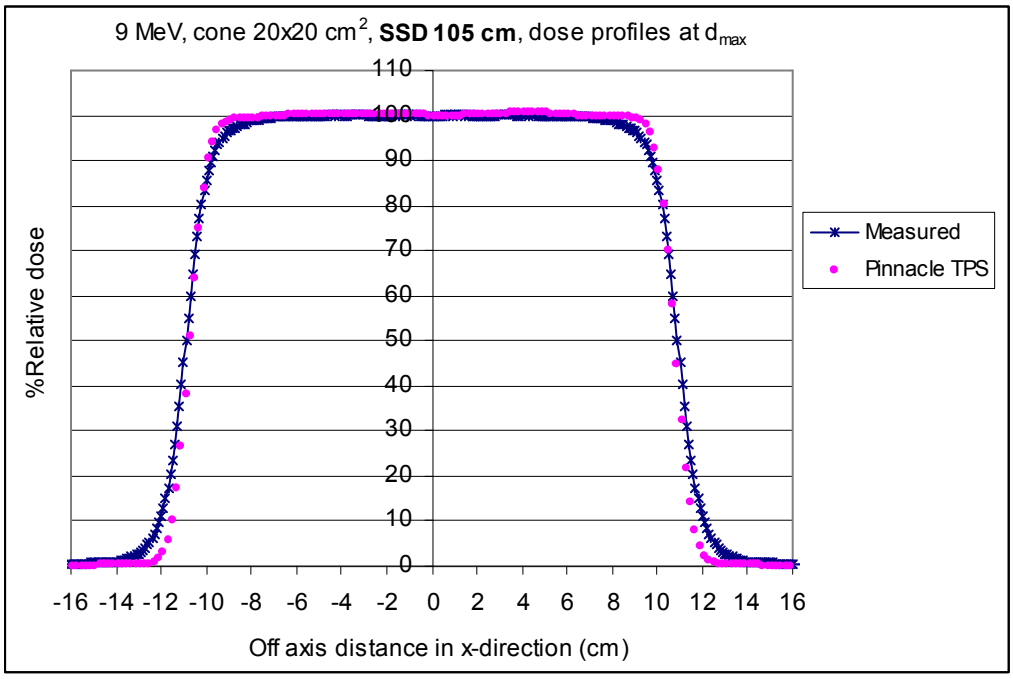

(a)

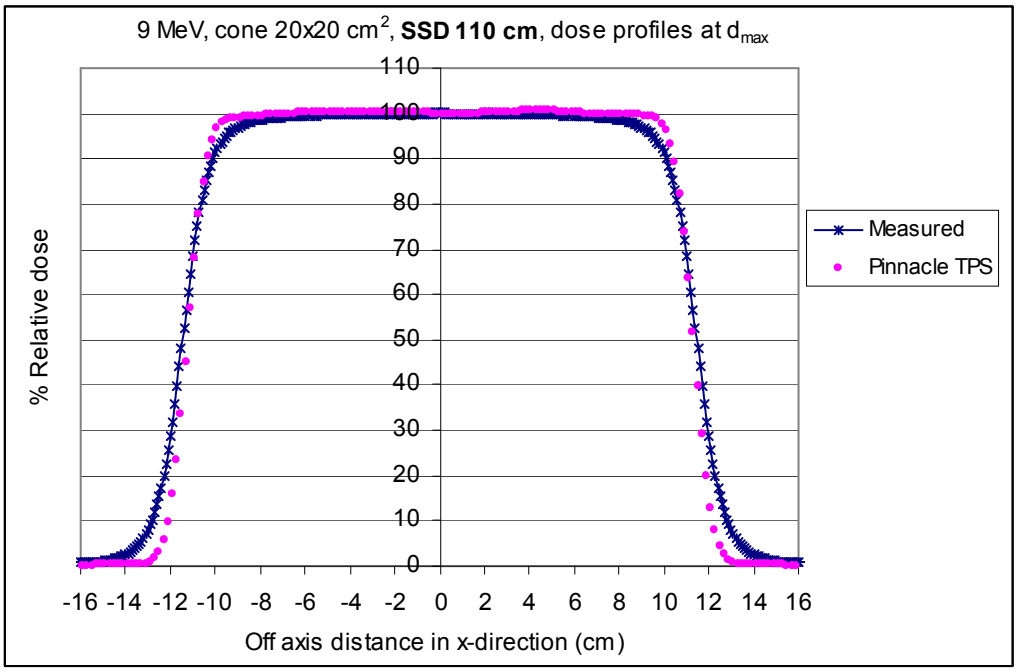

(b)

Figure 5.39 The comparison of relative dose profiles at the depth of maximum dose between Pinnacle TPS and diode measurement is shown for electron energy 9 MeV and field size 20 × 20 cm^2 at SSD (a) 105 cm and (b) 110 cm .

Table 5.11 The difference of beam fringe ($\delta_{50\text{-}90}$), radiological width (RW_{50}), penumbra width (δ_2), outside central beam axis region (δ_3) and outside beam edges (δ_4) between Pinnacle calculation and diode measurement for standard cone 4 × 4, 10 × 10 and 20 × 20 cm^2 at the maximum depths with extended SSD 105 and 110 cm, respectively and irradiated with electron energy 9 MeV electron beams.

SSD 105 cm			
	Distance to agreement (cm)		
	4 × 4 cm^2	**10 × 10 cm^2**	**20 × 20 cm^2**
$\delta_{50\text{-}90}$	0.24	0.288	0.275
RW_{50}	0	0.23	0.22
δ_2 (80-20%)	0.327	0.39	0.391
	% dose difference		
	4 × 4 cm^2	**10 × 10 cm^2**	**20 × 20 cm^2**
δ_3	-	1.50%	0.356%
δ_4	5.2%	6.04%	6.36%
SSD 110 cm			
	Distance to agreement (cm)		
	4 × 4 cm^2	**10 × 10 cm^2**	**20 × 20 cm^2**
$\delta_{50\text{-}90}$	0.283	0.434	0.51
RW_{50}	0.15	0.34	0.46
δ_2 (80-20%)	0.45	0.57	0.54
	% dose difference		
	4 × 4 cm^2	**10 × 10 cm^2**	**20 × 20 cm^2**
δ_3	-	2.588%	0.7%
δ_4	6%	6.26%	6.43%

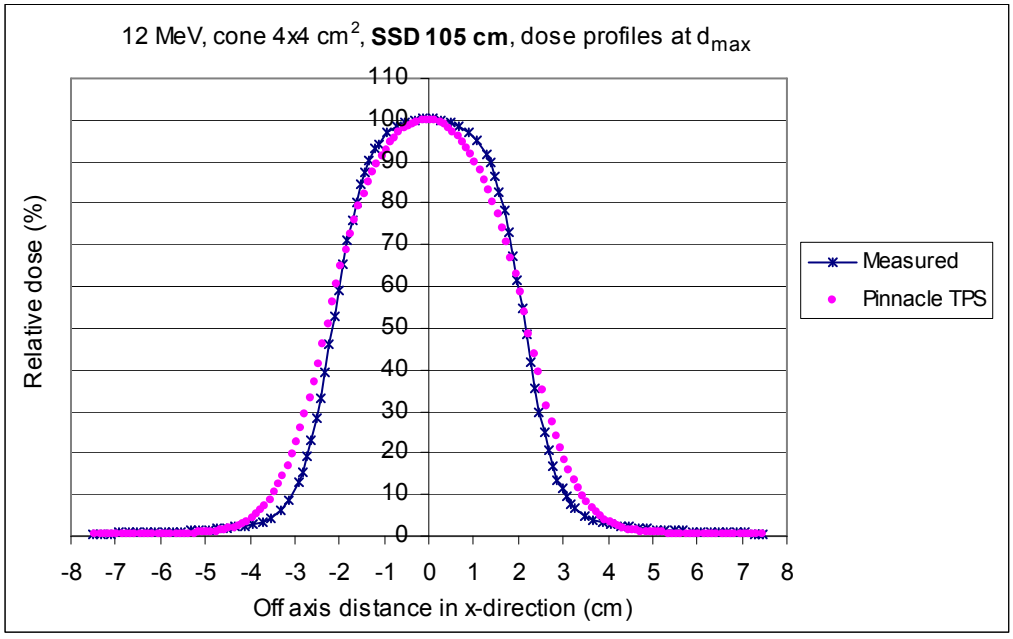

(a)

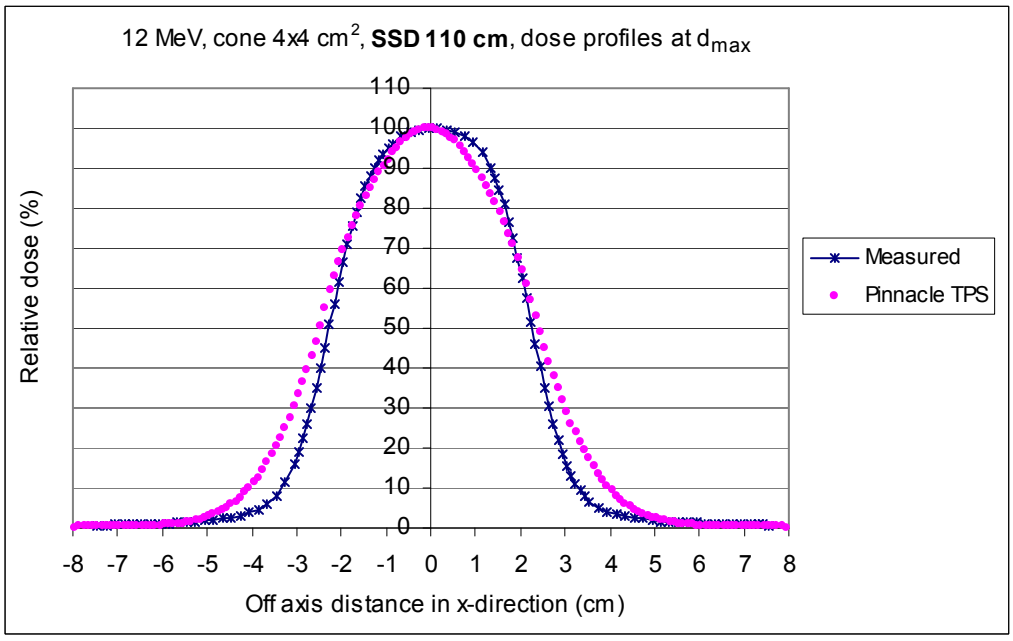

(b)

Figure 5.40 The comparison of relative dose profiles at the depth of maximum dose between Pinnacle TPS and diode measurement is shown for electron energy 12 MeV and field size 4×4 cm^2 at SSD (a) 105 cm and (b) 110 cm .

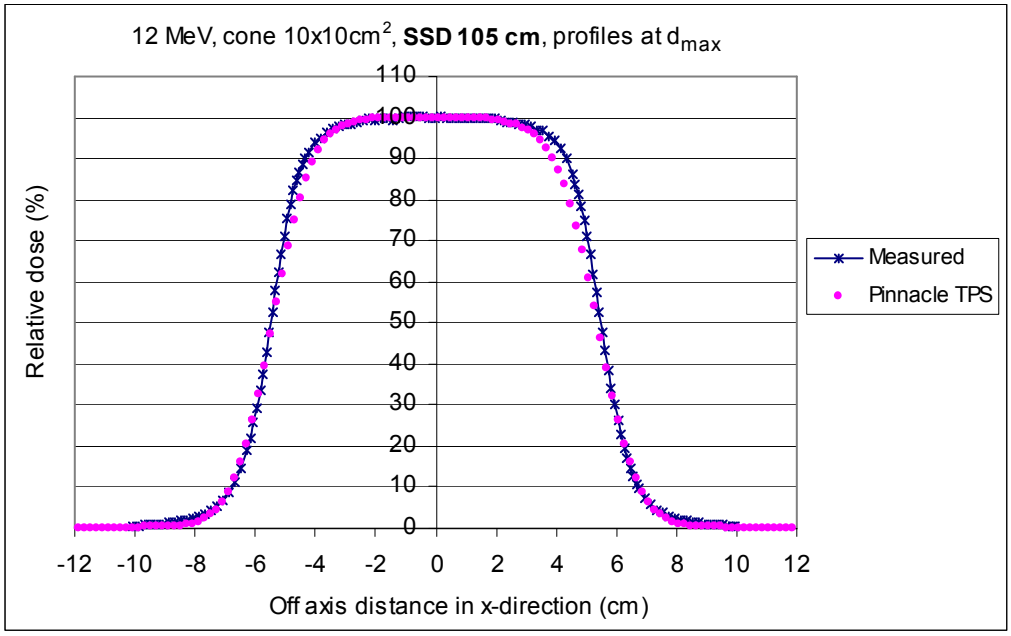

(a)

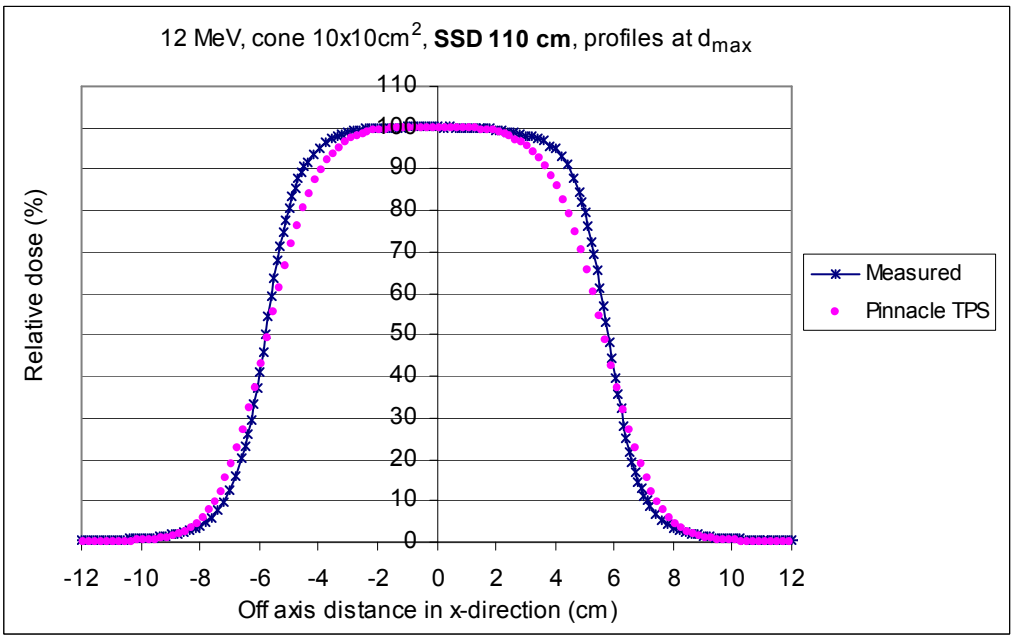

(b)

Figure 5.41 The comparison of relative dose profiles at the depth of maximum dose between Pinnacle TPS and diode measurement is shown for electron energy 12 MeV and field size 10 × 10 cm^2 at SSD (a) 105 cm and (b) 110 cm .

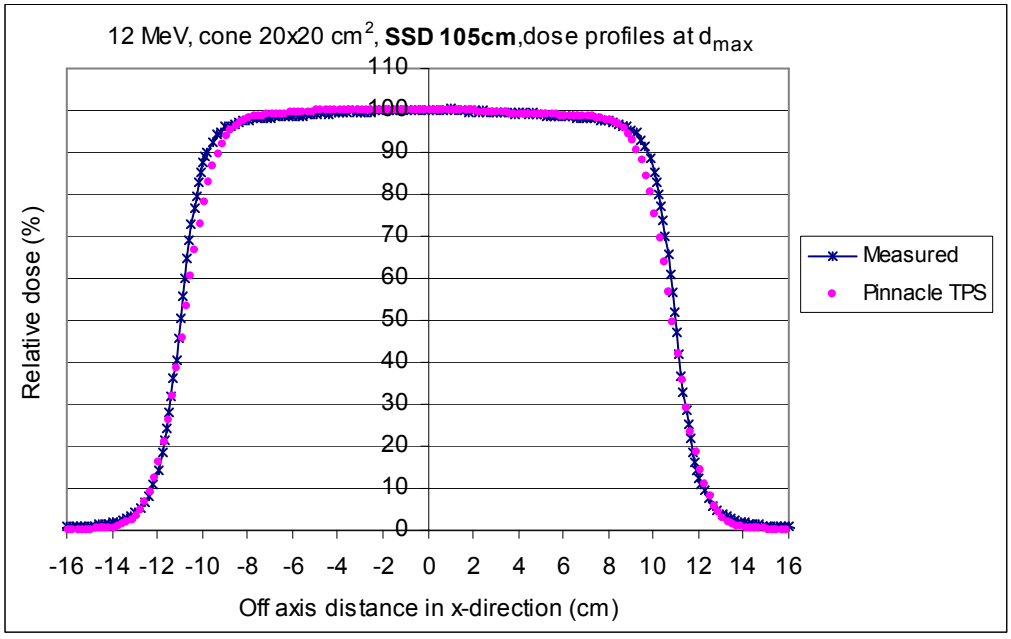

(a)

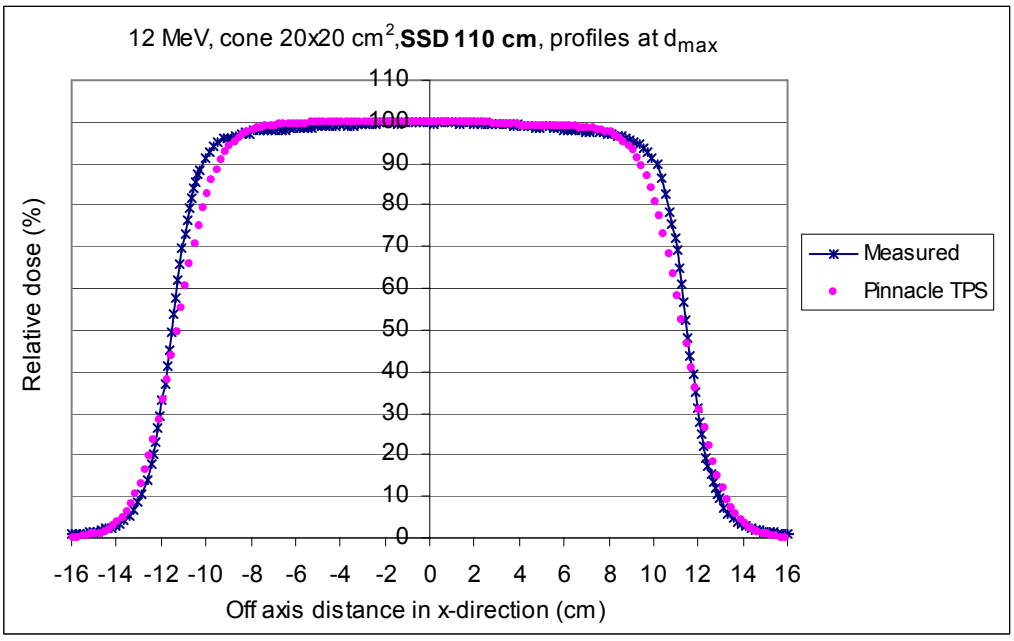

(b)

Figure 5.42 The comparison of relative dose profiles at the depth of maximum dose between Pinnacle TPS and diode measurement is shown for electron energy 12 MeV and field size 20 × 20 cm^2 at SSD (a) 105 cm and (b) 110 cm .

Table 5.12 The difference of beam fringe ($\delta_{50\text{-}90}$), radiological width (RW_{50}), penumbra width (δ_2), outside central beam axis region (δ_3) and outside beam edges (δ_4) between Pinnacle calculation and diode measurement for standard cone 4 × 4, 10 × 10 and 20 × 20 cm^2 at the maximum depths with extended SSD 105 and 110 cm, respectively and irradiated with electron energy 12 MeV electron beams.

SSD 105 cm			
	Distance to agreement (cm)		
	4 × 4 cm^2	**10 × 10 cm^2**	**20 × 20 cm^2**
$\delta_{50\text{-}90}$	0.38	0.34	0.3
RW_{50}	0.2	0.25	0.14
δ_2 (80-20%)	0.47	0.415	0.46
	% dose difference		
	4 × 4 cm^2	**10 × 10 cm^2**	**20 × 20 cm^2**
δ_3	-	1.714%	0.345%
δ_4	2.56%	0.79%	0.175%
SSD 110 cm			
	Distance to agreement (cm)		
	4 × 4 cm^2	**10 × 10 cm^2**	**20 × 20 cm^2**
$\delta_{50\text{-}90}$	0.51	0.62	0.6
RW_{50}	0.35	0.28	0.4
δ_2 (80-20%)	0.68	0.9	0.75
	% dose difference		
	4 × 4 cm^2	**10 × 10 cm^2**	**20 × 20 cm^2**
δ_3	-	4.043%	1.03%
δ_4	3.77%	2.6%	1.7%

D. Computed Tomography based inhomogeneity correction

Figure 5.43 to 5.45 show the results of an air cavity for electron energy 6, 9 and 12 MeV respectively. Table 5.13 shows the distance difference and % dose difference between Pinnacle calculation and X-Omat V film measurement of dose profiles in the transverse plane for an air cavity of standard cone 10 × 10cm^2 at the specified depths with 100 cm SSD.

In general, the calculation of dose beneath an air cavity by Pinnacle TPS was underestimated than that measured by the X-Omat V film. The maximum of the % dose difference beneath the air cavity found in 12 MeV electron beam is 4.56% which is still less than 5% of the criteria. However the agreement at the interface area is up to 10% because Pinnacle TPS misjudges the effect of side-scatter disequilibrium at lateral tissue discontinuities (interface). The maximum difference found in 6 MeV electrons beam and is about 15%. A measured dose at the distal interface between an air cavity and water was higher because the multiple scatter reflection back into the cavity from the water. This effect is more pronounced with lower energy and shallower depth. For 9 MeV beam, the measured dose at the interface area cannot predict the magnitude of the hot and cold spot because the measured depth is deeper so less effect by the multiple scatter reflection. The deviation of dose outside an air inhomogeneity agrees quite well. However except electron energy 6 MeV, the dose calculation outside the inhomogeneity by Pinnacle TPS was lower than dose measured by the XV film approximately 3-4%. That is because of the result of the central axis percent depth dose of the dose calculated by Pinnacle TPS (cone 10 × 10 cm^2, SSD 100 cm) at depth of the beam profile lower than that of the XV film measurement at the same depth.

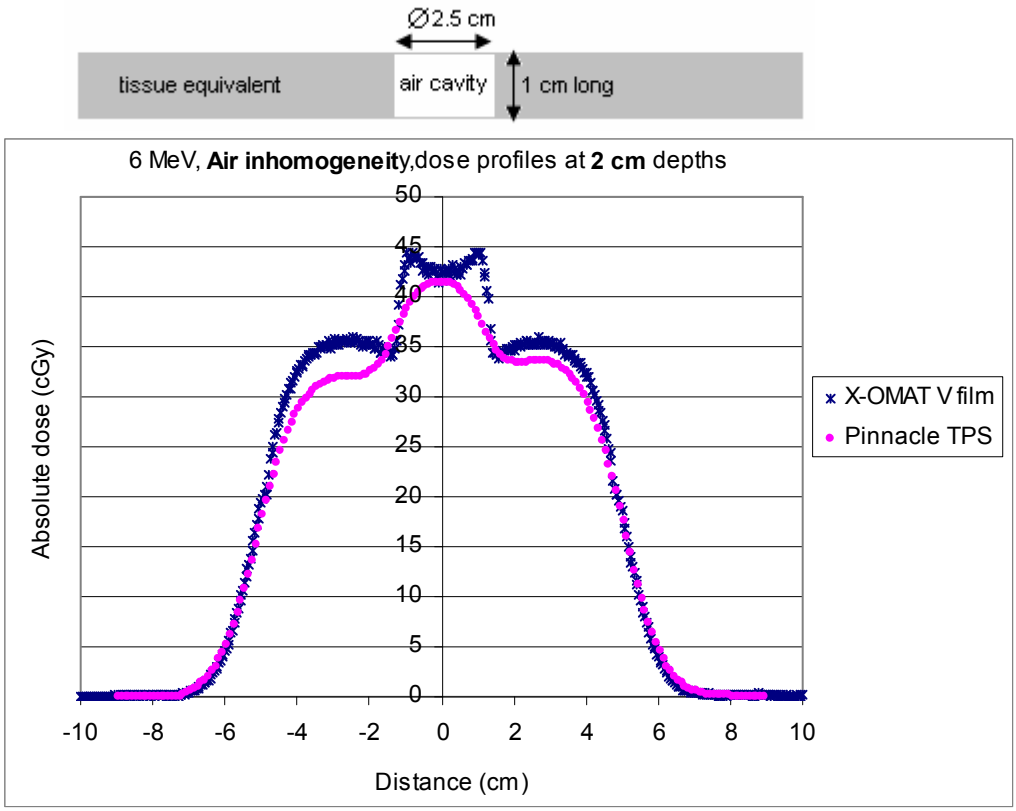

Figure 5.43 The comparison of dose profiles in the transverse plane for an air cavity between Pinnacle calculation and XV film measurement of electron energy 6 MeV, field size 10 × 10 cm^2 and SSD 100 cm. The dose profiles were obtained at 2 cm depth.

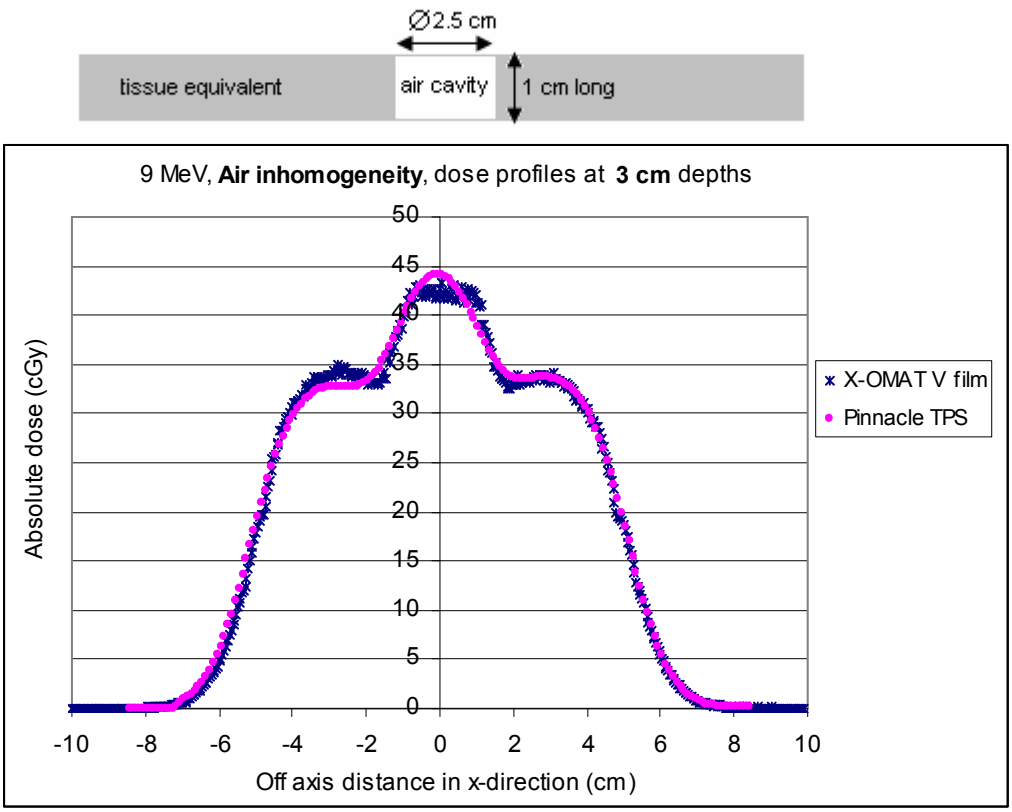

Figure 5.44 The comparison of dose profiles in the transverse plane for an air cavity between Pinnacle calculation and XV film measurement of electron energy 9 MeV, field size 10 × 10 cm^2 and SSD 100 cm. The dose profiles were obtained at 3 cm depth.

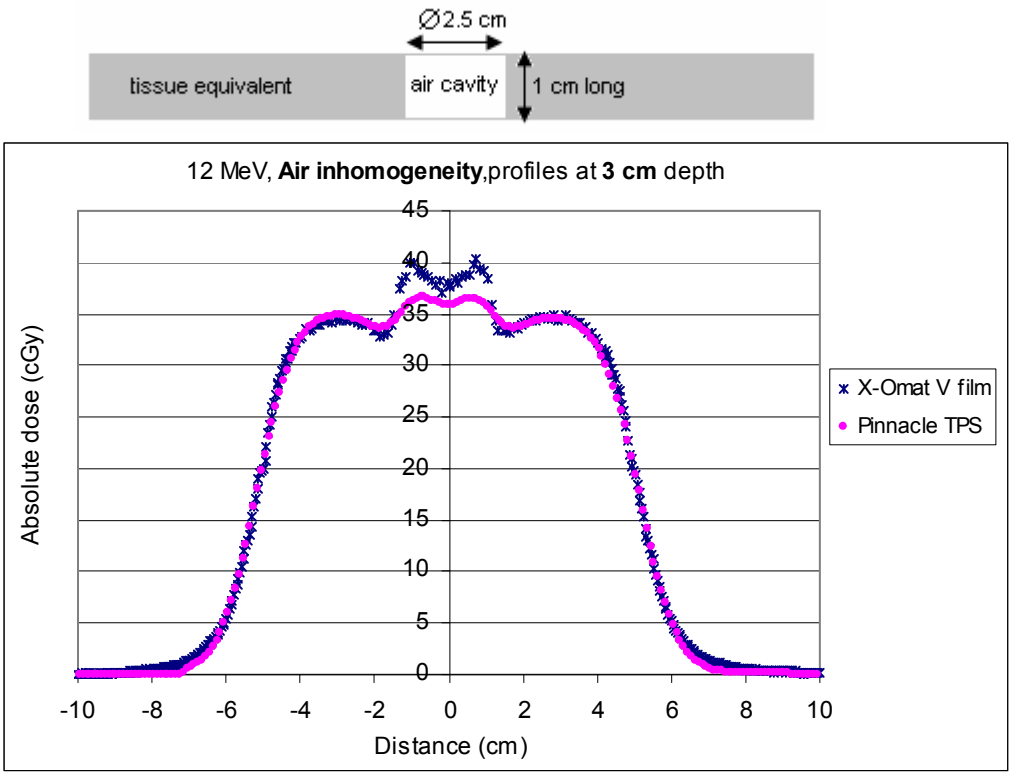

Figure 5.45 The comparison of dose profiles in the transverse plane for an air cavity between Pinnacle calculation and XV film measurement of electron energy 12 MeV, field size 10 × 10 cm^2 and SSD 100 cm. The dose profiles were obtained at 3 cm depth.

Table 5.13 The difference of dose profiles at the central axis (δ_1), interface area, and outside central axis region (δ_3) in the transverse plane for an air cavity between Pinnacle calculation and X-Omat V film measurement for standard cone 10 × 10 at the specified depths with 100 cm SSD .

Air inhomogeneity			
Region	**6 MeV**	**9 MeV**	**12 MeV**
	Distance to agreement (cm)		
δ_{50-90}	1.036	0.092	0.187
RW_{50}	0.17	0.14 2	0
δ_2 (80%-20%)	0.40	0.20	0.122
	%Different		
δ_1 (central axis)	3.36%	3.35%	4.56%
Interface area	15.09%	5.725%	9.87%
δ_3 (tissue equivalent)	10.52%	4.308%	1.14%
δ_4	0.188%	0.019%	0.657%

Figure 5.46 and 5.47 show the comparisons of dose profiles for the bone cavity for 9 and 12 MeV electron beams, respectively. The agreement between Pinnacle-calculated and X-Omat V film measured doses is remarkable although Pinnacle cannot predict the very fine details of the dose near the interface of the bone inhomogeneity. The deviation at the interface area of both electron energies was within criteria of acceptability (<7%). The calculation of dose beneath the bone cavity was overestimated than that of the measurements however the deviations were within 5% in which they were about 0.6% for 9 MeV beams and 3.3% for 12 MeV beams. Table 5.14 shows the % dose difference of dose profiles between Pinnacle calculation and X-Omat V film measurement in the transverse plane for a bone cavity for standard cone 10 × 10 cm^2 at the specified depths with 100 cm SSD.

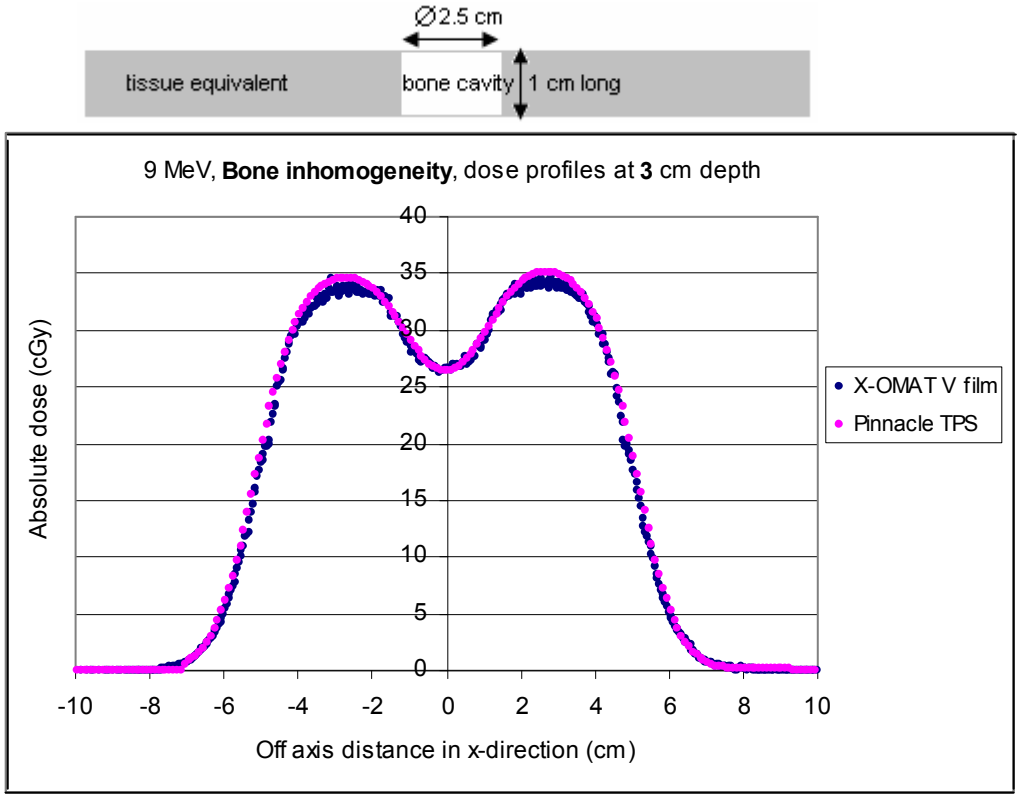

Figure 5.46 The comparison of dose profiles in the transverse plane for a bone cavity between Pinnacle calculation and XV film measurement of electron energy 9 MeV, field size 10 × 10 cm^2 and SSD 100 cm. The dose profiles were obtained at 3 cm depth.

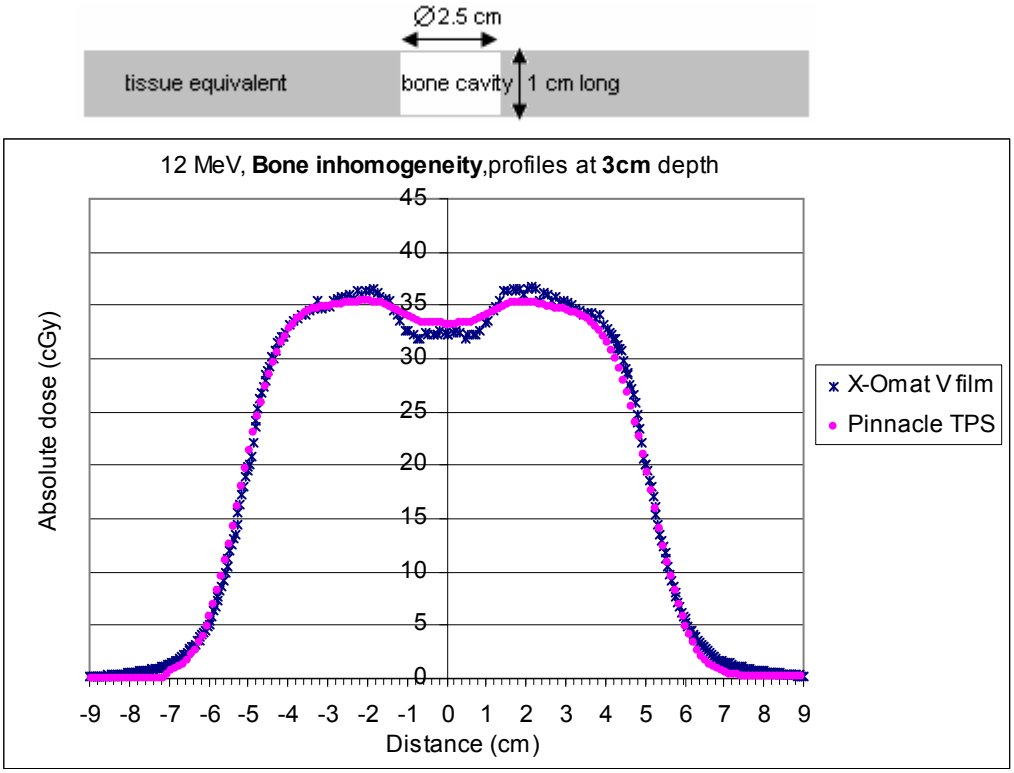

Figure 5.47 The comparison of dose profiles in the transverse plane for a bone cavity between Pinnacle calculation and XV film measurement of electron energy 12 MeV, field size 10 × 10 cm^2 and SSD 100 cm. The dose profiles were obtained at 3 cm depth.

Table 5.14 The difference of dose profiles at the central axis (δ_1), interface area, and outside central axis region (δ_3) in the transverse plane for bone cavity between Pinnacle calculation and X-Omat V film measurement for standard cone 10 × 10cm^2 at the specified depths with 100 cm SSD.

Bone inhomogeneity		
Region	**9 MeV**	**12 MeV**
	Distance to agreement (cm)	
δ50-90	0.06	0.232
RW_{50}	0.22	0.058
δ_2 (80%-20%)	0.08	0.159
	%Different	
δ_1 (central axis)	0.62%	3.29%
Interface area	0.5%	4.74%
δ_3 (tissue equivalent)	0.65%	1.054%
δ_4	2.4%	0.745%

5.2 Relative output factor

Tables 5.15 and 5.16 show the comparison of relative output factor for various electron cut-out sizes between Roos parallel plate chamber measurement and Pinnacle TPS for 6, 9, and 12 MeV electron beam of a 10 × 10 cm^2 and 15 × 15 cm^2 electron cone at depth of maximum dose and 100 cm SSD. The difference ranges between 0.1-4% which is less than 5% criteria of acceptability. Table 5.17 displays the result of the comparison of output factor for extended SSDs between Roos parallel plate chamber measurement and Pinnacle TPS for 6, 9, and 12 MeV electron beam of a 10 × 10 cm^2 electron cone at depth of maximum dose. The comparison results obtain excellent agreement smaller than 2%. Table 5.18 illustrates the comparison of output factor for oblique beam incidence (25°) between Roos parallel plate chamber measurement and Pinnacle TPS. The maximum difference is 4.56% for 6 MeV electron beam.

Table 5.15 Comparison of relative output factor for various electron cut-out sizes between Roos parallel plate chamber measurement and Pinnacle TPS for 6, 9, and 12 MeV electron beam of a 10 × 10 cm^2 electron cone at depth of maximum dose and 100 cm SSD.

Cut-out size (cm)	6 MeV			9 MeV			12 MeV		
	Measured	Pinnacle	%Diff	Measured	Pinnacle	%Diff	Measured	Pinnacle	%Diff
∅ 5.2	0.9956	1.0116	1.61	0.9687	1.0075	4	0.9747	0.9784	0.39
8.7x6.8	1.0066	1.0349	2.8	1.0051	1.0349	2.96	1.002	1.0124	1.04
9.5x4.2	0.9788	1.0116	3.35	0.9703	0.99	2.04	0.9747	0.9851	1.07

Table 5.16 Comparison of relative output factor for various electron cut-out sizes between Roos parallel plate chamber measurement and Pinnacle TPS for 6, 9, and 12 MeV electron beam of a 15 × 15 cm^2 electron cone at depth of maximum dose and 100 cm SSD.

Cut-out size (cm)	6 MeV			9 MeV			12 MeV		
	Measured	Pinnacle	%Diff	Measured	Pinnacle	%Diff	Measured	Pinnacle	%Diff
4.7x14.6	0.9886	1.0008	1.24	0.9707	0.9917	2.16	0.9691	0.9627	-0.67
6.7x13.7	0.9984	1.0215	2.31	0.9974	1.0232	2.59	0.9891	0.99	0.1

Table 5.17 Comparison of relative output factor for extended SSDs between Roos parallel plate chamber measurement and Pinnacle TPS for 6, 9, and 12 MeV electron beam of a 10 × 10 cm^2 electron cone at depth of maximum dose.

SSD (cm)	6 MeV			9 MeV			12 MeV		
	Measured	Pinnacle	%Diff	Measured	Pinnacle	%Diff	Measured	Pinnacle	%Diff
105	0.8923	0.9067	1.61	0.8962	0.8979	0.19	0.8988	0.893	-0.64
110	0.804	0.8026	-0.17	0.8084	0.8083	-0.02	0.8074	0.8018	-0.69

Table 5.18 Comparison of relative output factor for oblique beam incidence (25°) between Roos parallel plate chamber measurement and Pinnacle TPS for 6, 9, and 12 MeV electron beam of a 10 × 10 cm^2 electron cone at a depth of maximum dose and 105 cm SSD.

Energy (MeV)	Relative output factor		% Different
	Measurement	Pinnacle	
6	0.8772	0.9172	4.563
9	0.8637	0.8734	1.128
12	0.9167	0.9218	0.557

CHAPTER VI
CONCLUSIONS

The purpose of this study was to investigate the accuracy of the electron beam dose calculation algorithm in Pinnacle^3 treatment planning system version 7.6C (Philips radiation Oncology System, Milpitas, CA). It is very important for the users of any 3D RTP system to have a clear understanding of the limitations of the implemented electron beam dose calculation algorithm.

In general, the comparison between Pinnacle TPS and the measurements in both depth-dose curves and dose profiles for the homogeneous water phantom for square field size at standard and extended SSDs obtained good agreement within 4% or 0.4 cm. For shaped field size however the agreement showed within 5% or 0.5 cm. The most noticeable disagreement was found in the beam fringe and penumbra region at larger depths and larger SSDs due to the process of modeling. Most of the electron beams modeling gave higher accuracy at one particular depth and SSD.

For small inhomogeneities, the large deviation was found near the edge of an inhomogeneity (interface). Because of the approximation of the Hogstrom pencil beam algorithm[2, 22, 23], the dose contribution from each pencil beam is calculated as if the medium under the central ray of a pencil beam is infinite in their lateral extent (no inhomogeneity interface), produces calculation errors greatest in the shadow of inhomogeneities whose edge is parallel to the beam. This is due to a lack of subsequent scattering of the particles scattered from the denser medium into the less dense medium[2]. As a result in test 5, it produces calculation errors up to 10% when the inhomogeneity interface appears. However bone inhomogeneity calculation gives more acceptability than air inhomogeneity calculation. Similar to what has been observed by Anna Samuelsson *et al.* [17]. Moreover Pinnacle TPS calculates dose beneath the air and bone inhomogeneity quite reasonable within the criteria less than 5%.

The agreement between Pinnacle calculation and measurement in the relative output factor showed good agreement. The deviation was smaller than 2% for extended SSDs and 5% for shaped fields and oblique beam incidence.

This study indicates that the Pinnacle TPS is appropriate for electron beam dose calculations in clinical radiation therapy. However, the physicist and clinician should be aware of the limitations of the dose calculation at the interface area of the internal inhomogeneity.

REFERENCES

1. Khan FM. The Physics of radiation therapy.3rd ed. Baltimore: Williams& Wilkins; 2003.
2. Hogstrom KR, Mills MD, Almond PR. Electron beam dose calculations. Phys. Med. Biol 1981; 26: 445-459.
3. Cheng A, Harms WB, Gerber RL, Wong JW, Purdy JA. Systematic verification of a three-dimensional electron beam dose calculation algorithm. Med. Phys 1996; 23: 685-693.
4. Khan FM, Doppke KP, Hogstrom KR, Kutcher Gj, Nath R, Prasad SC, et al. American Association of in Medicine: Report of AAPM Rdiation Therapy Committee Task Group No.25. Clinical electron-beam dosimetry. Med Phys 1991; 18:73-109
5. Radiation oncology System. Electron Physics and data Requirements, Philips Medical System, USA, 2005.
6. Radiation oncology System. Electron Physics and Physics Utilities, Philips Medical System, USA, 2005.
7. International Atomic Energy Agency. Technical reports series no.430: Commissioning and quality assurance of computerized planning system for radiation treatment of cancer. Vienna; 2004: 148-154
8. Dyk JV, Barnett RB, Cygler JE, Ghragge PC. Commissioning and quality assurance of treatment planning computer. Int J Radiat Oncol Biol Phys 1993; 26: 261-273.
9. Hendee RW, Ibbott SG, Hendee GE. Radiation Therapy Physics. 3rd ed. New Jersey: John Wiley & Sons; 2005: 172-173.
10. Glegg. M.M. Electron dose calculations: A comparison of two commercial treatment planning computers. Medical Dosimetry 2003; 28: 99-105

11. Fraass B, Doppke K, Hunt M, Kutcher G, Starkschall G, Stern R, et al. American Association of Physicists in Medicine Radiation Therapy Committee Task Group 53: quality assurance for clinical radiotherapy treatment planning. Med Phys 1998; 25:1773-829.
12. Venselaar J, Welleweered H, Mignheer B. Tolerance for the accuracy of photon beam dose calculations of treatment planning system. Radiotherapy and Oncology 2001; 60: 191-201
13. International Atomic Energy Agency. Absorbed dose determination in external beam therapy. IAEA TRS 398, 2000: 84-107
14. AAPM Report No. 32. Clinical electron-beam dosimetry. New York, American Institute of Physics; 1991.
15.Kodak (Thailand) LTD. Kodak RP/TL X-OMAT Therapy Localization and Kodak RP/V X-OMAT Therapy Verification film. The manual of Kodak X-OMAT
16. El-Khatip E, Antolak J, Scrimger J. Evaluation of film and thermoluminescent dosimetry of high-energy electron beams in heterogeneous phantoms. Med. Phys 1992; 19:317-323
17. Samuelsson A, Hyodnmaa S, Johansson KA. Dose accuracy check 3D electron beam algorithm in a treatment planning system. Phy Biol 1998;43:1529-1544
18. Ding GX, Cygler GE, Zhang GG, Yu MK. Evaluation of a commercial three dimensional electron beam treatment planning system. Med Phys 1999;26:2571-2580
19. Muller-Runkel R, Cho SH. Evaluation of a three-dimensional electron pencil beam algorithm. Med Phys 1997;43:91-101
20. Shiu AS, Tung S, Hogstrom KR. Verification data for electron beam dose algorithm. Med Phys 1992;19:623-636
21. CIRS tissue simulation & Phantom technology. [cited 2006 Sep 10] Available from: URL:http://www.cirsinc.com/002pra_rad.htm
22. Shortt KR, Ross CK, Bielajew CK, Rogers DWO. Electron beam dose distributions near standard inhomogeneities. Phys. Med. Biol 1986;1: 235-249

23. Lax I. Inhomogeneity corrections in electron-beam dose planning. Limitations with the semi-infinite slab approximation. Phys. Med. Biol 1986; 31: 879-892.
24. Boyd AR, Hogstrom KR, Antolak JA, Shiu AS. A measure data set for evaluating electron beam dose algorithms. Med phys 1992;28:950-958
25. Cygler J, Allen Li X, Ding GX, Lawrence E. Practical approach to electron beam dosimetry at extended SSD. Phys. Med. Biol 1997; 42: 1505-1514.
26. Hogstrom K.R. et al. Dosimetric evaluation of a pencil-beam algorithm. Int. J. Radiat. Oncol. Biol. Phys 1984; 10: 561-569
27. Mah E, Antolak J, Scrimger JW, Battista J. Experimaental evaluation of a 2D and 3D electron pencil beam algorithm. Phys. Med. Biol 1 989; 34: 1179-1193.
28. Mcshan DL, Fraass BA, Ten Haken RK. Dosimetric verification of a 3-D electron pencil beam dose calculation algorithm. Med. Phys 1994; 21: 13-22

APPENDIX

APPENDIX A

Table 1a Dose difference (%) and distance difference of buildup region and fall-off region between diode-measurements and Pinnacle calculations of Percent Depth Dose (PDD) for standard cone 4 × 4, 6 × 6, 10 × 10, 15 × 15 and 20 × 20 cm^2 at standard SSD treatment and 6 MeV electron beam.

%Dose difference at build up region											
Depth (cm)	6 MeV					**Depth (cm)**	6 MeV				
	4×4	**6×6**	**10×10**	**15×15**	**20×20**		**4×4**	**6×6**	**10×10**	**15×15**	**20×20**
0.1	-4.09	2.447	1.518	5.824	-6.69	2.1					
0.2	-2.19	3.543	2.34	5.675	-1.95	2.2					
0.3	-1	4.347	2.982	5.853	-	2.3					
0.4	-0.28	4.927	3.507	6.212	1.111	2.4					
0.5	0.165	5.333	3.953	6.635	-	2.5					
0.6	0.478	5.602	4.338	7.026	0.776	2.6					
0.7	0.745	5.757	4.662	7.309	-	2.7					
0.8	1.007	5.805	4.908	7.428	0.805	2.8					
0.9	1.268	5.745	5.042	7.344	-	2.9					
1	1.492	5.562	5.018	7.037	2.62	3					
1.1	1.612	5.233	4.776	6.497		3.1					
1.2	1.527	4.721	4.241	5.726	0.868	3.2					
1.3	1.108	3.98	3.326	4.733		3.3					
1.4	0.19	2.95	1.927	3.526	0	3.4					
1.5		1.551	-0.08	2.115		3.5					
1.6		-0.32		0.499		3.6					
1.7						3.7					
1.8						3.8					
1.9						3.9					
2						4					
Ave.	**0.145**	**4.199**	**3.497**	**5.59**	**-0.308**	**Ave.**	**-**	**-**	**-**	**-**	**-**
SD	**1.62**	**1.769**	**1.51**	**1.983**	**2.8761**	**SD**	**-**	**-**	**-**	**-**	**-**

Distance difference at fall-off region					
Dose (%)	6 MeV				
	4×4	**6×6**	**10×10**	**15×15**	**20×20**
20	-0.20262	-0.14532	-0.1934	-0.23132	-0.17116
30	-0.21236	-0.15027	-0.19905	-0.22631	-0.17864
40	-0.22246	-0.15469	-0.19757	-0.21994	-0.18192
50	-0.22031	-0.15716	-0.19078	-0.21211	-0.18055
60	-0.20155	-0.15625	-0.18047	-0.20272	-0.17405
70	-0.17002	-0.15054	-0.16845	-0.19166	-0.16197
80	-0.13782	-0.13862	-0.15652	-0.17886	-0.14383
Ave.	**-0.19531**	**-0.15041**	**-0.18375**	**-0.20899**	**-0.1703**
SD	**0.030795**	**0.006621**	**0.016094**	**0.019044**	**0.013506**

Table 2a Dose difference (%) and distance difference of buildup region and fall-off region between diode-measurements and Pinnacle calculations of Percent Depth Dose (PDD) for standard cone 4 × 4, 6 × 6, 10 × 10, 15 × 15 and 20 × 20 cm^2 at standard SSD treatment and 9 MeV electron beam.

%Dose difference at build up region											
Depth (cm)	9 MeV					**Depth (cm)**	9 MeV				
	4×4	**6×6**	**10×10**	**15×15**	**20×20**		**4×4**	**6×6**	**10×10**	**15×15**	**20×20**
0.1	-5.54	-1.04	1.081	-0.81	-6.99	2.1		0.72	0.14	1.373	-
0.2	-4.68	-0.84	0.49	-0.02	-2.26	2.2		0.54	-0.24	0.603	0
0.3	-4.31	-0.67	0.11	0.419	-	2.3		0.3		-0.58	
0.4	-4.19	-0.51	-0.1	0.616	-0.8	2.4		-0.02			
0.5	-4.16	-0.37	-0.18	0.65	-	2.5					
0.6	-4.1	-0.23	-0.16	0.59	-0.9	2.6					
0.7	-3.94	-0.1	-0.06	0.49	-	2.7					
0.8	-3.64	0.03	0.089	0.393	-0.44	2.8					
0.9	-3.2	0.16	0.27	0.331	-	2.9					
1	-2.69	0.28	0.462	0.327	-0.44	3					
1.1	-2.79	0.41	0.651	0.392	-	3.1					
1.2	-2.77	0.52	0.82	0.528	0.104	3.2					
1.3	-2.64	0.63	0.959	0.731	-	3.3					
1.4	-2.4	0.73	1.056	0.985	0.1	3.4					
1.5	-2.07	0.81	1.104	1.268	-	3.5					
1.6	-1.67	0.87	1.096	1.55	0.211	3.6					
1.7	-1.23	0.91	1.03	1.794	-	3.7					
1.8	-0.8	0.92	0.902	1.954	0.002	3.8					
1.9	-0.42	0.9	0.711	1.978	-	3.9					
2	-0.13	0.83	0.457	1.806	-0.3	4					
Ave.	**-2.87**	**-**	**-**	**-**	**-**	**Ave.**	**-**	**0.24**	**0.486**	**0.755**	**-0.98**
SD	**1.488**	**-**	**-**	**-**	**-**	**SD**	**-**	**0.6**	**0.479**	**0.745**	**2.012**

Distance difference at fall-off region					
Dose (%)	9 MeV				
	4×4	**6×6**	**10×10**	**15×15**	**20×20**
20	-0.327801	-0.19309	-0.25306	-0.28645	-0.21603
30	-0.335379	-0.19196	-0.26505	-0.28026	-0.20386
40	-0.336251	-0.18829	-0.27175	-0.27836	-0.19534
50	-0.332055	-0.18229	-0.27235	-0.2779	-0.18965
60	-0.324429	-0.17419	-0.26608	-0.27605	-0.18595
70	-0.315009	-0.16418	-0.25214	-0.26996	-0.18343
80	-0.305433	-0.15249	-0.22974	-0.2568	-0.18123
Ave.	**-0.325194**	**-0.17807**	**-0.2586**	**-0.27511**	**-0.19364**
SD	**0.0113628**	**0.015293**	**0.015084**	**0.009452**	**0.012529**

Table 3a Dose difference (%) and distance difference of buildup region and fall-off region between diode-measurements and Pinnacle calculations of Percent Depth Dose (PDD) for standard cone 4 × 4, 6 × 6, 10 × 10, 15 × 15 and 20 × 20 cm^2 at standard SSD treatment and 12 MeV electron beam.

%Dose difference at build up region											
Depth (cm)	12 MeV					Depth (cm)	12 MeV				
	4×4	**6×6**	**10×10**	**15×15**	**20×20**		**4×4**	**6×6**	**10×10**	**15×15**	**20×20**
0.1	-2.64	-1.741	1.52	-1.8	-6.233	2.1	0.10	0.237	0.41		
0.2	-1.91	-0.941	0.7	-1.5	-2.386	2.2	0.01	0.225	0.22	0.69	0.0731
0.3	-1.37	-0.451	0.25			2.3		0.182	0.09		
0.4	-1.03	-0.18	0.04	-0.4	-1.38	2.4		0.111	-0.03	0.7	-0.126
0.5	-0.91	-0.061	-0.02			2.5		0.019	-0.05		
0.6	-1.02	-0.04	0.03	0.18	-1.197	2.6		-0.082	0.01	1.11	-0.209
0.7	-1.32	-0.076	0.14			2.7		-0.172	0.06		
0.8	-1.05	-0.138	0.26	0.09	-0.941	2.8		-0.228	0.09	0.71	0.3009
0.9	-1.01	-0.204	0.38			2.9		-0.218	0.06		
1	-1.01	-0.258	0.46	0.11	-0.898	3			0	0.71	0
1.1	-0.96	-0.289	0.5			3.1					
1.2	-0.85	-0.292	0.47	0.45	-0.568	3.2				0	
1.3	-0.72	-0.268	0.34			3.3					
1.4	-0.62	-0.217	0.13	0.23	-0.23	3.4					
1.5	-0.65	-0.147	0.19			3.5					
1.6	-0.86	-0.065	0.28	0.56	0.0041	3.6					
1.7	-0.86	0.022	0.41			3.7					
1.8	-0.86	0.104	0.55	0.36	-0.584	3.8					
1.9	-0.66	0.171	0.66			3.9					
2	-0.27	0.218	0.7	0.48	0.0538	4					
Ave.	**-**	**-**	**-**	**-**	**-**	**Ave.**	**-0.9**	**-0.165**	**0.3**	**0.07**	**-0.895**
SD	**-**	**-**	**-**	**-**	**-**	**SD**	**0.57**	**0.387**	**0.32**	**0.83**	**1.5839**

Distance difference at fall-off region					
Dose (%)	12 MeV				
	4×4	**6×6**	**10×10**	**15×15**	**20×20**
20	-0.34198	-0.1814	-0.25229	-0.27263	-0.17326
30	-0.3355	-0.17303	-0.25555	-0.27133	-0.1702
40	-0.32277	-0.16703	-0.25541	-0.26567	-0.16578
50	-0.29971	-0.16258	-0.25319	-0.25686	-0.15977
60	-0.26321	-0.15887	-0.25021	-0.24614	-0.15193
70	-0.21111	-0.15508	-0.24777	-0.23472	-0.14204
80	-0.14223	-0.1504	-0.2472	-0.22382	-0.12985
Ave.	**-0.27378**	**-0.16406**	**-0.25166**	**-0.25302**	**-0.15612**
SD	**0.074024**	**0.010694**	**0.003392**	**0.018839**	**0.015837**

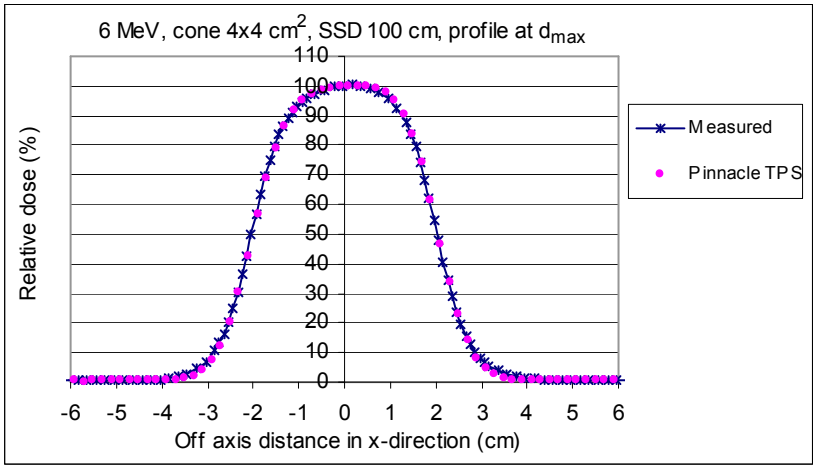
6 MeV, cone 4x4 cm2, SSD 100 cm, profile at dmax
Relative dose (%)
110
100
90
80
70
60
50
40
30
20
10
0
-6 -5 -4 -3 -2 -1 0 1 2 3 4 5 6
Off axis distance in x-direction (cm)
Measured
Pinnacle TPS

(a)

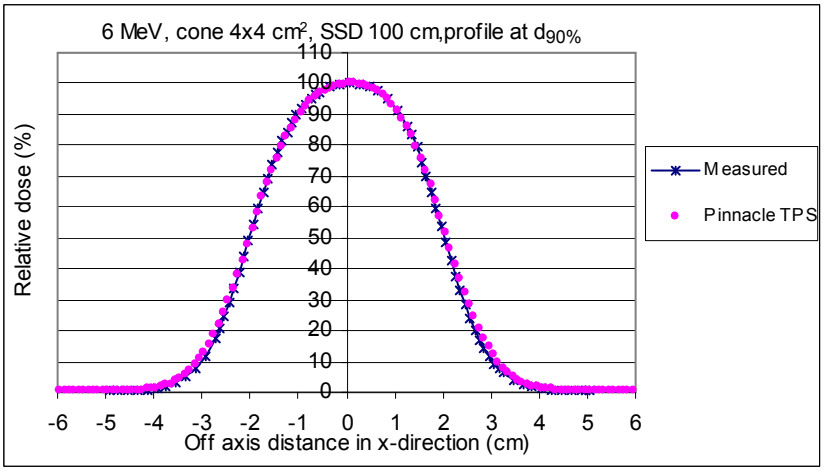
6 MeV, cone 4x4 cm2, SSD 100 cm,profile at d90%
Relative dose (%)
110
100
90
80
70
60
50
40
30
20
10
0
-6 -5 -4 -3 -2 -1 0 1 2 3 4 5 6
Off axis distance in x-direction (cm)
Measured
Pinnacle TPS

(b)

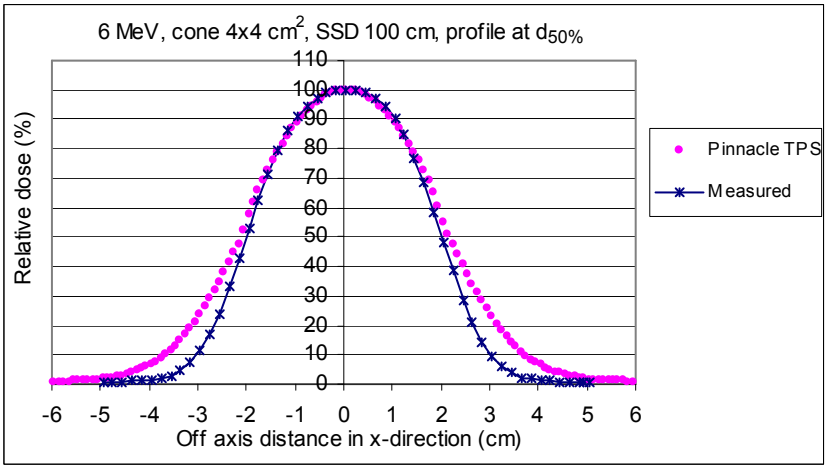
6 MeV, cone 4x4 cm2, SSD 100 cm, profile at d50%
Relative dose (%)
110
100
90
80
70
60
50
40
30
20
10
0
-6 -5 -4 -3 -2 -1 0 1 2 3 4 5 6
Off axis distance in x-direction (cm)
Pinnacle TPS
Measured

(c)

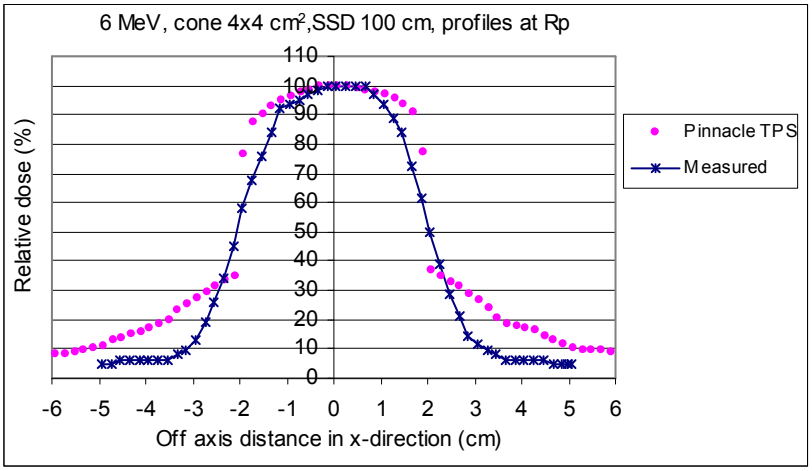

(d)

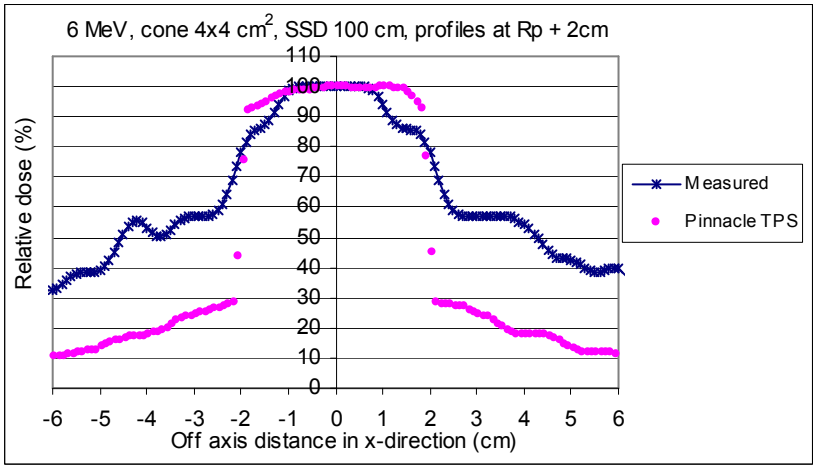

(e)

Figure 1a The comparison of relative dose profiles between Pinnacle TPS and diode measurement is shown for electron energy 6 MeV, SSD 100 cm and field size 4 × 4 cm^2 at (a) depth of dose maximum, (b) depth of dose 90%, (c) depth of dose 50%, (d) depth R_P and (e) depth R_P + 2 cm.

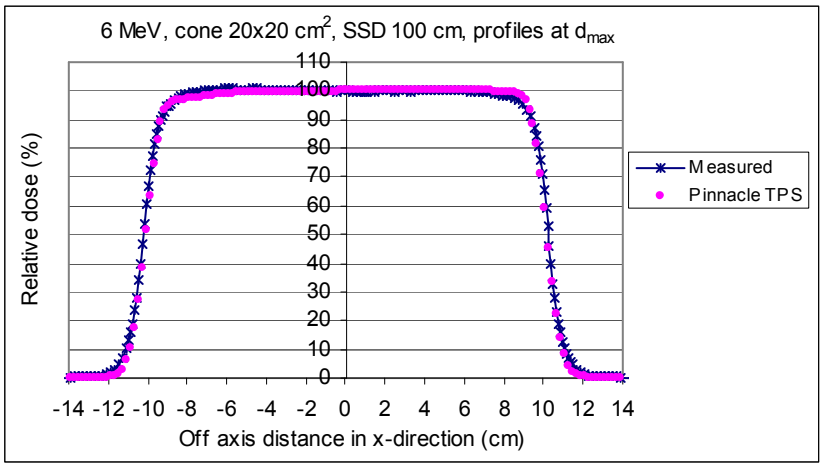
6 MeV, cone 20x20 cm2, SSD 100 cm, profiles at dmax
Relative dose (%)
110
100
90
80
70
60
50
40
30
20
10
0
-14 -12 -10 -8 -6 -4 -2 0 2 4 6 8 10 12 14
Off axis distance in x-direction (cm)
Measured
Pinnacle TPS

(a)

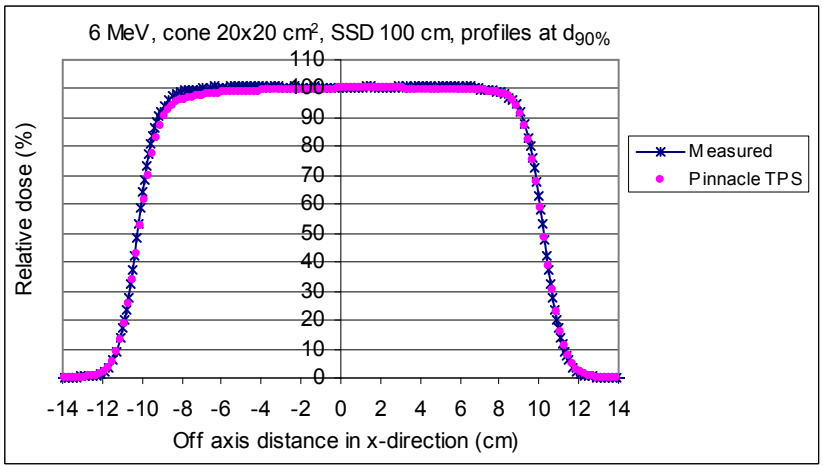
6 MeV, cone 20x20 cm2, SSD 100 cm, profiles at d90%
Relative dose (%)
110
100
90
80
70
60
50
40
30
20
10
0
-14 -12 -10 -8 -6 -4 -2 0 2 4 6 8 10 12 14
Off axis distance in x-direction (cm)
Measured
Pinnacle TPS

(b)

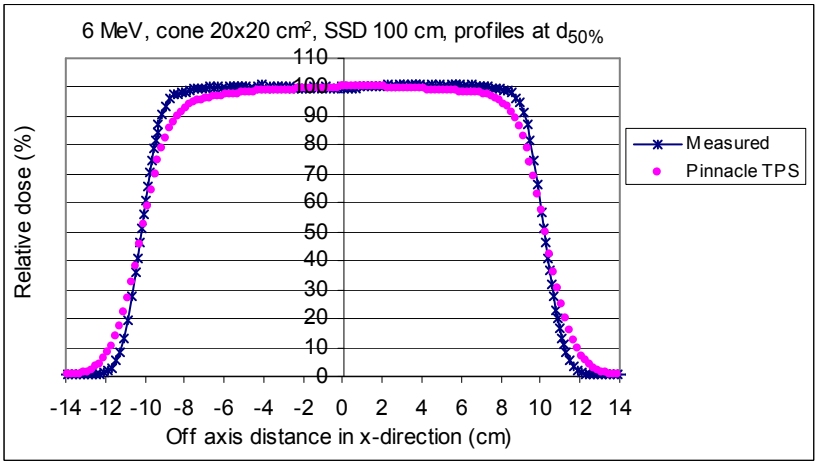
6 MeV, cone 20x20 cm2, SSD 100 cm, profiles at d50%
Relative dose (%)
110
100
90
80
70
60
50
40
30
20
10
0
-14 -12 -10 -8 -6 -4 -2 0 2 4 6 8 10 12 14
Off axis distance in x-direction (cm)
Measured
Pinnacle TPS

(c)

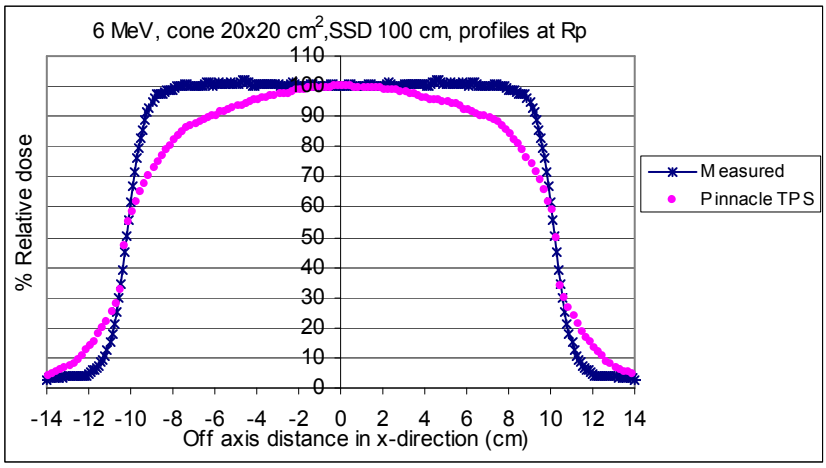

(d)

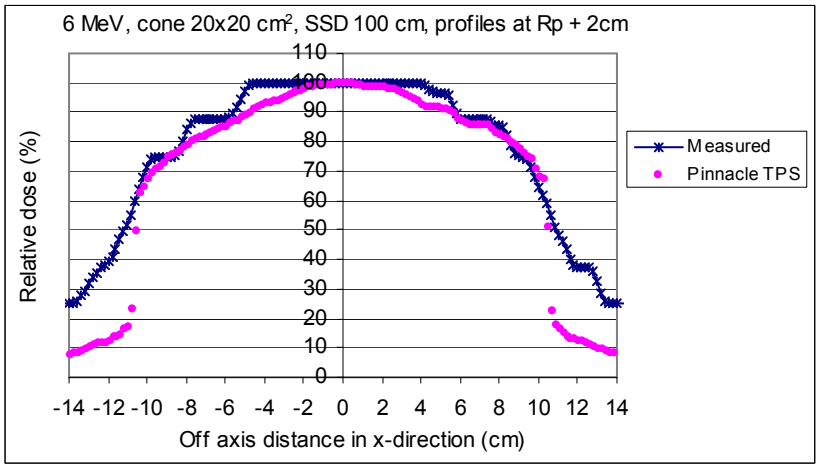

(e)

Figure 2a The comparison of relative dose profiles between Pinnacle TPS and diode measurement is shown for electron energy 6 MeV, SSD 100 cm and field size 20 × 20 cm^2 at (a) depth of dose maximum, (b) depth of dose 90%, (c) depth of dose 50%, (d) depth R_P and (e) depth R_P + 2 cm.

Table 4a The difference of beam fringe ($\delta_{50\text{-}90}$), radiological width (RW_{50}), penumbra width (δ_2), outside central beam axis region (δ_3) and outside beam edges (δ_4) between Pinnacle calculation and diode measurement for standard cone 4 × 4 and 20 × 20 cm^2 at the depths of d_{max}, $d_{90\%}$ $d_{50\%}$, Rp and Rp + 2 cm and irradiated with electron energy 6 MeV electron beams of 100 cm SSD.

	Depth	**Distance to agreement (cm)**	
		4 × 4 cm^2	**20 × 20 cm^2**
$\delta_{50\text{-}90}$	dmax	0.003	0.15
	d90%	0.05	0.251
	d50%	0.22	0.8
	Rp	0.44	3.01
	Rp+2cm	2.40	0.202
RW_{50}	dmax	0.05	0.09
	d90%	0	0.1
	d50%	0.3	0.1
	Rp	0.09	0.1
	Rp+2cm	4.8	1.2
δ_2 (80-20%)	dmax	0.021	0.06
	d90%	0.096	0.205
	d50%	0.475	0.85
	Rp	0.57	1.87
	Rp+2cm	-	0.53
	Depth	**% Different**	
		4 × 4 cm^2	**20 × 20 cm^2**
δ_3	dmax	-	2.011%
	d90%	-	1.824%
	d50%	-	3.83%
	Rp	-	12.10%
	Rp+2cm	-	6%
δ_4	dmax	2.246%	2.78%
	d90%	1.36%	1.36%
	d50%	5.56%	5.77%
	Rp	-	3.05%
	Rp+2cm	-	-

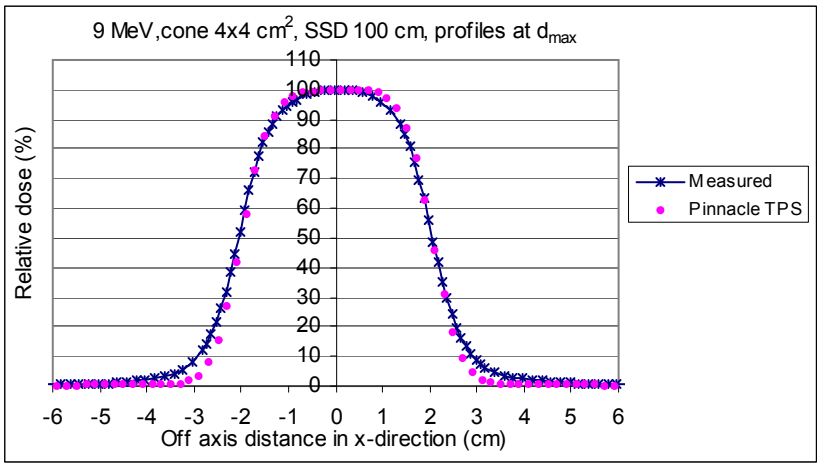
9 MeV,cone 4x4 cm2, SSD 100 cm, profiles at dmax
Relative dose (%)
Off axis distance in x-direction (cm)
Measured
Pinnacle TPS

(a)

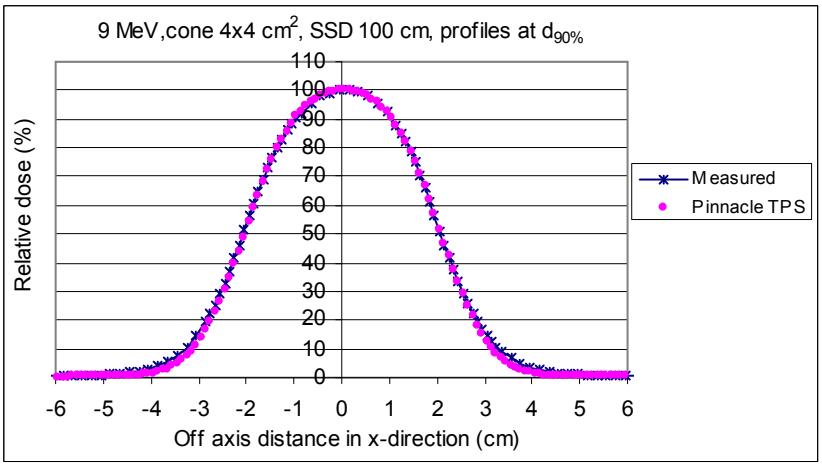
9 MeV,cone 4x4 cm2, SSD 100 cm, profiles at d90%
Relative dose (%)
Off axis distance in x-direction (cm)
Measured
Pinnacle TPS

(b)

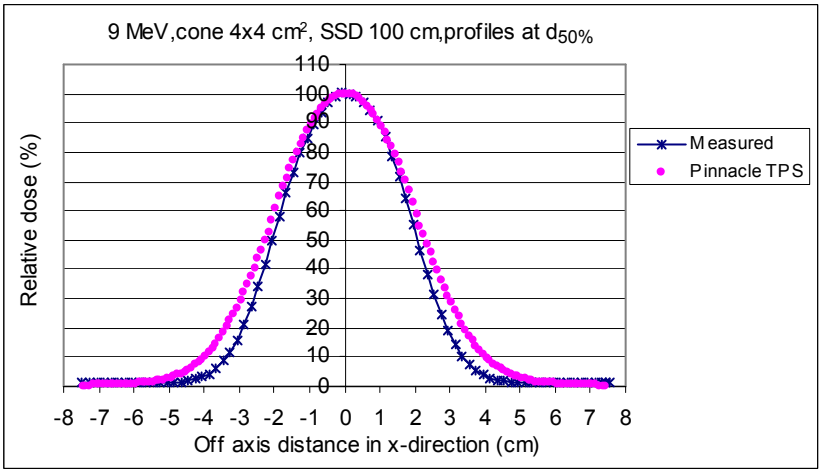
9 MeV,cone 4x4 cm2, SSD 100 cm,profiles at d50%
Relative dose (%)
Off axis distance in x-direction (cm)
Measured
Pinnacle TPS

(c)

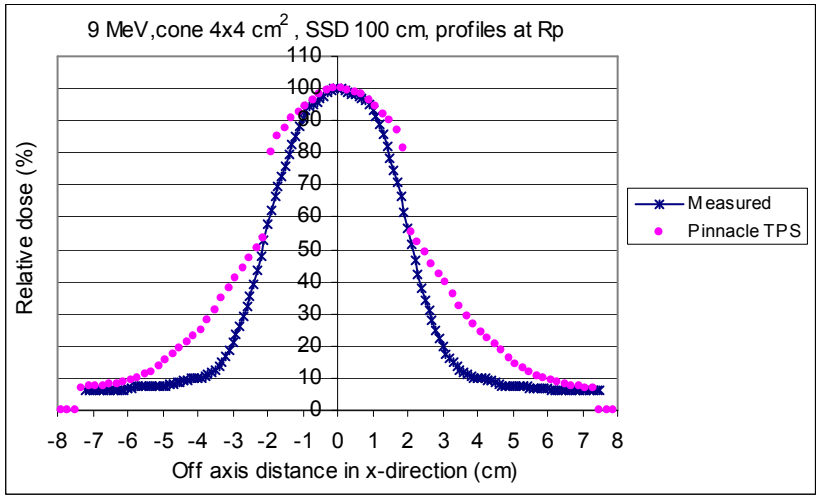

(d)

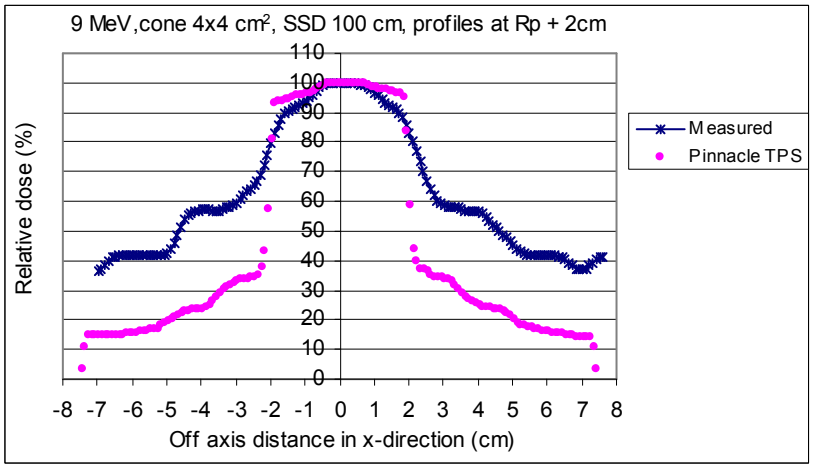

(e)

Figure 3a The comparison of relative dose profiles between Pinnacle TPS and diode measurement is shown for electron energy 9 MeV, SSD 100 cm and field size 4 × 4 cm^2 at (a) depth of dose maximum, (b) depth of dose 90%, (c) depth of dose 50%, (d) depth R_P and (e) depth R_P + 2 cm.

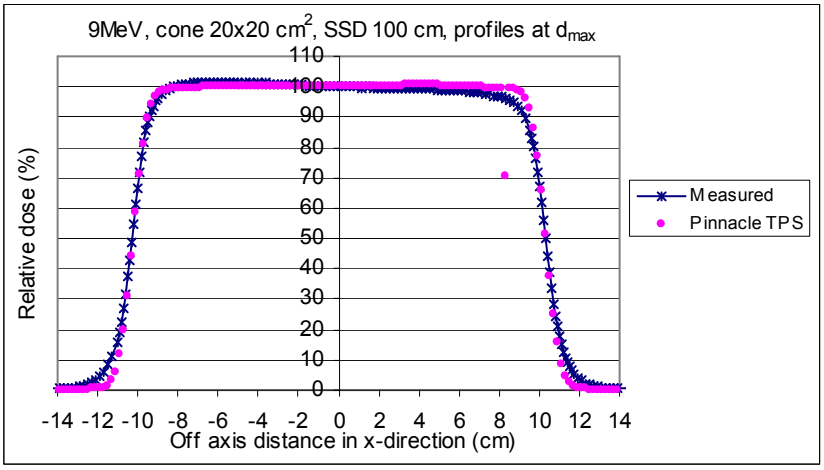
9MeV, cone 20x20 cm2, SSD 100 cm, profiles at dmax
Relative dose (%)
110
100
90
80
70
60
50
40
30
20
10
0
-14 -12 -10 -8 -6 -4 -2 0 2 4 6 8 10 12 14
Off axis distance in x-direction (cm)
Measured
Pinnacle TPS

(a)

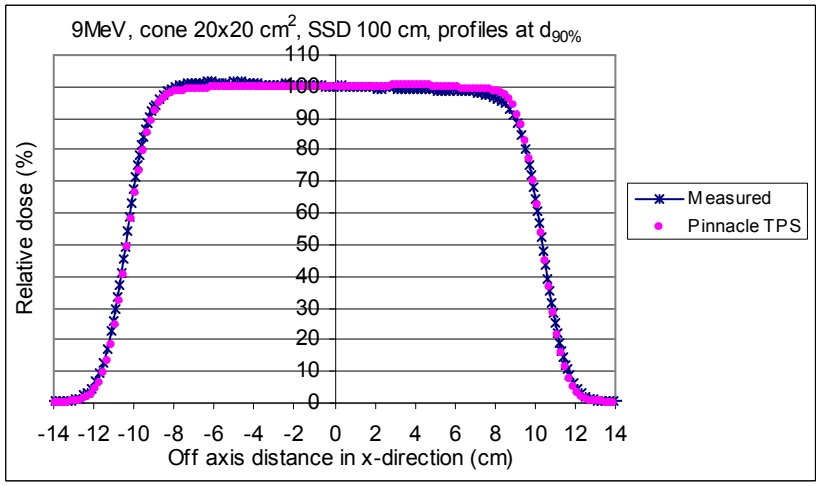
9MeV, cone 20x20 cm2, SSD 100 cm, profiles at d90%
Relative dose (%)
110
100
90
80
70
60
50
40
30
20
10
0
-14 -12 -10 -8 -6 -4 -2 0 2 4 6 8 10 12 14
Off axis distance in x-direction (cm)
Measured
Pinnacle TPS

(b)

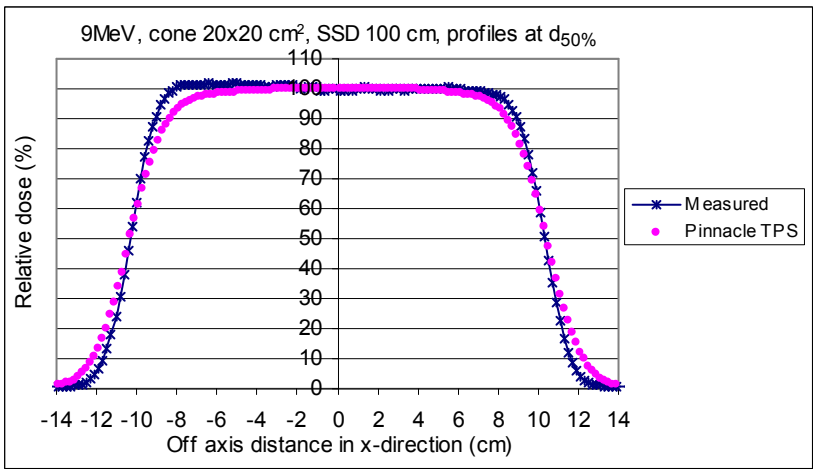
9MeV, cone 20x20 cm2, SSD 100 cm, profiles at d50%
Relative dose (%)
110
100
90
80
70
60
50
40
30
20
10
0
-14 -12 -10 -8 -6 -4 -2 0 2 4 6 8 10 12 14
Off axis distance in x-direction (cm)
Measured
Pinnacle TPS

(c)

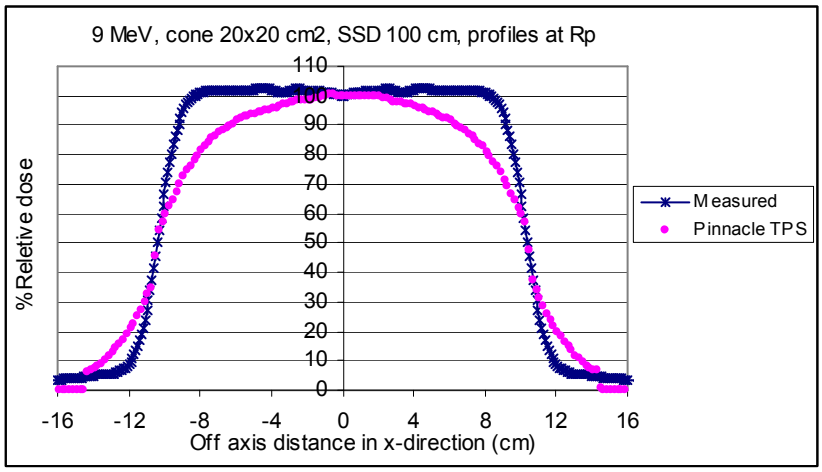

(d)

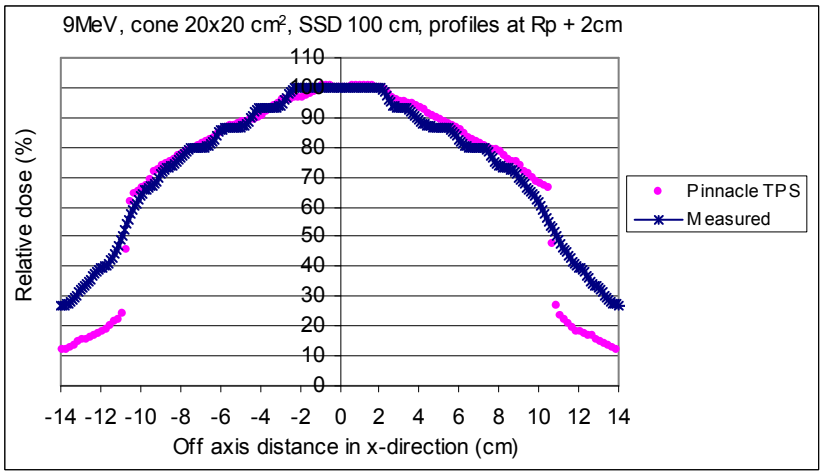

(e)

Figure 4a The comparison of relative dose profiles between Pinnacle TPS and diode measurement is shown for electron energy 9 MeV, SSD 100 cm and field size 20 × 20 cm^2 at (a) depth of dose maximum, (b) depth of dose 90%, (c) depth of dose 50%, (d) depth R_P and (e) depth R_P + 2 cm.

Table 5a The difference of beam fringe ($\delta_{50\text{-}90}$), radiological width (RW_{50}), penumbra width (δ_2), outside central beam axis region (δ_3) and outside beam edges (δ_4) between Pinnacle calculation and diode measurement for standard cone 4 × 4 and 20 × 20 cm^2 at the depths of d_{max}, $d_{90\%}$ $d_{50\%}$, Rp and Rp + 2 cm and irradiated with electron energy 9 MeV electron beams.

	Depth	**Distance to agreement (cm)**	
		4 × 4 cm^2	**20 × 20 cm^2**
$\delta_{50\text{-}90}$	dmax	1.305	0.30
	d90%	0.006	0.16
	d50%	0.12	0.76
	Rp	0.034	3.01
	Rp+2cm	2.9	1.92
RW_{50}	dmax	0.05	0.2
	d90%	0.05	0.02
	d50%	0.44	0.16
	Rp	0.49	0
	Rp+2cm	5.02	0.5
δ_2 (80-20%)	dmax	0.165	0.29
	d90%	0.04	0.13
	d50%	0.35	0.8
	Rp	1.14	2.29
	Rp+2cm	-	5.7
	Depth	**% Different**	
		4 × 4 cm^2	**20 × 20 cm^2**
δ_3	dmax	-	1.42%
	d90%	-	0.85%
	d50%	-	5.02%
	Rp	-	-14.36%
	Rp+2cm	-	6%
δ_4	dmax	5.28%	5.46%
	d90%	2.5%	2.2%
	d50%	4.57%	5.8%
	Rp	-	2.32%
	Rp+2cm	-	-

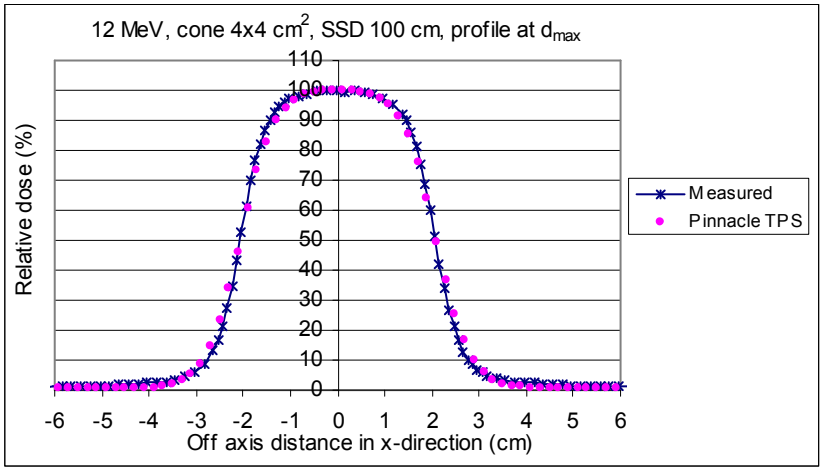
12 MeV, cone 4x4 cm2, SSD 100 cm, profile at dmax
Relative dose (%)
110
100
90
80
70
60
50
40
30
20
10
0
-6 -5 -4 -3 -2 -1 0 1 2 3 4 5 6
Off axis distance in x-direction (cm)
Measured
Pinnacle TPS

(a)

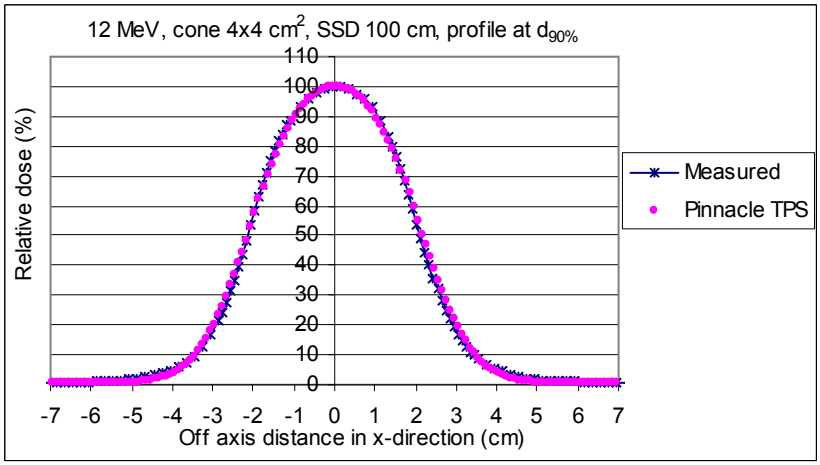
12 MeV, cone 4x4 cm2, SSD 100 cm, profile at d90%
Relative dose (%)
110
100
90
80
70
60
50
40
30
20
10
0
-7 -6 -5 -4 -3 -2 -1 0 1 2 3 4 5 6 7
Off axis distance in x-direction (cm)
Measured
Pinnacle TPS

(b)

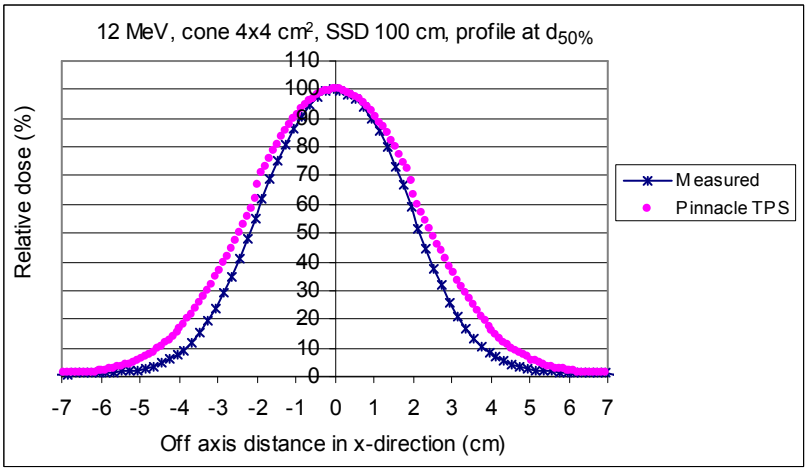
12 MeV, cone 4x4 cm2, SSD 100 cm, profile at d50%
Relative dose (%)
110
100
90
80
70
60
50
40
30
20
10
0
-7 -6 -5 -4 -3 -2 -1 0 1 2 3 4 5 6 7
Off axis distance in x-direction (cm)
Measured
Pinnacle TPS

(c)

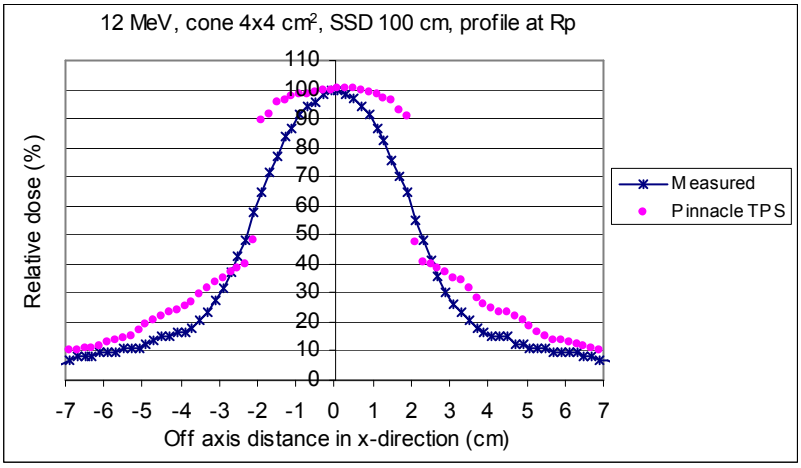

(d)

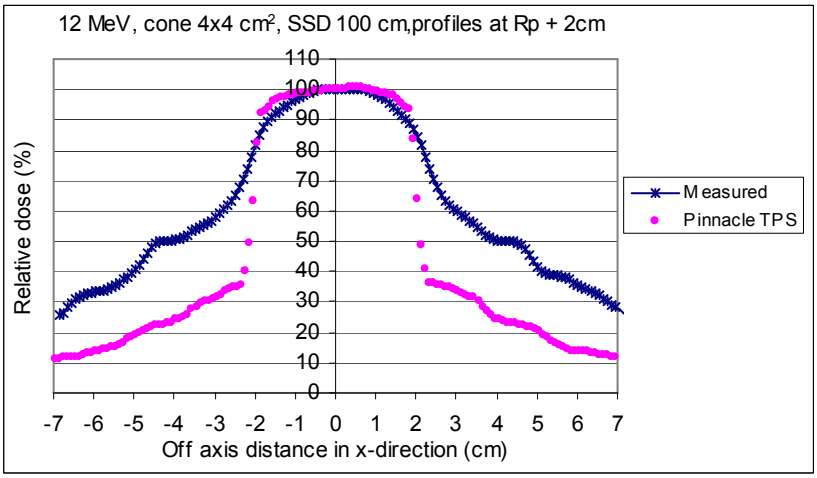

(e)

Figure 5a The comparison of relative dose profiles between Pinnacle TPS and diode measurement is shown for electron energy 12 MeV, SSD 100 cm and field size 4 × 4 cm^2 at (a) depth of dose maximum, (b) depth of dose 90%, (c) depth of dose 50%, (d) depth R_P and (e) depth R_P + 2 cm.

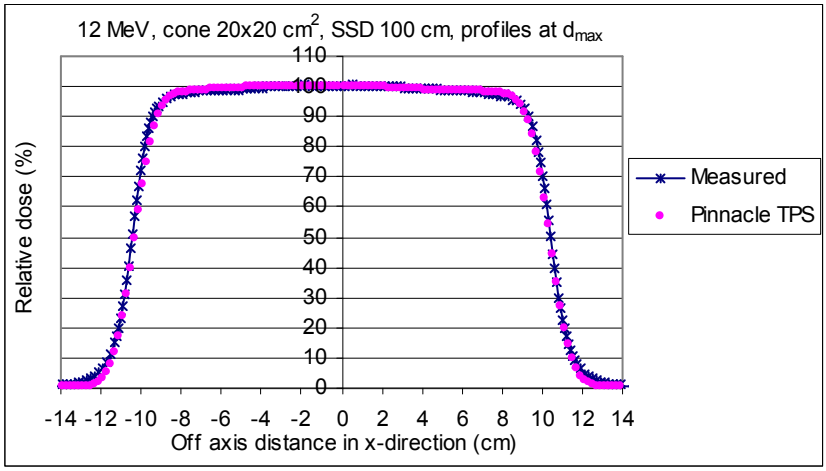
12 MeV, cone 20x20 cm2, SSD 100 cm, profiles at dmax
Relative dose (%)
110
100
90
80
70
60
50
40
30
20
10
0
-14 -12 -10 -8 -6 -4 -2 0 2 4 6 8 10 12 14
Off axis distance in x-direction (cm)
Measured
Pinnacle TPS

(a)

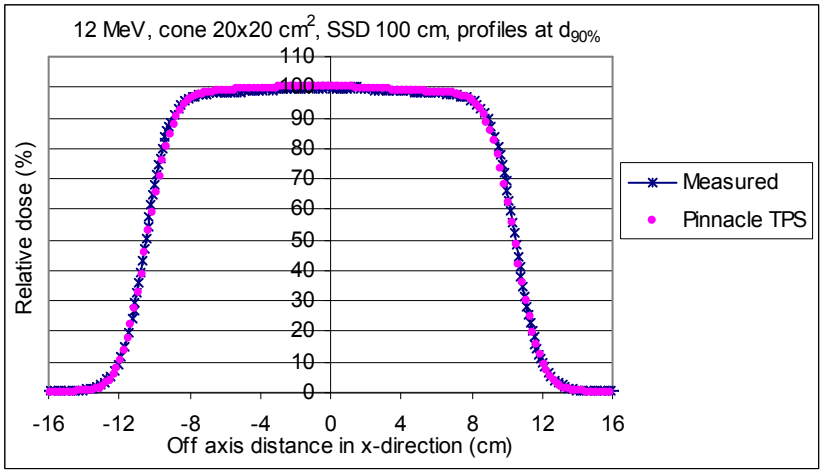
12 MeV, cone 20x20 cm2, SSD 100 cm, profiles at d90%
Relative dose (%)
110
100
90
80
70
60
50
40
30
20
10
0
-16 -12 -8 -4 0 4 8 12 16
Off axis distance in x-direction (cm)
Measured
Pinnacle TPS

(b)

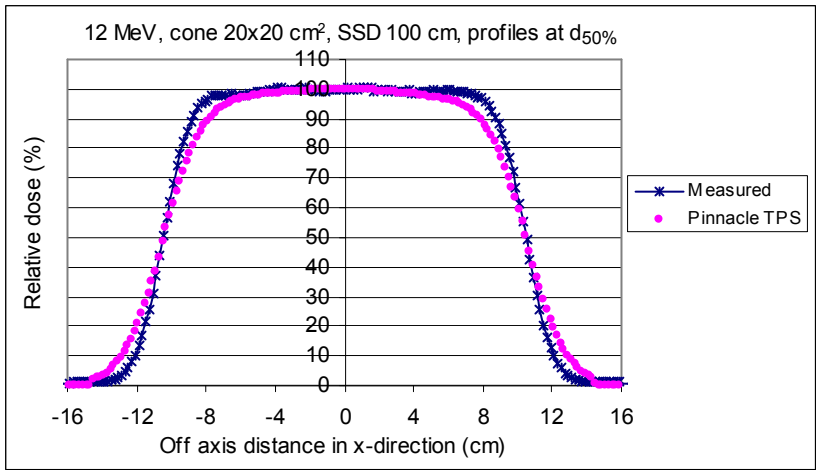
12 MeV, cone 20x20 cm2, SSD 100 cm, profiles at d50%
Relative dose (%)
110
100
90
80
70
60
50
40
30
20
10
0
-16 -12 -8 -4 0 4 8 12 16
Off axis distance in x-direction (cm)
Measured
Pinnacle TPS

(c)

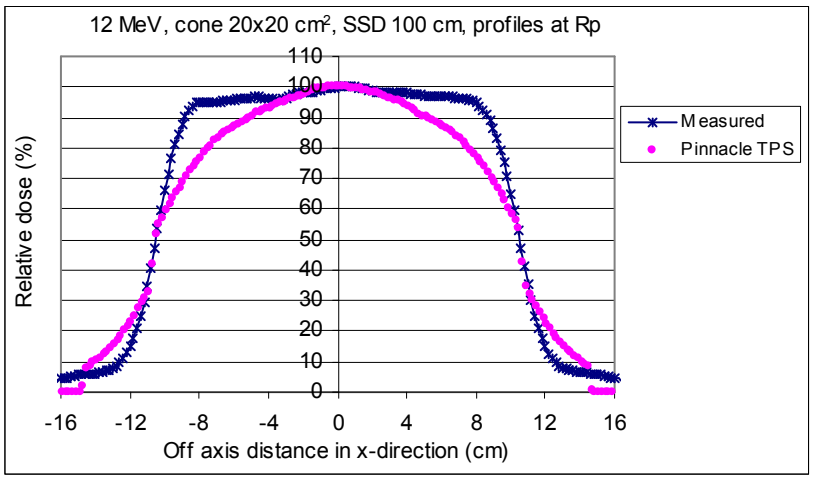

(d)

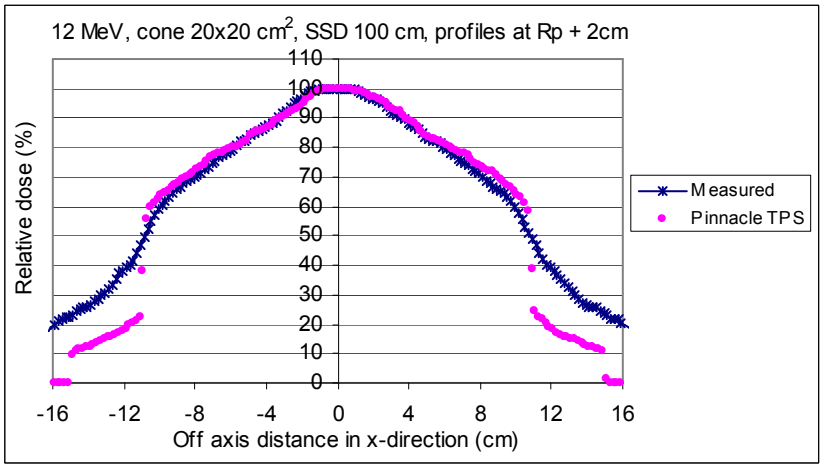

(e)

Figure 6a The comparison of relative dose profiles between Pinnacle TPS and diode measurement is shown for electron energy 12 MeV, SSD 100 cm and field size 20 × 20 cm^2 at (a) depth of dose maximum, (b) depth of dose 90%, (c) depth of dose 50%, (d) depth R_P and (e) depth R_P + 2 cm.

Table 6a The difference of beam fringe ($\delta_{50\text{-}90}$), radiological width (RW_{50}), penumbra width (δ_2), outside central beam axis region (δ_3) and outside beam edges (δ_4) between Pinnacle calculation and diode measurement for standard cone 4 × 4 and 20 × 20 cm^2 at the depths of d_{max}, $d_{90\%}$ $d_{50\%}$, Rp and Rp + 2 cm and irradiated with electron energy 12 MeV electron beams.

	Depth	**Distance to agreement (cm)**	
		4 × 4 cm^2	**20 × 20 cm^2**
$\delta_{50\text{-}90}$	dmax	0.12	0.075
	d90%	0.11	0.07
	d50%	0.26	1.1
	Rp	1.05	3.9
	Rp+2cm	2.27	0.36
RW_{50}	dmax	0.02	0.2
	d90%	0	0.22
	d50%	0.55	0
	Rp	0.28	0.2
	Rp+2cm	4.15	0.06
δ_2 (80-20%)	dmax	0.20	0.122
	d90%	0.13	0.16
	d50%	0.48	1
	Rp	0.9	2.7
	Rp+2cm	-	4.8
	Depth	**% Different**	
		4 × 4 cm^2	**20 × 20 cm^2**
δ_3	dmax	-	0.089%
	d90%	-	0.21%
	d50%	-	-4.08%
	Rp	-	-12.14%
	Rp+2cm	-	< 4%
δ_4	dmax	0.29%	3.11%
	d90%	2.6%	1.11%
	d50%	4.04%	5.15%
	Rp	-	-
	Rp+2cm	-	-

APPENDIX B

Table 1b Dose difference (%) and distance difference of buildup region and fall-off region between diode measurement and Pinnacle calculation for Percent Depth Dose (PDD) with insert circular cutout ∅5.2 cm and rectangular cutout of 8.7 × 6.8, 9.5 × 4.2, 6.7 × 13.7 and 4.7 × 14.6 cm^2 of electron energy 6 MeV beam.

%Dose difference at build up region											
Depth (cm)	6 MeV					Depth (cm)	6 MeV				
	∅ 5.2 cm	**8.7×6.8**	**9.5×4.2**	**4.7×14.6**	**6.7×13.7**		**∅ 5.2 cm**	**8.7×6.8**	**9.5×4.2**	**4.7×14.6**	**6.7×13.7**
0.1	-2.497	-1.557	-2.8133	-1.2952	-0.4313	2.1					
0.2	-2.913	-3.36	-1.567	-0.4369	1.02848	2.2					
0.3	-1.323	-0.574	0.7254	0.58144	2.13703	2.3					
0.4	0.0009	2.2134	1.7376	1.18784	2.9624	2.4					
0.5	0.4001	2.6999	2.1514	1.4501	3.34057	2.5					
0.6	0.5513	3.0509	1.9175	1.20398	3.35446	2.6					
0.7	0.4553	2.4417	1.4432	0.97011	3.30384	2.7					
0.8	0.3695	1.9761	1.8647	1.33081	3.24491	2.8					
0.9	0.9872	2.2275	2.5287	1.85899	3.22868	2.9					
1	1.3341	2.6813	2.6375	2.06007	3.19825	3					
1.1	0.9603	2.6664	2.5828	2.40098	2.6959	3.1					
1.2	0.669	2.6605	1.8289	1.3958	1.89341	3.2					
1.3	0.0683	2.1228	1.0607	0.43303	0.94598	3.3					
1.4	-0.018	1.8994	-0.0524	-0.3621	-0.1013	3.4					
1.5		0.6761				3.5					
1.6		-0.144				3.6					
1.7						3.7					
1.8						3.8					
1.9						3.9					
2						4					
Ave.	**-0.114**	**1.355**	**0.9864**	**0.81314**	**2.2001**	**Ave.**					
SD	**1.2472**	**1.8432**	**1.6742**	**1.07018**	**1.33268**	**SD**					

Distance difference at fall-off region					
Dose	6 MeV				
	∅ 5.2 cm	**8.7×6.8**	**9.5×4.2**	**4.7×14.6**	**6.7×13.7**
20	-0.08747	-0.204	-0.22228	-0.15084	-0.26463
30	-0.09022	-0.207	-0.22586	-0.14861	-0.26714
40	-0.08764	-0.212	-0.22514	-0.14454	-0.26678
50	-0.08126	-0.21	-0.22017	-0.13858	-0.26325
60	-0.07261	-0.197	-0.21096	-0.13068	-0.25625
70	-0.06322	-0.176	-0.19755	-0.1208	-0.24547
80	-0.05462	-0.154	-0.17997	-0.10889	-0.23059
Ave.	**-0.07672**	**-0.195**	**-0.21171**	**-0.1347**	**-0.2563**
SD	**0.013694**	**0.0214**	**0.017186**	**0.015499**	**0.013682**

Table 2b Dose difference (%) and distance difference of buildup region and fall-off region between diode measurement and Pinnacle calculation for Percent Depth Dose (PDD) with insert circular cutout ∅5.2 cm and rectangular cutout of 8.7 × 6.8, 9.5 × 4.2, 6.7 × 13.7 and 4.7 × 14.6 cm^2 of electron energy 9 MeV beam.

%Dose difference at build up region											
Depth (cm)	9 MeV					Depth (cm)	9 MeV				
	∅ 5.2 cm	**8.7×6.8**	**9.5×4.2**	**4.7×14.6**	**6.7×13.7**		**∅ 5.2 cm**	**8.7×6.8**	**9.5×4.2**	**4.7×14.6**	**6.7×13.7**
0.1	-3.4127	1.0221	-2.6718	-3.9784	0.1087	2.1	-0.085	0.3418	-0.0523	0.1268	0.6432
0.2	-3.7454	1.0786	-2.6268	-2.8612	1.0234	2.2	-0.2386	0.0037	-0.0347	-0.137	0.0002
0.3	-2.7196	1.2711	-2.0417	-1.087	1.3525	2.3					
0.4	-1.9939	0.6624	-1.8986	-0.9092	1.2345	2.4					
0.5	-1.905	0.0364	-1.9883	-0.905	1.141	2.5					
0.6	-1.9957	0.5838	-1.9958	-1.1969	1.2965	2.6					
0.7	-2.3782	1.2663	-2.0606	-1.5621	1.2489	2.7					
0.8	-2.6143	1.2017	-1.7598	-1.4506	1.0057	2.8					
0.9	-2.0657	1.0429	-1.4475	-1.2148	0.7912	2.9					
1	-1.8263	0.3614	-1.5691	-1.2999	0.4974	3					
1.1	-1.9939	-0.308	-2.0118	-1.4819	0.4464	3.1					
1.2	-1.9275	0.2792	-1.5959	-1.007	0.8423	3.2					
1.3	-1.4229	0.9574	-0.9754	-0.5281	1.1512	3.3					
1.4	-1.0028	1.1182	-0.6719	-0.2507	1.48	3.4					
1.5	-0.8638	1.2888	-0.3539	0.047	1.8288	3.5					
1.6	-0.7887	1.5803	-0.4177	-0.04	2.0964	3.6					
1.7	-0.8684	1.9048	-0.4246	-0.0795	2.0839	3.7					
1.8	-0.7887	1.1973	-0.3512	0.1457	1.7987	3.8					
1.9	-0.2416	0.4773	-0.1698	0.4438	1.4459	3.9					
2	0.0855	0.3482	-0.1504	0.2272	1.1262	4					
Ave.	**-**	**-**	**-**	**-**	**-**	**Ave.**	**-1.6261**	**0.8199**	**-1.2556**	**-0.9312**	**1.1201**
SD	**-**	**-**	**-**	**-**	**-**	**SD**	**1.0516**	**0.5535**	**0.8695**	**1.082**	**0.567**

Distance difference at fall-off region					
Dose	9 MeV				
	∅ 5.2 cm	**8.7×6.8**	**9.5×4.2**	**4.7×14.6**	**6.7×13.7**
20	-0.25636	-0.27823	-0.27048	-0.27623	-0.29641
30	-0.25797	-0.28668	-0.28037	-0.27667	-0.29399
40	-0.25443	-0.28524	-0.28001	-0.2754	-0.29434
50	-0.24526	-0.2761	-0.2703	-0.27038	-0.29415
60	-0.22999	-0.26146	-0.25213	-0.25958	-0.29013
70	-0.20813	-0.2435	-0.22638	-0.24095	-0.27896
80	-0.17922	-0.22441	-0.19396	-0.21246	-0.25734
Ave.	**-0.23305**	**-0.26509**	**-0.25338**	**-0.25881**	**-0.28647**
SD	**0.029716**	**0.023455**	**0.032345**	**0.024152**	**0.014111**

Table 3b Dose difference (%) and distance difference of buildup region and fall-off region between diode measurement and Pinnacle calculation for Percent Depth Dose (PDD) with insert circular cutout ∅5.2 cm and rectangular cutout of 8.7 × 6.8, 9.5 × 4.2, 6.7 × 13.7 and 4.7 × 14.6 cm^2 of electron energy 12 MeV beam.

%Dose difference at build up region											
Depth (cm)	12 MeV					Depth (cm)	12 MeV				
	∅ 5.2 cm	**8.7×6.8**	**9.5×4.2**	**4.7×14.6**	**6.7×13.7**		**∅ 5.2 cm**	**8.7×6.8**	**9.5×4.2**	**4.7×14.6**	**6.7×13.7**
0.1	-2.4668	1.242	-0.5382	-3.915	0.281933	2.1		0.355	0.1113	-0.407	
0.2	-3.0670	0.717	-0.7357	-3.374	0.273986	2.2	-0.6057	0.096	0.1577	-0.375	0.315882
0.3		0.384	-0.5152	-2.213		2.3		-0.149	0.1269	-0.412	
0.4	-1.1269	-0.112	-0.5741	-1.708	-0.27702	2.4	-0.1996	-0.176	-0.0732	-0.401	0.734011
0.5		-0.36	-0.5993	-1.304		2.5		-0.274	-0.1284	-0.226	
0.6	-1.288	-0.385	-0.7203	-1.349	-0.04373	2.6		-0.236	-0.1286	-0.079	0.289785
0.7		-0.212	-0.739	-1.414		2.7		-0.152			
0.8	-1.4696	-0.174	-0.7811	-1.405	0.013626	2.8		-0.204			0.611497
0.9		-0.18	-0.7553	-1.449		2.9		-0.086			
1	-1.1288	-0.137	-0.6758	-1.341	-0.18138	3		-0.174			0.057736
1.1		0.047	-0.6604	-1.202		3.1					
1.2	-1.1052	-0.055	-0.5087	-1.15	-0.0959	3.2					
1.3		-0.137	-0.4396	-1.085		3.3					
1.4	-0.7696	-0.206	-0.355	-0.905	0.024162	3.4					
1.5		-0.269	-0.3641	-0.829		3.5					
1.6	-0.9558	-0.024	-0.2629	-0.857	0.123887	3.6					
1.7		0.218	-0.2607	-0.99		3.7					
1.8	-1.045	0.254	-0.1517	-1.014	0.12422	3.8					
1.9		0.288	-0.1408	-1.033		3.9					
2	-0.9262	0.32	-0.0202	-0.728	0.33477	4					
Ave.	**-**	**-**	**-**	**-**	**-**	**Ave.**	**-1.2426**	**0.053**	**-0.3516**	**-1.242**	**0.161716**
SD	**-**	**-**	**-**	**-**	**-**	**SD**	**0.7563**	**0.425**	**0.3179**	**0.8851**	**0.270836**

Distance difference at fall-off region					
Dose	12 MeV				
	∅ 5.2 cm	**8.7×6.8**	**9.5×4.2**	**4.7×14.6**	**6.7×13.7**
20	-0.18646	-0.29888	-0.27241	-0.21112	-0.3255
30	-0.19686	-0.28754	-0.26481	-0.20236	-0.32367
40	-0.19836	-0.27747	-0.26415	-0.19861	-0.31778
50	-0.19031	-0.27048	-0.26364	-0.19448	-0.30774
60	-0.17201	-0.26631	-0.25645	-0.18457	-0.29348
70	-0.1428	-0.26263	-0.23577	-0.16348	-0.27492
80	-0.102	-0.25498	-0.1948	-0.12581	-0.25198
Ave.	**-0.16983**	**-0.27404**	**-0.25029**	**-0.18292**	**-0.2993**
SD	**0.035537**	**0.015149**	**0.027075**	**0.029424**	**0.027569**

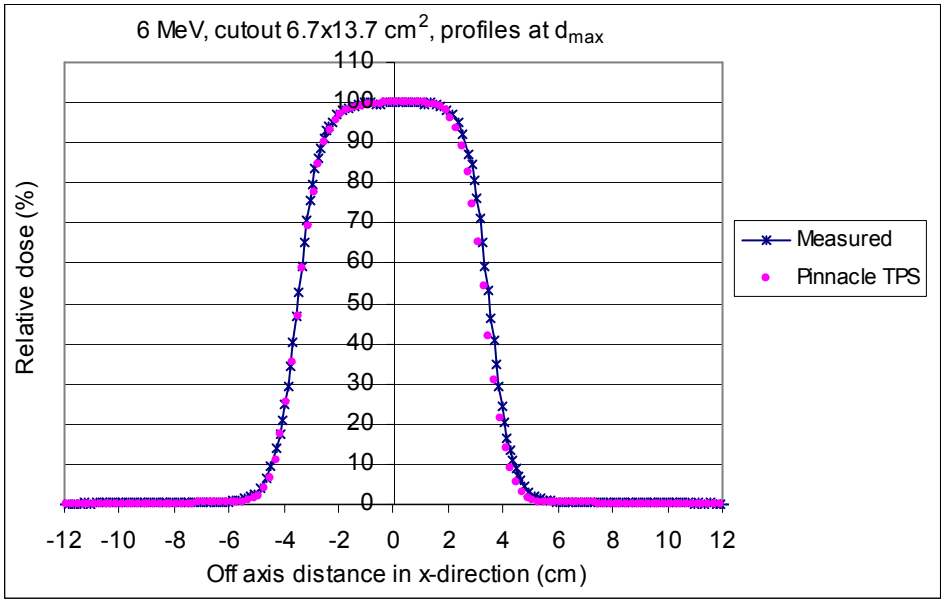

(a)

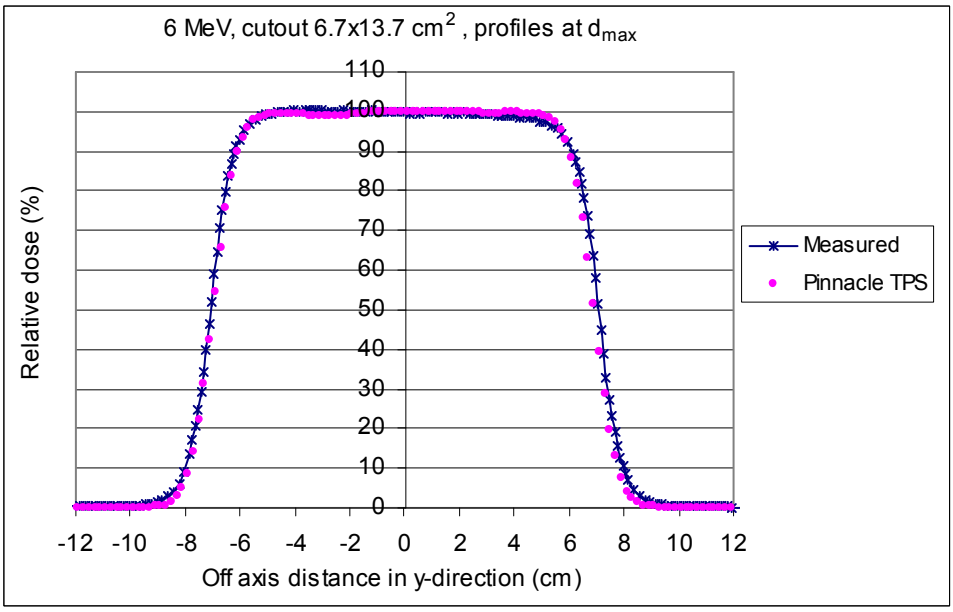

(b)

Figure 1b The comparison of relative dose profiles at the depth of maximum dose between Pinnacle TPS and diode measurement is shown for insert cutout 6.7 × 13.7 cm^2, SSD 100 cm with electron energy 6 MeV both in x-direction (a) and y-direction (b).

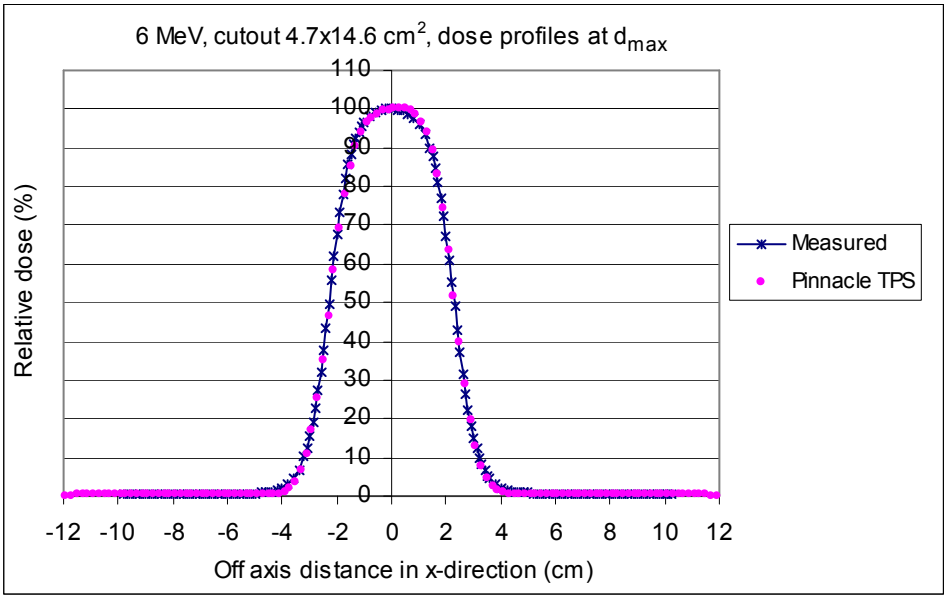

(a)

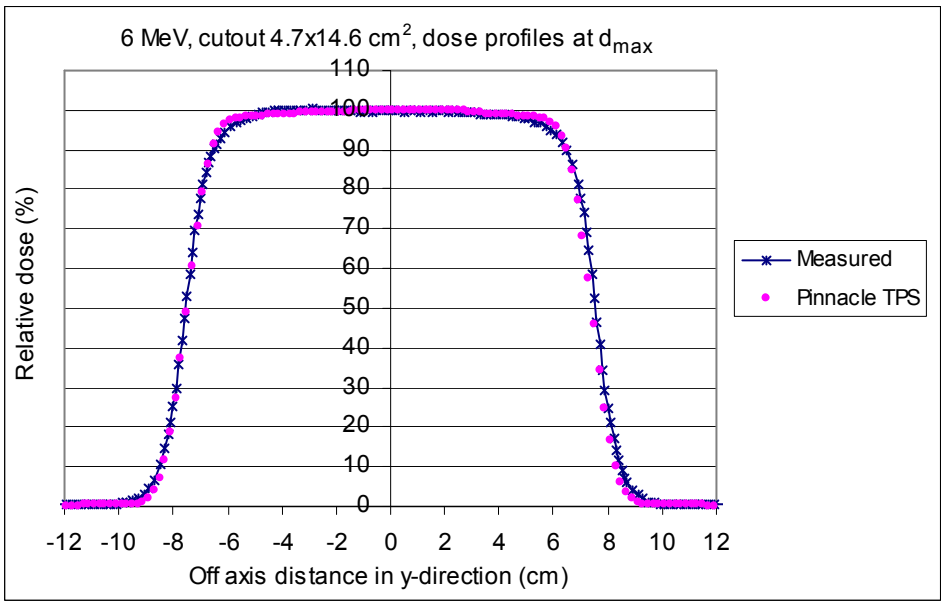

(b)

Figure 2b The comparison of relative dose profiles at the depth of maximum dose between Pinnacle TPS and diode measurement is shown for insert cutout 4.7 × 14.6cm^2, SSD 100 cm with electron energy 6 MeV both in x-direction (a) and y-direction (b).

Table 4b The difference of beam fringe ($\delta_{50\text{-}90}$), radiological width (RW_{50}), penumbra width (δ_2), outside central beam axis region (δ_3) and outside beam edges (δ_4) between Pinnacle calculation and diode measurement for rectangular cutout of 6.7 × 13.7 and 4.7 × 14.6 cm^2 at the maximum depth that insert to standard cone 15 × 15 cm^2 and irradiated with electron energy 6 MeV electron beams.

	Direction	**Distance to agreement (cm)**	
		6.7 × 13.7 cm^2	**4.7 × 14.6 cm^2**
$\delta_{50\text{-}90}$	X	0.03	0.027
	Y	0.06	0.15
RW_{50}	X	0.2	0
	Y	0.2	0.2
δ_2 (80-20%)	X	0.056	0.012
	Y	0	0.044
	Depth	**%Different**	
		6.7 × 13.7 cm^2	**4.7 × 14.6 cm^2**
δ_3	X	2.82%	-
	Y	1.15%	0.433%
δ_4	X	1.9%	0.22%
	Y	2.86%	2.83%

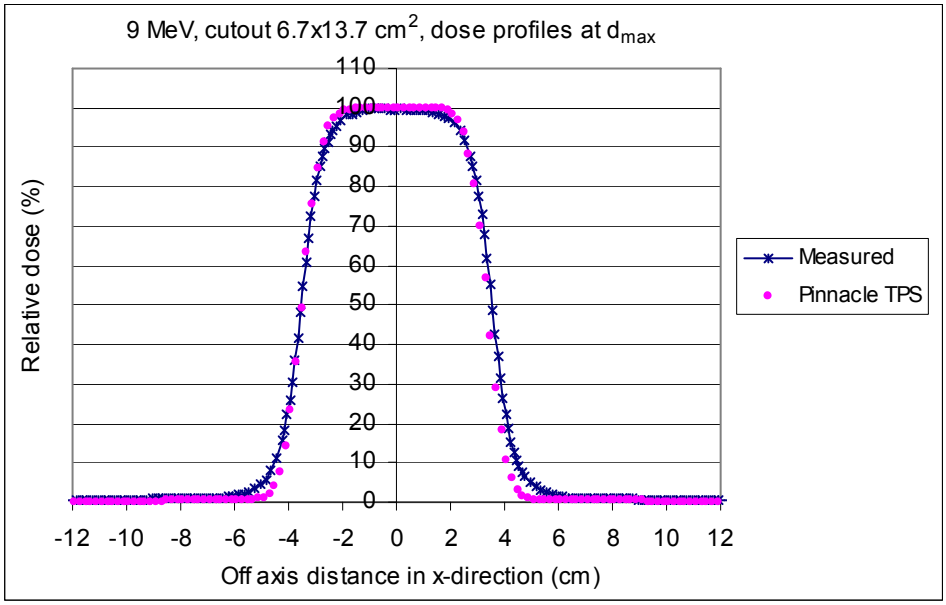

(a)

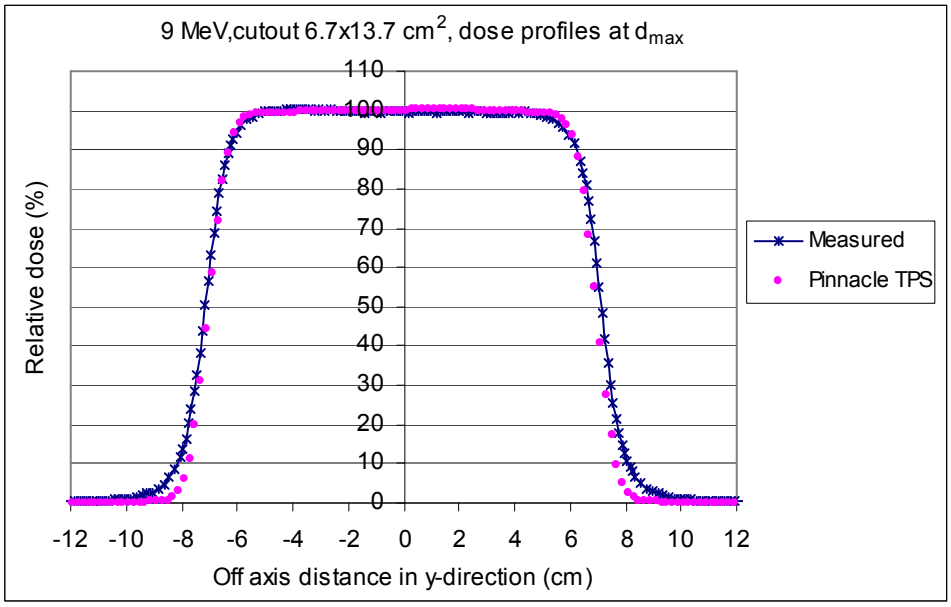

(b)

Figure 3b The comparison of relative dose profiles at the depth of maximum dose between Pinnacle TPS and diode measurement is shown for insert cutout 6.7 × 13.7 cm^2, SSD 100 cm with electron energy 9 MeV both in x-direction (a) and y-direction (b).

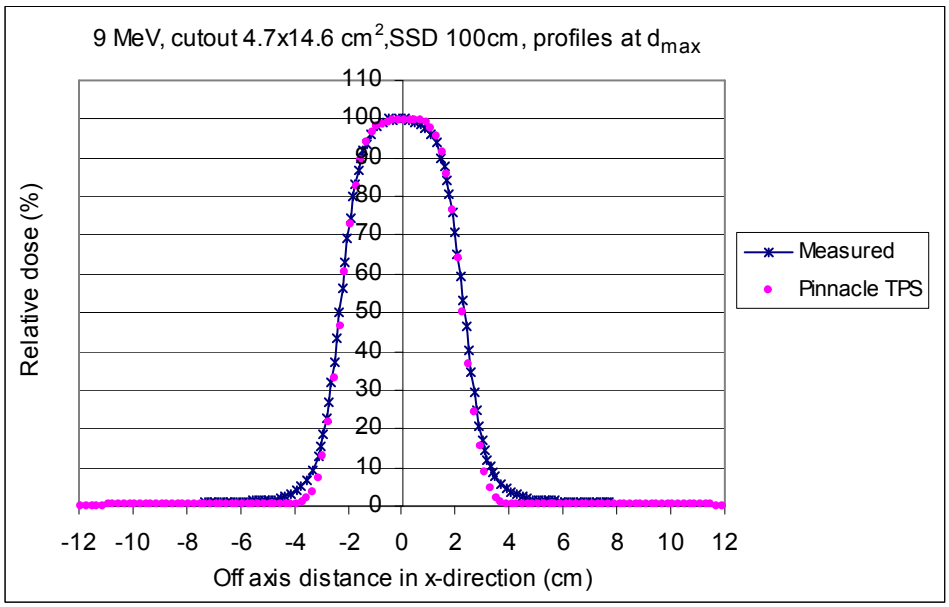

(a)

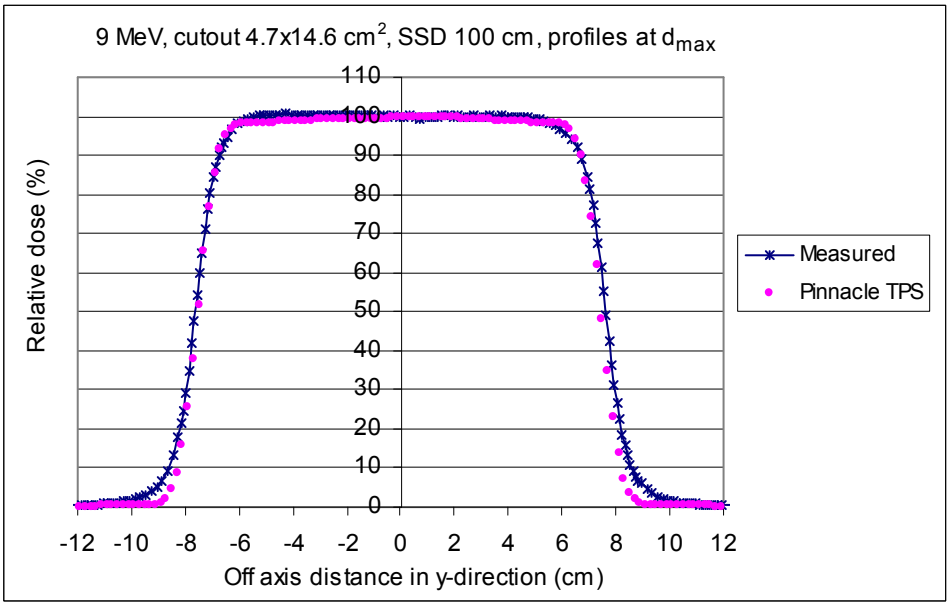

(b)

Figure 4b The comparison of relative dose profiles at the depth of maximum dose between Pinnacle TPS and diode measurement is shown for insert cutout 4.7 × 14.6 cm^2, SSD 100 cm with electron energy 9 MeV both in x-direction (a) and y-direction (b).

Table 5b The difference of beam fringe ($\delta_{50\text{-}90}$), radiological width (RW_{50}), penumbra width (δ_2), outside central beam axis region (δ_3) and outside beam edges (δ_4) between Pinnacle calculation and diode measurement for rectangular cutout of 6.7 × 13.7 and 4.7 × 14.6 cm^2 at the maximum depth that insert to standard cone 15 × 15 cm^2 and irradiated with electron energy 9 MeV electron beams.

	Direction	**Distance to agreement (cm)**	
		6.7 × 13.7 cm^2	**4.7 × 14.6 cm^2**
$\delta_{50\text{-}90}$	X	0.12	0.11
	Y	0.186	0.19
RW_{50}	X	0.22	0.05
	Y	0.3	0.24
δ_2 (80-20%)	X	0.17	0.16
	Y	0.16	0.175
	Depth	**%Different**	
		6.7 × 13.7 cm^2	**4.7 × 14.6 cm^2**
δ_3	X	1.78%	-
	Y	0.07%	2.01%
δ_4	X	5.3%	4.88%
	Y	5.8%	5.8%

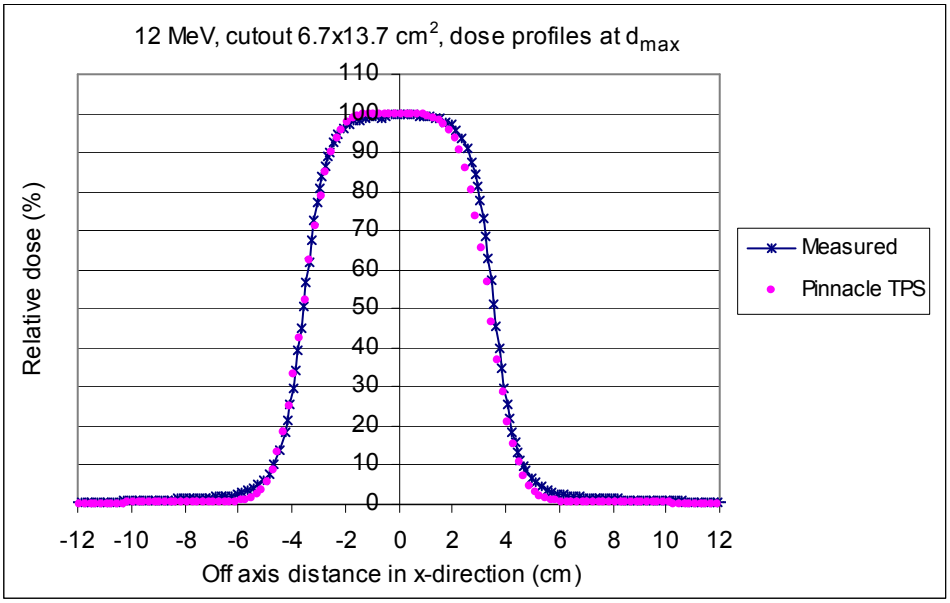

(a)

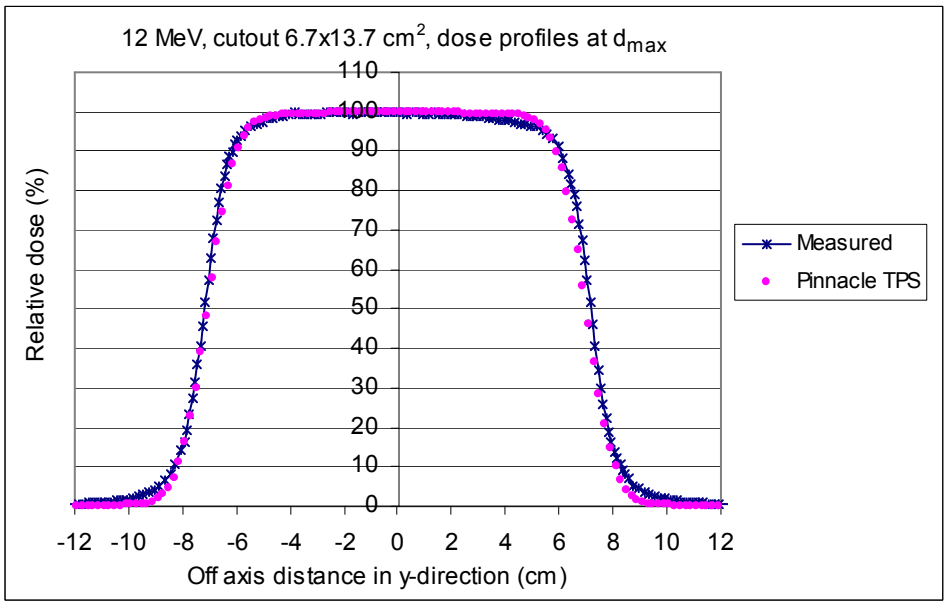

(b)

Figure 5b The comparison of relative dose profiles at the depth of maximum dose between Pinnacle TPS and diode measurement is shown for insert cutout 6.7 × 13.7 cm^2, SSD 100 cm with electron energy 12 MeV both in x-direction (a) and y-direction (b).

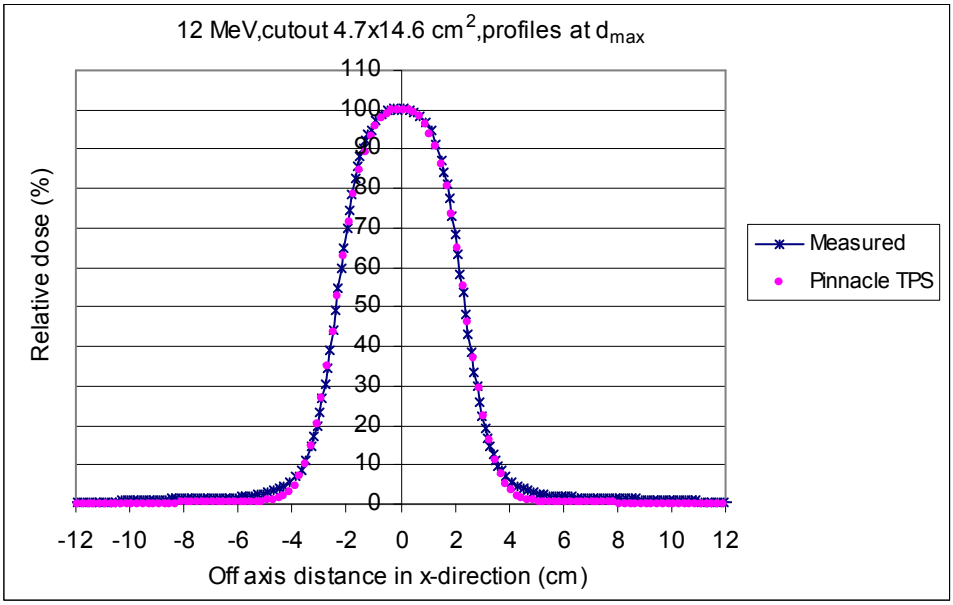

(a)

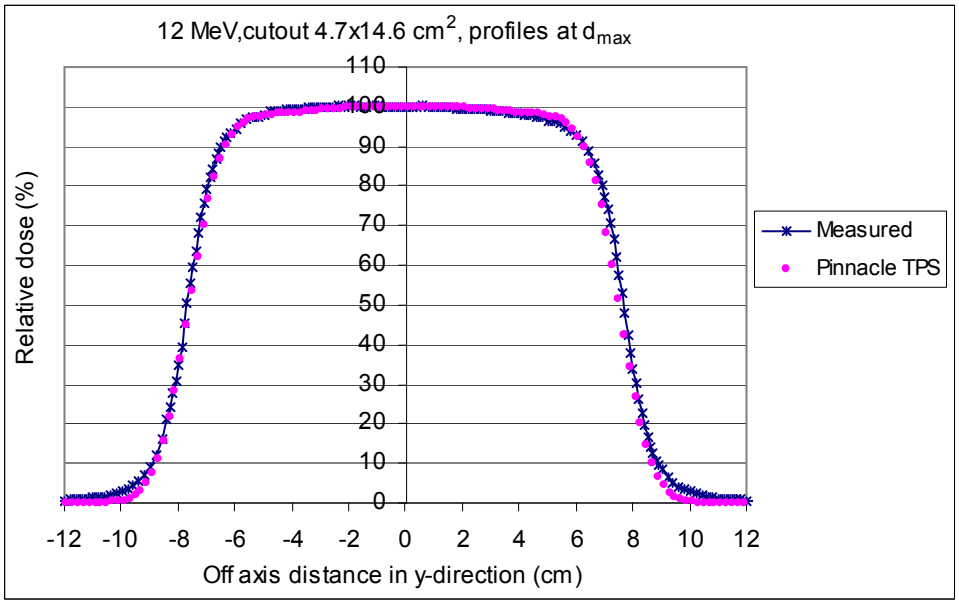

(b)

Figure 6b The comparison of relative dose profiles at the depth of maximum dose between Pinnacle TPS and diode measurement is shown for insert cutout 4.7 × 14.6 cm^2, SSD 100 cm with electron energy 12 MeV both in x-direction (a) and y-direction (b).

Table 6b The difference of beam fringe ($\delta_{50\text{-}90}$), radiological width (RW_{50}), penumbra width (δ_2), outside central beam axis region (δ_3) and outside beam edges (δ_4) between Pinnacle calculation and diode measurement for rectangular cutout of 6.7 × 13.7 and 4.7 × 14.6 cm^2 at the maximum depth that insert to standard cone 15 × 15 cm^2 and irradiated with electron energy 12 MeV electron beams.

	Direction	**Distance to agreement (cm)**	
		6.7 × 13.7 cm^2	**4.7 × 14.6 cm^2**
$\delta_{50\text{-}90}$	X	0.214	0.1
	Y	0.004	0.26
RW_{50}	X	0.15	0
	Y	0.4	0.2
δ_2 (80-20%)	X	0.268	0.1
	Y	0.197	0.005
	Depth	**%Different**	
		6.7 × 13.7 cm^2	**4.7 × 14.6 cm^2**
δ_3	X	4.77%	-
	Y	2.068%	1.06%
δ_4	X	2.05%	1.78%
	Y	2.72%	3.99%

APPENDIX C

Table 1c Dose difference (%) and distance difference at buildup region and fall-off region between diode measurements and Pinnacle calculations of Percent Depth Dose (PDD) for standard cone 4 × 4, 10 × 10 and 20 × 20 cm^2 at extended SSD 105 and 110 cm of electron energy 6 MeV.

%Dose difference at build up region						
Depth (cm)	105 cm			110 cm		
	4×4	**10×10**	**20×20**	**4×4**	**10×10**	**20×20**
0.1	-2.16432	-1.3712	-0.87735	3.959006	0.312256	2.41326
0.2	0.711286	0.778105	-0.61398	5.180057	3.146578	3.426934
0.3	2.786601	2.335747	1.041115	5.899939	4.694406	3.954533
0.4	3.418706	3.242535	2.424368	6.280162	5.389465	4.197098
0.5	3.896118	3.716438	1.899982	6.44464	5.574449	4.303515
0.6	3.021494	3.317633	1.432662	6.479987	5.502428	4.372014
0.7	2.167038	3.154194	1.069659	6.43763	5.342855	4.454057
0.8	2.983015	3.250934	0.852842	6.336763	5.189825	4.559257
0.9	3.972368	3.272254	1.813714	6.167351	5.07075	4.660272
1	3.892127	3.146219	2.627705	5.892638	4.954223	4.696948
1.1	3.983358	2.806234	2.080065	5.450749	4.756225	4.579244
1.2	2.421687	2.189163	1.645324	4.755065	4.344147	4.188616
1.3	1.153777	1.343896	0.639907	3.693103	3.538237	3.377613
1.4	-0.03993	-0.12411	-0.16393	2.123529	2.110084	1.967416
1.5				-0.12916	-0.22233	-0.25707
1.6						
1.7						
1.8						
1.9						
2						
Ave.	**2.300238**	**2.218431**	**0.977714**	**4.998097**	**3.98024**	**3.659581**
SD	**1.807336**	**1.518769**	**1.207805**	**1.897533**	**1.871788**	**1.358371**
Distance difference at fall-off region						
Dose	105 cm			110 cm		
	4×4	**10×10**	**20×20**	**4×4**	**10×10**	**20×20**
20	-0.236	-0.21252	-0.20286	-0.23834	-0.19304	-0.20708
30	-0.24642	-0.21698	-0.20953	-0.25141	-0.20005	-0.20728
40	-0.2557	-0.21511	-0.21461	-0.25393	-0.19962	-0.1997
50	-0.25424	-0.20835	-0.21294	-0.24777	-0.19279	-0.19195
60	-0.23879	-0.19818	-0.20312	-0.23482	-0.18061	-0.18632
70	-0.21239	-0.18604	-0.18755	-0.21698	-0.16412	-0.17972
80	-0.1844	-0.17339	-0.17244	-0.19611	-0.14436	-0.16373
Ave.	**-0.23256**	**-0.20151**	**-0.20043**	**-0.2342**	**-0.18209**	**-0.19083**
SD	**0.025737**	**0.016499**	**0.015292**	**0.020954**	**0.020868**	**0.015773**

Table 2c Dose difference (%) and distance difference at buildup region and fall-off region between diode measurements and Pinnacle calculations of Percent Depth Dose (PDD) for standard cone 4 × 4, 10 × 10 and 20 × 20 cm^2 at extended SSD 105 and 110 cm of electron energy 9 MeV.

%Dose difference at build up region						
Depth (cm)	105 cm			110 cm		
	4×4	**10×10**	**20×20**	**4×4**	**10×10**	**20×20**
0.1	-5.61102	1.920382	-0.8801	-4.16459	2.529897	-0.39254
0.2	-3.87835	2.004786	-0.71517	-4.46256	2.642299	-0.37336
0.3	-2.8662	1.874928	0.192836	-4.37343	2.407375	0.529257
0.4	-2.4	1.362722	1.016932	-3.79718	2.253436	1.232595
0.5	-1.91236	1.220278	0.715835	-3.99851	2.154186	1.001487
0.6	-2.99201	1.657535	0.464128	-4.37415	2.232057	0.694424
0.7	-4.13309	1.993112	0.627853	-4.34806	2.32362	0.853142
0.8	-3.25287	2.082029	0.686186	-4.09912	2.557069	1.030012
0.9	-2.98317	1.914477	0.389012	-3.94023	2.087243	0.662953
1	-2.92003	1.239884	0.109152	-3.73604	1.481872	0.302449
1.1	-3.30743	1.042299	0.448274	-3.49571	1.286847	0.614412
1.2	-2.75758	1.305294	0.66809	-3.08233	1.222483	0.778492
1.3	-2.1609	1.540064	0.772763	-2.64198	1.422362	0.800645
1.4	-1.64083	1.755216	0.76796	-2.03235	1.755173	0.820354
1.5	-1.19587	1.847102	0.660775	-1.80849	1.839158	0.717033
1.6	-1.55478	1.952413	0.690569	-1.81531	1.953714	0.633585
1.7	-1.85997	1.863706	0.632095	-1.48469	1.479917	0.584209
1.8	-0.91347	1.15912	0.723548	-0.94268	1.210531	0.585919
1.9	0.066101	0.671558	0.408449	-0.44526	0.787872	0.285291
2	-0.11716	0.428982	0.15512	0.032192	0.364646	0.083582
2.1		0.130985	-0.02467		0.091788	-0.11745
2.2		-0.06924	-0.11766		-0.0025	-0.04362
2.3						
2.4						
2.5						
2.6						
2.7						
2.8						
2.9						
3						
Ave.	**-2.41955**	**1.404438**	**0.323975**	**-2.95052**	**1.640048**	**0.487844**
SD	**1.360711**	**0.631414**	**0.541891**	**1.4454**	**0.788767**	**0.448722**
Distance difference at fall-off region						
Dose	105 cm			110 cm		
	4×4	**10×10**	**20×20**	**4×4**	**10×10**	**20×20**
20	-0.31632	-0.26012	-0.24174	-0.28218	-0.25706	-0.23382
30	-0.3171	-0.27712	-0.23175	-0.28404	-0.27305	-0.23
40	-0.30878	-0.28595	-0.23059	-0.27718	-0.27784	-0.22829
50	-0.29045	-0.28691	-0.23389	-0.26047	-0.2746	-0.22767
60	-0.26117	-0.28034	-0.23727	-0.23277	-0.26648	-0.22713
70	-0.22003	-0.26655	-0.23637	-0.19293	-0.25665	-0.22564
80	-0.16609	-0.24585	-0.22682	-0.1398	-0.2483	-0.2222
Ave.	**-0.26856**	**-0.27184**	**-0.23406**	**-0.23848**	**-0.26485**	**-0.22782**
SD	**0.057218**	**-0.27184**	**0.004907**	**0.054486**	**0.011073**	**0.0036**

Table 3c Dose difference (%) and distance difference at buildup region and fall-off region between diode measurements and Pinnacle calculations of Percent Depth Dose (PDD) for standard cone 4 × 4, 10 × 10 and 20 × 20 cm^2 at extended SSD 105 and 110 cm of electron energy 12 MeV.

%Dose difference at build up region						
Depth (cm)	105 cm			110 cm		
	4×4	**10×10**	**20×20**	**4×4**	**10×10**	**20×20**
0.1	2.165177	3.053646	-0.80729	6.542871	3.783434	0.341412
0.2	3.592627	2.64503	-1.0389	5.784038	3.388946	0.15775
0.3	4.45195	2.263656	-0.58293	5.782882	2.900101	0.660177
0.4	4.626591	1.766013	0.013186	6.115157	2.437082	1.117141
0.5	4.903142	1.51434	-0.02083	5.977974	2.116337	1.107663
0.6	4.248733	1.364074	-0.06684	5.732137	2.052206	1.054445
0.7	3.691733	1.300157	-0.14123	5.602785	1.945261	0.814025
0.8	3.472746	1.187576	-0.13648	5.268141	1.917062	0.791487
0.9	3.452119	1.137971	-0.06772	5.116594	1.951622	0.702736
1	3.121984	1.140775	-0.06913	4.850817	1.90003	0.80963
1.1	2.728432	1.186671	-0.15063	4.599089	1.886601	0.563792
1.2	2.759082	1.029472	-0.3208	4.357786	1.76723	0.361822
1.3	2.835011	0.902295	-0.22843	4.128662	1.66786	0.460076
1.4	2.584315	0.680876	-0.12149	3.917134	1.448794	0.44959
1.5	2.493564	0.596117	0.112959	3.595062	1.500932	0.587872
1.6	2.192827	0.758906	0.232931	3.171507	1.554084	0.735266
1.7	1.922785	0.929986	0.236696	2.654182	1.605271	0.755233
1.8	1.559233	0.990769	0.123809	2.18257	1.652893	0.644789
1.9	1.341472	1.056291	0.246028	1.891041	1.567487	0.662168
2	1.26646	1.125512	0.252128	1.639512	1.480559	0.804567
2.1	1.331799	1.083582	0.377838	1.416069	1.26645	0.813142
2.2	0.935606	0.818158	0.393834	1.066596	1.057971	0.820187
2.3	0.6784	0.560565	0.190487	0.561853	0.859913	0.574318
2.4	-0.03934	0.539466	0.005901	-0.27142	0.678229	0.340099
2.5		0.529283	-0.03825		0.645823	0.25368
2.6		0.53352	-0.04922		0.644174	0.198807
2.7		0.44418	-0.01759		0.43299	0.063597
2.8		0.3791	-0.04679		0.398855	0.118461
2.9		0.232262	-0.01047		0.179694	0.005633
3		0.010742	-0.00933		0.038023	0.00169
Ave.	**2.596519**	**1.0587**	**-0.05928**	**3.820126**	**1.55753**	**0.566703**
SD	**1.317135**	**0.672213**	**0.306621**	**1.993768**	**0.876217**	**0.316405**
Distance difference at fall-off region						
Dose	105 cm			110 cm		
	4×4	**10×10**	**20×20**	**4×4**	**10×10**	**20×20**
20	-0.33259	-0.25472	-0.21142	-0.292886967	-0.23974	-0.19531
30	-0.34453	-0.24503	-0.20436	-0.303600449	-0.23679	-0.19349
40	-0.34542	-0.24497	-0.20205	-0.312930991	-0.23474	-0.18543
50	-0.34217	-0.25003	-0.20144	-0.319979793	-0.23358	-0.17423
60	-0.33617	-0.25569	-0.1995	-0.323848055	-0.23334	-0.16303
70	-0.32329	-0.25741	-0.19318	-0.323636977	-0.23402	-0.15492
80	-0.29389	-0.25069	-0.17942	-0.318447759	-0.23563	-0.15304
Ave.	**-0.33115**	**-0.25122**	**-0.19877**	**-0.313618713**	**-0.23541**	**-0.17421**
SD	**0.01817**	**0.004993**	**0.010127**	**0.011542905**	**0.002263**	**0.01774**

APPENDIX D

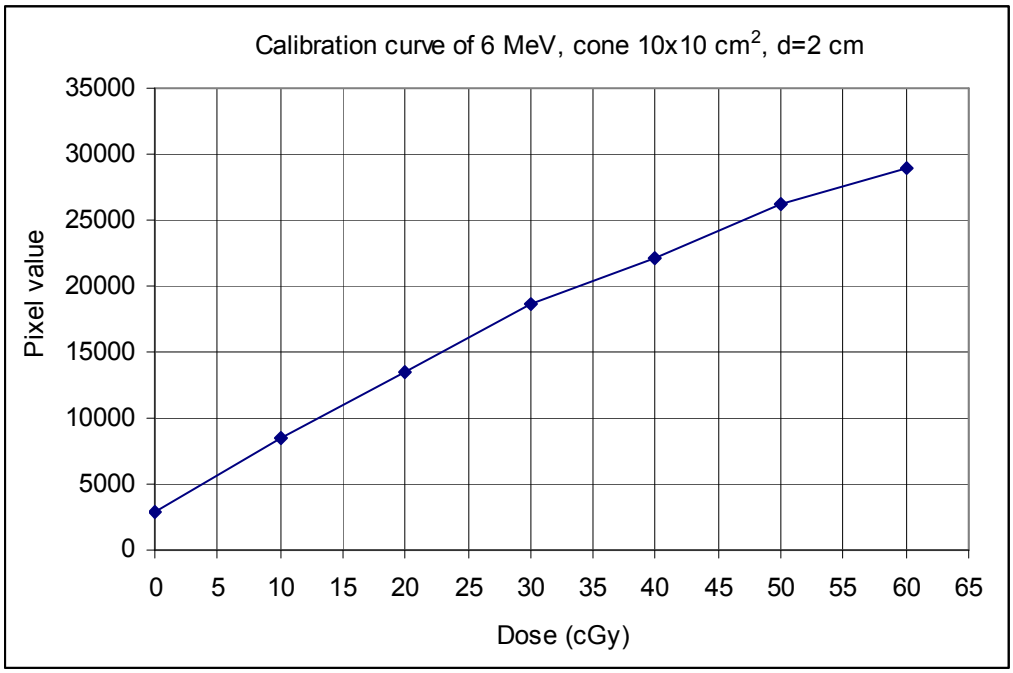

Figure 1d Calibration curves of XV film at depth 2 cm for standard cone 10 × 10 cm^2 of electron energy 6 MeV beam.

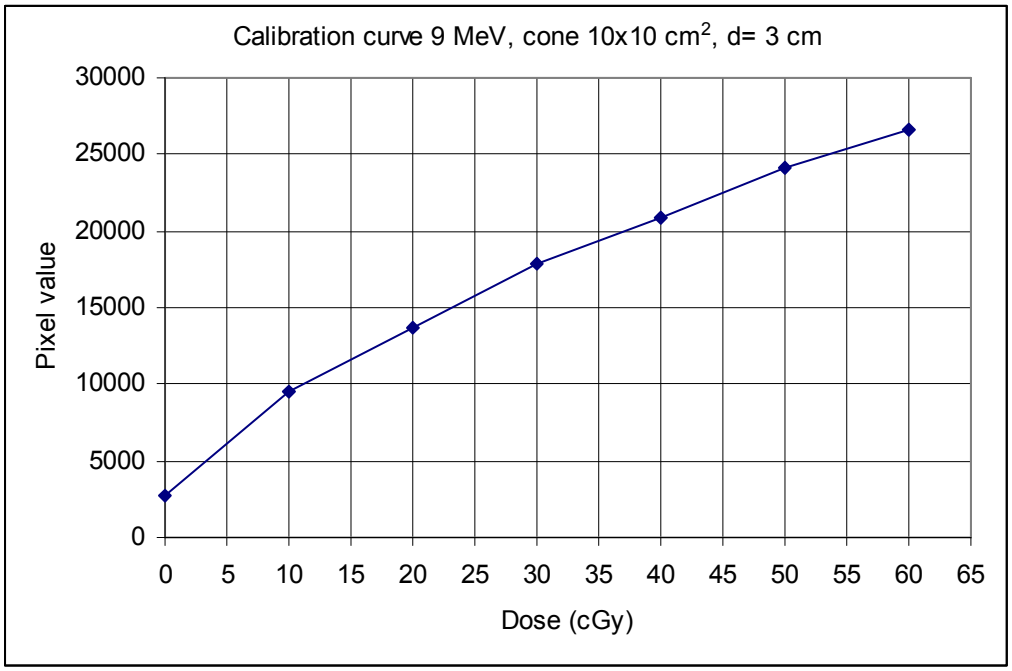

Figure 2d Calibration curves of XV film at depth 3 cm for standard cone 10 × 10 cm^2 of electron energy 9 MeV beam.

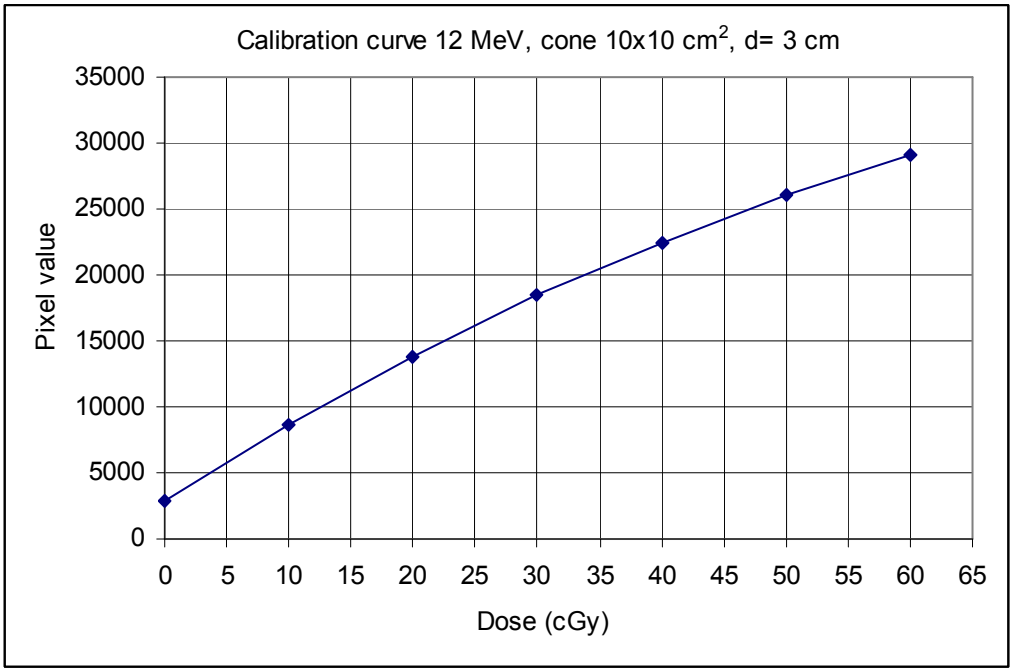

Figure 3d Calibration curves of XV film at depth 3 cm for standard cone 10 × 10 cm^2 of electron energy 12 MeV beam.

BIOGRAPHY

NAME	Ms.Saengduean Songsri
DATE OF BIRTH	29 December 1981
PLACE OF BIRTH	Surin, Thailand
INSTITUTIONS ATTENDED	Mahidol University, 2004: Bachelor of Science (Radiological Technology) Mahidol University, 2007: Master of Science (Medical physics)
HOME ADDRESS	21 Trabaekyai Village Kawao, Mueang Surin, Thailand 32000 Tel. 086-521-5722 E-mail: gamma_rt37@hotmail.com